Summer 2012

Bond, transfer length, and development length of prestressing strand in self-consolidating concrete

Krista Beth Porterfield

Department:

BOND, TRANSFER LENGTH, AND DEVELOPMENT LENGTH OF PRESTRESSING STRAND IN SELF-CONSOLIDATING CONCRETE

by

KRISTA BETH PORTERFIELD

A THESIS

Presented to the Faculty of the Graduate School of the

MISSOURI UNIVERSITY OF SCIENCE AND TECHNOLOGY

In Partial Fulfillment of the Requirements for the Degree

MASTER OF SCIENCE IN CIVIL ENGINEERING

2012

Approved by

Dr. Jeffery S. Volz, Advisor
Dr. John J. Myers
Dr. Lesley Sneed

ABSTRACT

Due to its economic advantages, the use of self-consolidating concrete (SCC) has increased rapidly in recent years. However, because SCC mixes typically have decreased amounts of coarse aggregate and high amounts of admixtures, industry members have expressed concerns that the bond of prestressing strand in SCC may be compromised. While the bond performance of prestressing strand in a new material such as SCC is an important topic requiring investigation, the results are only applicable if the research is completed on strands with similar bond quality as the strands used in the field. Therefore, the objectives of this research program were to investigate the transfer and development lengths of prestressing strand in SCC and also evaluate the effectiveness of two proposed bond tests in determining acceptable bond quality of strand.

Transfer and development lengths of 0.5-in. diameter (12.5 mm), Grade 270 prestressing strand were evaluated using rectangular beams constructed from normal and high strength conventional concrete and SCC mixes. End slips at release and strain readings over 28 days were used to calculate transfer lengths, and development lengths were evaluated through four-point loading at varying embedment lengths. Additionally, the NASP bond test and Large Block Pullout Tests (LBPT) were evaluated with strand from three different sources to determine if one test could be considered more reliable at predicting acceptable bond.

Results indicated that bond performance of SCC and conventional concrete were comparable, and that AASHTO and ACI equations for transfer and development length were generally conservative. The NASP bond test and LBPT were found to be equally valid, but the acceptance limits for both tests appear to require revisions.

ACKNOWLEDGMENTS

First, I would like to thank my advisor, Dr. Jeffery Volz, for making my time in grad school worthwhile and memorable. Not only did I learn a lot and greatly benefit from his knowledge and guidance, but his amiable personality and ability to connect with students made my experiences in grad school highly enjoyable.

I would also like to thank my committee members, Dr. John Myers and Dr. Lesley Sneed, for their time and advice.

Additionally, I would like to extend my thanks to the Missouri Department of Transportation and the Center for Transportation Infrastructure and Safety at Missouri S&T for providing funding. I would also like to thank PCI and the members of my PCI Daniel P. Jenny Fellowship committee, Roger Becker, Mike LaNier, Don Logan, Andrew Osborn and Larbi Sennour.

I would like to thank Coreslab Structures, Inc. in Marshall, MO and Prestressed Casting Co. in Springfield, MO for their time and assistance. Additionally, I would like to thank VSL for donation of resources.

I would like to thank the lab technicians, including Gary Abbott, John Bullock, Scott Parker, and Brian Swift, for their expertise and help with construction of test setups and specimens and data collection. Additionally, I owe a lot to my fellow grad students, Kyle Holman, Trevor Looney, Kyle Marlay, Carlos Ortega, Eric Sells, and Dane Shaw, for donating their time and effort to help me with my research. Working with everyone was always a pleasure, and I could never have completed my work without the help of the lab technicians and my colleagues and friends.

Finally, I would like to thank my parents, Sharon and Jim Porterfield, and my siblings, Joel and Elizabeth, for always supporting me and my decisions and for letting me know that they are proud of me.

TABLE OF CONTENTS

LIST OF ILLUSTRATIONS

LIST OF TABLES

NOMENCLATURE

Symbol	Description
A_{ps}	Area of prestressing strand, in^2
d_b	Nominal diameter of strand, in. (ACI 318-11 and AASHTO LRFD-07)
D	Nominal diameter of strand, in. (Tabatabai and Dickson 1993)
E_{ps}	Modulus of elasticity of prestressing strand, psi or ksi
f'_c	Concrete compressive strength at 28 days or otherwise specified, psi
f'_{ci}	Concrete compressive strength at release, psi
f_{ce}	Stress in concrete outside transfer zone due to stress in strand immediately after release, psi or ksi
f_{pe}	Effective stress in the strand after losses, psi (AASHTO LRFD-07)
f_{ps}	Stress in prestressing steel at nominal flexural strength, psi (ACI 318-11)
f_{pu}	Specified tensile strength of prestressing steel, psi (ACI 318-11)
f_{sb}	Average stress in the steel at general bond slip, psi or ksi (Tabatabai and Dickson 1993)
f_{si}	Stress in strand immediately after release, instead of after all losses, psi or ksi (Buckner 1995)
f_{si}	Stress in strand immediately before release, psi or ksi (Anderson and Anderson 1976)
f_{se}	Effective stress in prestressing strand after allowance for all prestress losses, psi or ksi (ACI 318-11 and Tabatabai and Dickson 1993)
f_{se}	Effective stress in prestressing strand immediately after release, psi or ksi (Anderson and Anderson 1976)
f_{su}	Stress developed in the strand at ultimate strength of a member, ksi (Tabatabai and Dickson 1993)
f_{su}*	Average stress in the prestressing steel at ultimate load, ksi (Tabatabai and Dickson 1993)
f_u	Ultimate tensile strength of prestressing strand as determined through a tension test in this research, ksi

l_e	Embedment length, in.
l_d	Development length, in. (AASHTO LRFD-07 and ACI 318-11)
l_{fb}	Flexural bond length, in.
l_t	Transfer length, in.
L	Embedment length, in. (Tabatabai and Dickson 1993)
L_T	Transfer length, in. (Tabatabai and Dickson 1993 and Anderson and Anderson 1976)
M_{cr}	Moment at which cracking first occurred in four-point load tests, k-in.
M_n	Calculated nominal moment capacity for four-point loading specimens, k-in.
M_u	Ultimate applied moment for four-point loading specimens, k-in.
U_t	Average bond stress, taken to be 0.4 ksi (Tabatabai and Dickson 1993)
Δ	Measured end slip of strand at release, in.
ε_{ce}	Strain in prestressing strand immediately after release, in./in.
ε_{se}	Strain in prestressing strand immediately after release, in./in.
ε_{si}	Strain in prestressing strand immediately before release, in./in.
Σ_0	Circumference of prestressing strand, in. (Tabatabai and Dickson 1993)
κ	Bond reduction factor of 1.6 for members greater than 24 in. deep (AASHTO LRFD-07)

1. INTRODUCTION

1.1. BACKGROUND

Self-consolidating concrete (SCC) is a material that is on the forefront of construction technology. The flowable nature of SCC eliminates the needs for mechanical vibration and finishing, which are typically required during placement of conventional concrete, saving costs in the form of labor, time, and equipment as well as increasing production rates at precast plants. In addition, the ability of SCC to securely fill formwork and congested areas of reinforcement under its own weight leads to a decrease in the potential for honeycombing and voids, resulting in better aesthetic appearance and structural quality. Despite the flowability of SCC, the concrete is still non-segregating due to the addition of certain admixtures and proper proportioning of the mix. The cost saving attributes, combined with the improved appearance and comparable structural quality compared to conventional concrete, make SCC especially of interest to precasters.

Although the economic and performance benefits make SCC desirable for use in construction, the addition of admixtures and adjustments to mix proportions that give SCC its unique qualities can alter structural properties when compared to conventional concrete, especially in terms of transfer and development lengths of prestressing strand. Because SCC mixes typically have decreased amounts of coarse aggregate and high amounts of admixtures, industry members have expressed concerns that the bond of prestressing strand in SCC may be compromised. In response to these concerns, some research programs have recently been implemented, especially by state Departments of Transportation, to investigate the effects of SCC on prestressing strand and determine if SCC is acceptable for precast plants to use in the construction of prestressed members, such as infrastructure elements (Boehm et al. 2010, Larson et al. 2007).

While the bond of prestressing strand in SCC has been a current research subject, the bond quality of prestressing strand in general has also been a topic of interest in recent years. Only in the past few decades have concerns regarding excessive end slips of strands and measured transfer lengths significantly longer than those predicted by the AASHTO LRFD and ACI 318 equations begun to surface (Cousins et al. 1990). Research has since indicated that bond quality is an inherent property of the strand and can vary

from source to source. These recent issues with bond quality are most likely due to the current production process of prestressing strand compared to the original production processes. Today's strands are typically heated through induction, while the original process employed convection heating. The convection process heated the strands to much higher temperatures, and it is hypothesized that the higher temperatures burned off more of the residues from the wire drawing process and combusted the organic impurities on the surfaces (Rose and Russell 1997). It is believed that the lower temperatures from induction heating result in more residues left on the strands, which could affect bond; however, a direct correlation has not yet been established.

While the exact relationship between production process and bond quality has yet to be determined, differences in bond quality of strands have still been proven to exist, and as a result, several tests for assessing the bond quality of strands have been proposed. These pullout tests consist of sections of strand cast in concrete or mortar, and acceptable bond quality is determined by comparing the average pullout load to a minimum value. The different pullout tests and the standard limits for the tests have been investigated since the mid 1990's, but a standard test and limit have still not been accepted.

Bond of prestressing strand has become an important topic in recent years, especially as new materials are being developed and put into use. While the bond of prestressing strand in a new material such as SCC is an important topic that deserves investigation, the results are only valid and applicable if the research tests are completed on strands with similar bond quality as the type of strand being used in the field. Therefore, it is important to develop a test that can pre-qualify strand based on bond so researchers as well as industry members can use similar strand types, so trends seen in test results will be accurately reflected in the field.

1.2. OBJECTIVES

In order to investigate the possibility of implementing specifications that would allow precasters to use SCC for the construction of infrastructure elements for Missouri projects, the Missouri Department of Transportation (MoDOT) funded a research project examining the effect of SCC on various structural properties, including shear, durability, creep and shrinkage, bond with mild steel reinforcement, and bond with prestressing

strand. The portion of the research program related to the bond of prestressing strand is presented in this thesis, and the main objectives of this portion of the research were to 1) investigate the transfer and development lengths of 0.5-in.-diameter (12.7 mm), Grade 270 prestressing strand in normal strength and high strength conventional and SCC mixes similar to those used by precast plants in Missouri, and 2) evaluate two pullout tests proposed for the acceptance or rejection of strand based on bond quality.

In terms of evaluating the transfer and development lengths, the goals were to 1) compare SCC results to conventional concrete results to determine if SCC compromises, enhances, or has no effect on bond performance of prestressing strand, 2) compare SCC and conventional concrete results to values predicted by AASHTO LRFD-07 and ACI 318 code equations to determine if the design equations are conservative, 3) compare the normal strength concrete results to high strength concrete results to determine the effect of concrete strength on bond, and 4) compare results from top-cast strands and bottom-cast strands to evaluate the top-bar effect on prestressing strand.

Regarding the investigation of pullout tests, the goals were to 1) compare bond quality of prestressing strand from three different sources using two proposed pullout test methods and 2) correlate pullout results to measured transfer lengths.

The ultimate goal was to analyze the results from the transfer and development length and bond portions of this research program and make recommendations to MoDOT for guidelines regarding the use of SCC by precast plants for infrastructure elements and the acceptance of prestressing strand based on bond.

1.3. SCOPE

In order to evaluate the bond of prestressing strand, first, a literature review that included studies examining the transfer and development lengths of prestressing strand in SCC as well as previous research related to pullout tests and strand bond quality was conducted. Based on the literature review, a research plan was developed.

The transfer and development lengths of 0.5-in.-diameter (12.7 mm), Grade 270 prestressing strand were evaluated and compared in four concrete mixes. The four mixes included a normal strength and high strength conventional concrete and a normal strength and high strength SCC. Three 17-ft.-long (5.18 m) beams were cast from each mix for a

total of 12 full-scale specimens. For each mix, two beams were cast with two strands, both on the bottom, and one beam was cast with four strands, two on the bottom and two on the top. The four-strand beams were constructed to evaluate the effect of casting position on transfer length. All beams were first used to measure transfer lengths periodically from release to 28 days after casting. Once all transfer length data was collected, the development lengths of the two-strand beams were evaluated through four-point loading.

In the bond testing portion of this research program, 0.5-in.-diameter (12.7 mm), Grade 270 strand from three different sources was evaluated through two different proposed bond tests, and the pullout loads were compared to each other and to the recommended minimum limit specified by each test. The strands were also then cast in a modified bond test using the four concrete mixes used to construct the transfer and development length beam specimens with the goal of determining if the pullout loads from the tests performed in concrete could be correlated to the measured transfer lengths and be an indicator of bond performance.

1.4. OUTLINE

This thesis is composed of six sections and six appendices. Section 1 gives a brief introduction to the subject area and explains why this research was done. The first section also presents the objectives and scope of work of the research covered in this thesis.

Section 2 contains the Literature Review conducted on the topics of bond and specifically bond of prestressing strand in SCC. First, relevant terms and the mechanisms of bond theory are defined and discussed. Next the AASHTO LRFD-07 and ACI 318-11 code equations for transfer and development length are presented along with a brief background of the development of the equations. Finally, summaries of previous research regarding general bond acceptance tests of prestressing strands and also bond, transfer length, and development length of prestressing strands in SCC are explained.

Section 3 presents the bond test program portion of this research. The design and fabrication of pullout specimens as well as the setup, procedure, and results for each test are discussed. Setup and procedure for tension testing performed on samples of the

prestressing strands and the resulting mechanical properties are also included in this section.

The transfer length and development length test program is explained in Section 4. This section outlines the design and fabrication of the prestressed beams used for this research as well as the set-up, procedure, and results for the transfer length and development length tests.

Section 5 contains the discussion of all results, including evaluation of bond performance of prestressing strand in conventional concrete versus SCC and comparison of results to AASHTO and ACI code provisions. A comparison and discussion of the two bond tests evaluated in this program are also included in this section, along with discussion of the correlation between results of the pullout tests and measured transfer lengths.

Finally, the findings obtained from each section of the study along with the conclusions that were drawn based on the findings are presented in Section 6. This section also includes recommendations for proposed specifications and future research.

There are also six appendices included in this thesis. Appendix A includes the summary of concrete compressive strengths from 1 to 28 days for the four concrete mixes. Appendix B contains the load vs. deflection plots for the NASP in concrete tests, while the load vs. time curves from the LBPT specimens are presented in Appendix C. The 95% Average Mean Strain plots for transfer length determination are included in Appendix D, and the end slip plots from the linear potentiometers connected to the Synergy data acquisition system can be found in Appendix E. Finally, Appendix F includes photos, moment and end slip vs. deflection plots, and descriptions of all four-point load tests.

2. LITERATURE REVIEW

2.1. INTRODUCTION

This Literature Review first explains the relevant terms related to bond of prestressing strand and then discusses theory of bond mechanisms and the factors that affect transfer and development lengths. Next, the current AASHTO and ACI provisions for transfer length and development length of prestressing strand are presented along with information on the background of the development of the equations. Finally, previous research regarding bond acceptance tests for prestressing strand and the bond of prestressing strand in SCC are discussed.

2.2. EXPLANATION OF TRANSFER LENGTH, FLEXURAL BOND LENGTH, AND DEVELOPMENT LENGTH

Transfer length, l_t, is defined as the length from the free end of the member to the point along the length of the beam where the effective prestress in the strand is fully transferred to the concrete. The stress in the strand along the length of the transfer length is assumed to vary linearly from zero at the free end to f_{pe}, the effective prestress after losses, at the end of the transfer length.

Flexural bond length, l_{fb}, is defined as the length of fully bonded strand beyond the transfer length that is required to fully develop the stress in the strand to f_{ps}, the ultimate stress at nominal flexural capacity, when load is applied to the member.

Development length, l_d, is the sum of the transfer length and flexural bond length. The transfer length, flexural bond length, and development length are illustrated in Figure 2.1.

Additionally, the term embedment length, l_e, is discussed frequently in this thesis. Embedment length is the distance from the free end of the beam to the point along the strand where the cross-section of the member is being assessed for strength. This is often the closest point from the end of the strand to where the critical cross-section is, or where the maximum moment is in the member, and the point where the strand would need to be fully developed to maximum nominal flexural resistance. To investigate development length, a beam is typically loaded with a point load, and the embedment length is the

distance from the free end of the beam to the point load. If the beam fails in flexure, the strand is fully developed and the embedment length is greater than the development length, but if the beam fails in bond, the embedment length is shorter than what is needed to fully develop the strand.

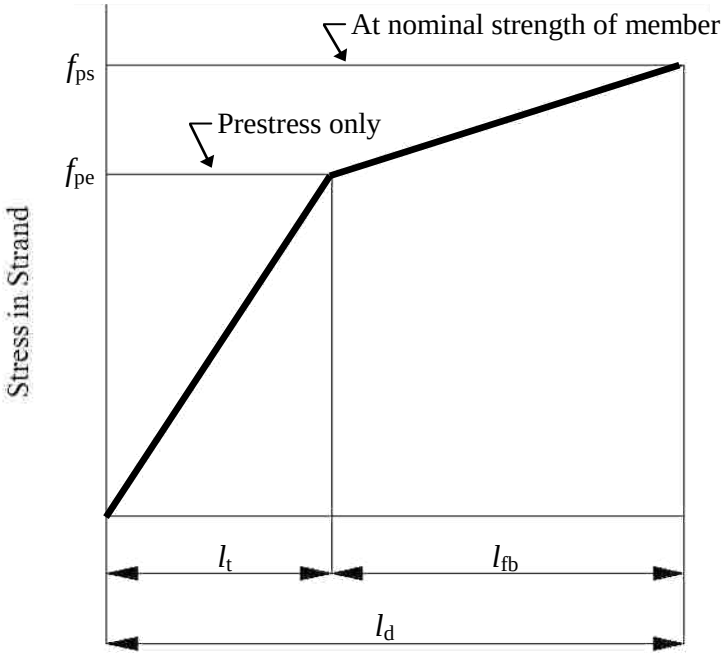

Figure 2.1 – Variation of Stress in a Strand Along the Length of a Beam (Adapted from ACI 318-11)

2.3. BOND THEORY

Combinations of several factors have been shown to contribute to bond of prestressing strand to concrete. Depending on the circumstances, adhesion, Hoyer effect, and mechanical interlocking can act singly or in combinations to resist slippage of the strand in concrete (Russell and Burns 1993). Research completed by Janney (1953) regarding bond of plain wires and strand in concrete led him to conclude that friction is a

major contributor to bond. While friction is not individually discussed in this section, friction plays a large role in both the Hoyer effect and mechanical interlocking.

2.3.1. Adhesion. Adhesion is the thin layer of glue that chemically forms between the strand and the concrete. As soon as the strand slips, adhesion is lost, and the bond stress that had been contributed by adhesion goes to zero and is transferred to other bond mechanisms. Since the transfer zone is characterized by the strand moving relative to the concrete, adhesion does not contribute to the bond in the transfer zone (Russell and Burns 1993).

2.3.2. Hoyer Effect. In the transfer zone, a major contributor to bond is a factor known as the Hoyer effect. As a strand is stressed, the strand becomes longer, but also thinner due to Poisson's effect. When the strand is cut, the release of the stress causes the wires in the strand to expand back to their original forms, but this expansion is resisted by the concrete. As a result, wedging action occurs between the strand and concrete as the strand produces a normal force on the concrete from radial expansion, and the resulting friction resists the movement of the strand into the concrete (Figure 2.2).

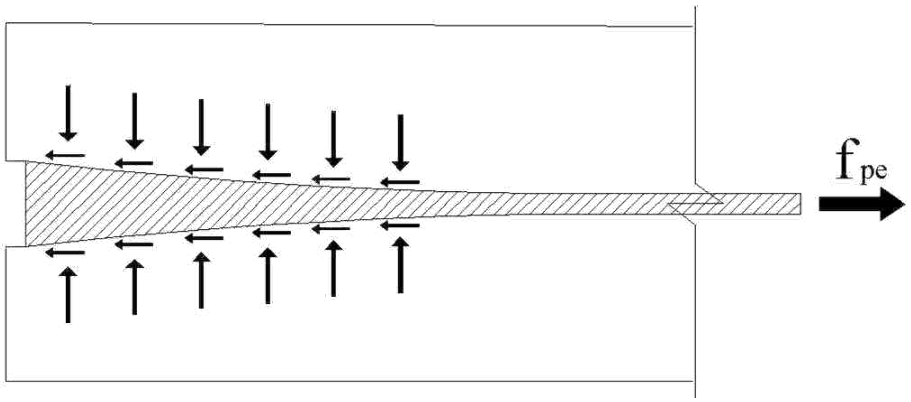

Figure 2.2 – Hoyer Effect (Adapted from Russell and Burns 1993)

The Hoyer effect is only applicable in the transfer zones because the radial expansion only occurs at the ends where the strand slips relative to the concrete. Once an outside load is applied, as the wave of stress that starts at the maximum moment zone gets pushed into the transfer zone, the stress in the strand increases and the strand

becomes thinner again. The frictional forces from Hoyer effect decrease and mechanical interlock is then the only force resisting bond.

2.3.3. Mechanical Interlock. When concrete is cast around prestressing strand, the concrete molds around the strand and between the grooves of the wires. When the strand tries to move through the concrete and untwist due to release of stress, the concrete ridges formed between the wires resist the movement. This effect is known as mechanical interlock. While some of this friction helps bond the strand in the transfer zone, mechanical interlock is the main form of resistance in flexural bond (Russell and Burns 1993).

2.4. FACTORS AFFECTING TRANSFER AND DEVELOPMENT LENGTHS

Over the years, many studies have been completed regarding transfer length and development length of prestressing strands, and although the current equations are functions of only stress in the strand after losses and at ultimate as well as nominal strand diameter, many other factors have also been proven to affect bond. Zia and Mostafa (1977) conducted an extensive literature review on previous testing regarding development length and attempted to pinpoint the many factors that affect bond. Based on their findings, some of the factors that have been found to influence transfer length and development length include:

1. Strand size (diameter)
2. Strand stress level
3. Concrete strength
4. Time dependent effects (losses)
5. Type of release (gradual or sudden)
6. Consolidation and consistency of concrete around strand
7. Surface condition of strand (clean, rusted, epoxy-coated)
8. Confinement
9. Cover and spacing
10. Type of strand (stress relieved, low relaxation)
11. Type of loading (static, repeated, impact)

The effects of the first six factors are briefly discussed below.

2.4.1. Strand Size. It is commonly accepted that an increase in strand diameter results in an increase in transfer and development lengths. Kaar, LaFraugh, and Mass (1963) were some of the first researchers to document this aspect. Based on transfer length testing of 0.25-in., 0.375-in., 0.5-in., and 0.6-in.-diameter (6.35 mm, 9.53 mm, 12.7 mm, and 15.2 mm) strands, it was noted that larger diameter strands yielded longer transfer lengths, and the relationship between strand diameter and transfer length at release was approximately linear (Kaar, et al. 1963). Based on this research, the direct relationship between strand diameter and transfer length was adopted into current code equations for transfer length and development length.

2.4.2. Steel Stress Level. With an increase of initial stress in the strand, the surface area that is required to transfer the stress to the concrete also increases, resulting in longer transfer lengths. The current equations for transfer and development lengths are based on f_{se}, or effective stress after all losses. While this is reasonable for flexural bond length, it has been noted that the use of f_{se} does not necessarily seem applicable to transfer length at release, and that f_{si}, or the stress in the strand immediately after release instead of after all losses, should instead be applied to the calculation of transfer length (Buckner 1995). This approach would result in longer, more conservative transfer length calculations. As discussed, the equation for transfer length was developed based on research performed in the 1950's and 60's using Grade 250 strands which were also stressed to lower levels than what is commonly used today theoretically rendering the equation unconservative for today's use. Some researchers have proposed equations for transfer length expressed as a function of f_{si} instead of f_{se} (Zia and Mostafa 1977, Buckner 1995), but research has not consistently shown that the current equation is, in fact, unconservative, so no changes have yet been made to the current AASHTO and ACI equations.

2.4.3. Concrete Strength. Although the study performed by Kaar, LaFraugh, and Mass in 1963 indicated that concrete strength had little effect on transfer length, many studies since have proven the correlation between high concrete strengths and decreased transfer lengths. The bond over the transfer length is primarily due to friction between the strand and the concrete caused by radial expansion of the strand at release that occurs due

to Poisson's effect. According to Barnes et al. (2003), this friction depends on how well the concrete surrounding the strand reacts to the pressure caused by the increasing circumference. The release results in radial cracking in the concrete surrounding the strand, which softens the concrete. Therefore, a higher tensile strength and stiffness means the concrete can respond better to the radial expansion, resulting in better friction and shorter transfer lengths. Since the ACI 318-11 Sections 8.5.1 and 9.5.3.2 show that modulus of elasticity and modulus of rupture are directly related to the square root of concrete strength, it follows that transfer length should also be related to the square root of concrete strength at release (Barnes et al. 2003).

While Kaar, LaFraugh, and Mass only studied concrete release strengths up to 5,000 psi (34.5 MPa), today's release strengths can range to over 10,000 psi (68.9 MPa). Many researchers, including Mitchell et al. (1993), Lane (1998), and Ramirez and Russell (2008), have since published studies relating increased concrete strengths to decreased transfer lengths. The studies have also resulted in a number of proposed, revised equations for transfer length and development length (Zia and Mostafa 1977, Mitchell et al. 1993, Lane 1998, Ramirez and Russell 2008), almost all of which relate transfer length to the square root of concrete compressive strength. However, much debate still exists over the exact effect of concrete strength on transfer and development lengths, and since the current equation is considered conservative for high concrete strengths, there is no immediate rush to update the equation.

2.4.4. Time Dependent Losses. Research has shown that transfer lengths tend to increase over time. Barnes et al. (2003) suggested although stress in the strand decreases over time due to losses, transfer lengths still do not decrease over time because of the inelasticity of the concrete immediately surrounding the strand. The increases in transfer lengths are most likely due to propagation of the radial cracking and the resulting softening of the concrete grip (Barnes et al. 2003). Transfer lengths measured by Kaar, LaFraugh, and Mass showed average increase in transfer lengths of 6% over one year, with the maximum increase being 19% (1963). In FHWA research, transfer lengths of 32 AASHTO Type II beams increased 30% in 28 days and then an additional 7% between 28 and 185 days (Lane 1998). Research by Barnes et al. (2003) showed 28 day average transfer lengths increases of 10-20%, with some individual increases as high as 50%.

Also, Boehm et al. (2010) reported 0.5-in.-diameter (12.7 mm) strands in conventional concrete had a 38% increase in transfer length over three months.

2.4.5. Type of Release. Sudden release methods, such as flame cutting, have been proven to result in longer transfer lengths than more gradual release methods, such as detensioning. In their review of data from previous studies for the establishment of a new development length equation, Zia and Mostafa separately plotted transfer lengths vs. the ratio of the initial stress in the strand at release to concrete strength at release (f_{si}/f'_{ci}) for ends exposed to sudden release and ends exposed to gradual release and found that for a given f_{si}/f'_{ci} value, the transfer lengths from sudden release were longer than transfer lengths from gradual release (1977).

Similarly, transfer lengths have also been shown to be longer at live ends, or locations where the strand is first cut to relieve tension, as opposed to dead ends, or ends not directly adjacent to the first release point in the strand. Kaar, LaFraugh, and Mass found that for strands up to 0.5-in. (12.7 mm) in diameter, live end transfer lengths averaged 20% longer than dead end transfer lengths, while 0.6-in.-diameter (15.2 mm) strands showed a 30% increase from dead to live ends (1963). For uncoated strands, Cousins et al. (1990) found that transfer lengths at live ends for 0.5-in. and 0.6-in.-diameter (12.7 mm and 15.2 mm) strands averaged 8% higher than dead ends, while 0.375-in.-diameter (9.53 mm) strands actually had live end transfer lengths 6% shorter than the dead ends. Additionally, Russell and Burns (1997) reported live end transfer lengths to be 34% longer than dead end transfer lengths.

2.4.6. Consolidation and Consistency of Concrete around Strand. As the use of new types of concrete, such as SCC, becomes more prevalent, the properties of the concrete surrounding the strand is becoming an increasingly important topic. Since SCC is not mechanically vibrated, it is still being debated whether the flowable nature of SCC results in adequate consolidation around the strand, or if it could actually improve the condition of consolidation around the strand compared to vibrated conventional concrete (Larson et al. 2007). Several studies reporting conflicting results on the effect of SCC on bond of prestressing strand are discussed in Section 2.7 of this thesis.

Related to the aspect of condition of concrete surrounding the strand is the subject of strand locations in members. ACI-318-11 and the AASHTO LRFD-07 code account

for the "top bar effect" for mild deformed reinforcing bars, which implies that bars located in the top of a member during casting have longer development lengths than bars located at the bottom. This phenomenon has been attributed to various reasons, including bleed water and air getting trapped on the bottom surfaces of the top bars (Peterman 2007) and the idea that concrete-bar friction results mainly from concrete consolidated above bars than immediately below (Wan et al. 2002). In a research study by Petrou and Joiner (2000), end slips of strands in prestressed piles from five plants were analyzed, and top strands were found to have end slips an average of 2.3 times longer than bottom strands, with some instances showing end slips of top strands up to 4-5 times longer. In a subsequent research program, Wan measured end slips of strands in 32 18-in.-square (457 mm) concrete piles and noted that top-cast strands had average end slips of 0.140 in. (3.56 mm), while bottom-cast strands had end slips of only 0.058 in. (1.47 mm) (2002). However, ACI and AASHTO currently have no provision for increasing development lengths of prestressing strands located in the top of a member. A 1.3 multiplier was suggested by Buckner (1995) and Lane (1998) and incorporated to Section 5.11.4.2 of the AASHTO code shortly after, but the provision has since been removed (Peterman 2007).

2.5. ACI AND AASHTO CODE EQUATIONS

The *AASHTO LRFD Bridge Design Specifications* (2007), which shall hereby be referred to as the AASHTO code, is the governing document for the design of prestressed bridge girders used by the Missouri Department of Transportation, so the AASHTO equations for transfer length and development length were used as the basis for the analyses in this program. Additionally, results were compared to values determined by equations in ACI's *Building Code Requirements for Structural Concrete*, or ACI 318-11. This subsection identifies the relevant code equations and discusses the backgrounds behind the equations.

2.5.1. AASHTO LRFD Bridge Design Specifications. The guidelines for the development of prestressing strand can be found in Section 5.11.4 of the AASHTO code. Although there is no specific equation for transfer length in the AASHTO code, Section 5.11.4.1 states that "the transfer length may be taken as 60 strand diameters." Therefore,

the AASHTO equation for transfer length in inches, l_t, can be represented by Eq. 2.1, where d_b is the nominal diameter of the strand in inches.

$$l_t = 60 d_b \quad \textbf{(2.1)}$$

In terms of development length, Section 5.11.4.2 of AASHTO then defines the minimum development length in Eq. 5.11.4.2-1, which is shown here as Eq. 2.2, where l_d is the development length in inches, κ is a multiplier of 1.0 for members with depth less than or equal to 24 in. (610 mm) and 1.6 for members deeper than 24 in. (610 mm), f_{ps} is the average stress in the prestressing steel at the time for which the nominal resistance of the member is required in ksi, f_{pe} is the effective stress in the prestressing steel after losses in ksi, and d_b is the nominal strand diameter in inches.

$$l_d = \kappa \left(f_{ps} - \frac{2}{3} f_{pe} \right) d_b \quad \textbf{(2.2)}$$

The 1.6 multiplier for deep members is based on research performed by Shahawy (2001), which indicated a relationship between shear and bond. Three-point load tests were performed on 83 prestressed pile specimens with six different cross-sections and 12 AASHTO Type II girders at varying embedment lengths and shear spans, and the slippage of strands, applied moments, and final failure modes were noted. These tests indicated that members with depths greater than 24 in. (610 mm) needed development lengths up to 50% longer than those predicted by the original AASHTO equation, or Eq. 2.2 without the κ factor. Shahawy came to the conclusion that for deep members, the shear-flexural interaction has a significant effect on development length, and he proposed a new development length equation with factors to take into account the effect of shear on strand slippage before failure. AASHTO did not adopt the proposed equation, but based on the research, added a 1.6 multiplier for members with a depth greater than 24 in. (610 mm) to the development length equation, which when applied to Shahawy's research results, proved to give mostly conservative results.

The AASHTO equation for and provisions regarding development length has undergone many revisions and will likely continue to be adjusted. In 1988, the FHWA administered a memorandum that imposed a 1.6 multiplier on the AASHTO development length equation, increased strand spacing requirements, and banned the use of 0.6-in.-diameter (15.2 mm) strand (Lane 1998). This memorandum, and specifically the clause regarding the 1.6 multiplier, was issued mostly in response to research completed in the mid 1980's by Cousins, Johnston, and Zia, which indicated development lengths much longer than those predicted by the AASHTO equation (Lane 1998). The research covered transfer and development length of epoxy coated and uncoated strands and tested square and rectangular members with one strand, but the research program is mainly known for showing the measured transfer and development length results of the uncoated strands to be 48-67% longer, depending on the strand size, than the lengths predicted by the AASHTO and ACI equations (Cousins et al. 1990).

Based on the alarming results, FHWA initiated a test program focusing on development length, and more research has since shown that the ban on 0.6-in.-diameter (15.2 mm) strand and limits on spacing requirements could be repealed, and the restrictions were lifted in 1996 (Lane 1998). Shortly after, the 1.6 safety factor was proven over-conservative in most cases, and that safety factor was lifted as well. However, as discussed, now the 1.6 multiplier is applied in certain cases to account for shear effects on bond of strand in deep members. Also, based on the surge in development length research spawned by the FHWA memorandums, many new development length equations have been proposed (Zia and Mostafa 1977, Mitchell 1993, Buckner 1995, Lane 1998, Ramirez and Russell 2008), a number of which take into account the effect of concrete strength, which has proven to affect bond. However, much debate still exists, and none of these equations have yet been adopted.

2.5.2. ACI 318-11. In the ACI 318-11 code, the provisions for the development of prestressing strand are presented in Section 12.9. The equation for development length is shown in the ACI 318-11 code as Eq. 12-4, and consists of two terms, where the first term is equal to the transfer length and the second term represents the flexural development length, as noted by the commentary in R12-9. The ACI 318-11 equations for transfer and development length are shown here as Eqs. 2.3 and 2.4,

respectively, where l_t is the transfer length in inches, l_d is the development length in inches, f_{se} is the effective stress in the prestressing steel after losses in psi, f_{ps} is the stress in the prestressing steel at the nominal flexural strength in psi, and d_b is the nominal diameter of the strand in inches.

$$l_t = \left(\frac{f_{se}}{3000}\right) d_b \quad \textbf{(2.3)}$$

$$l_d = \left(\frac{f_{se}}{3000}\right) d_b + \left(\frac{f_{ps} - f_{se}}{1000}\right) d_b \quad \textbf{(2.4)}$$

It should be noted that the ACI equation for development length (Eq. 2.4) is equal to the AASHTO equation for development length (Eq. 2.2) when the depth of the member is less than or equal to 24 in. (610 mm).

ACI 318-11 also provides an additional equation for transfer length for the shear design of prestressed members. In Section 11.3.4, ACI 318-11 requires that shear designs of prestressed members be based on a reduced stress in the strand for sections of a member that are closer to the support than the transfer length. For this design, the transfer length is to be taken as 50 times the nominal diameter of the strand. This additional ACI transfer length equation is presented here as Eq. 2.5, where l_t is the transfer length in inches and d_b is the nominal diameter of the strand in inches.

$$l_t = 50 d_b \quad \textbf{(2.5)}$$

2.5.3. Background of the AASHTO and ACI Development Length Equations. As discussed, although the AASHTO and ACI equations for development length (Eq. 2.2 and Eq. 2.4, respectively) are formatted differently, they are essentially the same equation (when $\kappa = 1.0$ for Eq. 2.2). The equation was first incorporated into ACI-318 in 1963, and AASHTO also adopted it 10 years later. According to an extensive study conducted by Tabatabai and Dickson (1993) on the origins of the equation, the basis of the equation stems from research conducted by Hanson and Kaar and Kaar, LaFraugh, and Mass for the Portland Cement Association (PCA) in the 1950's and 1960's. The studies were

conducted with 250 ksi (1.72 GPa), stress relieved strands, which were stressed to 60%-70% of capacity and cast in concrete strengths up to 5,500 psi (34.5 MPa). Majority of today's prestressed members are constructed with 270 ksi (1.86 GPa), low relaxation strands that are often subjected to higher initial stresses and cast in concrete with higher strengths. These differences between practices today vs. practices decades ago could be cause for concern as to whether the design equations derived on outdated construction methods can still adequately apply to members today.

Hanson and Kaar tested 0.25-in., 0.375-in., and 0.5-in.-diameter (6.4 mm, 9.5 mm, and 12.7 mm) Grade 250 prestressing strands in members at varying embedment lengths. Although Hanson and Kaar recommended minimum embedment lengths based on their research, the current transfer length and development length equations were actually developed by Alan H. Mattock. The values calculated from Mattock's equations, which are based on Hanson and Kaar's data and findings, are actually less conservative than Hanson and Kaar's recommendations (Tabatabai and Dickson 1993).

Based on the assumption that the force in the steel must equal the transfer bond force, Mattock used Eq. 2.6 to solve for transfer length in inches, L_t, where U_t is the average bond stress in ksi, Σ_0 is the circumference of the prestressing strand in inches, A_{ps} is the area of prestressing strand in ksi, and f_{se} is the effective stress in the strand after losses in ksi.

$$U_t \Sigma_0 L_t = A_{ps} f_{se} \tag{2.6}$$

U_t was assumed to be 0.4 ksi (2.76 MPa) based on the data from Hanson and Kaar, and Σ_0 and A_{ps} were taken to be $4/3\pi D$ and $0.725\pi D^2/4$, respectively, where D is the nominal diameter of the strand in inches, to account for the actual circumference and area of the prestressing strand. Substituting these values into Eq. 2.6 yielded Eq. 2.7, which is equal to the current transfer length equation specified by ACI.

$$L_t \approx \frac{f_{se} D}{3} \tag{2.7}$$

It should be noted that the basis for the transfer length equation is an average of the results from Hanson and Kaar, and is not meant to be conservative. The same is true of the equation derived for flexural development length. When evaluating flexural bond length, for each specimen, Mattock plotted the increase in steel stress from the effective prestress at the point of general bond slip ($f_{sb} - f_{se}$) and the increase in steel stress from the effective prestress at ultimate failure ($f_{su} - f_{se}$) vs. the embedment length minus the transfer length divided by the nominal diameter, as seen in Figure 2.3. The trend line is presented in Eq. 2.8, and as shown in Figure 2.3, in many cases the line runs above the point of general bond slip but below ultimate failure. According to Mattock, the line is "a reasonable mean line for general bond slip" (Tabatabai and Dickson 1993).

$$f_{su}^{*} - f_{se} = 0.9\left(\frac{L - L_t}{\mathrm{D}}\right) \qquad \textbf{(2.8)}$$

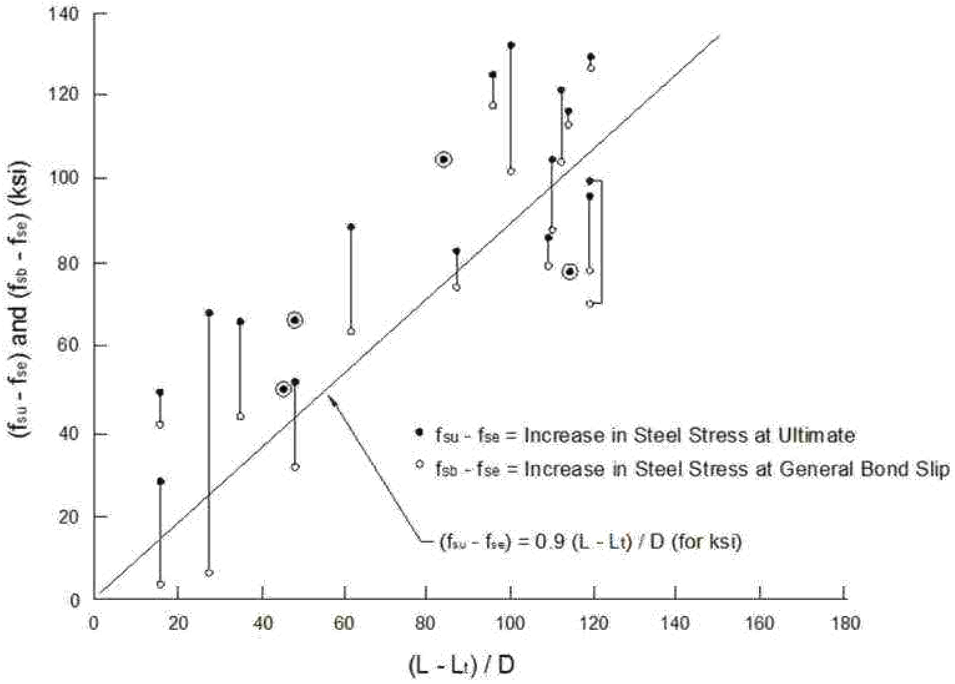

Conversion: 1 ksi = 6.89 MPa
1 in. = 25.4 mm

Figure 2.3 – Original Representation of Flexural Bond Length (adapted from Tabatabai and Dickson, 1993)

Eq. 2.8 was later revised to Eq. 2.9, and substituting in $L_t/D = f_{se}/3$ from Eq. 2.7 and rearranging the equation yields Eq. 2.10. Eq. 2.10 is equivalent to Eq. 2.2, or the current AASHTO development length equation without the κ factor, and functionally equivalent to the ACI development length equation in Eq. 2.4 as well.

$$f_{su}^{*} - f_{se} = \frac{L - L_t}{\mathrm{D}} \tag{2.9}$$

$$L = \left(f_{su}^{*} - \frac{2}{3} f_{se}\right) \mathrm{D} \tag{2.10}$$

In conclusion, the current transfer length and development equations are based on research completed almost 60 years ago involving 250 ksi (1.72 GPa), stress-relieved strands stressed to 60%-70% capacity in lower strength concretes, while today's practices commonly use 270 ksi (1.86 GPa), low-relaxation strands stressed to 75% capacity in higher strength concretes. Additionally, the equations were not developed to be conservative, but rather, they were derived based on averages. Many researchers wonder how applicable these equations are to today's prestressed concrete, and although many new transfer length and development length equations based on recent research have been proposed in the past two decades to update the equations and include the effect of concrete strength, a revised equation has yet to be agreed upon.

2.6. RESEARCH REGARDING ACCEPTANCE OF A STANDARD BOND TEST

Since the mid 1990's, several test programs have been completed in order to investigate the potential of different bond tests to produce consistent results from test to test and site to site. The ultimate goal of the research programs has been to develop a standardized test that would be able to pre-qualify strand in terms of having acceptable bond performance.

2.6.1. Logan (1997). The main purpose of Logan's test program was to see if bond quality of strand could be assessed through simple untensioned pullout tests by correlating the pullout values to results from end slip monitoring and flexural testing on prestressed beams. In order to obtain a wide representation of the prestressing strand used

in the western hemisphere, Logan collected samples of strand from six sources from across the country.

First, pullout tests based on the method developed by Saad Moustafa in 1974 were run on each strand source. Six strands from each source were cast vertically with an 18 in. (457 mm) embedment length in a block of standard structural concrete. The blocks were cured overnight, and then a jack was used to pull out each strand until the peak load could no longer be sustained. Four of the six samples had average maximum pullout loads ranging from 36.8 kips to 41.6 kips (164 kN to 185 kN), while the other two sources had average values of 11.2 (49.8 kN) and 10.7 kips (47.6 kN). When these results were compared to the performance of the strands in the end slip and flexural testing of the beams, the beams with the four strands with high pullout values had transfer and development lengths less than predicted by ACI 318-95, while the beams with the strands with low pullout capacities failed in bond, meaning the transfer length and development lengths predicted by ACI 318-95 were unconservative for those strands. Based on these results, Logan proposed lowering the minimum pullout value from 38.2 kips (170 kN), as determined by Moustafa, to 36 kips (160 kN) because the strands with pullout values of 37.7 kips (168 kN) and 36.8 kips (164 kN) performed well in the beam testing. Logan suggested that this minimum pullout limit could be even further reduced, but further testing would have to be done on strands with pullout capacities between 11.2 kips (49.8 kN) and 36.8 kips (164 kN).

In order to test the transfer length and development length of the strands, 17-ft.-long (5.18 m) beams with 6.5 in. x 12 in. (165 mm x 305 mm) cross-sections and one strand located at 2 in. (50.8 mm) from the bottom were constructed. The end slips of the strands into the concrete at release were measured, and then the end slip values were used in conjunction with Mast's strand slip theory to calculate transfer lengths. The calculated transfer lengths were then compared to transfer lengths calculated by the equation in ACI 318-95. Each end of the beam was then tested in flexure at a different embedment length, and it was noted whether each test resulted in either a flexural or bond failure. By comparing the transfer lengths calculated by end slip to the calculated and actual moment capacities, it was found that Mast's strand slip theory accurately predicted which beams failed in bond and which failed in flexure.

Logan also investigated whether factors such as color, noticeable residue, rust, and pitch of the outer strands could be used to predict bond quality. Before each of the pullout tests, Logan noted the color and rust of the strands, wiped a clean towel over each strand to visually quantify the amount of residue on each, and measured the pitch of the outside wires, or the distance for one wire to make a complete revolution around the strand. Overall, Logan found no strong correlation between any of the factors and the pullout capacities of the strands, so it was concluded that neither color, residue, rust, nor pitch can be considered a reliable predictor of bond.

2.6.2. Rose and Russell (1997). The research program was designed to evaluate the effectiveness of three test methods that could be used to assess the bond of prestressing strand. Data from simple untensioned direct tension pullout tests, pretensioned direct pullout tests, and measured end slips and transfer lengths on beams were used to determine the relative bond performance of Grade 270 0.5-in.-diameter (12.7 mm) strands from different manufacturers and having different surface conditions of as-received, cleaned, silane treated, and weathered. The ultimate goal was to see if one test could be considered superior.

The simple untensioned pullout tests were based on Logan's method (1997) and consisted of strands cast vertically with 18 in. (457 mm) of embedment length in 2 ft. x 3 ft. x 4 ft. (610 mm x 914 mm x 1,219 mm) blocks of concrete. The tensioned pullout tests had 5.5 in. (127 mm) square cross-sections and were 12 in. (305 mm) in length with 12 in. (305 mm) embedment. It was thought that the tensioned pullout tests would more closely represent the bond in prestressed members because these tests would include the Hoyer effect resulting from the release of tension. The beams used for end slip and transfer length measurements had 6 in. x 12 in. (152 mm x 305 mm) cross-sections and were 17 ft. (5.18 m) in length, except for the beams with the silane-treated strand, which were 24 ft. (7.32 m) long. Each beam contained two strands, and the beams were instrumented so that strain readings could be taken with a detachable mechanical strain gage (DEMEC gage). The 95% Average Mean Strain Method was then used to analyze the transfer lengths.

Ultimately, it was concluded that the end slip measurements consistently gave the most accurate assessment of bond. The greater the end slip, the longer the transfer length,

and the typical equation was found to be adequate. In terms of the pullout tests, the simple untensioned test was found to be better than the tensioned pullout test, but no strong correlation existed between the simple pullout results and the transfer lengths. The tensioned pullout test was found to be difficult to set up and run and also yielded inconsistent results. Except for the silane treated strand, the simple tension test showed that the lower the maximum pullout value, the higher the transfer length. The silane-treated strand showed adequate bond performance in the simple pullout test, but had the largest measured transfer lengths. Therefore, it was concluded that simple untensioned pullout test mirroring Logan's method is still not an overly reliable predictor of bond.

2.6.3. NASP Bond Testing Rounds I-IV. In the late 1990's, the North American Strand Producers (NASP) funded a research project to compare tests designed to assess strand bond and ultimately determine a test suitable for strand bond acceptance. This project consisted of several rounds of testing and was based out of the University of Oklahoma (OU).

The first round of testing compared the Moustafa test, the PTI bond test, and the friction bond test (Russell and Paulsgrove 1999a). From the results, it was determined the friction bond test gave inconclusive and inconsistent results, so in Rounds II and III, researchers continued to investigate the Moustafa Test and the PTI test, but in these rounds, the friction bond test was discarded and the NASP bond test was added. The NASP bond test was similar to the PTI test, but a mortar with Type III cement, sand, and water was used in place of the grout of Type I cement and water that was specified by the PTI test. The addition of sand made the mix stiffer and minimized shrinkage (Russell and Paulsgrove 1999b).

In Round II, in order to determine the repeatability and reproducibility of the three tests, several series of the three tests were completed at different locations. The Moustafa test was run at Stresscon in Colorado, the Florida Wire and Cable Company (FWC), and OU, while the PTI and NASP tests were only completed at FWC and OU.

One conclusion that was reached from the Round II of testing was that results indicated that the Moustafa test was a good predictor of relative bond but was not a good absolute predictor of bond; the rank of strands was always the same at each site, but the specific pullout values did not correlate well between sites. This conclusion was further

confirmed in Round III of testing. In terms of the NASP bond test vs. the PTI test, the NASP test showed slightly more consistent results. For both tests, it was noted that the pullout values had the least variation at a slip of 0.1 in. (2.54 mm). For this slip value, plotting results comparing NASP test series from OU and FWC resulted in coefficients of determination (R^2 values) of 0.97 and 0.98, indicating a strong correlation of test results between tests at the same site as well as between sites, as seen in Table 2.1. These coefficients of determination were significantly higher than R^2 values derived from comparing results from different sites for either the Moustafa or PTI test (Table 2.1). Therefore, a main conclusion from this round of testing was that the NASP bond test was standing out as the most replicable of the three (Russell and Paulsgrove 1999b).

Table 2.1 – NASP Round II R2 Values Comparing Moustafa, PTI, and NASP Pullout Results Between Sites (Russell and Paulsgrove 1999b)

Data Comparison	Moustafa	PTI Pull-Out			NASP Pull-Out		
	Maximum Strand Force	Maximum Strand Force	Force at 0.10 in. SLIP	Force at 0.01 in. SLIP	Maximum Strand Force	Force at 0.10 in. SLIP	Force at 0.01 in. SLIP
	r^2	r^2	r^2	r^2	r^2	r^2	r^2
Series 1 vs. Series 1							
OU vs. FWC	0.88	0.87	0.90	0.73	0.97	0.98	0.90
OU vs. STRESSCON	0.92						
STRESSCON vs. FWC	0.94						
OU Series 1 vs. OU Series 2					0.97	0.97	0.71
OU Series 1 vs. FWC Series 2					0.87	0.97	0.72
r^2 (coefficient of determination) regression about "best fit" line							

Round III of the testing included flexural beam specimens, and one of the main goals was to see if transfer lengths and development lengths could be correlated to pullout values from the three tests to determine if absolute limits of pullout values could be set for any of the tests. Single strand beams and double strand beams were constructed at OU and FWC with strand from four different sources. Transfer lengths were computed

by measuring the strand draw-in at release and at 28 days. Table 2.2 shows the R^2 values correlating 28 day transfer length to pullout values for the three tests. The Moustafa test had generally low correlations across the board, while the PTI test had low correlations at one site but high correlations at the other. The NASP test had consistently reasonable correlations at both sites for both beam types. Comparing the pullout values to 28 day transfer lengths further strengthened the argument for focusing further research on developing the NASP bond test (Hawkins and Ramirez 2010).

Table 2.2 – Round III Coefficient of Variation (R^2) Values Relating 28 Day Transfer Lengths to Bond Test Pullout Values (adapted from Hawkins and Ramirez 2010)

Test	OU		FWC	
	Single Strand Transfer Lengths	Double Strand Transfer Lengths	Single Strand Transfer Lengths	Double Strand Transfer Lengths
Moustafa Pullout Values	0.50	0.50	0.73	0.87
PTI Pullout Values	0.52	0.29	0.95	0.84
NASP Pullout Values	0.83	0.73	0.98	0.76

In order to evaluate development length, each end of each beam was tested in four-point loading at an embedment length of either 73 in. (1,854 mm) or 58 in. (1,473 mm) and the mode of failure was noted. The results are summarized in Table 2.3 for the single strand beams and Table 2.4 for the double strand beams. N corresponds to tests completed at 73 in. (1,854 mm) embedment, and S represents tests completed at 58 in. (1,473 mm) embedment. Bond failures indicated that the embedment length was not sufficient to develop sufficient stress in the strand, and the results from the development length testing were used to help set 10,500 lb. (46.7 kN) average pullout value and 9,000 lb. (40.0 kN) individual pullout value minimum limits for bond acceptance for the NASP test (Hawkins and Ramirez 2010).

Table 2.3 – Round III NASP Pullout Values and Failure Modes from Flexural Testing of Single Strand Beams (Hawkins and Ramirez 2010)

Single Strand Beams: NASP P.O. Values vs. Failure Mode							
Strand	Lt @ 28 Days (in.)	NASP P.O. Value (lbs.)		Failure Mode			
		Average	Low	1N	2N	1S	2S
AA	16.2	14950	11500	F	F	F	F
FF	31.2	7300	5500	F	F	V	B
HH	30.2	10700	8900	F	F	F	B
II	39.2	4140	2620	F	B	B	B

- F = Flexural Failure
- V = Shear Failure
- B = Bond Failure

Table 2.4 – Round III NASP Pullout Values and Failure Modes from Flexural Testing of Double Strand Beams (Hawkins and Ramirez 2010)

Double Strand Beams: NASP P.O. Values vs. Failure Mode							
Strand	Lt @ 28 Days (in.)	NASP P.O. Value (lbs.)		Failure Mode			
		Average	Low	1N	2N	1S	2S
AA	17.4	14950	11500	F	F	F	F
FF	24.2	7300	5500	F	F	F	F
HH	26.3	10700	8900	F	F	F	F
II	42.7	4140	2620	F	B	B	B

- F = Flexural Failure
- V = Shear Failure
- B = Bond Failure

From Rounds II and III of testing, it was determined that the NASP test showed the most promise for becoming a test that could accurately and consistently assess strand bond. Therefore, Round IV of testing focused on taking steps to standardize the NASP bond test. First, a parametric study was run at OU to study the effects of mortar strength, mortar flow, temperature and curing conditions, load vs. displacement control, and loading rate on the NASP test results. From this study, current limits for each variable as seen in the proposed standard were determined. After the testing at OU established the

more specific standard limits and procedures, round robin testing was completed on several strand samples at OU, Purdue University, and University of Arkansas to see how well the test would replicate between sites using various cement and sand sources. Plotting the NASP results from Purdue and University of Arkansas to results from OU resulted in R^2 values of 0.92 and 0.89, respectively, and trends from both comparisons were very close to the "perfect fit" line, or the same pullout load from both sites. From these observations, it was concluded that the NASP test is reproducible and can be replicated from site to site with acceptably consistent results (Russell 2006).

2.6.4. Ramirez and Russell (2008). As part of testing done for the National Cooperative Highway Research Program (NCHRP) Report 603, Ramirez and Russell investigated bond and corresponding transfer and development lengths of 0.5-in. and 0.6-in.-diameter (12.7mm and 15.2mm) prestressing strand in high strength concretes**.** Due to the recent increase in use of high strength concrete, the main purpose of this program was to investigate the effect of concrete strength on bond of prestressing strands and propose revised transfer and development length equations to AASHTO.

Eight I-shaped beams and 43 rectangular beams were constructed using four strand sources and concretes with one day target strengths ranging from 4 to 10 ksi (27.5 to 68.9 MPa) to monitor transfer lengths through DEMEC readings and end slips and to evaluate development lengths through four-point flexural testing at varying embedment lengths. Another goal of the research program was to refine and standardize the NASP test, and Rounds III and IV of NASP round-robin testing were completed as a part of this test program. Additionally, a modified NASP test in concrete was also implemented to determine how concrete strength directly affects bond.

From their research, Ramirez and Russell concluded that increasing concrete strength results in improved bond performance. Pullout values for the modified NASP in concrete test increased as concrete strength increased, and members with high concrete strength displayed shorter transfer lengths. In terms of bond, the results from this program showed the NASP test in mortar to be a good indicator of bond performance. The pullout results from the standard NASP test in mortar correlated well with transfer and development length results; strands with high NASP pullout values consistently had shorter transfer and development lengths.

Ultimately, based on their results, the research team made recommendations to AASHTO for updates to the bond, transfer, and development provisions in the code. First, the report proposed new transfer and development length equations, which take into account the effect of concrete strength. Additionally, the researchers recommended that the NASP test be accepted as the Standard Test for Strand Bond and implemented to control bond quality of strands. However, to date, no official revisions have yet been made to the AASHTO code.

2.6.5. Current Status and Recent Developments. Currently, Logan's modified Moustafa test, now known as the Large Block Pullout Test (LBPT), is required to be conducted in PCI member plants to assure the bond quality of strand (Precast/Prestressed Concrete Institute 2003). However, as the current research has shown, LBPT results are difficult to reproduce from site to site, and the NASP test is proving to be more reliable than the LBPT. Although the NASP test shows promise for becoming the "Standard Test Method to Assess the Bond of 0.5-in. (12.7 mm) and 0.6-in. (15.2 mm) Seven Wire Strand with Cementitious Material," a due diligence report conducted on the four rounds of testing came to several conclusions that show more testing is required before the test is accepted as a standard (Hawkins and Ramirez 2010).

First, since Round IV testing exposed the NASP test's sensitivity to mortar flow and strength, it can be assumed that sand angularity can also have a significant effect on results. Hawkins and Ramirez suggest that a range of angularity be specified since angularity greatly affects workability. Also, although the goal of Round IV round robin testing was to prove that the test was reproducible between sites, Hawkins and Ramirez deemed the results as not "statistically defensible," and suggested that more testing be done at between four to six independent sites. They also recommend that more development length testing be done to identify pullout limits (Hawkins and Ramirez 2010). A research program funded by PCI addressing these issues about the NASP test is currently beginning to get underway at the time of this thesis.

Although the NASP test appears to be the front runner for becoming the standard bond test, recent developments with the LBPT have shown that the test may still be potentially viable as a reproducible test. Based on a recent, unpublished study, Logan has discovered a correlation between soft limestone coarse aggregates and low pullout values,

and test results have suggested that using a coarse aggregate with a Mohs hardness value of 6.0 or higher will improve the consistency of results (Logan, personal communication, October 20, 2011). Further testing needs to be completed in order to determine if the standardization of the hardness of the coarse aggregate will truly improve reproducibility of the LBPT from site to site.

2.7. RESEARCH REGARDING BOND OF PRESTRESSING STRAND IN SCC

As the use of SCC has become more and more popular, an increasing number of studies have been completed in order to investigate the bond of prestressing strand in SCC. In these studies, transfer and development lengths of prestressing strand in SCC were compared to the lengths measured in conventional concrete to determine if bond behavior between the two concretes is comparable. Experimentally determined transfer and development lengths were also compared to values calculated by the AASHTO and ACI equations. The findings of these studies are presented in this section.

2.7.1. Girgis and Tuan (2005). Three mixes were investigated in this study: two SCC mixes (Mix 1 and Mix 2) and one conventional mix (Mix 3). The SCC mixes had partial replacement of cement with Class C fly ash and also contained a viscosity modifying admixture (VMA). One full scale NU bridge girder was cast per mix and each girder contained 0.6-in.-diameter (15.2 mm) strand, which was pre-qualified through the Moustafa test, now known as the Large Block Pullout Test, using Logan's concrete mix. The bridge girders, which were parts of three different projects around Nebraska, were instrumented with DEMEC points, and readings were taken at 1, 3, 7, 14, and 28 days after casting. Transfer lengths were calculated using the 95% Average Mean Strain Method. Moustafa pullout tests were also completed on the 0.6-in.-diameter (15.2 mm) strands with the three concrete mixes to determine if pullout values in the concrete mix could be correlated to transfer lengths. Smaller pullout tests were also performed on #4, #6, and #8 deformed bars and 0.6-in.-diameter (15.2 mm) strand.

The SCC mixes had much longer initial transfer lengths than the conventional mix; Mix 1 had an average initial transfer length 80% higher than Mix 3, and Mix 2 had an average initial transfer length over two times that of Mix 3. However, the Moustafa pullout values from the tests completed in the concrete mixes did not predict the longer

transfer lengths in the SCC. It would be assumed that higher pullout values would correspond to shorter transfer lengths, but, in fact, Mix 2 had the highest average pullout load, yet had the longest initial transfer length. The Moustafa pullout values from the concrete mixes and initial transfer lengths from this study are presented in Table 2.5.

Table 2.5 – Girgis and Tuan Results

Mix	Concrete Type	Girder Type	Average Pullout Load (kip)	Average Initial Transfer Length (in.)
Mix 1	SCC	NU1100	43.4	36
Mix 2	SCC	NU900	54.2	43
Mix 3	Conventional	NU1350	48.0	20

Conversion: 1 kip = 4.45 kN
1 in. = 25.4 mm

2.7.2. Larson, Peterman, and Esmaeily (2007). Larson, Peterman, and Esmaeily undertook a project funded by the Kansas Department of Transportation (KDOT) to investigate the bond performance of prestressing strand in SCC. The main goal was to determine if ACI and AASHTO equations would still be conservative when applied to SCC so Kansas precasters would be permitted to use the material to construct bridge girders.

First, Large Block Pullout Tests were run on strand that was to be used in the project. Pullout tests were performed using Logan's specified mix in order to qualify the strand based on pullout values determined by Logan, and strands were also cast in blocks of SCC to compare pullout values in SCC to those of the standard mix. The strands in Logan's mix passed the bond acceptance criteria, but in terms of comparing pullout values from the two concretes, the pullout values for the SCC tests were significantly lower than the pullout values from the conventional concrete; the average SCC pullout value was 22.5 kips (100 kN) while the average pullout value from Logan's concrete mix was 39.5 kips (176 kN).

Several types of beams were then constructed with 0.5-in.-diameter (12.7 mm), Grade 270 prestressing strand to measure transfer lengths due to end slip and then to evaluate development length through four-point load testing. The same SCC mix, which contained no VMA or supplemental cementitious materials, was used for all specimens. Six single strand beams (SSB) with 8 in. x 12 in. (203 mm x 305 mm) cross-sections were cast with one strand located 2 in. (50.8 mm) from the bottom, and six top strand beams (TSB) with 8 in. x 24 in. (203 mm x 610 mm) cross-sections were cast with one strand located at 22 in. (559 mm) from the bottom in order to study the top strand effect. The depth of the TSB's was decreased to 12 in. (305 mm) at the maximum moment range so the SSB and TSB results could be compared. Finally, four T-beams (TB) were cast with strands at a depth of 19 in. (483 mm).

The transfer lengths were determined by measuring strand end slips with a caliper at release and at 21 days and using the values to calculate transfer lengths according to Mast's slip theory. The 21 day average transfer lengths were found to be 21 in. (533 mm) for the SSB specimens, 30 in. (762 mm) for the TSB specimens, and 29 in. (737 mm) for the TB specimens. Additionally, the specimens with bottom strands (TB and SSB) showed increases in transfer length ranging from 10-20%, while the top strands (TSB specimens) had increases of 40-45%.

All development length tests failed in flexure due to strand rupture. The actual maximum moments surpassed the calculated nominal moment capacities by 10-20% for the beams tested at 100% of the calculated development length and 25-30% for the beams tested at 80% of the calculated development length.

Overall, several conclusions were made based on the results of this test program. First, the "top strand effect" theory appeared to be supported; average measured 21 day transfer lengths for the TSB specimens were approximately 50% longer than measured bottom strand transfer lengths, and top strand transfer lengths also showed a much higher increase over 21 days than the bottom strands. Top-cast strands in the study also had on average over 60% longer transfer lengths than the current ACI provision of $50d_b$. Another main conclusion that was drawn was that the ACI and AASHTO code equations for transfer length and development length of bottom strands are conservative and adequate for SCC. Finally, even though the SCC pullout values were low, the results from the

transfer and development length tests for the strand in SCC were acceptable, so therefore, Logan's pullout acceptance limits should not be applied to pullouts performed in SCC.

2.7.3. Pozolo and Andrawes (2011). In order to study the effect of SCC on the bond and transfer lengths of 0.5-in.-diameter (12.7 mm), Grade 270 prestressing strand in Illinois bridge girders, SCC and conventional concrete mixture designs conforming to standards set by the Illinois Department of Transportation (IDOT) were used to cast modified Moustafa pullout test blocks, and hollow box girders and I-girders were constructed out of SCC. The modified Moustafa pullout tests were first run to determine if the bond of strand in SCC was comparable to the bond of strand in conventional concrete, and then transfer lengths were measured on the SCC girders.

In order to compare bond properties of SCC versus conventional concrete, one SCC mix and one conventional concrete (CC) mix were used to cast modified Moustafa pullout test blocks. The SCC mix contained no VMA or supplementary cementitious materials. For each mix, two 2 ft. x 2 ft. x 5.5 ft. (610 mm x 610 mm x 1,676 mm) blocks were cast with 14 strands each, and pullout tests were then completed at 1, 3, 7, and 28 days. Tests were completed using a hollow core hydraulic jack applying load at 0.4 in./min. (10.2 mm/min.). The non-linear slip load and maximum pullout load were recorded. The normalized pullout values for both concrete types at the different days showed the nonlinear slip loads and peak pullout loads were comparable for SCC and CC; in fact, except for an anomaly in the 7 day testing, the SCC peak pullout loads were higher than the CC peak pullout loads. From these results, it was concluded that strands exhibited acceptable bond in SCC, and the project could be continued to test the strand in SCC girders.

The next phase of the project involved casting two I-girders (I-1 and I-2) and two hollow box girders (Box-1 and Box-2) with the SCC mix and monitoring the change in transfer lengths over time by using DEMEC points attached to the concrete surface at the level of the prestressing strand. Strain measurements were taken at 1, 3, 7, 14, and 28 days, and the 95% Average Mean Strain Method was employed to determine transfer lengths. The measured transfer lengths were then compared to transfer lengths calculated by ACI-318-08 and AASHTO equations for transfer length, and it was found that every measured transfer length except for one end were shorter than the ACI and AASHTO

limits. The one end that did not meet the ACI and AASHTO criteria had low concrete strength and was the end that was first released. Overall, the measured lengths averaged 86% below $50d_b$, 72% below $60d_b$, and 69% below $f_{pe}d_b/3$, so it was determined that strands would exhibit acceptable bond in SCC girders in Illinois.

2.7.4. Staton, Do, Ruiz, and Hale (2009). For this program, the researchers evaluated the transfer lengths of 0.6-in-diameter (15.2 mm), Grade 270 prestressing strand in two different SCC mixtures and a high strength conventional concrete. The mixes included an SCC with Type I cement (SCC-I), an SCC with Type III cement and Class C fly ash (SCC-III), and a high-strength conventional concrete (HSC). The strand was first prequalified through the NASP bond test, and then beams were constructed and instrumented with DEMEC points to measure the transfer lengths of the strands over time.

In order to evaluate transfer lengths, 18-ft.-long (5.49 m) beams with 6.5 in. x 12 in. (165 mm x 305 mm) cross-sections, two strands at 2 in. (50.8 mm) from the bottom, and stirrups at 6 in. (152 mm) on center were constructed from three different mixes. Eight beams were cast with the SCC-I, and the SCC-III and HSC were used to cast 6 beams each for a total of 20 beams. The beams were instrumented with DEMEC points, and readings were taken at 1, 3, 7, 14, and 28 days. The 95% Average Mean Strain Method was then used to determine transfer lengths.

The transfer lengths at all ages were compared for all mixes using 90% confidence intervals. Overall, it was found that there was no statistical difference between the HSC and SCC-I transfer lengths, but transfer lengths at 28 days were 3.5 in. (88.9 mm) shorter for the SCC-III beams than for the HSC beams. In terms of transfer length growth, both the SCC-I and SCC-III beams averaged about 8% growth, while the HSC transfer lengths averaged around 12% growth. Also, all measured transfer lengths were shorter than lengths calculated by the ACI and AASHTO equations. For SCC, the measured transfer lengths averaged about 60% below the transfer length predicted by the ACI equation. However, it should be noted that the strands in this research were released by detensioning, and a harsher release method might have resulted in longer transfer lengths.

2.7.5. Floyd, Ruiz, Do, Staton, and Hale (2011). This research program was a continuation of the study of transfer lengths of 0.6-in.-diameter (15.2 mm) strand in SCC by Staton, Do, Ruiz, and Hale. The same beams that were used to measure transfer lengths were also then tested to evaluate the effects of SCC on development length. One end of each beam was tested by applying a single point load to a simple span at a predetermined embedment length. For each test, the failure moment and first slip moment were noted and compared to the calculated nominal moment capacity, and from these observations, it was determined whether the beam failed in bond or flexure. The embedment length for each test was varied based on whether the embedment length of the previous test resulted in a bond or flexural failure. Ultimately, the development length for each concrete type was narrowed down to a range based on failure modes resulting from the different embedment lengths (Table 2.6). For instance, based on results, the development length for 0.6-in.-diameter (15.2 mm) strand in SCC-I is most likely longer than 35 in. (889 mm) but shorter than 37.5 in (953 mm).

Table 2.6 – Concrete Strength at Testing and Development Length Ranges

Concrete Type	$f'_{c,test}$ (psi)	Development Lengths	
		Low End (in)	High End (in)
SCC-I	14,770	35	37.5
SCC-III	13,190	30	32.5
HSC	14,510	30	35

Conversion: 1 psi = 6.89 kPa
1 in. = 25.4 mm

In conclusion, it was determined that the HSC and SCC specimens had comparable development lengths, although SCC-I appeared to have development lengths slightly greater than the HSC. Still, all experimentally determined development lengths were much shorter than lengths calculated by the ACI/AASHTO equation; SCC-I and HSC development lengths were 60-66% shorter, and SCC-III lengths were 64-67% shorter.

2.7.6. Boehm, Barnes, and Schindler (2010). The Alabama Department of Transportation funded a study dedicated to determining if the use of SCC is feasible for bridge girder construction in Alabama. Six AASHTO Type I girders with 0.5-in.-diameter (12.7 mm) "special" Grade 270 prestressing strand composite decks were used to evaluate transfer lengths and development lengths. A moderate strength conventional concrete (STD-M), a moderate strength SCC (SCC-MS), and a high strength (SCC-HS) were used for comparison, and two beams were constructed per mix. All three mixes contained Type III cement, and the two SCC mixes also contained ground granulated blast furnace slag (GGBFS). Also, for the SCC mixes, SCC-MS contained a VMA, while SCC-HS did not. The moderate strength conventional concrete and SCC had target release strengths of 5,000 psi (34.5 MPa), while the high strength SCC had a target release strength of 10,000 psi (68.9 MPa). DEMEC points and the 95% Average Mean Strain Method were used to monitor transfer lengths over three months, and strand draw-in was measured at release with a steel ruler. Flexural bond length was evaluated using four-point loading, and for each mix, one test was completed at an embedment length of 135 in. (3,429 mm), one at 85 in. (2,159 mm), and two at 65 in. (1,651 mm). The development length calculated by AASHTO was 124 in. (3,150 mm).

Through the transfer lengths determined by the 95% Average Mean Strain Method, the study concluded that there was no significant difference between transfer lengths of strands in conventional concrete or SCC for full size girders. Additionally, the ACI and AASHTO equations for transfer length were found to be generally conservative, especially for high strength concretes. Also, SCC transfer lengths were found to increase an average of 28% over three months, while transfer lengths in conventional concrete increased 38%. In terms of the transfer lengths determined from the draw-in measurements, the study found little correlation between these values and the transfer lengths determined by the 95% Average Mean Strain Method.

All four-point load tests failed in flexure, even at the embedment lengths significantly shorter than the value recommended by AASHTO. Therefore, the AASHTO equation was deemed conservative. Results also showed that SCC performed comparably to conventional concrete, exceeding calculated nominal moment capacities by similar amounts.

Overall, SCC was determined to be comparable to conventional concrete in terms of bond. Additionally, the AASHTO and ACI equations for transfer length and development length were found to be conservative for both SCC and conventional concrete. Ultimately, this study approved the potential use of SCC in bridge girders in Alabama.

2.7.7. Burgueño and Haq (2007). Burgueño and Haq investigated the effect of how the different methods and admixtures used in making SCC can affect bond of prestressing strand. The study included three SCC mixes (SCC1, SCC2, and SCC3) and one conventional mix (NCC). SCC1 had a 0.35 water to cement ratio with decreased coarse aggregate, increased fines, and a significant amount of high range water reducer (HRWR), while SCC3 had a 0.45 water to cement ratio, proportions of aggregate similar to those of conventional concrete, and additions of a HRWR and a viscosity modifying admixture (VMA) to produce the fluidity and stability. SCC2 had a 0.40 water to cement ratio and admixture and aggregate proportions between those of SCC1 and SCC3. The three SCC mixes were also compared to a conventional concrete (NCC). Large Block Pullout Tests were completed using the four mixes, and 38-ft. long T-beams using 0.5-in.-diameter (12.7 mm), Grade 270 prestressing strand were cast from each mix to monitor transfer length using DEMEC points and the 95% Average Mean Strain Method and evaluate development length through three-point flexural tests.

Overall, the NCC was found to have slightly better bond than the SCC mixes. The SCC mixes on average had 12% lower pullout values, 36% longer transfer lengths, and 3% longer development lengths. Although transfer lengths were longer for SCC than NCC, the transfer lengths in all SCC mixes were still shorter than the transfer lengths predicted by the ACI code. In terms of comparing the three SCC mixes to determine effects of mix proportioning on bond, it appeared that SCC1 (high fines mix) had the lowest bond capacity of the three, and SCC3 (conventional mix with HRWR and VMA) showed the highest bond capacity of the three.

3. BOND TEST PROGRAM AND RESULTS

3.1. INTRODUCTION

The bond test program involved two types of pullout tests: the North American Strand Producers (NASP) Pullout Test and the Large Block Pullout Test (LBPT). The NASP test consists of six pullout specimens, where each specimen is composed of a section of strand cast concentrically in a cylinder of specified mortar. The LBPT is comprised of six strands cast in a block of concrete having a specific mix design. Both the NASP test and LBPT specify that the pullout tests are to be performed 24 hours after casting. Because there is currently no accepted standard for the testing of bond of prestressing strand, the main purpose of the bond test program was to compare the NASP test in mortar and the LBPT to see if one test could be deemed more reliable than the other in terms of qualifying strand based on bond. In order to compare the two tests, prestressing strand from three different sources was obtained, and the standard NASP test in mortar and the LBPT were performed on strand from each source.

Additionally, the NASP test was also performed using the four concrete mixes that were developed for the transfer length and development length portions of the project, instead of the specified mortar. The NASP tests in concrete were performed only on strands from the same source as the beams, and the purpose of the testing was to see if any correlation could be made between the pullout values and transfer lengths. For each mixture, six total NASP specimens were made and three specimens were tested at 1 day and the remaining three were tested at 8 days. While the standard NASP test in mortar assesses only the bond quality of the strand itself, the NASP test in concrete gives an idea of the actual bond behavior of the strand in a specific concrete and concrete strength.

Prestressing strand from three different sources was used for comparing the standard NASP test in mortar and the LBPT. In this thesis, the strands will be identified as 101, 102, or 103 to designate the source. Strand type 101was the strand type that was used in the beams, and strands 102 and 103 were samples of strand remaining from previous bond testing completed during NCHRP 10-62. Samples 102 and 103 were used to provide a comparison between different strand manufacturers. Because three different

sources of strand were used for multiple pullout tests, an identification code was developed to distinguish the specific bond test and strand combinations (Figure 3.1).

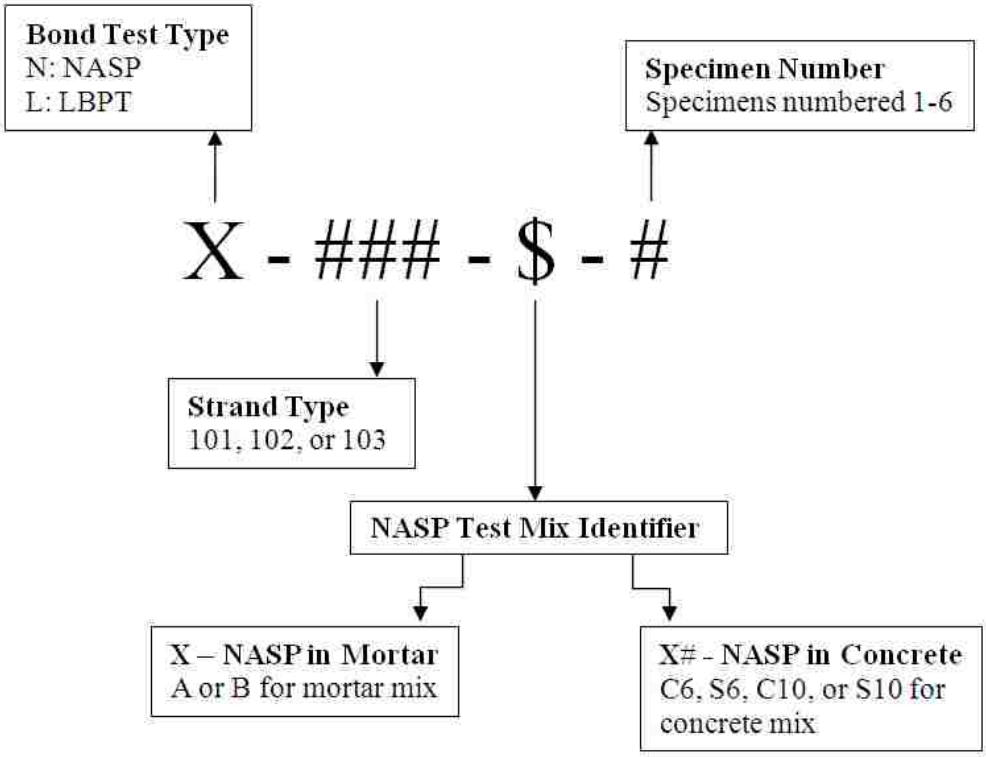

Figure 3.1 – Bond Test Identification Code

For instance, N-101-A-1 designates the first specimen in the group of six NASP tests using strand type 101 in mortar Mix A, while N-101-C6-1 designates the first specimen in a group of six NASP tests using strand type 101 in the conventional concrete, 6,000 psi (41.4 MPa) target strength mix.

A few notes should be made concerning the NASP test in concrete specimens. First, the concrete mix designs used for the beams, and consequently the NASP tests in concrete, are discussed in Section 4.2. Also, all NASP in concrete tests were completed with strand type 101 because this was the strand type used in the beams. Finally, the NASP tests in concrete were run with three specimens tested at 1 day and three specimens tested at 8 days; therefore, it should be noted that for the NASP tests in

concrete, specimens numbered 1-3 were tested at 1 day, and specimens numbered 4-6 were tested at 8 days. Consequently, N-101-C6-1 indicates a C6 NASP specimen tested at 1 day, while N-101-C6-4 indicates a C6 NASP specimen tested at 8 days.

Finally, L-101-1 designates the first specimen in the group of the six type 101 strands cast for the LBPT. Since one concrete mix was used for the LBPT, the mix identification label was dropped for the LBPT identifiers.

This section first describes program used to determine the strands' tensile properties in Section 3.2. Section 3.2 also summarizes ultimate tensile strength, f_u, and modulus of elasticity, E_{ps}, of each source. Next, Section 3.3 presents the set-up, instrumentation, procedure, and results for the standard NASP tests in mortar as well as the NASP tests in concrete. Finally, the set-up, instrumentation, procedure, and results for the LBPT are reported in Section 3.4.

3.2. TENSILE PROPERTIES OF PRESTRESSING STRANDS

The tensile properties of the three strand types used were found in order to aid in the evaluation of the pullout tests and to determine the ultimate moment capacities of the full-scale prestressed beams. Tensile tests were completed on strand types 101, 102, and 103, and the average ultimate strength and modulus of elasticity were found for each source.

3.2.1. Tension Test Setup and Procedure. Three tension specimens were tested for each strand source. The strands were cut into 18-in.-long (457 mm) sections and 3-in.-long (76.2 mm) aluminum tube sleeves were placed on each end of each test specimen to protect the strand from the grip serrations and facilitate gripping, as suggested in ASTM A1061/A1061M-09: Standard Test Methods for Testing Multi-Wire Steel Strand. The aluminum sleeves consisted of 6061 aluminum tubing with a 0.625 in. (15.9 mm) outside diameter, 0.527 in. (13.4 mm) inside diameter, and 0.049 in. (1.24 mm) wall thickness. Two sleeves were slid onto each specimen, and then small welds were placed on each end of the strand to ensure the wires would be loaded uniformly and also to keep the aluminum sleeves from sliding off the specimen. A set of three tension test specimens can be seen in Figure 3.2.

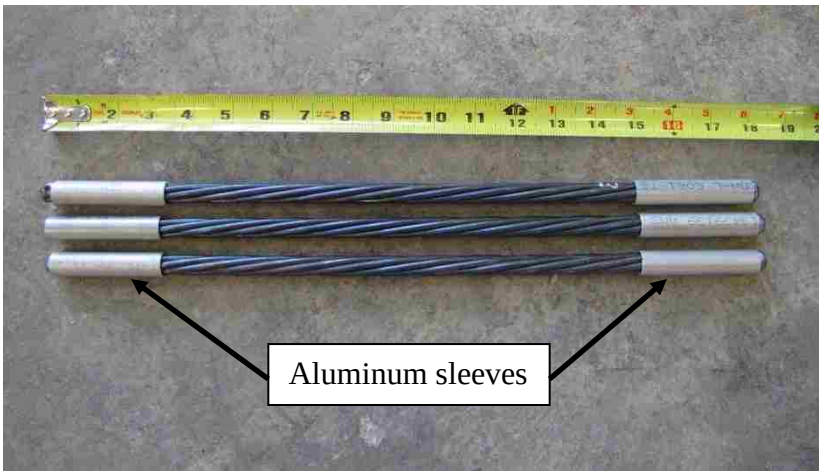

Figure 3.2 – Tension Test Specimens

An MTS 880 Universal Testing Machine was used to apply tension to each specimen until fracture. Each strand was centered and clamped into the grips. The gripping strength was initially set at 3.5 ksi (24.1 MPa), but the first set of tests exhibited slippage. As a result, after the first set of tests, the gripping strength was increased to 7.5 ksi (51.2 MPa), and no further slippage was experienced. The initial set that showed slippage in the grips was discarded, and an additional three specimens of the same strand type were tested using the 7.5 ksi (51.2 MPa) gripping strength to determine the final properties.

After setting the specimen in the grips, an initial load of 4,130 lb. (18.3 kN), which corresponds to 10% of the minimum specified fracture load, was applied based on ASTM A416/A416M-10: Standard Specification for Steel Strand, Uncoated Seven-Wire for Prestressed Concrete. Then, a 2-in.-long (50.8 mm) extensometer was attached near the middle of the section between the grips. The tension test setup with the extensometer is shown in Figure 3.3. Each specimen was then loaded at a rate of 3,235 lb./min. (14.4 kN/min.) until fracture. The load rate was chosen based on the limitations in ASTM A370-11a: Standard Test Methods and Definitions for Mechanical Testing of Steel Products, the limitations of the MTS equipment, and previous strand tensile testing performed on the MTS test machine. The majority of specimens fractured in the grips, but all specimens failed above the minimum fracture load of 41,300 lb (184 kN), so the

tests were considered valid according to ASTM A1061. A fractured specimen that failed away from the grips is pictured in Figure 3.4.

The data acquisition system recorded load, strain, and stroke and was set to record four readings per second. For each tension specimen, the extensometer was removed after a strain reading of approximately 0.008 in./in. was reached, and then the specimen continued to be loaded until failure. The extensometer was able to record sufficient data for the determination of the modulus of elasticity but was removed at a safe margin before fracture so the extensometer would not be damaged. Yield strength, which would have corresponded to a strain of 0.01 in./in., was not determined.

3.2.2. Tension Test Results. The collected load and extensometer data was used to determine the ultimate tensile strength (f_u) and the modulus of elasticity (E_{ps}) for each strand source. The average, standard deviation, and coefficient of variation (COV) results for f_u and E_{ps} presented in Table 3.1 are based on three tension specimens per strand type.

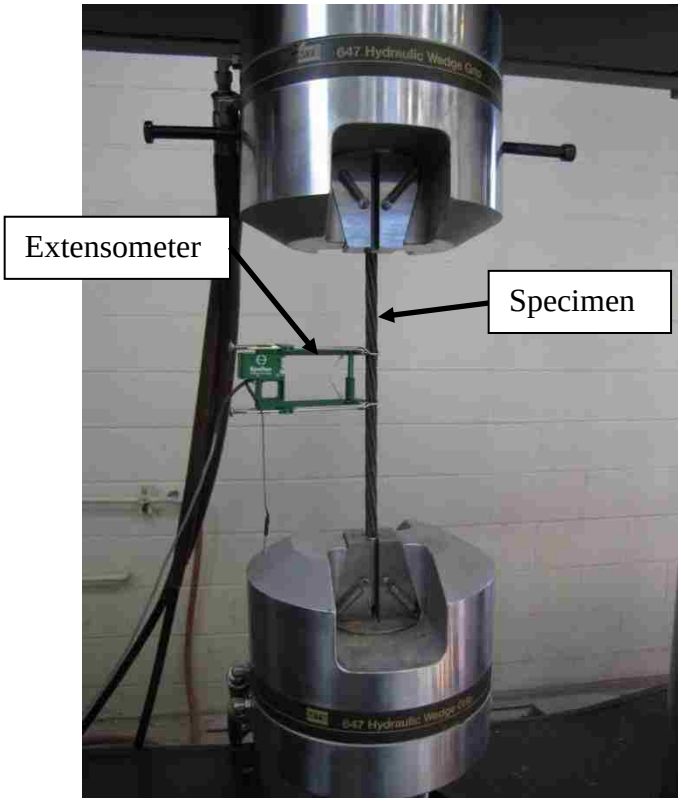

Figure 3.3 – Tension Test Setup

Figure 3.4 – Fractured Tension Test Specimen

Table 3.1 – Direct Tension Test Results

Strand Type	Statistic	f_u (ksi)	E_{ps} (ksi)
101	Average	287.5	29,400
	Std. Dev.	1.8	1,131.4
	COV	0.63%	3.85%
102	Average	285.0	27,500
	Std. Dev.	0.2	193.0
	COV	0.06%	0.70%
103	Average	287.7	28,500
	Std. Dev.	0.3	71.6
	COV	0.12%	0.25%

Conversion: 1 ksi = 6.89 MPa

3.3. NASP BOND TEST

The NASP Bond Test was performed in both the specified mortar, so results could be compared to the LBPT results, and the four concrete mixes, so pullout results could be correlated to transfer lengths. Aside from the mortar vs. concrete mixes, the specimen design and testing methods were virtually identical for both types of NASP tests.

3.3.1. NASP Test Specimen Design. The NASP specimen molds were identical for both the mortar and concrete NASP tests. The molds were constructed from 18-in.-long (457 mm) sections of 5 in. (127 mm) outside diameter, $^{1}/_{8}$-in.-thick (3.18 mm) steel tubing. The sections of tube were welded to 6 in. x 6 in. x ¼ in. (152 mm x 152 mm x 6.35 mm) steel plates with a $^{5}/_{8}$-in.-diameter (15.9 mm) hole in the center. A 1 ¾ in. (44.5 mm) section of inverted 2 in. x 2 in. (50.8 mm x 50.8 mm) angle was welded onto the side of the tube at the open end to allow for the attachment of an LVDT during testing. Before testing, the angle piece on each specimen mold was checked with a level to ensure a horizontal surface and adjusted as necessary. A diagram of the steel mold is shown in Figure 3.5.

The strands were cut into 32-in.-long (813 mm) segments and were positioned so that 2 in. (50.8 mm) of strand would protrude from the top in order for the LVDT to measure slip, and 12 in. (305 mm) would extend from the bottom so the chuck would have sufficient strand to grip. A grinder was used to shape the top end of each strand, so that the outer wires were tapered upwards to the center wire, which had a level surface for the LVDT. Additionally, a 2-in.-long (50.8 mm) bond breaker constructed from foam insulation was wrapped around the strand and secured with duct tape. As shown in Figure 3.5, the bond breaker was positioned immediately above the hole in the bottom plate, and extended upward 2 in. (50.8 mm) into the mortar or concrete. The bond breakers are depicted in Figure 3.6.

For the NASP test in mortar, a significant number of trial batches of mortar were required in order to develop a mortar mix design that would meet the specific requirements set forth by the proposed standard in Appendix H of NCHRP 603 (Ramirez and Russell 2008). The proposed standard requires a mortar flow greater than or equal to 100 but less than or equal to 125 as measured in accordance with the procedure in ASTM C1437-07: Standard Test Method for Flow of Hydraulic Cement Mortar. Furthermore,

the 24-hour average compressive strength of three mortar cubes was required to fall within the range of 4,500 psi (31.0 MPa) to 5,000 psi (34.5 MPa). The mortar consisted of Type III cement, fine aggregate, and water. The fine aggregate gradation conformed to ASTM C33/C33M-11a: Standard Specification for Concrete Aggregates. For the first few trial batches, the moisture content of the fine aggregate was measured and factored into the mix design; however because of the variability of results obtained, all fine aggregate for the remaining trial and final batches was oven dried to maintain more precise control of the water-cement ratio.

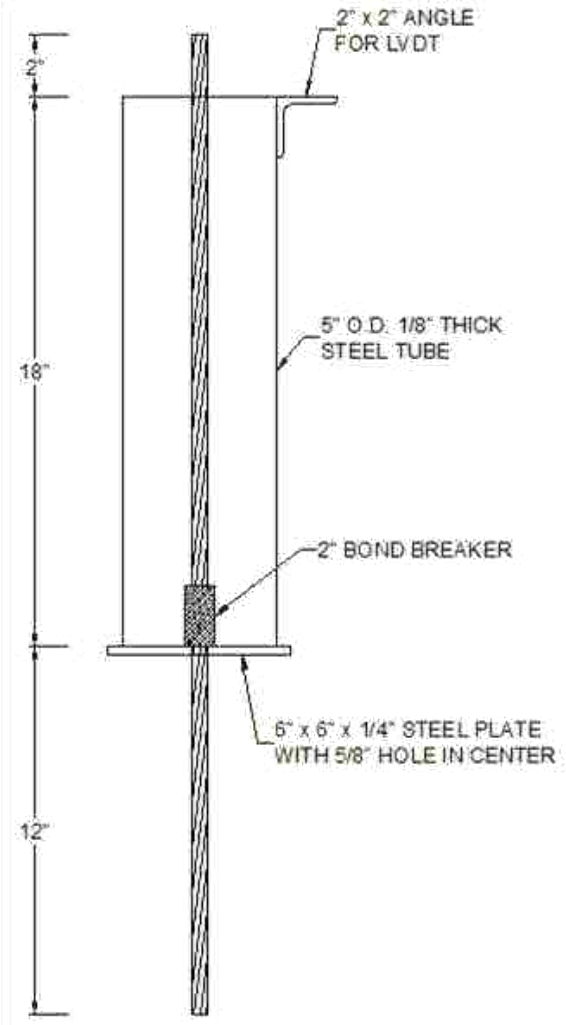

Conversion: 1 in. = 25.4 mm

Figure 3.5 – NASP Specimen Mold

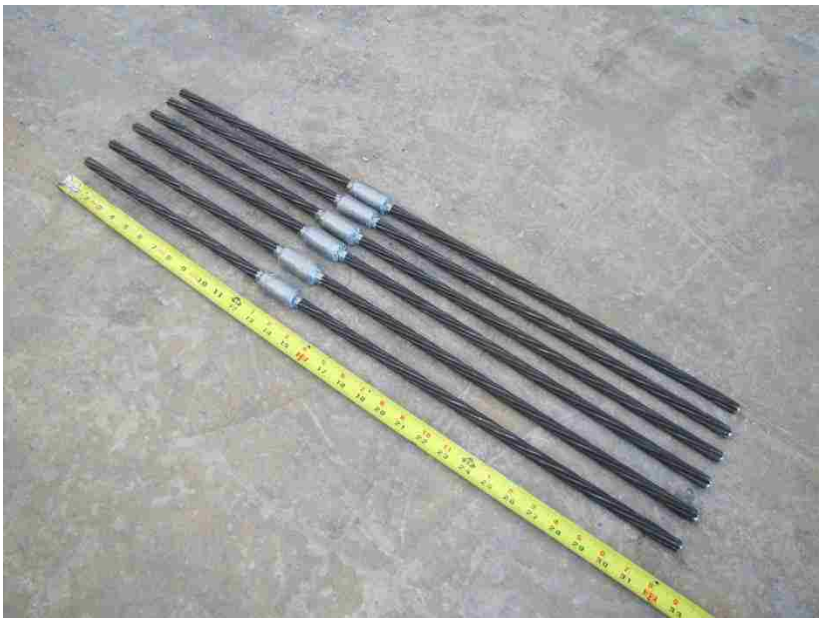

Figure 3.6 – Strands with Bond Breakers

The initial NASP test for strand type 101 was completed during the summer of 2011, but the NASP tests for strand types 102 and 103 were completed over six months later in February of 2012. The mix design that was developed during the summer, Mix A, for strand type 101 did not meet the requirements of the proposed standard when used for testing strand types 102 and 103. When trial batches of Mix A were produced in February, the batches gave comparable 24 hour strengths to the trial batches of Mix A that were produced the previous summer, but the flow values were consistently lower than the previous batches and did not meet the criteria of the standard. Therefore, a revised mix design, Mix B, meeting the flow and strength criteria was developed for testing of strand types 102 and 103. Mix B was significantly different from Mix A in terms of proportioning, and because extra samples of strand type 101 were still available during the testing of types 102 and 103, the NASP test was performed again on strand type 101 in March 2012 with the new mix design, Mix B. The final mortar mix designs can be found in Table 3.2, and the test matrix for the NASP test in mortar is shown in Table 3.3.

For the NASP tests in concrete, the NASP specimens were poured at Coreslab Structures in Marshall, Missouri from the same batches that were used for the beams and

using strand type 101, which was the same strand type used in the beams. The mix designs for the C6, S6, C10, and S10 concretes can be found in Table 4.1 in Section 4.2.

Table 3.2 – Mortar Mix Design for NASP Tests

Mix ID	Water/Cement Ratio	Sand/Cement Ratio	Oven Dried Sand (lb/ft^3)	Type III Cement (lb/ft^3)	Water (lb/ft^3)
A	0.38	1.2 : 1	64.3	53.4	20.7
B	0.395	0.9 : 1	52.7	58.6	23.5

Conversion: 1 lb/ft^3 = 16.0 kg/m^3

Table 3.3 – NASP Test in Mortar Test Matrix

Strand Type	Mix A	Mix B
101	X	X
102		X
103		X

3.3.2. NASP Test Specimen Fabrication. For the mortar specimens, the mortar was mixed in a 2 ft^3 (0.056 m^3) drum mixer according to a procedure based on ASTM C192/C192M-07: Standard Practice for Making and Curing Concrete Test Specimens in the Laboratory. The mixer was started and all of the sand and enough water to produce a slurry were added. After the sand and water had thoroughly mixed, the cement and remaining water were then added in approximately three equal increments, allowing time for mixing between each increment. Once all the components were in the mixer, the mortar was mixed for three minutes. Then, the mixer was stopped for approximately two minutes while the blades were scraped with a spatula. Finally, the mortar was mixed for an additional two minutes. Figure 3.7 shows the mortar in the drum mixer.

The flow test was performed according to ASTM C1437-07: Standard Test Method for Flow of Hydraulic Cement Mortar immediately after mixing. After conducting the flow test, the mortar cube molds and NASP steel casings were filled. Three sets of three 2 in. x 2 in. x 2 in. (50.8 mm x 50.8 mm x 50.8 mm) mortar cubes were made according to ASTM C109/C109M-11a: Standard Test Method for

Compressive Strength of Hydraulic Cement Mortars (Using 2 in. or 50 mm Cube Specimens). Three sets of cubes were made so that the mortar strength could be monitored before, during, and after testing. During the casting process, cube molds were also weighed before and after being filled in order to determine fresh unit weight. The flow test and cube-making process are depicted in Figures 3.8 and 3.9, respectively.

Figure 3.7 – Mortar Mix in Drum Mixer

In order to fill the NASP molds, the six molds were placed on a custom wooden platform with two rows of three $^{5}/_{8}$-in.-diameter (15.9 mm) holes on the top and bottom sections of plywood so that the strands could be placed vertically in the molds and rest at the correct height, as seen in Figure 3.10. The steel tubes were filled in three equal layers, and each layer was vibrated with a handheld 1 in^2 (645 mm^2) battery powered vibrator. Once the specimen molds were filled and vibrated, wooden caps designed to fit securely around the mold and with $^{5}/_{8}$-in.-diameter (15.9 mm) holes in the center of each were placed on the top of each specimen to ensure the strands would remain plumb and concentric within the mold. The cube molds and table holding the six specimens were placed in the moist cure room for 24 hours.

Figure 3.8 – Flow Test

Figure 3.9 – Mortar Cubes

Figure 3.10 – NASP Mold and Strand Setup

For the NASP tests in concrete, the only difference is the steel molds were filled with the appropriate concrete mix instead of mortar. Once again, the molds were filled in three equal layers, and each layer was vibrated with the 1 in^2 (645 mm^2) handheld vibrator. Filling of the molds for one of the concrete mixes can be seen in Figure 3.11. The caps were placed on the molds to keep the strands plum and concentric, and the outside of the molds were vibrated once more to ensure consolidation. The specimens were match cured with the beams. Six specimens were made for each mix, and for each mix, three specimens were tested at 24 hours and three specimens were tested at 8 days. Concrete cylinders measuring 4 in. x 8 in. (102 mm x 203 mm) were used to determine the compressive strength of the concrete at the times of testing. The final capped NASP specimens and cylinders for one of the concrete mixes can be seen in Figure 3.12.

Figure 3.11 – Filling Specimens for NASP Test in Concrete

Figure 3.12 – Capped NASP in Concrete Specimens and Cylinders

3.3.3. NASP Test Setup and Procedure. On the day after casting, cubes or cylinders were first tested to determine compressive strength. For the mortar, one set of three cubes was tested between 22 and 23 hours to ensure the compressive strength of the

mortar was at or near 4,500 psi (31.0 MPa). The second set of cubes was tested at around 24 hours, which corresponded to the beginning of NASP testing, and the third set was tested after the NASP testing was complete, or at around 25 or 26 hours. The average compressive strengths from immediately before and immediately after testing were averaged to determine the reported mortar compressive strength during testing. For the concrete NASP tests, a target compressive strength range was not required, so one set of three cylinders was tested at around 24 hours to determine compressive strength.

For the mortar NASP tests, all six specimens were tested at approximately 24 hours, while three specimens were tested at 24 hours and three specimens were tested at 8 days for each concrete mix. The specimens were tested using an MTS 880 Universal Testing Machine and steel frames that had been constructed specifically for the test. The frames, which are illustrated and dimensioned in Figure 3.13, were subsequently secured within the grips of the MTS via vertical plates welded to the top and bottom. The top frame held the cylindrical NASP specimen, and a chuck gripped the strand and bore against the top plate of the bottom frame, securing the specimen at approximately 6 in. (152 mm) from the bottom plate of the specimen, as show in Figure 3.14. Additionally, a steel plate was placed between the chuck and the bottom frame, and a steel plate and neoprene pad were placed under the specimen on the top frame, as seen in Figure 3.15.

The bottom crosshead remained stationary, while the top crosshead moved upwards, applying load to the strand. The test method specifies that the load be applied at a rate of 0.1 in./min. (2.54 mm/min.), but the rate also must not exceed 8,000 lb./min. (35.6 kN/min.). The specimen was loaded at 0.1 in./min. (2.54 mm/min.) but a calculation was performed later using Eq. 3.1, which was also used by researchers in Round IV of the NASP testing (Russell 2006) to ensure the load rate was under 8,000 lb./min. (35.6 kN/min.). In Eq. 3.1, T_{6000} is the time elapsed in seconds when the pullout load was 6,000 lb. (26.7 kN) and T_{4000} is the time elapsed in seconds when the pullout load was 4,000 lb. (17.8 kN). Time and load values were interpolated from the data.

$$Load\ Rate = \frac{(6{,}000lb - 4{,}000lb)}{(T_{6000} - T_{4000})(60)} \quad \textbf{(3.1)}$$

An LVDT was secured in a specially constructed steel apparatus that was designed to be clamped to the specimen and would position the LVDT onto the center wire of the portion of strand protruding from the top, as seen in Figure 3.16. The data acquisition system collected the MTS stroke and load data and the LVDT readings at a rate of two readings per second. The load rate was applied to the specimen until a slip of 0.1 in. (2.54 mm) was observed.

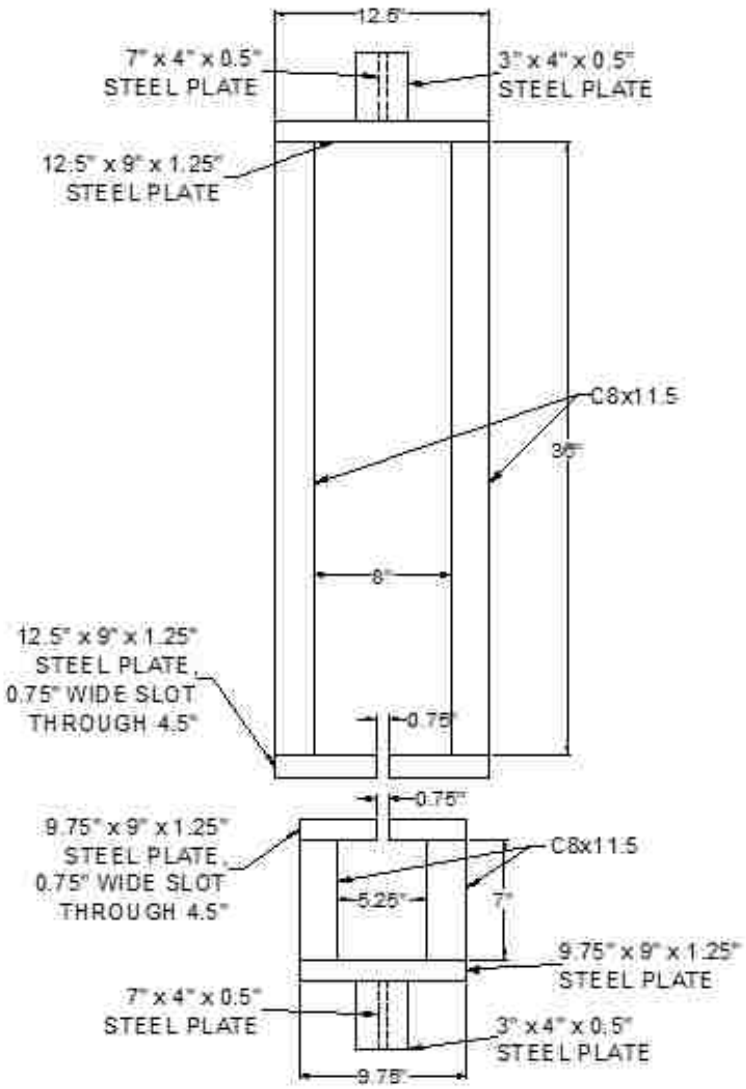

Conversion: 1 lb = 4.45 N
1 in. = 25.4 mm

Figure 3.13 – NASP Test Frame

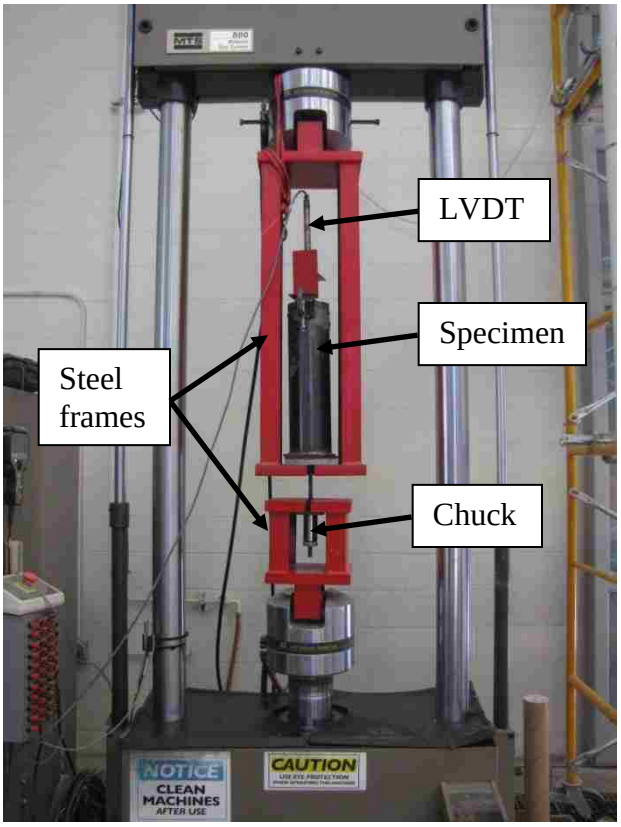

Figure 3.14 – NASP Test Setup

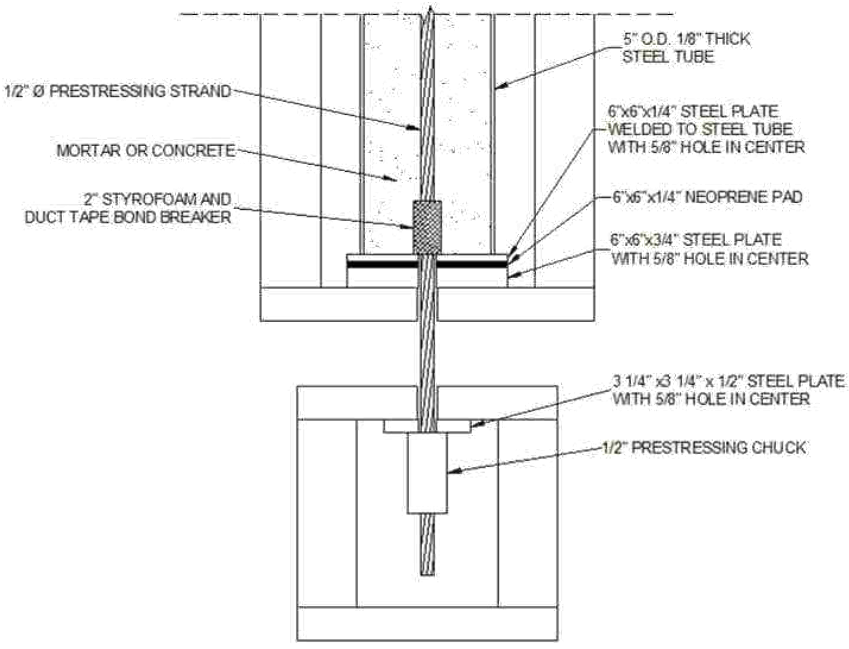

Conversion: 1 in. = 25.4 mm

Figure 3.15 – NASP Test Setup Details

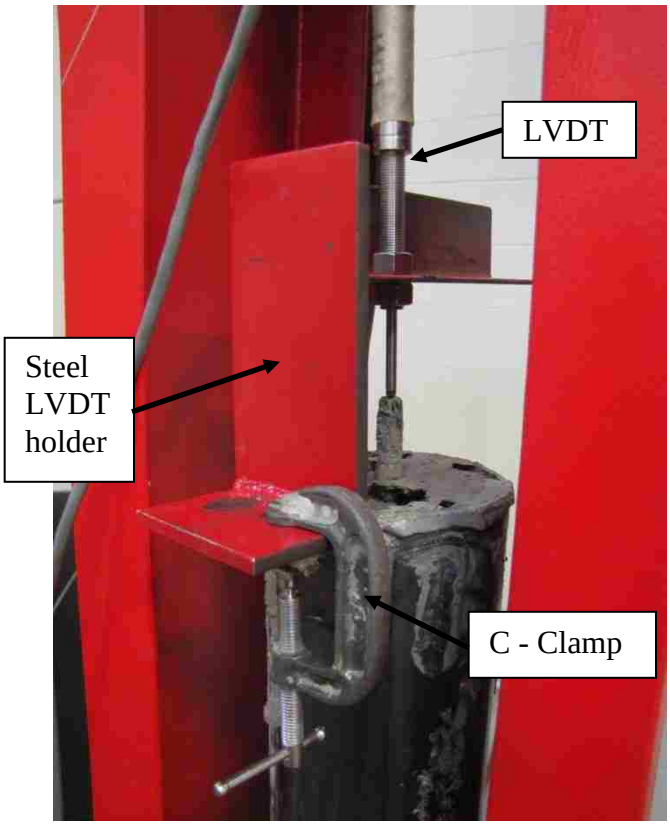

Figure 3.16 – NASP Test LVDT Setup

3.3.4. NASP Test Results. In this section, the NASP test results have been divided into the results for the tests in mortar and the tests in concrete. The results are presented in load vs. slip plots, and the loads at 0.001 in. (0.025 mm) and 0.1 in. (2.54 mm) slips for each specimen are presented in tables.

3.3.4.1 Results from standard NASP test in mortar. The results from the NASP tests in mortar performed on the samples of strand from three different sources are presented in this subsection. First, the load data from the MTS and the slip data from the LVDT were organized into load vs. slip plots. An example load vs. slip plot can be found in Figure 3.17. The plot shows the load vs. slip curves for all six specimens of the same strand type, and the average minimum pullout load for acceptable bond quality as suggested by the proposed standard is also marked on each plot. For 0.5-in.-diameter (12.7 mm) strand, the average minimum pullout value is 10,500 lb (46.7 kN). All plots

for the mortar NASP tests for strand types 101, 102, and 103 can be found in the discussion of the NASP test results in Section 5.2.1.

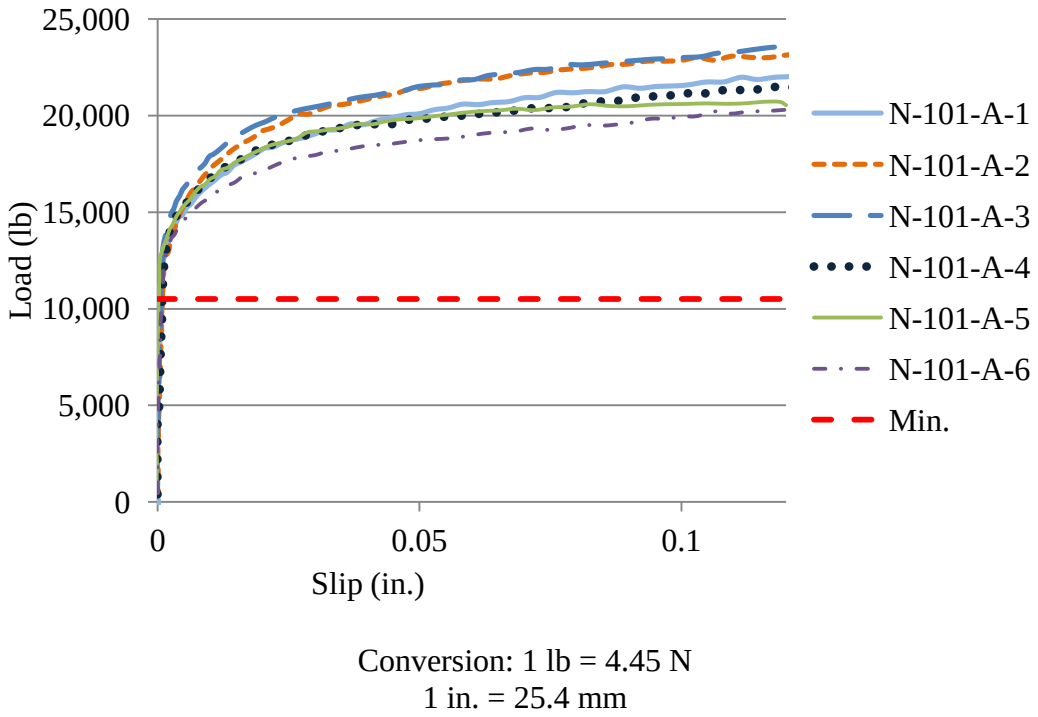

Figure 3.17 – Typical Load vs. Slip Plot for NASP Test in Mortar (N-101-A)

Tables 3.4, 3.5, 3.6, and 3.7 present the loads at strand slip values of 0.001 in. (0.025 mm) and 0.1 in. (2.54 mm) for the NASP tests performed on strand and mortar mix combinations of 101-A, 101-B, 102-B, and 103-B, respectively. The mortar strength, mortar flow, and average loading rate for each set of tests are also reported in each table. Table 3.8 summarizes the average loads at 0.001 in. (0.025 mm) and 0.1 in. (2.54 mm) slip, as well as fresh and hardened properties of the mortar used for each test so the results from the different tests can be compared side by side.

Table 3.4 – NASP in Mortar Results for Strand 101 Mix A

Specimen ID	Load at 0.001 in. Slip (lb)	Load at 0.1 in. Slip (lb)
N-101-A-1	12,500	22,100
N-101-A-2	10,600	22,900
N-101-A-3	12,600	23,000
N-101-A-4	11,100	21,100
N-101-A-5	13,100	20,600
N-101-A-6	11,500	20,000
Average	**11,900**	**21,600**
Std. Dev.	**965**	**1,249**
COV	**8.1%**	**5.8%**
f'_c = 4,980 psi		
Flow = 112.1		
Average Load Rate = 6,539 lb./min.		

Conversion: 1 lb = 4.45 N
1 psi = 6.89 kPa
1 in. = 25.4 mm

Table 3.5 – NASP in Mortar Results for Strand 101 Mix B

Specimen ID	Load at 0.001 in. Slip (lb)	Load at 0.1 in. Slip (lb)
N-101-B-1	8,100	19,100
N-101-B-2	6,500	17,300
N-101-B-3	7,800	17,800
N-101-B-4	7,200	19,100
N-101-B-5	8,900	18,200
N-101-B-6	5,200	17,800
Average	**7,300**	**18,200**
Std. Dev.	**1,311**	**751**
COV	**18.0%**	**4.1%**
f'_c = 5,000 psi		
Flow = 100.2		
Average Load Rate = 6,933 lb/min.		

Conversion: 1 lb = 4.45 N
1 psi = 6.89 kPa
1 in. = 25.4 mm

Table 3.6 – NASP in Mortar Results for Strand 102 Mix B

Specimen ID	Load at 0.001 in. Slip (lb)	Load at 0.1 in. Slip (lb)
N-102-B-1	3,200	11,000
N-102-B-2	3,300	12,400
N-102-B-3	4,200	12,600
N-102-B-4	1,900	9,300
N-102-B-5	3,800	12,400
N-102-B-6	2,400	12,300
Average	**3,100**	**11,700**
Std. Dev.	**860**	**1,289**
COV	**27.4%**	**11.0%**
f'_c = 4,820 psi		
Flow = 116.0		
Average Load Rate = 6,420 lb./min.		

Conversion: 1 lb = 4.45 N
1 psi =6.89 kPa
1 in. = 25.4 mm

Table 3.7 – NASP in Mortar Results for Strand 103 Mix B

Specimen ID	Load at 0.001 in. Slip (lb)	Load at 0.1 in. Slip (lb)
N-103-B-1	3,500	15,800
N-103-B-2	2,600	20,500
N-103-B-3	1,800	18,600
N-103-B-4	700	16,000
N-103-B-5	8,700*	19,700
N-103-B-6	1,200	21,300
Average	**2,000**	**18,700**
Std. Dev.	**1,091**	**2,295**
COV	**55.6%**	**12.3%**
f'_c = 4,770 psi		
Flow = 111.6		
Average Load Rate = 6,590 lb./min.		

* - Value was statistically removed from average and std. dev.

Conversion: 1 lb = 4.45 N
1 psi = 6.89 kPa
1 in. = 25.4 mm

Table 3.8 – Summary of NASP Test in Mortar Pullout Values and Mortar Properties

Strand/Mix ID	Avg. Load at 0.001 in. (lb.)	Avg. Load at 0.1 in. (lb.)	f'_c (psi)	Flow	Unit Weight (lb/ft^3)	Average Load Rate (lb/min.)
N-101-A	11,900	21,600	4,980	112.1	142.9	6,539
N-101-B	7,300	18,200	5,000	100.2	136.5	6,933
N-102-B	3,100	11,700	4,820	116.0	134.2	6,420
N-103-B	1,960	18,700	4,770	111.6	134.9	6,590

Conversion: 1 lb = 4.45 N
1 psi = 6.89 kPa
1 lb/ft^3 = 16.0 kg/m^3
1 in. = 25.4 mm

3.3.4.2 Results from modified NASP test in concrete. The results from the 24 -hour and 8 day NASP tests run on the concrete NASP specimens are presented here. First, the load data from the MTS and the slip data from the LVDT were organized into load vs. slip plots. An example load vs. slip plot can be found in Figure 3.18. Each plot shows the curves for the three specimens of the same concrete mix tested at either 1 day or 8 days. All plots for the concrete NASP tests can be found in Appendix B.

The written procedure specifies that the pullout load is defined as the load at 0.1 in. (2.54 mm) of strand slip, but the pullout load at 0.001 in. (0.025 mm) of slip was also recorded. Table 3.9 contains the individual and average loads corresponding to 0.001 in. (0.025 mm) and 0.1 in. (2.54 mm) of slip for concrete mixes C6 and S6 tested at 1 day and 8 days, as well the standard deviation and coefficient of variation for each set of three loads. Table 3.10 contains the same data for the C10 and S10 mixes.

In Table 3.9, specimen N-101-C10-1 does not have a 0.1 in. (2.54 mm) pullout load value because this was the first test completed, and the test reached the maximum stroke of the MTS before the slip reached 0.1 in. (2.54 mm). The allowable stroke distance was increased after this test, so this problem was not encountered again.

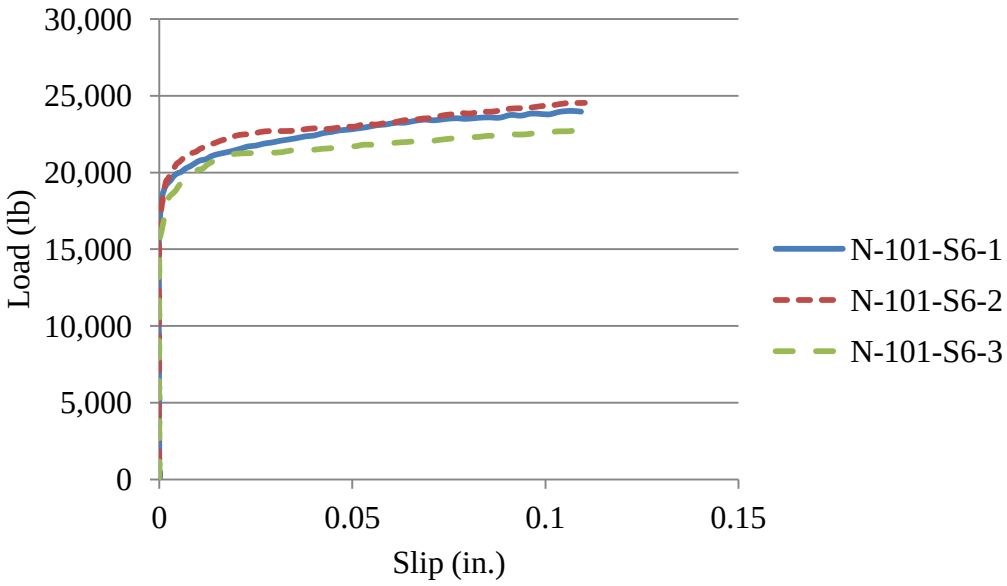

Conversion: 1 lb = 4.45 N
1 in. = 2.54 mm

Figure 3.18 – Typical Load vs. Slip Plot for Concrete NASP Test (N-101-S6)

Table 3.9 – Concrete NASP Results – C6 and S6

Mix	Day	Specimen ID	f'_c (psi)	Load at Slip of 0.001 in.				Load at Slip of 0.1 in.			
				Load (lb.)	Average (lb.)	Std. Dev. (lb.)	COV	Load (lb.)	Average (lb.)	Std. Dev. (lb.)	COV
C6	1 Day	N-101-C6-1	4,810	16,900	17,700	971	5.49%	20,900	21,100	529	2.51%
		N-101-C6-2		17,500				20,700			
		N-101-C6-3		18,800				21,700			
	8 Day	N-101-C6-4	5,620	18,200	18,900	2,676	14.16%	24,900	24,200	907	3.75%
		N-101-C6-5		16,700				24,600			
		N-101-C6-6		21,900				23,200			
S6	1 Day	N-101-S6-1	5,660	18,700	18,000	1,127	6.26%	23,900	23,700	874	3.69%
		N-101-S6-2		18,600				24,400			
		N-101-S6-3		16,700				22,700			
	8 Day	N-101-S6-4	6,690	18,100	19,000	1,137	5.99%	24,700	26,200	1,375	5.25%
		N-101-S6-5		18,700				26,500			
		N-101-S6-6		20,300				27,400			

Conversion: 1 lb = 4.45 N
1 in. = 2.54 mm

Table 3.10 – Concrete NASP Results – C10 and S10

Mix	Day	Specimen ID	f'_c (psi)	Load at Slip of 0.001 in.				Load at Slip of 0.1 in.			
				Load (lb.)	Average (lb.)	Std. Dev. (lb.)	COV	Load (lb.)	Average (lb.)	Std. Dev. (lb.)	COV
C10	1 Day	N-101-C10-1	5,670	14,000	15,000	850	5.67%	N/A	26,700	1,202	4.51%
		N-101-C10-2		15,300				27,500			
		N-101-C10-3		15,600				25,800			
	8 Day	N-101-C10-4	7,950	15,500	17,100	2,600	15.20%	24,400	28,600	3,707	12.96%
		N-101-C10-5		15,700				30,200			
		N-101-C10-6		20,100				31,300			
S10	1 Day	N-101-S10-1	6,330	13,600	12,900	1,358	10.52%	29,000	27,300	9,420	34.51%
		N-101-S10-2		11,300				17,100			
		N-101-S10-3		13,700				35,700			
	8 Day	N-101-S10-4	8,600	18,500	16,900	1,550	9.17%	39,600	36,700	3,799	10.35%
		N-101-S10-5		15,400				38,100			
		N-101-S10-6		16,900				32,400			

Conversion: 1 lb = 4.45 N
1 in. = 2.54 mm

3.4. LARGE BLOCK PULLOUT TEST

The large block pullout test was performed on all three strand sources to compare results to those of the standard NASP test in mortar. Samples of strand 101 were received four months before samples of 102 and 103, so the samples of strand type 101 were wrapped in plastic, secured with duct tape, and stored in a closed container until testing to keep the strands in as-received condition. A single block was cast with six strands from each source, and the pullout tests to determine load at first slip and peak load were performed approximately 24 hours after casting.

3.4.1. LBPT Specimen Design. The LBPT specimen was designed based on Logan's study completed in 1997. The 2 ft. x 2 ft. x 6 ft.-8 in. (610 mm x 610 mm x 203 mm) block of concrete was designed to hold 18 strand samples, six samples from each of the three strand sources. Strands were cut to 52 in. (1321 mm) lengths, so each strand could have 18 in. (457 mm) of bonded length, a 2 in. (50.8 mm) bond breaker made from foam insulation and duct tape, and 32 in. (813 mm) of strand protruding from the concrete surface to accommodate the test setup. The strands were spaced in two rows 12 in. (305 mm) apart, and each row contained nine strands spaced at 8 in. (203 mm) on center. The mild reinforcing and strand layout are shown in Figures 3.19 and 3.20. All mild reinforcing conformed to ASTM A615, Grade 60. Steel chairs measuring 5 in. (127 mm) high were used to support the mild steel cage, which in turn provided attachment points and support for the strand samples.

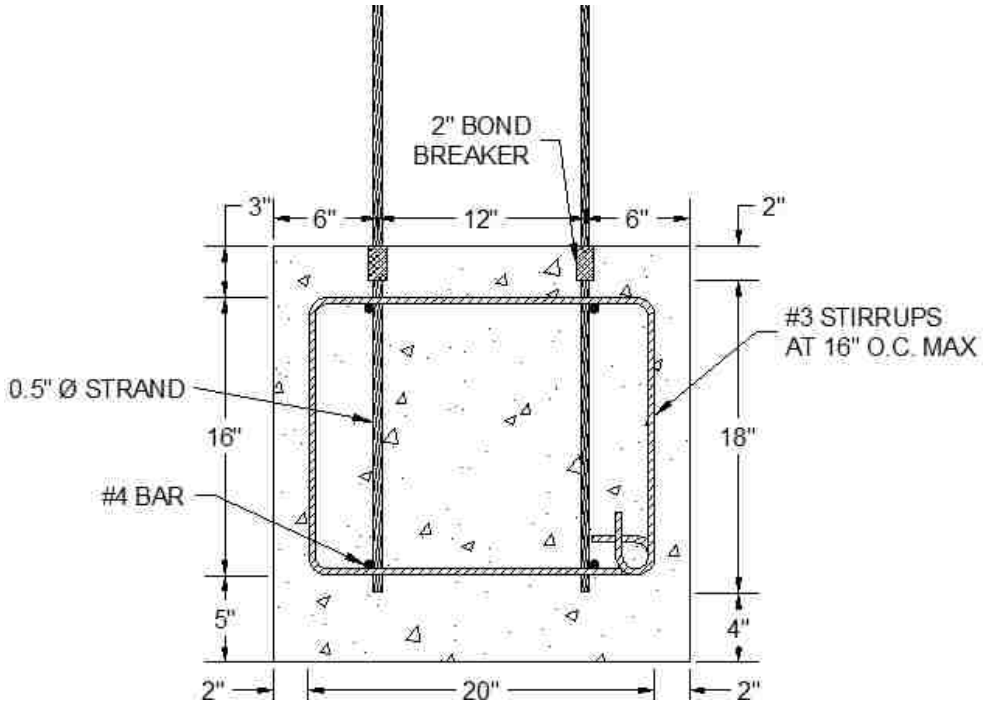

Conversion: 1 in. = 25.4 mm

Figure 3.19 – Cross-Section of LBPT Specimen

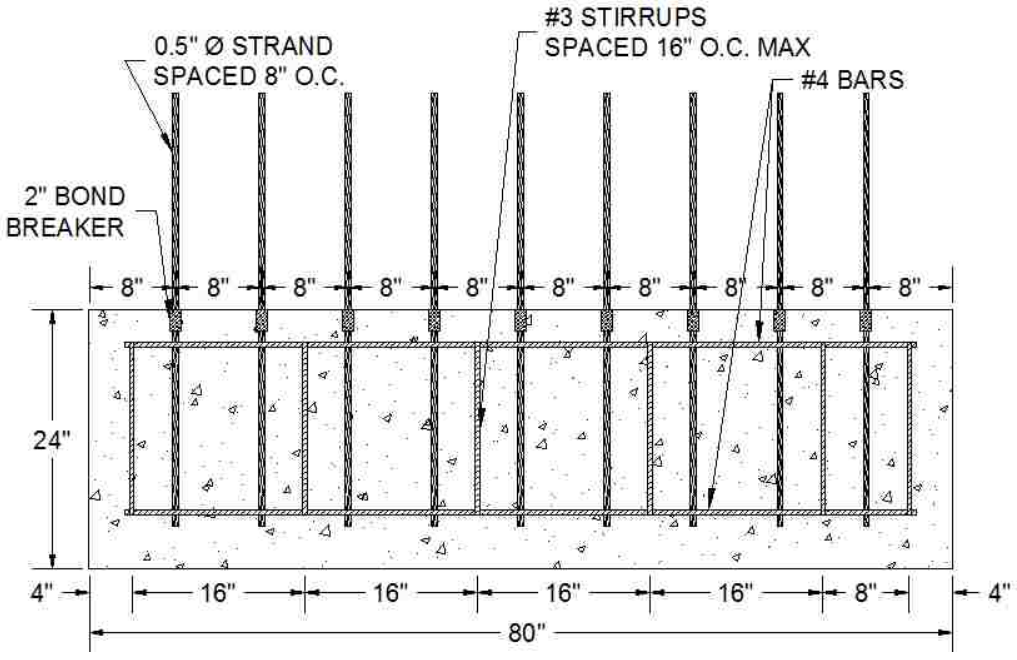

Conversion: 1 in. = 25.4 mm

Figure 3.20 – Profile of LBPT Specimen

3.4.2. LBPT Specimen Fabrication. Due to the large volume of concrete required, the LBPT specimen was cast at a precast plant, and the test was performed on site the day after casting. The form was constructed out of three 8 ft. x 2 ft. (2438 mm x 610 mm) standard formwork panels, which made up the sides and bottom of the form. Standard formwork panels measuring 2 ft. x 3 ft. (610 mm x 914 mm) were secured on each end, but an end block made of a plywood panel and 2x4's was placed at one end of the form to shorten the standard form to the required length of 6 ft.-8 in. (2032 mm). The formwork and reinforcing cage were constructed at the Missouri S&T High Bay Structures Laboratory, and then for casting, the formwork and cage were transported by truck to Prestressed Casting Company, a precast plant located in Springfield, Missouri.

Upon arrival at the plant, the formwork and mild steel cage were placed on top of a precasting bed, and the strands were tied to the designated locations on the longitudinal bars of the reinforcing cage using wire ties. The strands were labeled with duct tape flags and were arranged so that the different strand sources were mixed throughout locations on the specimen to randomize the test in case any inconsistencies in the concrete existed. The strand layout pattern was the same pattern used by Logan (1997) and is shown in Figure 3.21. A picture of the LBPT specimen before casting can be seen in Figure 3.22.

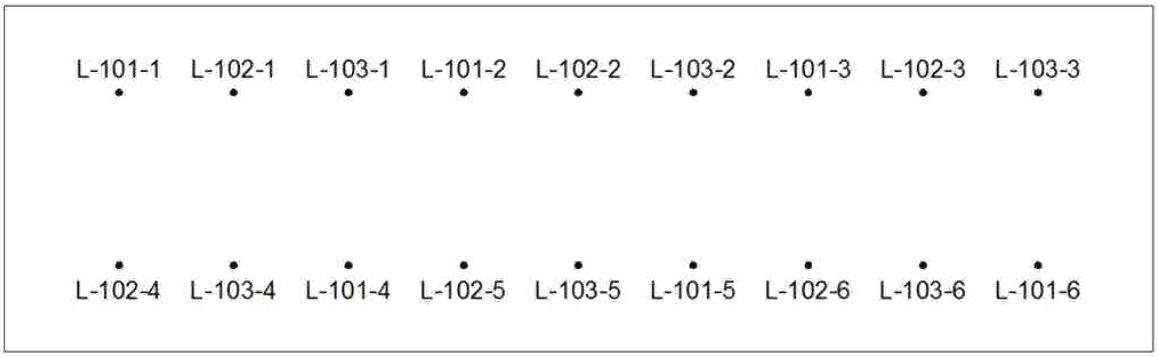

Figure 3.21 – Strand Layout Pattern

Figure 3.22 – LBPT Specimen Before Casting

The specimen was fabricated from structural concrete with no admixtures. The mix design was extremely similar to Logan's (1997), and both mix designs are shown in Table 3.11. Also, it is important to note that Granite-Iron Mountain Trap Rock with an average Mohs Hardness of approximately 6.5 was used for the coarse aggregate. Recent unpublished research by Logan indicates that the Mohs Hardness of the coarse aggregate can affect the test results, and softer aggregates lead to lower pullout values. Therefore, Logan has recently recommended that when conducting the LBPT, the coarse aggregate should have a Mohs Hardness of 6.0 or greater to achieve consistency among testing (D. Logan, personal communication, October 20, 2011).

Table 3.11 – Missouri S&T's and Logan's LBPT Mix Designs

Material	Weight (lb/yd^3)	
	Missouri S&T	Logan
Type III Cement	660	660
¾" Coarse Aggregate	1785	1900
Fine Aggregate	1033	1100
Water	290	290

Conversion: 1 lb/yd^3 = 0.593 kg/m^3

The concrete was mixed at the batch plant on site and delivered by a sidewinder to the specimen form. Before the concrete was placed, a slump test was run according to ASTM C143/C143M–10a: Standard Test Method for Slump of Hydraulic Cement Concrete to ensure the slump was close to the 3 in. (76.2 mm) target slump. Once the slump was deemed acceptable, the LBPT form was filled. Due to the low slump, the concrete was heavily vibrated, but great care was taken during placement and vibration to avoid jostling the strands. The concrete placement process is illustrated in Figure 3.23. During placement, 6 in. x 12 in. (152 mm x 305 mm) cylinders were also cast to determine unit weight and monitor compressive strength, and air content was determined in the field as well. The fresh and hardened concrete properties are presented in Table 3.12.

Figure 3.23 – Casting the LBPT Specimen

After casting, the surface of the LBPT specimen was finished, and then the specimen was cured overnight by means of wet burlap, plastic sheeting, and the heated prestressing bed. The burlap was placed on the surface of the concrete around the strands, and the plastic sheeting was tented over the entire specimen and supported by a frame of

2x4's so the plastic would not touch the strands. The finished specimen and part of the wooden frame for the plastic sheeting is shown in Figure 3.24.

Table 3.12 – Fresh and Hardened Properties of LBPT Concrete Mix

Fresh or Hardened Concrete Property	Value
f'_c at Test (psi)	4,250
Slump (in.)	4
Unit Weight (lb./ft^3)	143.3
Air Content	2.5%

Conversion: 1 psi = 6.89 kPa
1 in. = 25.4 mm
1 lb./ft^3 = 16.0 kg/m^3

Figure 3.24 – Finished LBPT Specimen

3.4.3. LBPT Test Setup and Procedure. On the night before the day of casting, all strands were labeled with duct tape flags and then subjected to a visual inspection and towel wipe test, as prescribed by Logan (1997). The strands were first visually observed for color, rust spots, and rust coatings, and then a clean, white rag was

wiped down the length of the strand, and the amount of residue on the rag was noted. The results of the visual observations and towel wipe tests are presented in Section 3.4.4. After completing the visual observations and towel wipe tests, the strands were packed in a shipping box for transportation to the precast plant for casting the next day.

The strands were cast in the LBPT specimen as described in Section 3.4.2, and then the research team returned to the precast plant approximately 24 hours after casting to perform the pullout tests. The average strength of the concrete at the time of testing was 4,250 psi (29.3 MPa). Logan maintains that LBPT can be performed in concrete strengths ranging from 3,500 psi (24.1 MPa) to 5,900 psi (40.7 MPa) and still give consistent results, so the compressive strength of the concrete at the time of testing was deemed acceptable. Also, it should be noted that no honeycombing or voids were observed in the concrete, indicating adequate consolidation.

Upon arrival at the plant, the form was removed, and then the data acquisition system, 100 kip (4.45 kN) load cell, and 30 ton (8.90 kN) hollow core hydraulic jack were set up. For each strand, first, a steel table was placed over the strand, and then the jack was placed on the strand, followed by a steel plate, the load cell, another steel plate, and a prestressing chuck. The setup is illustrated in Figure 3.25.

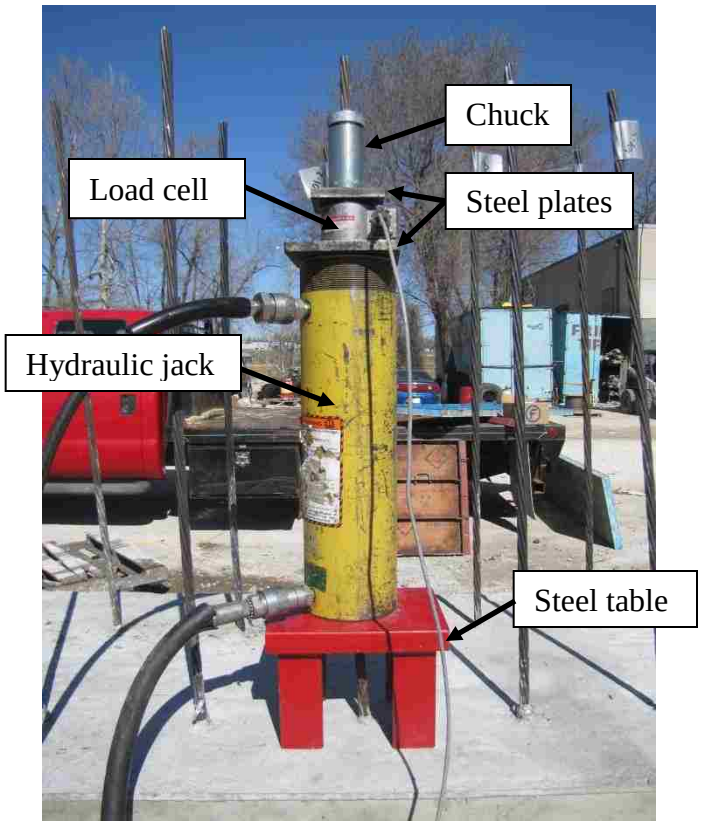

Figure 3.25 – LBPT Hydraulic Jack and Load Cell Setup

The 8 in. x 6 in. x 6-in. (203 mm x 152 mm x 152 mm) steel table, which is pictured in Figure 3.26, was constructed from a 1-in.-thick (25.4 mm) steel plate with a $^{5}/_{8}$-in.-diameter (15.9 mm) hole in the center and four 2 in. x 2 in. (50.8 mm x 50.8 mm) sections of angle. The table was designed based on the one used by Logan, and the purpose of the table was to give the jack a flat surface to contact and help distribute the load to the concrete.

Figure 3.26 – Steel Table for LBPT

Once the jack and load cell were positioned on the strand, a three-person team was used to run the test, as shown in Figure 3.27. One person operated the pump to apply load to the strand, one person observed the strand and reported first slip, and one person monitored the data acquisition system to record the load at first slip and peak load. According to Logan, load is supposed to be applied at approximately 20 kips/min. (89.0 kN/min.). Since the load was applied via a manual pump, there was no direct way to monitor the load rate, so the individual at the data acquisition system used a stopwatch and monitored the load. Based on the load cell and stopwatch, the individual instructed the pump operator to either increase or decrease the loading rate. Additionally, a sample test block with two strands was cast at the same time as the LBPT specimen, and the test block was used to refine the test procedure prior to performing the actual strand pullout tests.

Load was applied until the data acquisition system indicated a distinct drop off in load or until there was a loud noise and a sudden drop off in load. The load noise was determined to be the chuck slipping as the strand stretched and tried to untwist, but then suddenly snapped back into its twisted state. The load at first slip was determined through coordination between the individual watching the strand and the individual monitoring

the data acquisition system. At first noticeable movement, the person watching the strand called out “Slip!”, and the person monitoring the data acquisition system recorded the load value at that moment. Peak load was estimated in the field and then refined through analysis of the collected load data.

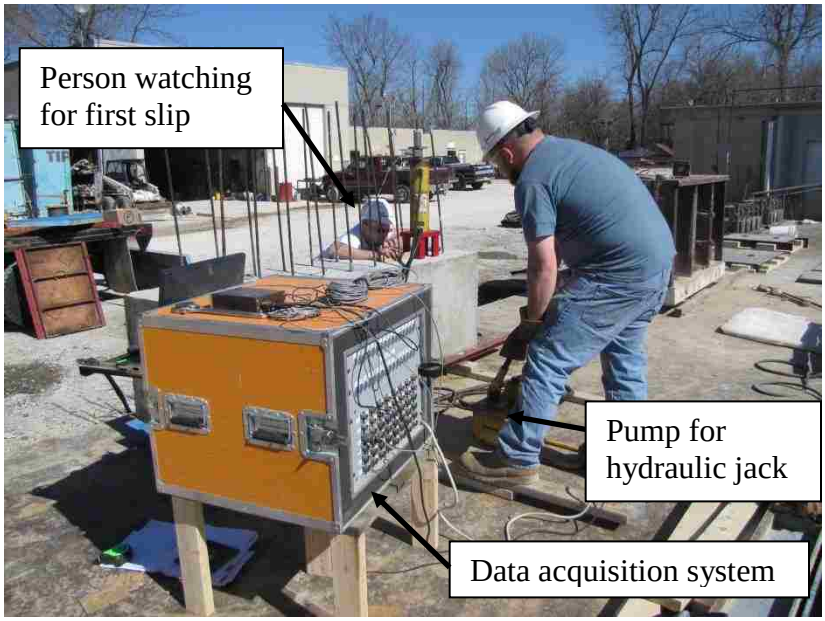

Figure 3.27 – Full LBPT Setup

3.4.4. LBPT Results. The results from the visual observations, towel wipe tests, and the actual pullout tests are discussed summarized for each strand in Table 3.13 and discussed in the following paragraphs.

In terms of the visual observations, a comparison of the strands can be seen in Figure 3.28. Strand type 102 showed the largest number of rust spots and also appeared to have a dull, light rust over all surfaces. Strand types 101 and 103 appeared to be similar in terms of very little noticeable rust, but strand type 103 actually had a slightly shiny, almost blue tinge to the wires. A written description of the visual observations for each strand can be found in Table 3.13.

Table 3.13 – LBPT Results

Specimen ID	First Slip Load (kips)	Peak Load (kips)	Surface Condition (Visual and Towel Wipe)	Test Description
L-101-1	15.9	34.3	No rust Light/moderate residue	Gradual slip to loud noise abrupt drop off in load 2” pullout
L-101-2	17.9	34.2	No rust Light/moderate residue	Gradual slip to peak load, test stopped 1” pullout
L-101-3	20.2	35.9	Light rust Moderate residue	Gradual slip to clear peak load, then load noise and abrupt drop off in load
L-101-4	31.2	38.8	Moderate rust spots in bonded area Moderate residue	Gradual slip to loud noise and abrupt drop off in load 1.5” pullout
L-101-5	19.2	38.5	Moderate/heavy rust spots in bonded area Moderate residue	Gradual slip to loud noise and abrupt drop off in load 2.75” pullout
L-101-6	22.1	38.1	No rust Light residue	Gradual slip to loud noise and abrupt drop off in load 3” pullout
L-102-1	9.7	27.1	Dull, light rust layer Heavy Residue	Gradual slip to loud noise and abrupt drop off in load 2.5” pullout
L-102-2	12.3	27.1	Dull, light rust layer Moderate residue	Gradual slip to peak load, test stopped 2” pullout
L-102-3	13.8	31.0*	Dull, light rust layer Moderate residue	Gradual slip to peak load, test stopped 2” pullout Data recording accidently stopped at

* - Data collection was accidently stopped midway through the test, and this is the estimated value from the field.

Table 3.13 – LBPT Results (Cont.)

Specimen ID	First Slip Load (kips)	Peak Load (kips)	Surface Condition (Visual and Towel Wipe)	Test Description
L-102-4	13.9	40.1	Dull, light rust layer and many heavy rust spots in bonded area Heavy orange residue	Gradual slip, strand broke in concrete 4.5” pullout
L-102-5	12.1	25.1	Dull, light rust layer and some rust spots in bonded area Moderate/heavy residue	Gradual slip to loud noise and abrupt drop off in load 2” pullout
L102-6	14.3	31.9	Dull, light rust layer Moderate/heavy residue	Gradual slip to loud noise and abrupt drop off in load 2.25” pullout
L-103-1	19.7	33.5	Blue tinge, some rust spots at bottom of bonded area Light residue	Gradual slip to loud noise and abrupt drop off in load 2” pullout
L-103-2	21.3	33.5	Blue tinge, little rust specks Moderate residue	Gradual slip to loud noise and abrupt drop off in load 3” pullout
L-103-3	15.9	38.7	Blue tinge, light rust spots in bonded area Moderate residue	Gradual slip to loud noise and abrupt drop off in load 4” pullout, but wedge
L-103-4	17.3	35.6	Blue tinge, light rust spots in bonded area Moderate residue	Gradual slip to loud noise and abrupt drop off in load 3.5” pullout
L-103-5	16.7	26.6	Blue tinge, light rust spots in bonded area Light residue	Gradual slip to loud noise and abrupt drop off in load 2.25” pullout
L-103-6	24.6	39.2	Blue tinge, light rust spots in bonded area Light residue	Gradual slip to loud noise and abrupt drop off in load 3.5” pullout

Conversion: 1 kip = 4.45 kN
1 in. = 25.4 mm

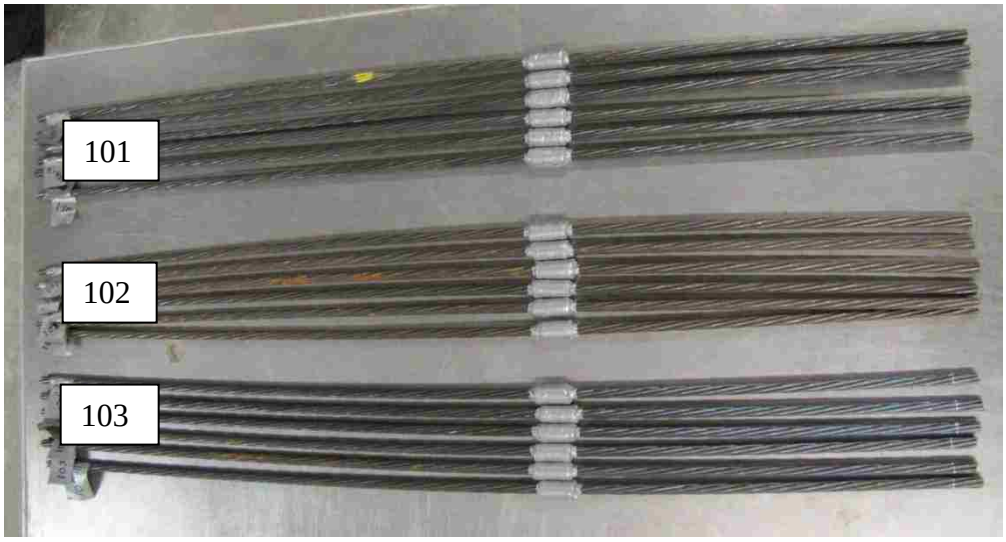

Figure 3.28 – Visual Comparison of Strands

The results of the towel wipe test for strand types 101, 102, and 103 are displayed in Figures 3.29, 3.30, and 3.31, respectively. Compared to the other strand types, type 102 had a noticeable moderate to heavy brown/orange residue on almost all strands (Figure 3.30). Strand type 103 showed very light residue (Figure 3.31), and strand type 101 exhibited light to moderate amounts of residue (Figure 3.29). A written description of the results of the towel wipe test for each strand can be found in Table 3.13.

Figure 3.29 – Towel Wipe Results for Strand Type 101

Figure 3.30 – Towel Wipe Results for Strand Type 102

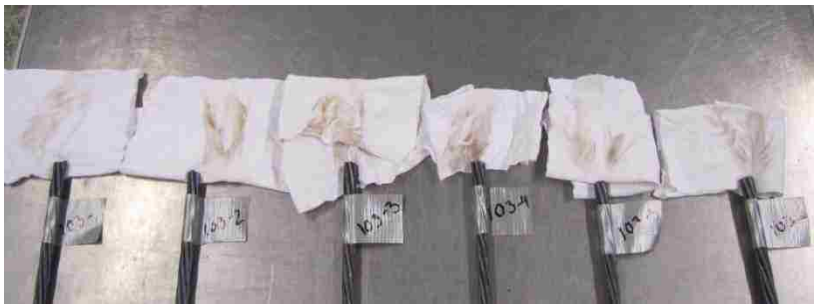

Figure 3.31 – Towel Wipe Results for Strand Type 103

Time and load were collected by the data acquisition system at a sampling rate of two points per second, and the data was converted into excel files to plot load vs. time and determine the maximum applied load. The load vs. time plots can be found in Appendix C. The estimated first slip load and peak load determined from the collected data are summarized for each strand in Table 3.13. A summary of just the first slip and peak pullout loads, along with the averages, standard deviations, and coefficients of variation for each strand type are presented in Table 3.14. For comparison, it should be noted that Logan's limits for first slip and peak load are 16 kips (71.2 kN) and 36 kips (160 kN), respectively.

As the footnote on Tables 3.13 and 3.14 indicate, the peak load for L-102-3 is load from field observations because the data was not collected electronically. However, this value is still considered valid because during analysis, it was noted that estimated values were very close to the values determined through analysis of the electronically collected data. Additionally, as noted in the footnote in Table 3.14, the peak load for L-

102-4 and the first slip load for L-101-4 were not included in their respective averages or standard deviations. For L-102-4, because the peak load exceeded 40 kips and it was observed that the strand became untwisted above the concrete at failure, it was determined that this specimen actually ruptured in the concrete. This was seen as an anomaly, especially since this was the strand type with the worst bond overall, so the peak load value was not used in the analysis. Additionally, the first slip load of L-101-4 was deemed high, so the value was not included in the first slip average for that specimen.

Table 3.14 – Summary of LBPT Pullout Loads

Strand Type	Specimen ID	First Slip Load				Peak Load			
		Load (kips)	Avg. (kips)	Std. Dev. (kips)	COV	Load (kips)	Avg. (kips)	Std. Dev. (kips)	COV
101	L-101-1	15.9	19.1	2.3	12.27%	34.3	36.6	2.1	5.76%
	L-101-2	17.9				34.2			
	L-101-3	20.2				35.9			
	L-101-4	31.2**				38.8			
	L-101-5	19.2				38.5			
	L-101-6	22.1				38.1			
102	L-102-1	9.7	12.7	1.7	13.53%	27.1	27.8	2.9	10.40%
	L-102-2	12.3				27.1			
	L-102-3	13.8				31.0*			
	L-102-4	13.9				40.1**			
	L-102-5	12.1				25.1			
	L-102-6	14.3				31.9			
103	L-103-1	19.7	19.3	3.3	17.16%	33.5	34.5	4.6	13.30%
	L-103-2	21.3				33.5			
	L-103-3	15.9				38.7			
	L-103-4	17.3				35.6			
	L-103-5	16.7				26.6			
	L-103-6	24.6				39.2			

Conversion: 1 kip = 4.4 kN

* - Data collection was accidently stopped midway through the test, and this is the estimated value from the field.

** - Load was removed from average and std. dev.

4. TRANSFER LENGTH AND DEVELOPMENT LENGTH TEST PROGRAM AND RESULTS

4.1. INTRODUCTION

In order to study the effect that different concrete mixes have on transfer length and development length, twelve 17-foot long (5,182 mm) rectangular prestressed beams with either two or four strands were constructed. The beams were first used to measure transfer lengths at release and then periodically over two months. After all transfer length measurements had been taken, each end of each beam was tested in flexure at different span lengths to determine if development lengths calculated from AASHTO and ACI codes are conservative for the concrete mixes tested. The design and fabrication of the beams are presented in Sections 4.2 and 4.3, respectively. Section 4.4 covers the setup, procedure, and result for each transfer length test, and the setup, procedure, and results from the development length test program are presented in Section 4.5.

4.2. TRANSFER AND DEVELOPMENT LENGTH BEAM DESIGN

In terms of specimen design, the concrete mixes were based on typical mix designs produced around Missouri, and the dimensions and reinforcement layouts of the specimens were based on previous research done by Ramirez and Russell (2008). The details of the mix designs and specimen designs are discussed in this subsection.

4.2.1. Mix/Specimen Identifications and Mix Designs. The goal of the research was to evaluate the effects of type of concrete and concrete strength on strand bond performance. As a result, four mix designs were developed: a normal and high strength conventional concrete and a normal and high strength self-consolidating concrete (SCC). The target strengths for the normal strength and high strength mixes were 6,000 psi (41.4 MPa) and 10,000 psi (69.0 MPa), respectively. An identification code was developed to distinguish the mixes and specimens, as shown in Figure 4.1.

For example, C6 simply refers to the conventional concrete, 6,000 psi (41.4 MPa) target strength mix, while C6-2-1 refers to the beam fabricated with the conventional concrete, 6,000 psi (41.4 MPa) target strength mix, having two strands, and being the first of two beams constructed with the specific mix and strand layout. Since the two-strand

beams were used for testing both transfer length and development length, an additional code was added to distinguish between the tests. For instance, C6-2-1_NE indicates the transfer length testing on the north end of the strand on the east side of the beam previously described, while C6-2-1_58 indicates the testing of the 58 in. (1,473 mm) embedment length on the same beam. All directions for transfer length designation are relative to the cardinal position of casting.

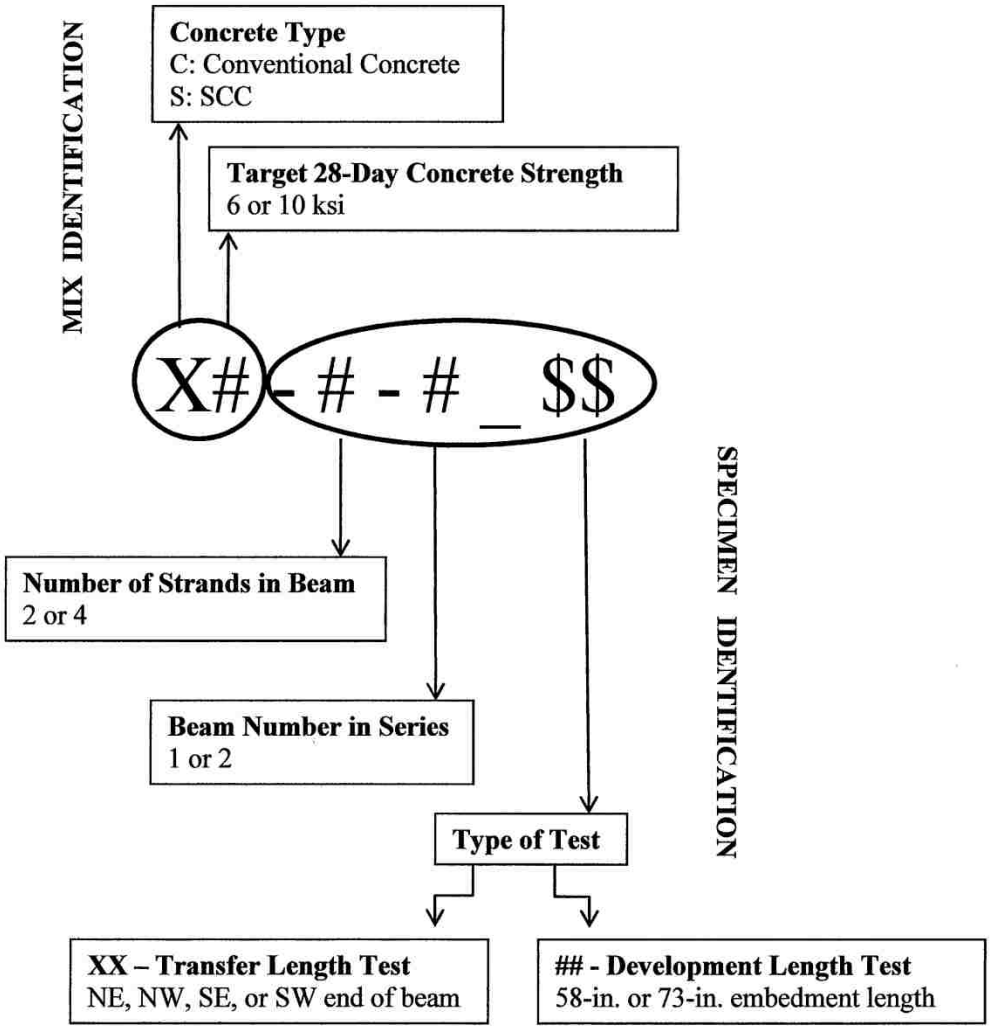

Figure 4.1 – Mix and Specimen Identification Code

The normal strength conventional mix (C6) is MoDOT's A-1 precast/prestressed mix, and the remaining mix designs were developed based on results from surveys that were sent to precast plants around Missouri and previous research performed at Missouri S&T. This step ensured that the concrete used in the research would be comparable to the concrete that is being used in the field. The mix designs are broken down in Table 4.1.

Table 4.1 – Mix Designs

Material	Concrete Mix ID			
	C6	**S6**	**C10**	**S10**
Type III Cement (lb/yd^3)	750	750	840	840
Class C Fly Ash (lb/yd^3)	0	0	210	210
Water (lb/yd^3)	278	278	315	315
Fine Aggregate (lb/yd^3)	1166	1444	1043	1291
Coarse Aggregate (lb/yd^3)	1611	1333	1440	1192
MB-AE-90 (oz/yd^3) [oz/cwt]	11.3 [1.5]	11.3 [1.5]	13.7 [1.3]	10.5 [1.0]
Glenium 7700 (oz/yd^3) [oz/cwt]	29.3 [3.9]	46.5 [6.2]	52.5 [5.0]	75.6 [7.2]

Conversion: 1 lb/yd^3 = 0.593 kg/m^3
1 oz/yd^3 = 38.7 mL/m^3

4.2.2. Fresh and Hardened Properties of Concrete Mixtures. All mixes were first tested in trial batches in the Materials Lab at Missouri S&T in order to work out the correct mix proportions to obtain the target fresh and hardened properties before the final specimens were constructed at Coreslab Structures, Inc. (Coreslab) in Marshall, MO. Final fresh and hardened properties of all four concrete mixtures were measured and recorded.

In terms of fresh properties, slump, slump flow, and J-ring were performed on the appropriate mixes, and unit weight and air content were found for all mixes. The standard slump test was run on the conventional concrete mixes according to ASTM C143/C143M-10a: Standard Test Method for Slump of Hydraulic Cement Concrete.

Slump flow for the SCC mixes was measured according to ASTM C1611/C1611M-09 Standard Test Method for Slump Flow of Self-Consolidating Concrete using Filling Procedure B in Section 8.2.2 with the inverted slump mold. Additionally, passing ability of the SCC mixes was evaluated using ASTM C1621/C1621M-09b: Standard Test Method for Passing Ability of Self-Consolidating Concrete by J-Ring. Air content for all mixes was determined using a Type B pressure meter and following ASTM C231/C231M-10: Standard Test Method for Air Content of Freshly Mixed Concrete by the Pressure Method. Finally, unit weight of each mix was determined through the rodding procedure specified in Section 6.3 of ASTM C138/C138M-10b: Standard Test Method for Density (Unit Weight), Yield, and Air Content (Gravimetric) of Concrete. The fresh properties of all four mixtures are shown in Table 4.2.

Table 4.2 – Fresh Concrete Properties

Property	Concrete Mix ID			
	C6	S6	C10	S10
Slump (in.)	8.5	N/A	4.5	N/A
Slump Flow (in.)	N/A	28	N/A	22
J-Ring (in.)	N/A	28	N/A	18
Unit Weight (lb/ft^3)	137.6	139.2	142.4	141.6
Air Content (%)	6	7.5	6.5	7

Conversion: 1 in. = 25.4 mm
1 lb/ft^3 = 16.0 kg/m^3

In terms of hardened concrete properties, compressive strength was measured at 1, 4, 8, 14, and 28 days, and the modulus of elasticity was determined at 28 days. The normal strength mixes had target one day strengths of 4,000 psi (27.6 MPa) and target 28 day strengths of 6,000 psi (41.4 MPa), while the high strength mixes were designed to reach 6,000 psi (41.4 MPa) and 10,000 psi (69.0 MPa) at one day and 28 days, respectively. All compressive strengths were determined by testing 4 in. x 8 in. (102 mm x 203 mm) cylinders on the Forney compressive testing machine and following ASTM

C39/C39M-11a: Standard Test Method for Compressive Strength of Cylindrical Concrete Specimens.

In addition to testing compressive strength, the modulus of elasticity of each concrete mix was tested and recorded at 28 days. To determine modulus of elasticity of each mix, a two-ring modulus test frame was used in accordance with the procedure specified by ASTM C469/C469M-10: Standard Test Method for Static Modulus of Elasticity and Poisson's Ratio of Concrete in Compression.

Table 4.3 summarizes the initial and 28 day compressive strengths and the 28-day moduli of elasticity for the four mixes. The C10 mix was the only mix that did not reach the one day target strength, and three of the four mixes did not reach the target 28 day strengths. C6 was just slightly under the goal of 6,000 psi (41.4 MPa), while the two high strength mixes fell short of the 10,000 psi (69.0 MPa) target strength. However, the 28 day strengths of C10 and S10 were still high enough to be significantly different than the 28 day C6 and S6 strengths. A full 28 day strength curve can be found in Appendix A.

Table 4.3 – Concrete Strengths and 28 Day Moduli of Elasticity

Property	C6	S6	C10	S10
f'_{ci} (psi)	4810	5660	5670	6330
f'_{c} (psi)	5730	6950	8480	9250
Modulus of Elasticity (psi)	4,126,500	4,820,500	4,806,800	4,736,900

Conversion: 1 psi = 6.89 kPa

4.2.3. Strand and Mild Reinforcement Design. The beams used for measuring transfer length and testing development length were designed based on the specimens constructed for similar research completed by Ramirez and Russell (2008). The beams were designed to be 17 ft. (5,182 mm) in length with 6.5 in.-wide (165 mm) by 12 in.-high (305 mm) cross-sections. The prestressing strand for all beams consisted of 0.5 in.-diameter (12.7 mm), Grade 270, low relaxation seven wire strand from the same roll. As illustrated in Figure 4.2, the two-strand beams were constructed with two strands placed 2

in. (50.8 mm) from the bottom and spaced 2.5 in. (63.5 mm) on center. The four strand beams were constructed with two strands at 2 in. (50.8 mm) from the bottom and two strands at 2 in. (50.8 mm) from the top, with both sets again spaced at 2.5 in. (63.5 mm) on center, as shown in Figure 4.3. The four-strand beams were included in the research program in order to study the effect of casting position on transfer length.

The mild reinforcement consisted of closed stirrups constructed out of ASTMA615, Grade 60, #3 mild reinforcing steel. The stirrups were placed at 2 in. (76.2 mm) on center at the ends of the beams to conservatively meet AASHTO requirements for cracking at release and spaced 6 in. (152 mm) on center elsewhere to ensure the beams would not fail in shear when undergoing flexural testing for development length. Two ASTM A615, Grade 60, #6 bars were placed in the top of each beam to control stresses during release. The profiles and strand and reinforcement layouts of the two-strand and four-strand beams are illustrated in Figure 4.4 and Figure 4.5, respectively.

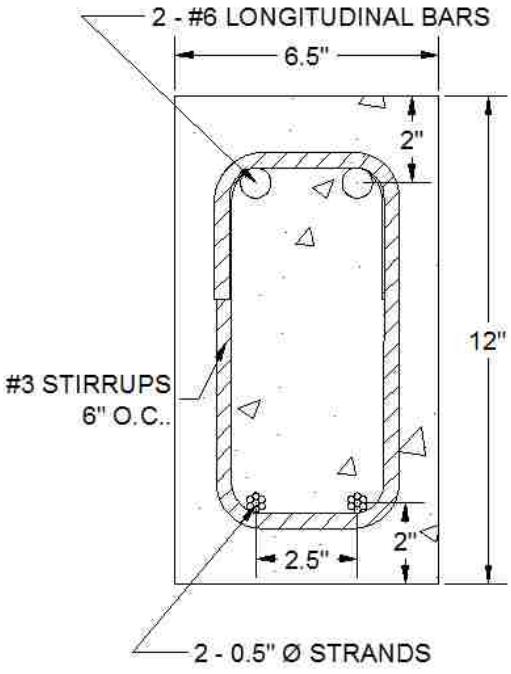

Conversion: 1 in. = 25.4 mm

Figure 4.2 - Two-Strand Beam Cross-Section

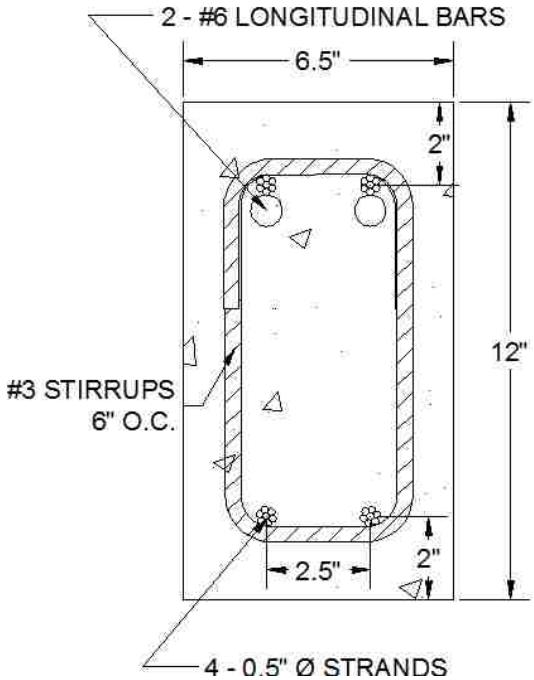

Conversion: 1 in. = 25.4 mm

Figure 4.3 – Four-Strand Beam Cross-Section

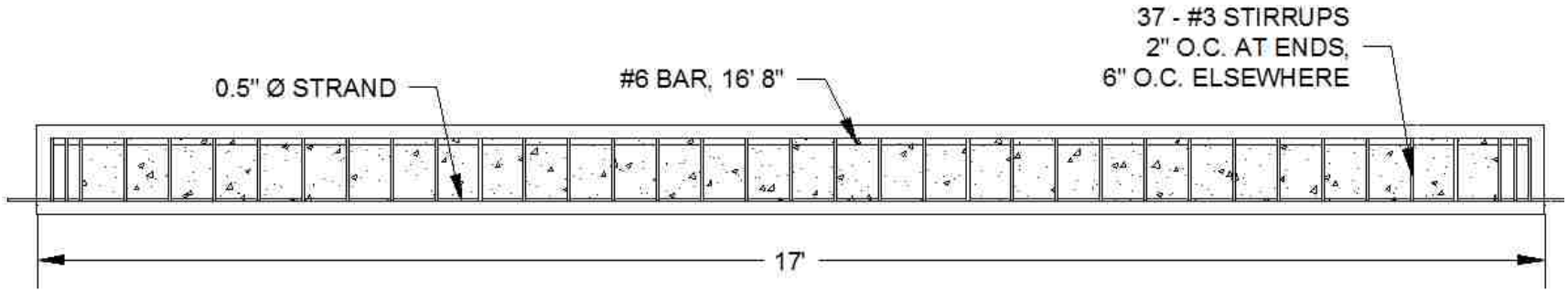

Conversion: 1 in. = 25.4 mm
1 ft. = 305 mm

Figure 4.4 – Profile of Two-Strand Beams

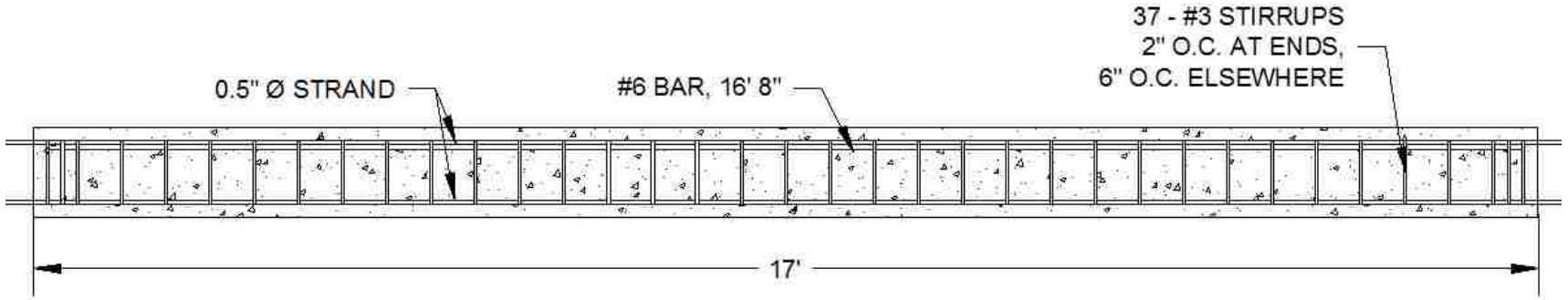

Conversion: 1 in. = 25.4 mm
1 ft. = 305 mm

Figure 4.5 – Profile of Four-Strand Beams

4.3. TRANSFER AND DEVELOPMENT LENGTH BEAM FABRICATION

The beams were cast at Coreslab, a precast plant in Marshall, Missouri. Three beams designed to measure transfer length and development length were cast per mix: two two-strand beams and one four-strand beam. Additionally, one beam designed for shear testing was fabricated from each mix. While the shear beams are shown in the prestressing bed layout (Figures 4.6 and 4.7), the testing of these beams is not covered in this thesis.

The C6 and S6 beams were cast on July 21, 2011, while the C10 and S10 beams were cast on July 25, 2011. All sets of beams were released at approximately 24-26 hours after casting. The beams were cast in a 100-ft.-long (30.48 m) prestressing bed with the two-strand beams cast in one line, the four-strand beams cast in another line, and the shear beams cast in a third line. The prestressing bed layout for the C6 and S6 beams is depicted in Figure 4.6, while the layout for the C10 and S10 beams is shown in Figure 4.7.

For each mix, the concrete was mixed at the on-site batch plant and then delivered to the bed by a sidewinder. Fresh properties were measured and recorded, and once the batch was deemed acceptable, the sidewinder proceeded to fill the four beam molds (two two-strand beams, one four-strand beam, and one shear beam). One batch in the sidewinder was sufficient to complete all four beams, so the mix was kept consistent from beam to beam. The beams constructed with the conventional concretes were heavily vibrated, and the SCC beams were also lightly vibrated to ensure full consolidation. The sidewinder and beam fabrication process is illustrated in Figure 4.8.

Casting for both the normal strength and high strength mixes took place between late morning and early afternoon on the days of casting. The beams were cured with wet burlap and plastic overnight, and then the forms were removed early the next morning so the instrumentation could be applied before releasing the strands. Figure 4.9 shows the transfer length and the development length beams after removal of the forms and before instrumentation.

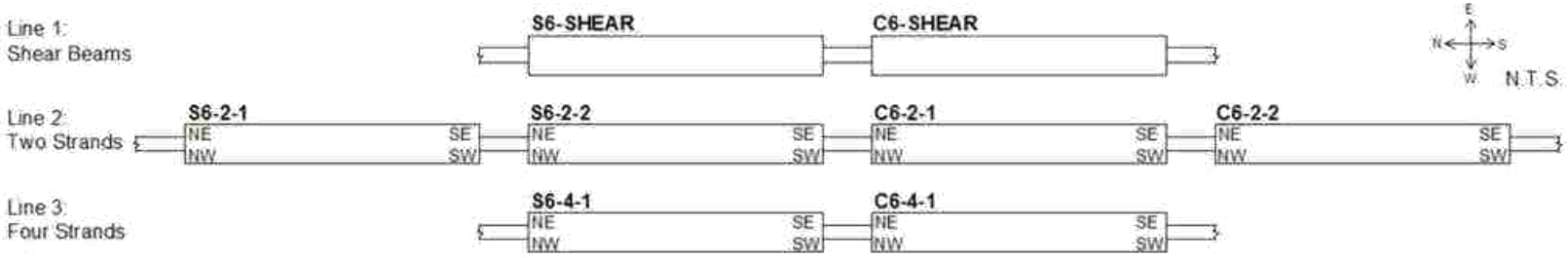

Figure 4.6 – C6 and S6 Prestressing Bed Layout

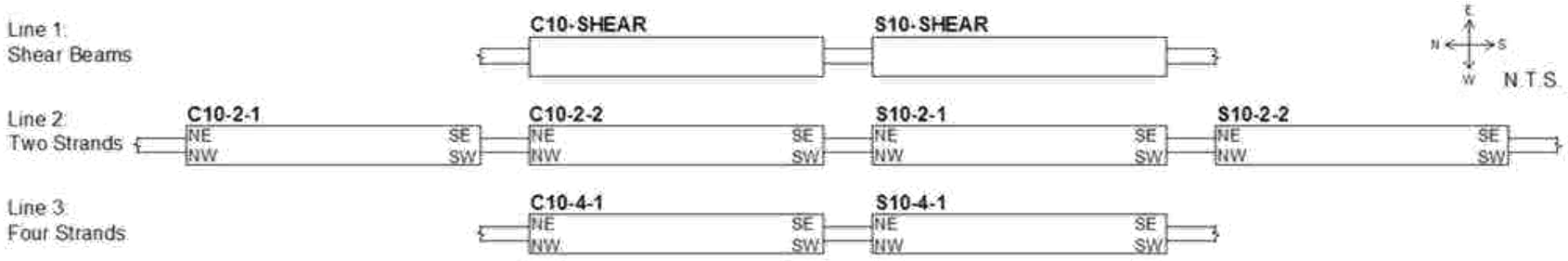

Figure 4.7 – C10 and S10 Prestressing Bed Layout

Figure 4.8 – Beam Fabrication at Coreslab Structures in Marshall, MO

Figure 4.9 – Beams After Form Removal and Before Instrumentation

Strands were released between 24-26 hours after casting, and bolt cutters were used to release the strands one at a time. Since transfer length is affected by method of release, and the harsher the release method, the longer the transfer length, cutting the

strands abruptly with bolt cutters was a conservative, or worst-case, method of release. Inorder to try and release each strand all at once, one person lined up at each location where the strand would need to be cut to separate all the beams, and then the strands were ordered to be cut at the same time on cue. Figure 4.10 demonstrates how bolt cutters were used to release the strands. It should be noted that often, not all strands were cut on the first try at all locations. Consequences of the sequence of strand release will be discussed in Section 5.3.1.

Figure 4.10 – Bolt Cutting Strands at Release

4.4. TRANSFER LENGTH TEST SETUPS, PROCEDURES, AND RESULTS

Tests were done to determine transfer length at release as well as monitor the change in transfer length over time. The 95% Average Mean Strain Method, which depended on readings from demountable mechanical (DEMEC) points and a DEMEC strain gauge, was the main method employed to determine transfer lengths periodically from release to approximately 56 days after casting. Additionally, transfer lengths at release were also determined by the end slip method, which involves calculating an initial transfer length based on how much the strand slips into the concrete upon cutting. End

slip of the strands was measured by linear potentiometers as well as by hand with a steel tape measure.

4.4.1. 95% Average Mean Strain Method. The 95% Average Mean Strain Method relies on the theory of strain compatibility between the strand and concrete. When a pretensioned strand is released, the strand loses some stress due to elastic shortening. In the transfer zone, the stress and strain in the steel and concrete are equal to zero at the unrestrained end of the beam and increase linearly as the strand transfers its stress to the concrete through bond. Beyond the transfer zone in the fully bonded area, the change in strain of the strand from the initial strain to the strain after release is equal to the strain in the concrete. By measuring concrete surface strain with DEMEC points and a DEMEC gauge, the point where the concrete strain, or the change in strain of the strand, becomes constant can be determined, and this point is the transfer length. Russell and Burns (1993) explained the use of DEMEC points and the 95% Average Mean Strain Method in depth, and many researchers have since used this process to successfully determine transfer lengths.

The following subsections explain the process of affixing the DEMEC points, taking DEMEC readings, converting the readings into strains, plotting the strains, and determining transfer lengths based on the plots. The final transfer lengths at 1, 4, 8, 14, 28, and approximately 56 days as determined by the 95% Average Mean Strain Method are presented in Subsection 4.4.1.3.

4.4.1.1 DEMEC instrumentation. On the morning after casting, the forms were removed, and a permanent marker was used to mark each beam with the correct beam identification code and to mark each end with cardinal points of NE, NW, SE, or SW based on casting position. Since each beam contained two strands of interest (the top two strands on the four strand beams), and each strand had two ends once the beam was released, the direction labels identified the four distinct transfer lengths per beam.

The DEMEC points were to be applied on the concrete surface at each transfer length location at the level of the prestressing strand. Therefore, after identifying the beams, a 5-ft.-long (1.52 m) line was marked starting from the end of the beam at each of the four transfer length locations on each beam at 2 in. (50.8 mm) from the bottom on the two strand beams and 2 in. (50.8 mm) from the top on the four-strand beams. A

plexiglass template with nine 1/8-in.-diameter (3.18 mm) holes was then used to mark where the DEMEC points should be applied. The holes in the template began 0.98 in. (25 mm) from each end, and the holes were spaced 3.94 in. (100 mm) apart. The template was lined up with the closest end of the beam, and the first nine holes were marked along the line that had been drawn. Then the template was repositioned such that the first hole in the template lined up with the last hole that was marked, and an additional eight points were marked for a total of 17 points per transfer length location.

Once all the points were marked, a three-person team worked to apply a dab of 5-minute, concrete-metal epoxy to each marking, affix a DEMEC point, and set the points with the 7.87 in. (200 mm) setting bar. Figure 4.11 depicts setting the DEMEC points. A few points could not be set due to surface honeycombing over the area where the point was supposed to be located. In these cases, the point was simply skipped. An example of this can be seen in Figure 4.12, where point 4 on C10-4-1_SW could not be placed due to honeycombing.

Figure 4.11 – Setting DEMEC Points with Setting Bar

Figure 4.12 – Honeycombing Preventing DEMEC Placement at Point 4 on C10-4-1_SW

After all the points were set, initial readings were taken with the DEMEC gauge before the strands were cut. Figure 4.13 shows an example of how the DEMEC readings were taken. Since the DEMEC gauge is designed to measure points set with the 7.87 in. (200 mm) setting bar, and the points were spaced 3.94 in. (100 mm) apart, overlapping readings were taken. If points were missing due to honeycombing or set incorrectly and unreadable, the readings involving that point were simply skipped. After the initial reading, subsequent readings were taken immediately after release (1 day), and then at 4, 8, 14, and 28 days, and then at the time of development length testing, or around 56 days. All subsequent readings were compared back to the initial reading to determine the change from the initial point prior to strand release.

The beams were stored in the storage yard at Coreslab through 28 days so that the DEMEC points would not be disturbed by travel from the plant to the university. Figure 4.14 shows the storage conditions for the beams. Although the beams were subject to temperature and humidity changes from being stored outdoors, the DEMEC reference bar was not needed for corrections. For this research, the absolute change from the initial reading did not matter, only the relative change. The 95% Average Mean Strain Method

is not based on the strain readings themselves, but simply where the strain readings along the length of the beam become constant.

Figure 4.13 – Taking DEMEC Readings

Figure 4.14 – C6 and S6 Beams in Storage Yard at Coreslab

4.4.1.2 95% Average Mean Strain procedure. The first step in the 95% Average Mean Strain Procedure was determining the strains. The initial readings were subtracted from the final DEMEC readings on a given day, and the change in DEMEC reading was multiplied by the calibration factor provided by the manufacturer to convert the DEMEC number into microstrain. Consecutive sets of three readings were then averaged so the final plot would have a "smoothed curve." The first point consisted of the mean of the first two readings, and the mean of every three readings was taken after that. An illustration of how the readings were averaged can be found in Figure 4.15, and the pattern shown would continue for all points. If readings were missing due to missing or faulty points, the other two readings in the set of three were averaged to obtain the mean strain for that point.

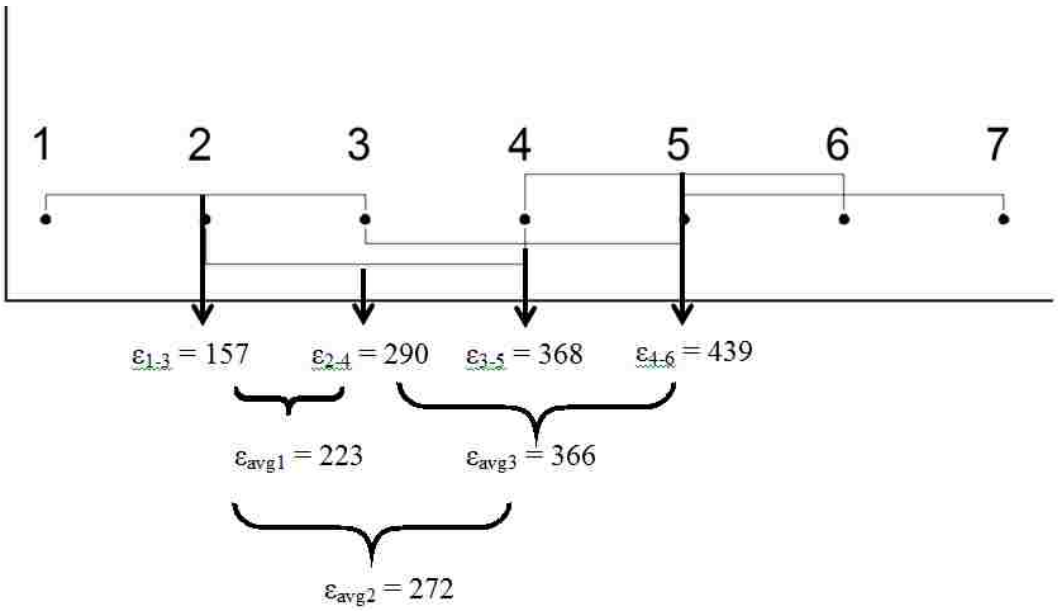

Figure 4.15 – Mean Strains

Once the mean strains and the values' corresponding distances from the end of the beam were determined, a plot of microstrain vs. distance from the end of the beam was created for each strand. A typical smoothed mean strain plot for one strand with readings from immediately after release is illustrated in Figure 4.16. In this particular case, the plot

shows the strains along the north and south ends of the east strand of beam S10-2-2. The plateaus on each of the curves indicate where the strain became constant, which indicates that the prestressing force had been fully transferred to the beam.

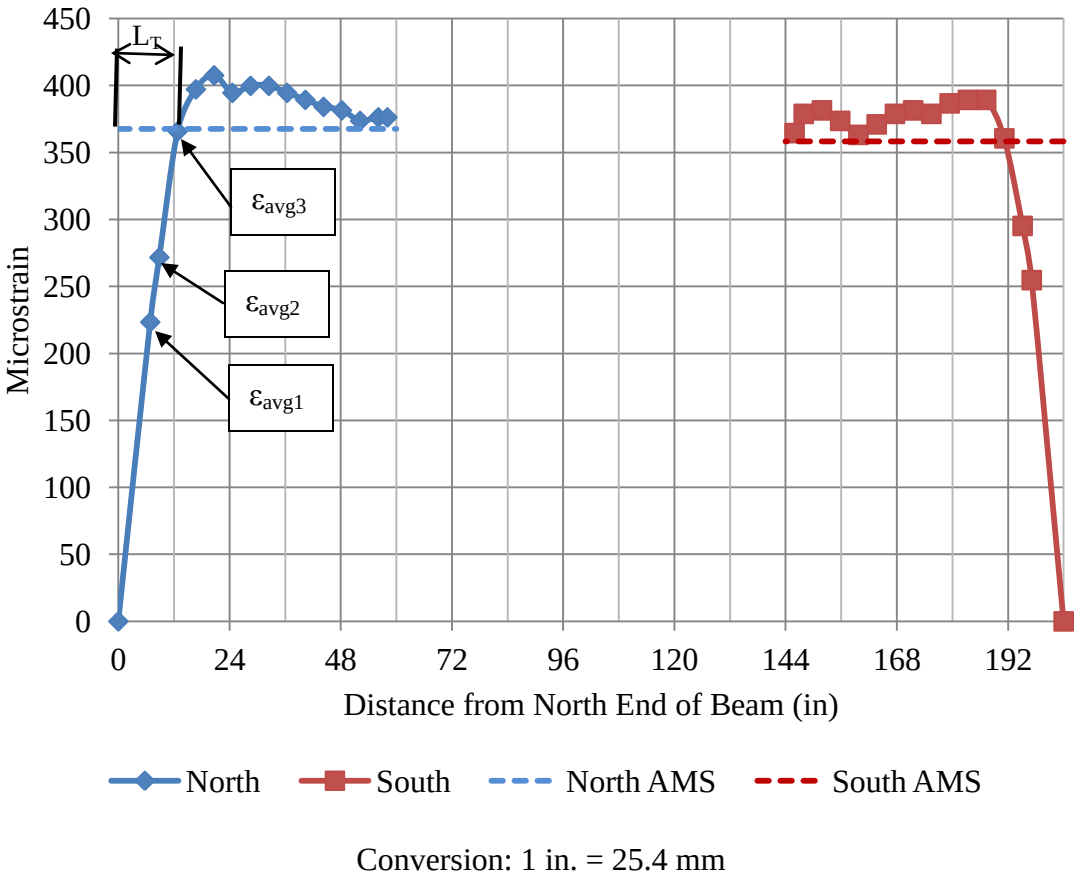

Figure 4.16 – Typical 95% Average Mean Strain Smoothed Curve for Determining Transfer Lengths – S-10-2-2-NE and S10-2-2_SE

In order to apply the 95% Average Mean Strain Method, the points on each plateau were averaged to come up with an average mean strain value. Determining which points should be included in the plateau is subjective, but the method is designed so that subtle fluctuations in including or not including a point one way or the other has a negligible effect on the transfer length (Russell and Burns 1993). After an average value of the plateau was determined, a line was drawn on the plot at 95% of the average mean

strain value. The intersection of the 95% average mean strain line and the smoothed curve on each plot indicates the transfer length for that strand end. This intersection calculation was done by linearly interpolating between the two curve points where the 95% average mean strain line met the curve.

4.4.1.3 95% Average Mean Strain transfer lengths. Four transfer lengths were determined per beam for a total of eight bottom transfer lengths and four top transfer lengths per day, per mix. A typical strain plot for one strand is shown in Figure 4.17. The plot contains the strain profiles for DEMEC readings taken at 1, 4, 8, 14, 28, and approximately 56 days. All strain plots, like the typical plot shown in Figure 4.17, are included in Appendix D.

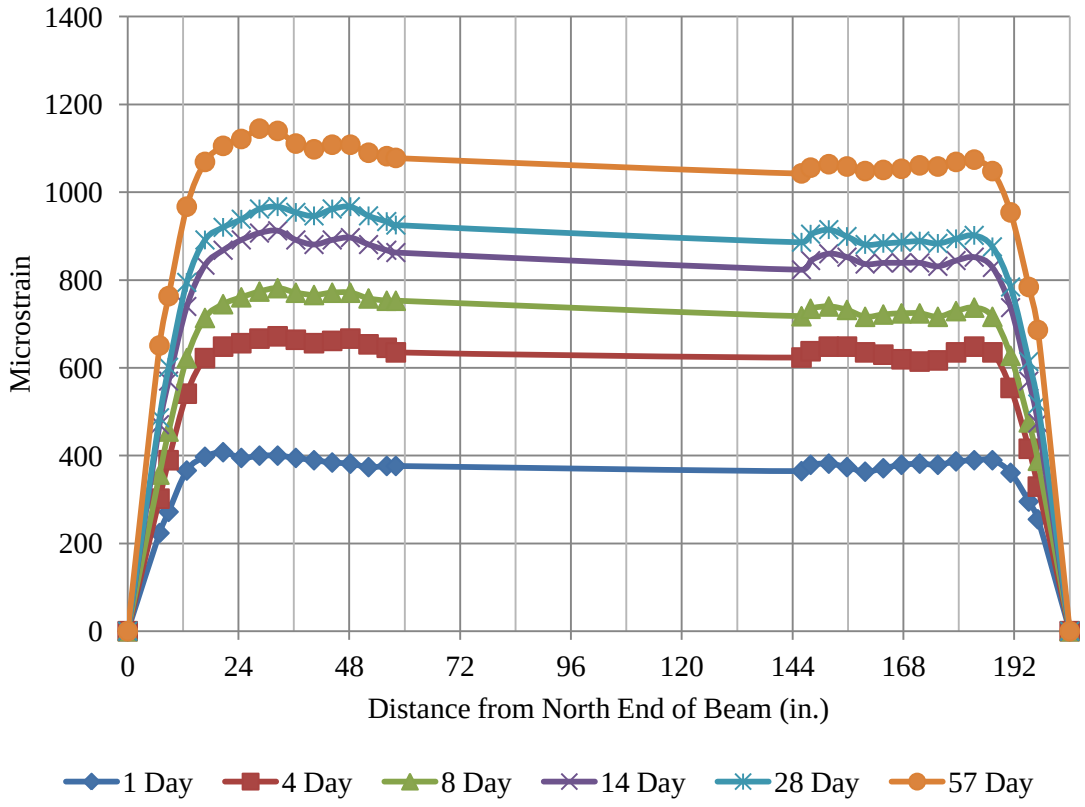

Conversion: 1 in. = 25.4 mm

Figure 4.17 – Typical 95% Average Mean Strain Smoothed Curves for Determining Transfer Lengths from 1 to 28 Days – S10-2-2-NE and S10-2-2_SE

Tables 4.4 and 4.5 list transfer lengths for all specimens for 1, 4, 8, 14, 28 and approximately 56 days as determined by the 95% Average Mean Strain Method. Table 4.4 reports transfer lengths of the top strands of the four-strand beams, while Table 4.5 reports the transfer lengths of the bottom strands of the two-strand beams. Table 4.6 summarizes the average transfer lengths, standard deviations, and coefficients of variation (COV) for the top strands for each mix at each day. Table 4.7 contains the same average value, standard deviation, and COV summary for the bottom strands. N/A indicates that a transfer length reading could not be obtained because the DEMEC readings did not result in a plot where a conclusive transfer length could be determined.

Table 4.4 – Transfer Lengths for Top Strands of Four-Strand Beams (1-28 Days)

Transfer Length ID		1 Day (in.)	4 Day (in.)	8 Day (in.)	14 Day (in.)	28 Day (in.)	~56 Day (in.)
C6-4-1	NE	N/A	N/A	N/A	N/A	N/A	N/A
	NW	N/A	N/A	N/A	N/A	N/A	N/A
	SE	31.3	N/A	30.0	31.2	31.8	N/A
	SW	18.2	N/A	24.9	24.1	25.9	26.3
S6-4-1	NE	20.5	24.7	22.6	22.2	20.9	22.8
	NW	N/A	N/A	N/A	N/A	N/A	N/A
	SE	N/A	N/A	N/A	N/A	N/A	N/A
	SW	15.9	18.9	21.9	20.1	19.2	22.0
C10-4-1	NE	18.8	19.7	19.4	19.8	23.9	22.3
	NW	15.3	16.5	17.6	16.6	17.0	18.8
	SE	15.1	13.3	14.7	14.8	15.8	N/A
	SW	18.9	19.2	19.2	18.8	19.2	19.7
S10-4-1	NE	18.0	15.5	14.2	14.7	14.7	15.2
	NW	17.6	18.4	17.1	17.5	16.6	18.2
	SE	27.7	21.2	28.1	27.9	28.0	29.0
	SW	14.0	12.8	14.8	15.9	14.0	15.6

Conversion: 1 in. = 25.4 mm

Table 4.5 – Transfer Lengths for Bottom Strands of Two-Strand Beams (1-28 Days)

Transfer Length ID		1 Day (in.)	4 Day (in.)	8 Day (in.)	14 Day (in.)	28 Day (in.)	~56 Day (in.)
C6-2-1	NE	19.6	20.1	27.7	29.2	31.9	28.6
	NW	20.3	22.0	22.0	23.5	24.4	23.9
	SE	19.8	22.3	30.4	30.4	30.6	N/A
	SW	15.5	20.0	21.2	24.1	26.0	23.6
C6-2-2	NE	17.0	27.3	19.7	22.1	20.6	25.6
	NW	13.8	16.1	16.6	17.0	17.6	18.7
	SE	14.2	15.2	17.0	16.5	16.4	15.9
	SW	N/A	N/A	23.6	26.5	21.3	23.0
S6-2-1	NE	10.6	19.2	20.2	20.3	20.4	22.5
	NW	14.2	16.7	16.7	15.3	18.9	19.9
	SE	N/A	N/A	N/A	N/A	N/A	N/A
	SW	19.1	21.4	21.5	22.1	22.8	20.2
S6-2-2	NE	15.9	23.9	16.4	18.1	16.5	19.2
	NW	13.4	15.5	17.8	17.6	19.2	19.9
	SE	13.4	16.2	17.1	16.6	16.7	16.5
	SW	14.3	16.1	17.8	19.9	19.5	16.1
C10-2-1	NE	14.9	18.2	18.5	18.9	18.6	18.7
	NW	15.4	18.5	18.8	17.7	18.5	16.4
	SE	30.1	31.2	31.0	29.6	30.1	31.4
	SW	31.4	33.9	34.5	34.4	33.7	34.8
C10-2-2	NE	22.0	25.3	24.1	24.2	27.1	26.2
	NW	22.3	25.8	29.0	29.7	30.4	30.1
	SE	11.9	13.7	13.8	14.4	14.9	14.0
	SW	12.8	14.8	17.8	16.6	16.6	16.4
S10-2-1	NE	13.7	17.7	15.6	15.9	16.0	15.2
	NW	14.2	15.8	15.6	16.0	15.9	15.8
	SE	12.3	12.4	12.9	13.2	13.1	13.8
	SW	13.5	15.9	16.1	15.9	16.1	15.8
S10-2-2	NE	13.0	17.1	18.5	17.9	18.3	16.1
	NW	17.9	21.0	19.6	20.6	20.1	19.7
	SE	12.7	15.0	15.5	15.5	15.5	14.9
	SW	12.9	16.3	16.7	17.2	17.5	16.4

Conversion: 1 in. = 25.4 mm

Table 4.6 – Average Transfer Lengths for Top Strands of Four-Strand Beams

Transfer Length ID		1 Day (in.)	4 Day (in.)	8 Day (in.)	14 Day (in.)	28 Day (in.)	~56 Day (in.)
C6-4	Avg.	24.8	N/A	27.5	27.6	28.9	26.3
	Std. Dev.	9.25	N/A	3.63	4.98	4.15	N/A
	COV	37.4%	N/A	13.2%	18.0%	14.4%	N/A
S6-4	Avg.	18.2	21.8	22.2	21.1	20.1	22.4
	Std. Dev.	3.26	4.15	0.55	1.50	1.20	0.58
	COV	17.9%	19.0%	2.5%	7.1%	6.0%	2.6%
C10-4	Avg.	17.0	17.2	17.7	17.5	19.0	20.3
	Std. Dev.	2.08	2.95	2.19	2.22	3.59	1.80
	COV	12.2%	17.1%	12.3%	12.7%	18.9%	8.9%
S10-4	Avg.	19.3	17.0	18.6	19.0	18.3	19.5
	Std. Dev.	5.86	3.63	6.50	6.02	6.52	6.46
	COV	30.3%	21.4%	35.0%	31.7%	35.6%	33.1%

Conversion: 1 in. = 25.4 mm

Table 4.7 – Average Transfer Lengths for Bottom Strands of Two-Strand Beams

Transfer Length ID		1 Day (in.)	4 Day (in.)	8 Day (in.)	14 Day (in.)	28 Day (in.)	~56 Day (in.)
C6-2	Avg.	17.2	20.4	22.3	23.7	23.6	24.2
	Std. Dev.	2.76	4.07	4.85	5.09	5.69	5.55
	COV	16.1%	19.9%	21.8%	21.5%	24.1%	24.4%
S6-2	Avg.	14.4	18.4	18.2	18.6	19.2	19.2
	Std. Dev.	2.61	3.20	1.90	2.35	2.17	2.21
	COV	18.1%	17.4%	10.5%	12.7%	11.3%	11.5%
C10-2	Avg.	20.1	22.7	23.4	23.2	23.7	23.5
	Std. Dev.	7.63	7.53	7.38	7.38	7.35	8.06
	COV	37.9%	33.2%	31.5%	31.8%	31.0%	34.3%
S10-2	Avg.	13.8	16.4	16.3	16.5	16.6	15.9
	Std. Dev.	1.76	2.44	2.04	2.15	2.09	1.71
	COV	12.8%	14.9%	12.5%	13.0%	12.6%	10.7%

Conversion: 1 in. = 25.4 mm

4.4.2. End Slip Method of Determining Initial Transfer Length. While the 95% Average Mean Strain Method was the main method used for determining both the transfer lengths at release and the transfer lengths over time, the end slip method was also used to determine initial transfer lengths. The end slip method computes the initial transfer length, L_T, based on the amount the strand slips into the concrete upon release. The relationship between the end slip and transfer length can be seen in Eq. 4.1, where E_{ps} is the modulus of elasticity of the steel strand in ksi, f_{si} is the stress in the strand immediately before release in ksi, and Δ is the measured end-slip of the strand in inches.

$$L_T = \frac{2E_{ps}\Delta}{f_{si}} \quad \textbf{(4.1)}$$

The theory of the relationship between end slip and transfer length was first thoroughly explained by Anderson and Anderson (1976), and has since been explained and successfully used by other researchers. When a tensioned strand is cut, the prestressing force is transferred to the member, shortening the member as well as the strand. The strand loses some of its prestress, and this loss in stress is known as elastic shortening. This is shown in Figure 4.18, where f_{si} is the stress in the strand immediately before release, and f_{se} is stress in strand after elastic shortening immediately after release. The stress in the strand varies linearly from zero at the end of the member to f_{se} at a certain distance from the end of the member, or the transfer length, L_T. Because of the linear relationship between stress and strain, it can also be said that the strain varies linearly in the transfer zone, from zero at the end to $\varepsilon_{se} = f_{se}/E_{ps}$ at the transfer length. Due to strain compatibility, it is assumed that in the fully bonded area, the strain in the concrete, ε_{ce}, equals the change in strain of the steel, $(f_{si}-f_{se})/E_{ps}$. The strain in the concrete therefore varies linearly from zero at the end to $(f_{si}-f_{se})/E_{ps}$ at the transfer length. As a result, in the transfer zone, there is a differential strain that varies from $\varepsilon_{si} = f_{si}/E_{ps}$ at the end of the member, where both the strain in the concrete and steel are zero, to zero at the transfer length, where the strain in the concrete equals the change in strain of the steel. This differential strain is represented by the shaded area in Figure 4.18, and the area is equal to the slip of the strand relative to the concrete. The area is represented by the

integral in Eq. 4.2, but because the variations in concrete and steel strains in the transfer zone are linear, the integral can be simplified to Eq. 4.1.

$$L_T = \int_0^{L_T} [\varepsilon_{si} - \varepsilon_s(x)]dx - \int_0^{L_T} \varepsilon_c(x)dx \quad \textbf{(4.2)}$$

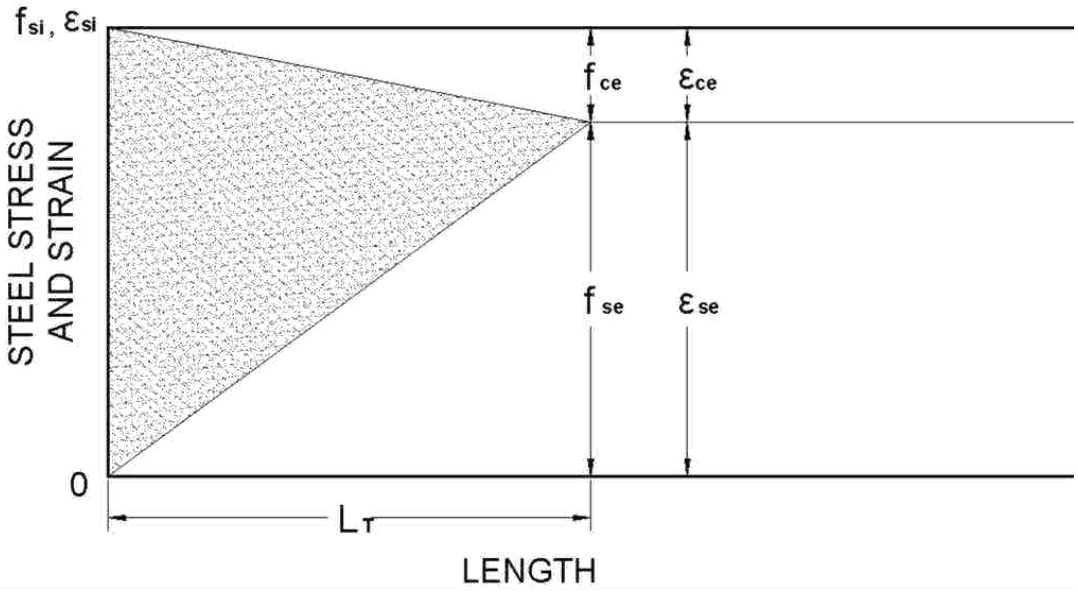

Figure 4.18 – Relationship Between Steel Stress and Strain and Transfer Length (adapted from Russell and Burns, 1993)

In this test program, the end slips of the strands were measured in two ways: by computer with electronic linear potentiometers and by hand with a steel ruler. The end slips measured by each method were then used in conjunction with Eq. 4.1 to determine transfer lengths.

4.4.2.1 Linear potentiometer setup and procedure. The first method of end slip determination involved securing linear potentiometers to the ends of the strands before they were cut and attaching the potentiometers to a Synergy data acquisition computer (Synergy). The linear potentiometer setup on the strands of a two strand beam

is depicted in Figure 4.19, while the Synergy data acquisition computer is shown in Figure 4.20.

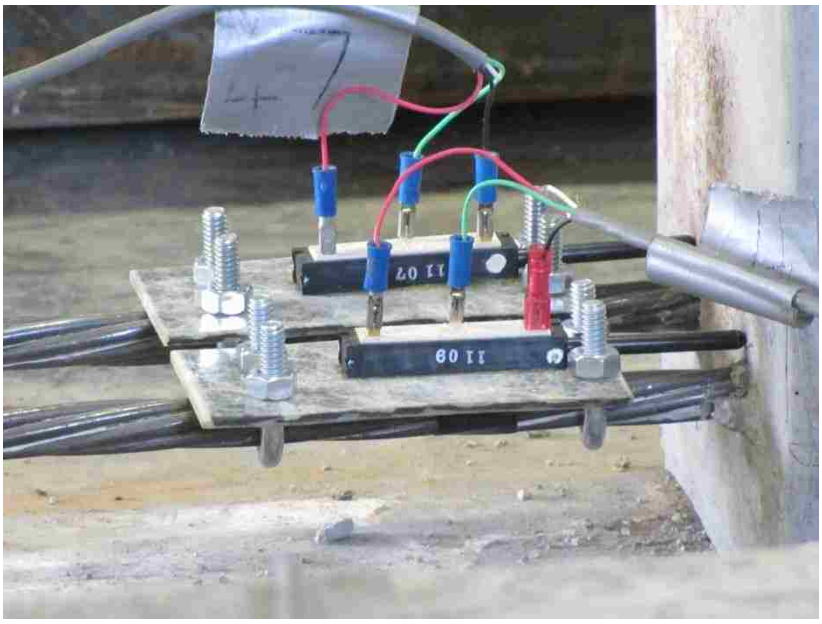

Figure 4.19 – Linear Potentiometer Setup

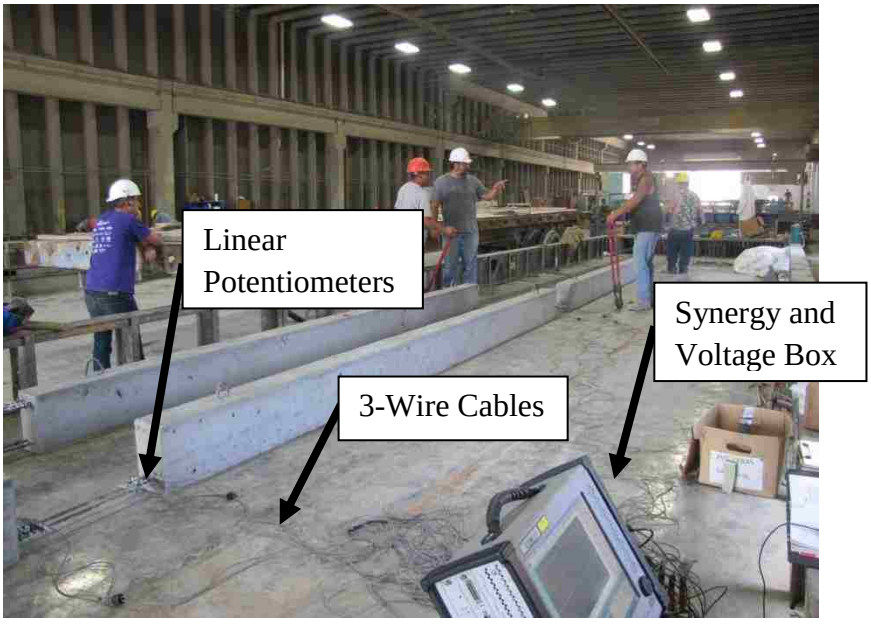

Figure 4.20 – Synergy Data Acquisition Computer Setup

The linear potentiometers, which could measure displacements up to 1.5 in. (38.1 mm), were epoxied on to 2 in. x 4 in. (50.8 mm x 102 mm) sections of FRP, which were then bolted to the strands. The initial epoxy that was used to bond the potentiometers to the FRP did not perform well on the first set of beams and resulted in numerous failures between the potentiometer and FRP, so different epoxies and methods of securing the potentiometers to the sections of FRP were experimented with when the potentiometers were used on the next release day. The methods of securing the potentiometers to the FRP bases are described later in this subsection. Two sets of holes were drilled through the FRP bases, and the potentiometer-FRP assemblies were bolted to the strands with two 0.5-in.-diameter (12.7 mm) U-bolts, as seen in Figure 4.19. Each potentiometer-FRP assembly was rotated about its strand until the free end was lined up with a smooth portion of the beam end. Once the potentiometers were lined up in a suitable position, the U-bolts were securely tightened with a wrench. The potentiometers were attached to the strands so that initial readings of approximately 0.1 in. (2.54 mm) to 0.5 in. (12.7 mm) could be read on the Synergy, meaning that the potentiometers were slightly depressed and making solid contact with the beam. The initial readings were subtracted from the final slip readings to determine the amount of strand slip. The potentiometers were attached to a power box with 3-wire cables, and the power box was hooked up to the Synergy via banana jack cables. The sample rate on the Synergy was set to record data at 1000 samples per second.

The Synergy could record up to 16 data sets at one time. The beams were cut one line at a time, so the potentiometers were first attached to the line of two-strand beams, and after all the two-strand beams had been released, the potentiometers were then attached to the strands of the four-strand beams. Although there were 16 transfer length locations on the line of the four two-strand beams, only 12 readings could be taken on each day because the cables could not reach the far north and south ends of the line of beams. In regards to the four-strand beams, on the first day (C6 and S6 beams), only two readings could be taken because only two potentiometer-FRP assemblies remained intact after the release of the two-strand beams. On the second release day (C10 and S10 beams), significantly more potentiometer-FRP assemblies survived the release of the two-strand beams due to improved bonding methods, so potentiometers were attached to

all 16 transfer length locations on the two four-strand beams. Although the eight transfer length locations on the top strands were the only locations of importance on the four-strand beams, the potentiometers were attached to the bottom strands as well in order to collect as much data as possible and also determine if any relationship existed between the bottom strand readings from the two-strand beams and the four-strand beams.

As mentioned, the bonding of the potentiometers to the FRP bases proved to be problematic. Initially, the surfaces of the FRP sections were roughened with sandpaper, and an 8-minute multi-use epoxy was used to attach the potentiometers to the FRP plates. On the first day of use, almost all potentiometers detached or loosened from their FRP bases due to the sudden release of the strands. It was noted that the epoxy on the broken bonds had a slightly tacky texture, and because the testing was completed in an open shed during the summer, one hypothesis was that the heat affected the epoxy's bonding ability.

Before the potentiometers were used on the next set of beams, several methods were used to try to improve the bond of the potentiometers to the FRP plates. First, the surfaces of the FRP plates were roughened to a greater degree by using a very small grinding wheel attached to a Dremmel. Then, several different epoxies were tested with the intent of determining which one performed the best. The three epoxies tested included a 5-minute plastic bonder epoxy, gorilla glue epoxy, and gorilla glue expanding foam. Additionally, two plastic zip ties were added to each potentiometer-FRP assembly to facilitate bonding as the epoxy dried as well as add an extra securing measure to the assembly. A picture of the improved potentiometer-FRP assemblies with zip ties, plastic epoxy, and gorilla glue expanding foam can be seen in Figure 4.21. Although significantly more assemblies remained intact on the second release day, there was no improvement in the acquisition of readable results.

In order to determine the end slips from the data collected on the Synergy, the files were first downloaded from the Synergy to a personal computer and saved as Microsoft Excel files. Data was then organized into potentiometer reading vs. time plots. Since the potentiometers were attached to one line of beams at a time during the release process, plots were organized to include data from the same line of beams so the same amount of elapsed time could be shown. Each data series from each potentiometer shows

readings from a few seconds before the first strand in the line was cut to a few seconds after the last cut had been made on the line of beams.

Figure 4.21 – Improved Potentiometer-FRP Assemblies with Zip Ties and Plastic Epoxy (Top) and Gorilla Glue Expanding Foam (Bottom)

An example potentiometer vs. time plot is shown in Figure 4.22, which illustrates the end slips for the C6 line of two-strand beams (C6-2-1 and C6-2-2). The plot shows the plateau of initial readings for each location where a potentiometer was applied and then shows the gradual change in the potentiometer readings over time as the strands were cut. End slip values were determined by averaging the values on the initial and final plateaus and then subtracting the average initial reading from the average final reading. However, very few potentiometers actually showed changes in readings that could be accepted as valid data.

The potentiometer readings vs. time plots show that there were several standard ways that the potentiometer readings changed as the strands were cut. Sudden jumps to zero, such as 2-1_NE in Figure 4.22, indicate that the white or red wires in the three wire cable became disconnected from the potentiometer, or the assembly broke or slipped off

the strand. Sudden jumps to readings of 1.5 in. (38.1 mm) indicate only the black wire became disconnected from the potentiometer. Although 1.5-in. (38.1 mm) is not shown on the y-axis of the plots because the majority of readings were within the range of 0 in. to 0.5 in. (12.7 mm), it can be assumed that any data series that exits the top of the plot, such as 2-1_SW in Figure 4.22, goes to 1.5 in. (38.1 mm).

Of the data series that show jumps not immediately going to 0 in. or 1.5 in. (38.1 mm), many of these are negative jumps. In the case of a negative jump, this means the potentiometer moved out from its initial position and slipped backwards, resulting in an invalid reading. A positive jump indicates a potentially good reading, where the strand slipped into the concrete, and the potentiometer was pushed in. However, there is still no guarantee that a positive jump is a valid end slip. After seeing how sensitive the potentiometers ended up being in terms of bond to the plate, disconnected wires, and slippage on the strand, there is a strong possibility that outside stimuli other than the slipping of the stand, such as accidentally bumping the strand or potentiometer, could have affected the readings. Despite this possibility, it was determined that all positive jumps greater than 0.01 in (0.25 mm), which still only corresponds to a transfer length of approximately 3 in. (76.2 mm), were deemed reasonable to report as valid end slips.

Several other special situations also had to be considered when evaluating the end slip data. A few of the potentiometers registered a valid positive jump, but after a while the readings went to 0 in. or 1.5 in. (38.1 mm). For example, 2-1_SE, 2-1_NE, and 2-2_NW in Figure 4.22 all seemed to register a slight positive slip, but then the readings abruptly went to 0 in. after 10 to 35 seconds. In these cases, it was determined that the plateau of the final potentiometer reading was held long enough to be considered valid. The other type of special case involved series that showed a significant amount of noise in the data, such as 2-1_NW in Figure 4.22. Noise most likely indicates that the strand or potentiometer was bumped or somehow affected by outside stimuli. In these cases, if the potentiometer registered a stable reading after the noise, the ultimate change from initial to final reading was still considered valid if the change was positive and significant. In the specific case of C6-2-1_NW, it was decided that even though there was a stable plateau after the noise, the data should be rendered invalid. The fact that the reading first

dropped to 0 in. and then increased back up again put the stability and validity of the potentiometer into question.

In conclusion, the interpretation of end slip data was highly subjective at times, and a lot of assumptions had to be made about which data could be considered valid. All potentiometer reading vs. time plots can be found in Appendix E.

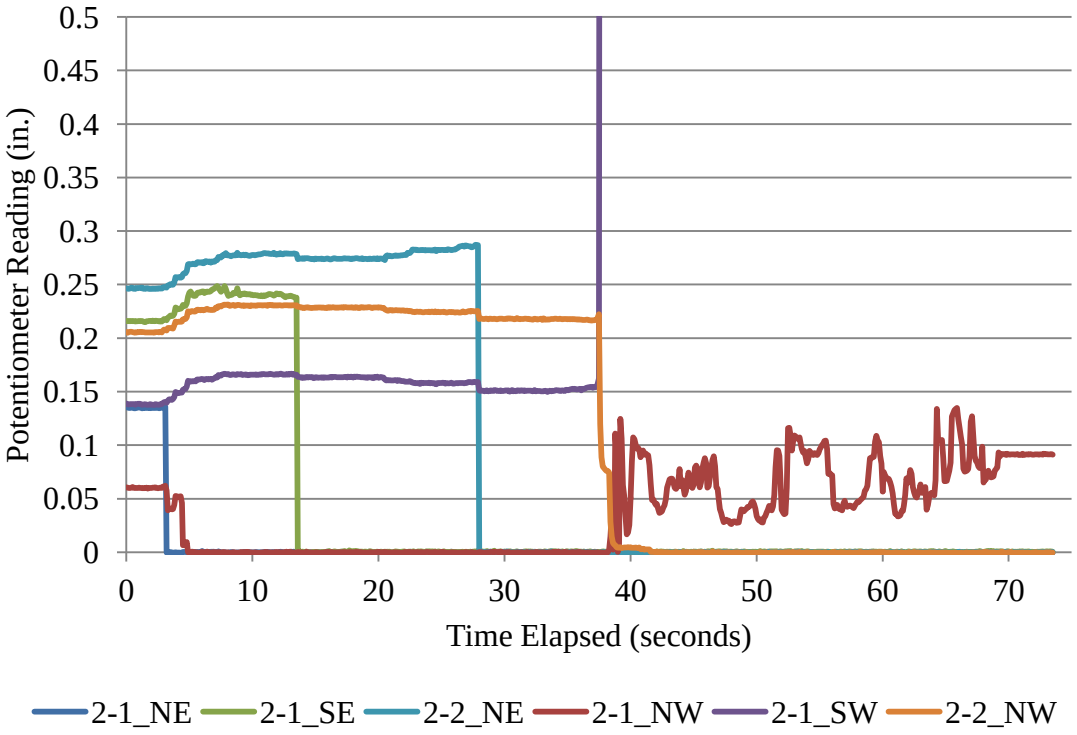

Conversion: 1 in. = 25.4 mm

Figure 4.22 – Typical End Slip Plot: C6 Two-Strand Beams Potentiometer Reading vs. Time Elapsed Plot from Synergy

Table 4.8 shows the end slips measured from the data acquisition system. Each two-strand beam had four possible locations (bottom), while each four strand beam had eight possible locations (bottom and top). A dash indicates a potentiometer was not applied at that location due to either the cables being unable to reach the end of the beam line or a lack of a sufficient number of potentiometers. "N/A" indicates that no

reasonable data could be obtained from the readings, while a number in the cell is the measured end slip in inches.

Table 4.8 – Measured End Slips from Linear Potentiometers

Specimen ID	Bottom				Top			
	NE (in.)	NW (in.)	SE (in.)	SW (in.)	NE (in.)	NW (in.)	SE (in.)	SW (in.)
C6-2-1	N/A	N/A	0.025	0.028				
C6-2-2	0.033	0.025	-	-				
C6-4-1	-	-	-	-	N/A	-	-	-
S6-2-1	-	-	N/A	N/A				
S6-2-2	N/A	0.050	N/A	0.051				
S6-4-1	-	-	-	-	-	-	-	N/A
C10-2-1	-	-	N/A	N/A				
C10-2-2	N/A	N/A	0.041	0.036				
C10-4-1	N/A	N/A	0.066	N/A	N/A	N/A	N/A	N/A
S10-2-1	0.029	0.083	0.025	0.016				
S10-2-2	0.031	0.016	-	-				
S10-4-1	N/A	N/A	N/A	0.050	N/A	N/A	N/A	N/A

Conversion: 1 in. = 25.4 mm

4.4.2.2 Steel ruler setup and procedure. In addition to electronic collection of end slip data, a steel ruler was also used to measure end slip by hand. First, black electrical tape was wrapped around the strand with approximately 2 in. (50.8 mm) of strand showing between the end of the beam and the beginning of the tape. The taped strands can be seen in Figure 4.23. Next, a steel ruler was used to measure the initial distance from the surface of the beam to the beginning of the tape. The measurements were taken to the nearest $^{1}/_{32}$ in. (0.79 mm). In order to keep the measurements as consistent as possible, initial and final measurements were taken by the same individual. Additionally, for each measurement, a permanent marker was used to mark a line on the concrete surface, indicating where the steel ruler had been placed to take the initial measurement. This way, the ruler could be lined up in the same place to take the final

measurement. Measurements were taken at all possible transfer length locations on all beams.

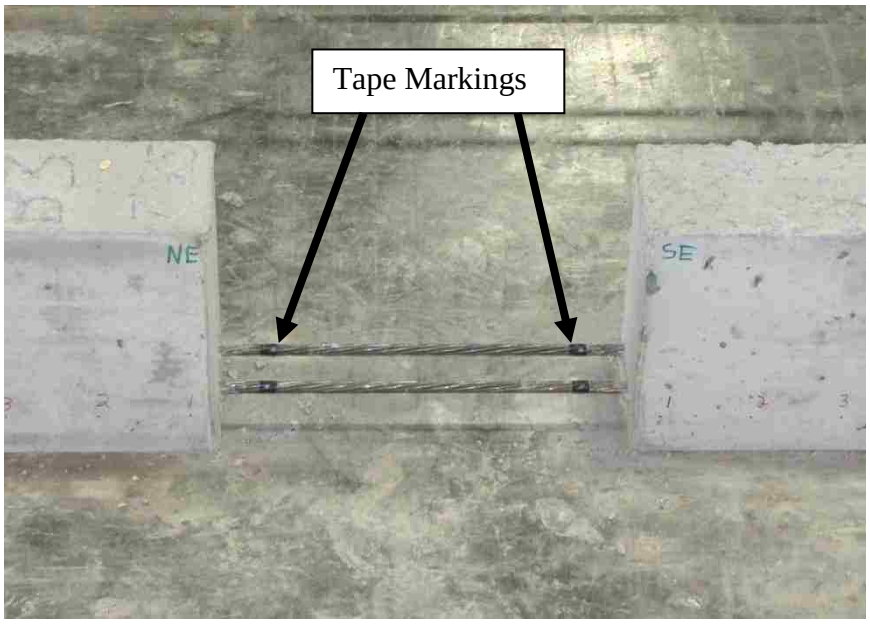

Figure 4.23 – Electrical Tape on Strands for Steel Ruler Measurements of End Slip

The end slip measurements in inches as measured by hand with the steel ruler are presented in Table 4.9. C10-2-1_SW and S10-4-1_NW (bottom) did not have final readings because on each beam, the portion of concrete with the mark where the ruler had been lined up to take the initial reading had broken off when the beam was released. Additionally, C6-4-1_NE (bottom), S6-4-1_SE (bottom), C10-2-2_NW, and S10-4-1_NE (bottom) showed increases in end slip, which is contrary to what was expected.

Table 4.9 – Measured End Slips from Steel Ruler

Specimen ID	Bottom				Top			
	NE (in.)	NW (in.)	SE (in.)	SW (in.)	NE (in.)	NW (in.)	SE (in.)	SW (in.)
C6-2-1	0.125	0.031	0.031	0.063				
C6-2-2	0.063	0.063	0.031	0.063				
C6-4-1	-0.156	0.063	0.094	0.063	0.094	0.063	0.094	0.063
S6-2-1	0.063	0.031	0.031	0.094				
S6-2-2	0.063	0.063	0.063	0.000				
S6-4-1	0.031	0.063	-0.094	0.031	0.031	0.094	0.063	0.063
C10-2-1	0.000	0.063	0.000	N/A				
C10-2-2	0.047	-0.125	0.063	0.063				
C10-4-1	0.000	0.047	0.000	0.031	0.031	0.016	0.031	0.047
S10-2-1	0.063	0.047	0.047	0.063				
S10-2-2	0.047	0.063	0.078	0.094				
S10-4-1	-0.016	N/A	0.047	0.031	0.016	0.000	0.031	0.063

Conversion: 1 in. = 25.4 mm

4.4.2.3 Transfer length determination from end slip data. Once all of the end slip values were determined, the values were used to calculate initial transfer lengths, using Eq. 4.1, as discussed in Section 4.3.2. E_{ps} was taken to be the experimentally determined modulus of elasticity of the prestressing strand, or 29400 ksi (203 GPa), and f_{si}, or the stress in the strand before release, was taken to be 75% of 270 ksi (1,862 MPa). The measured end slips in inches were inserted into the equation to calculate a transfer length at each applicable location.

$$L_T = \frac{2E_{ps}\Delta}{f_{si}} \quad \textbf{(4.1)}$$

Tables 4.10 – 4.12 summarize the transfer lengths in inches calculated from the measured end slips from both the linear potentiometers (Synergy) and the steel ruler. The last column in each table also includes the transfer lengths determined by the 95% Average Mean Strain Method from the 1 Day DEMEC data for comparison. Table 4.10 reports the transfer lengths for the bottom strands of the C6 and S6 beams, while Table

4.11 reports the transfer lengths for the bottom strands of the C10 and S10 beams. Table 4.12 reports the transfer lengths for all of the top strands.

Table 4.10 – Initial Transfer Lengths from Steel Ruler End Slips, Synergy End Slips, and DEMEC Data for Bottom Strands on C6 and S6 Beams

Transfer Length Location		Steel Ruler End Slip L_T (in.)	Synergy End Slip L_T (in.)	DEMEC 1 Day L_T (in.)
C6-2-1	NE	35.8	N/A	19.6
	NW	9.0	N/A	20.3
	SE	9.0	7.2	19.8
	SW	17.9	8.0	15.5
C6-2-2	NE	17.9	9.5	17.0
	NW	17.9	7.2	13.8
	SE	9.0	-	14.2
	SW	17.9	-	N/A
C6-4-1	NE	N/A	-	-
	NW	17.9	-	-
	SE	26.9	-	-
	SW	17.9	-	-
S6-2-1	NE	17.9	-	10.6
	NW	9.0	-	14.2
	SE	9.0	N/A	N/A
	SW	26.9	N/A	19.1
S6-2-2	NE	17.9	N/A	15.9
	NW	17.9	14.3	13.4
	SE	17.9	N/A	13.4
	SW	0.0	14.6	14.3
S6-4-1	NE	9.0	-	-
	NW	17.9	-	-
	SE	N/A	-	-
	SW	9.0	-	-

Conversion: 1 in. = 25.4 mm

Table 4.11 – Initial Transfer Lengths from Steel Ruler End Slips, Synergy End Slips, and DEMEC Data for Bottom Strands on C10 and S10 Beams

Transfer Length Location		Steel Ruler End Slip L_T (in.)	Synergy End Slip L_T (in.)	DEMEC 1 Day L_T (in.)
C10-2-1	NE	0.0	-	14.9
	NW	17.9	-	15.4
	SE	0.0	N/A	30.1
	SW	N/A	N/A	31.4
C10-2-2	NE	13.4	N/A	22.0
	NW	N/A	N/A	22.3
	SE	17.9	11.7	11.9
	SW	17.9	10.3	12.8
C10-4-1	NE	0.0	N/A	-
	NW	13.4	N/A	-
	SE	13.4	18.9	-
	SW	17.9	N/A	-
S10-2-1	NE	13.4	8.3	13.7
	NW	17.9	23.8	14.2
	SE	13.4	7.2	12.3
	SW	17.9	4.6	13.5
S10-2-2	NE	13.4	8.9	13.0
	NW	17.9	4.6	17.9
	SE	22.4	-	12.7
	SW	26.9	-	12.9
S10-4-1	NE	N/A	N/A	-
	NW	N/A	N/A	-
	SE	13.4	N/A	-
	SW	9.0	14.3	-

Conversion: 1 in. = 25.4 mm

Table 4.12 – Initial Transfer Lengths from Steel Ruler End Slips, Synergy End Slips, and DEMEC Data for Top Strands on C6, S6, C10, and S10 Beams

Transfer Length Location		Steel Ruler End Slip L_T (in.)	Synergy End Slip L_T (in.)	DEMEC 1 Day L_T (in.)
C6-4-1	NE	26.9	N/A	N/A
	NW	17.9	-	N/A
	SE	26.9	-	31.3
	SW	17.9	-	18.2
S6-4-1	NE	9.0	-	20.5
	NW	26.9	-	N/A
	SE	17.9	-	N/A
	SW	17.9	N/A	15.9
C10-4-1	NE	9.0	N/A	18.8
	NW	4.5	N/A	15.3
	SE	9.0	N/A	15.1
	SW	13.4	N/A	18.9
S10-4-1	NE	4.5	N/A	18.0
	NW	0.0	N/A	17.6
	SE	9.0	N/A	27.7
	SW	17.9	N/A	14.0

Conversion: 1 in. = 25.4 mm

4.5. DEVELOPMENT LENGTH TEST SETUP, PROCEDURE, AND RESULTS

A four-point loading test setup was used to test each end of the beams in flexure at different embedment lengths, where the embedment length is the distance from the end of the beam to the first load point, and then determine if the beam failed in flexure or bond. There is no direct way to test development length, but iterative testing of different embedment lengths can indicate a range in which the development length falls. Theoretically, if the embedment length at testing was exactly equal to the development length, the member would fail in bond and flexure at the same time. A bond failure indicates the strand could not be fully developed, so the development length is longer than the tested embedment length, while a flexural failure indicates that the strand was able to be fully developed, so the embedment length was longer than the actual development length.

For each beam, one end was first tested at an embedment length of 58-in. (1,473 mm), and then the other end was tested at an embedment length of 73-in. (1,854 mm). The shorter length corresponds to approximately 80% of the ACI/AASHTO recommended development length, and the longer length is approximately equal to the calculated ACI/AASHTO development length. As noted in Section 2.5, the ACI and AASHTO equations for development length are equal when the member is less than or equal to 24-in. (610 mm) deep. The mode of failure was determined through a combination of noting the crack pattern, determining if the applied moment at failure fell below or exceeded the calculated nominal moment capacity, and noting if the strands on the tested end experienced any significant slip. A flexural failure, which would be indicated by strand yielding or concrete crushing, a failure moment at or above the nominal moment, and negligible end slips in the strands, would imply that the strand had enough effective, bonded length to fully develop the moment capacity.

4.5.1. Four-Point Loading Setup and Instrumentation. The four-point load tests were completed on a steel frame designed for flexural beam testing at the Missouri S&T Structural Engineering High Bay Research Laboratory (SERL). The beams were supported on two steel plates on top of rollers, and two hydraulic actuators were used to apply two point loads at 24 in. (610 mm) apart using spreader beams (Figure 4.24). Since the beams were tested one end at a time, the supports were positioned so the end of the beam could be tested at the correct embedment length, and the two point loads would be positioned in the middle of the simply supported span. The end not being tested was cantilevered over one of the supports.

For each beam, the 58 in. (1,473 mm) embedment length was tested first, and then the beam was shifted to test the 73 in. (1,854 mm) embedment length on the other end. The beam test setups for the 58 in. (1,473 mm) and 73 in. (1,854 mm) embedment length tests are illustrated in Figures 4.25 and 4.26, respectively. Figures 4.25 and Figure 4.26 also show how portions of the beam overlapped during each test. The shaded portion of the beam in Figure 4.25 indicates where the maximum moment region would be during the 73 in. (1,854 mm) test. This shows that the 73 in. (1,854 mm) embedment length was largely unaffected by the 58 in. (1,473 mm) test because the majority of the end tested in the 73-in. (1,854 mm) test was cantilevered over one support during the 58 in. (1,473

mm) test, and therefore unaffected by the loading. Figure 4.26 shows cracks indicating approximately where the failed portion from the 58 in. (1,473 mm) test would have been located on the beam during the 73 in. (1,854 mm) test. Although the failed portion of the beam from the 58 in. (1,473 mm) test fell partly within the span of the 73 in. (1,854 mm) test, the failed portion did not fall within the maximum moment zone of the 73 in. (1,854 mm) test. Furthermore, additional development length was available on the side of the beam containing the failed portion from the 58 in (1,473 mm) test due to the cantilevered portion extending beyond the support.

Figure 4.24 – Four-Point Loading Test Setup for Evaluating 58-in. (1,473 mm) Embedment Length

From these observations, several assumptions were made regarding the effect the first flexural test would have on the second. First, it was assumed that the bond of 73 in. (1,854 mm) embedment length would have been negligibly affected by the 58 in. (1,473

mm) test because 68 in. (1,727 mm) of the 73 in. (1,854 mm) was cantilevered. It was also assumed that the zone experiencing maximum moment during the 73 in. (1,854 mm) test would still be able to develop full moment capacity because the area was assumed to be fully bonded to begin with, and the area also should not have seen a moment close to the nominal capacity during the 58 in. (1,473 mm) test. Figure 4.26 corroborates this by showing that while cracks did form and extend outside the region between the two point loads, the failed portion from the 58 in. (1,473 mm) test still did not affect the maximum moment zone of the 73 in. (1,854 mm) test. Based on these assumptions, the 73 in. (1,854 mm) test on each beam was assumed to be valid. Furthermore, this test setup has been successfully used in previous research (Ramirez and Russell 2008).

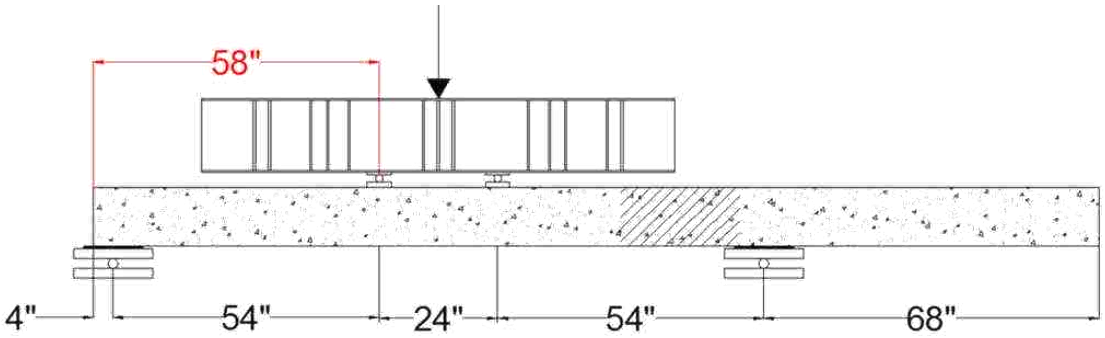

Figure 4.25 – 58 in. (1,473 mm) Embedment Length Test Setup

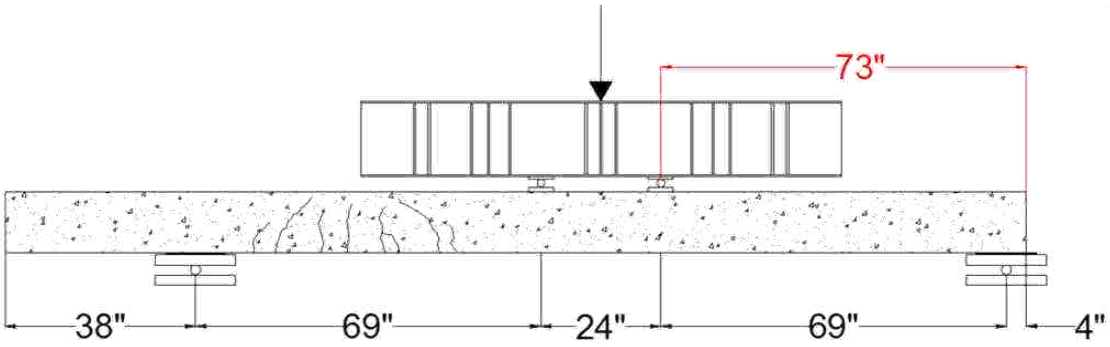

Figure 4.26 – 73 in. (1,854 mm) Embedment Length Test Setup

Instrumentation was installed to measure deflection of the beam and slip in the strands. In order to measure deflection, a Linear Voltage Differential Transformer (LVDT) was placed on a level section of angle bolted at midspan of the span (Figure 4.27). Also, the linear potentiometers that were used to measure initial end slip of the strands at release were attached to the strands on the end of the beam to monitor slipping of the strands (Figure 4.28). In order to keep the slip measurements consistent, the free end of the potentiometer was lined up at the top of the strands. On some beams, the area of contact was uneven, so in these cases, 1 in. x 1 in. (25.4 mm x 25.4 mm) sections of plexiglass were attached to the contact areas with an epoxy, which is also shown in Figure 4.28. A description of the linear potentiometers can be found in Section 4.3.2.1. A data acquisition system was used to record the load applied by each actuator, deflection as measured by the LVDT, and slip in the strands as measured by the linear potentiometer on each strand.

Figure 4.27 – LVDT Setup for Measuring Deflection at Midspan

Figure 4.28 – Linear Potentiometer Setup on Four-Point Loading Tests

4.5.2. Four-Point Loading Procedure. Once the beam was positioned at the correct tested embedment length and the instrumentation was installed, the beam was loaded in a displacement controlled method until failure. Most of the beams were loaded at increments of 0.05 in. (1.27 mm) of deflection until the total deflection reached 1.0 in. (25.4 mm). After 1.0 in. (25.4 mm) of total deflection, the beam continued to be loaded at increments of 0.05 in. (1.27 mm), but the beam was only checked and marked for cracks at increments of 0.1 in. (2.54 mm) of deflection until failure. Failure was determined to be when the beam would no longer support any additional load.

At each deflection step, the beam was checked for cracks, and any crack or continuation of a crack were marked with permanent marker, and the maximum load for that step was written next to the end of the crack (Figure 4.29). The load that corresponded to initial flexural cracking and the ultimate failure mode were visually noted. The loads applied by the hydraulic actuators, end slips as measured by the potentiometers, and deflection at midspan as measured by the LVDT were monitored throughout the test by the data acquisition systems. From the recorded data, moment vs. deflection and end-slip vs. deflection were plotted for each test, and a typical plot of both relationships can be found in Figure 4.30. The applied moments include the moment from

the self-weight of the beam. Additionally, the load cells were located above the spreader beam, so moment resulting from the dead load of the spreader beam was also added into the final applied moment.

Figure 4.29 – Cracks Marked with Permanent Marker during Development Length Test

4.5.3. Four-Point Loading Results. In Figure 4.30, the dashed line on the plot indicates the calculated nominal moment capacity for the beam. The experimentally determined ultimate strength and modulus of elasticity of the strand as well as the actual strength of the concrete were used in the calculations of the nominal moment capacities. In Figure 4.30, the peak of the moment curve exceeds the calculated nominal moment capacity, and the end slip remained negligible throughout the test. The combination of these results indicates C10-2-1_58 failed in flexure. Plots, photographs, and a summary of the loading method and results of each test can be found in Appendix F.

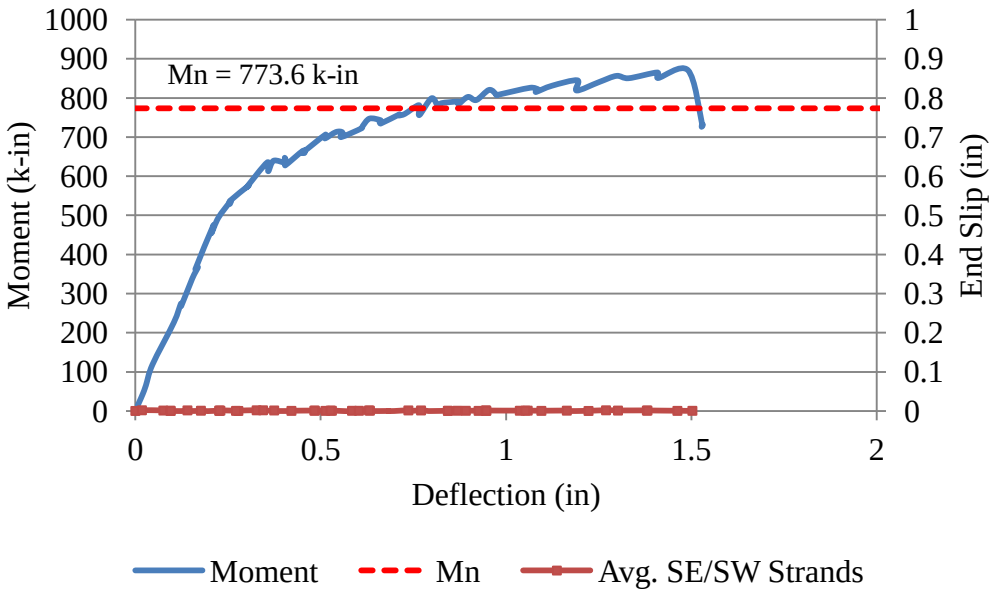

Conversion: 1 in. = 25.4 mm
1 k-in. = 113 N-m

Figure 4.30 – Typical Moment vs. Deflection and Strand End Slip vs. Deflection Plot from Four-Point Loading Data

Table 4.13 identifies the observed cracking moment (M_{cr}), ultimate applied moment (M_u), and calculated nominal moment (M_n) for each test as well as the ratio of the ultimate applied moment to the calculated nominal moment, average strand end slip, visual observations regarding failure, and the final failure mode. In terms of the M_u/M_n ratio, a ratio greater than one indicates the beam had a greater moment capacity than predicted, and therefore, the embedment length was conservative. The final failure mode was determined through analysis of a combination of the M_u/M_n ratio, average strand end slip, and visual observations. Since all beams had a M_u/M_n ratio greater than one, showed virtually no end slip in the strands, and largely exhibited concrete crushing in the maximum moment zone (Figure 4.31), all tests were determined to have failed in flexure. Table 4.14 summarizes the average moment capacities and average M_u/M_n ratios for each mix at each embedment length.

Table 4.13 – Nominal and Actual Moment Capacities

Test ID	M_{cr} (k-in)	M_u (k-in)	M_n (k-in)	M_u/M_n	Average End Slip (in.)	Visual Observations	Failure Mode
C6-2-1_58	469.2	811.8	742.7	1.093	0.000	Concrete Crushing	Flexural
C6-2-1_73	529.5	834.8	742.7	1.124	0.000	Concrete Crushing	Flexural
C6-2-2_58	482.7	836.6	742.7	1.126	0.000	Concrete Crushing	Flexural
C6-2-2_73	498.4	837.6	742.7	1.128	0.000	Concrete Crushing	Flexural
S6-2-1_58	523.3	867.7	757.9	1.145	0.000	Concrete Crushing	Flexural
S6-2-1_73	505.5	878.4	757.9	1.159	0.000	Concrete Crushing*	Flexural
S6-2-2_58	501.7	889.9	757.9	1.174	0.000	Concrete Crushing	Flexural
S6-2-2_73	460.7	843.1	757.9	1.112	0.000	Concrete Crushing	Flexural
C10-2-1_58	534.2	880.3	773.6	1.138	0.000	Concrete Crushing	Flexural
C10-2-1_73	495.6	880.7	773.6	1.138	0.000	Concrete Crushing	Flexural
C10-2-2_58	466.7	875.3	773.6	1.132	0.001	Concrete Crushing	Flexural
C10-2-2_73	492.1	885.8	773.6	1.145	0.000	Concrete Crushing	Flexural
S10-2-1_58	499.1	883.3	790.7	1.117	0.000	Concrete Crushing	Flexural
S10-2-1_73	519.7	904.2	790.7	1.144	0.000	Concrete Crushing	Flexural
S10-2-2_58	553.1	901.1	790.7	1.140	0.000	Concrete Crushing	Flexural
S10-2-2_73	530.1	871.7	790.7	1.102	0.000	Concrete Crushing	Flexural

* Concrete crushing occurred outside the maximum moment zone

Conversion: 1 in. = 25.4 mm
1 k-in. = 113 N-m

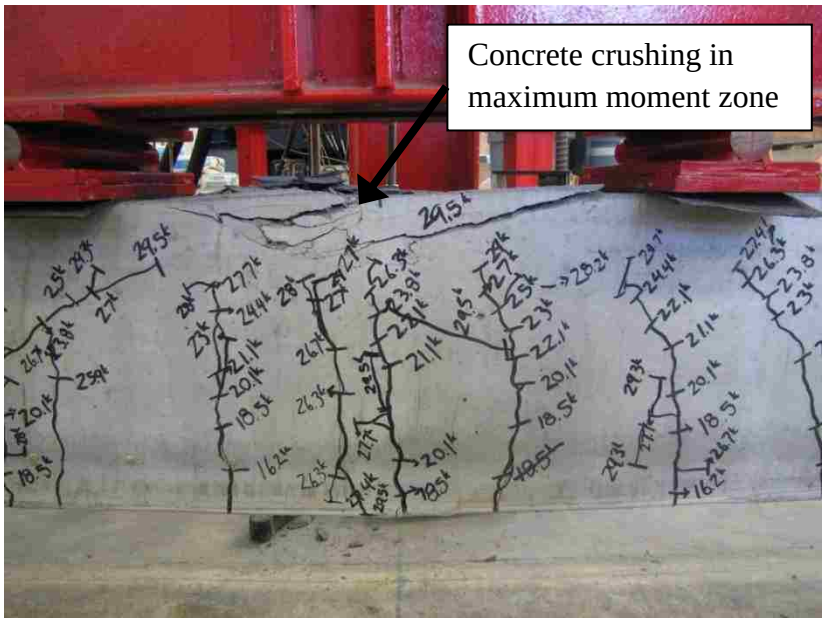

Figure 4.31 – Typical Concrete Crushing Failure for Development Length Tests

Table 4.14 – Summary of Average Nominal and Actual Moment Capacities

Mix ID	M_n (k-in)	58 in. (1,473 mm)		73 in. (1,854 mm)	
		M_u (k-in)	M_u/M_n	M_u (k-in)	M_u/M_n
C6	742.7	824.2	1.110	836.2	1.126
S6	757.9	878.8	1.160	860.8	1.136
C10	773.6	877.8	1.135	883.3	1.142
S10	790.7	892.2	1.128	888.0	1.123

Conversion: 1 k-in. = 113 N-m

5. DISCUSSION AND COMPARISON OF RESULTS

5.1. INTRODUCTION

The two main objectives of this research program were to 1) evaluate two different bond tests and 2) compare bond performance of SCC vs. conventional concrete through a test program investigating transfer and development lengths of 0.5-in.-diameter (12.7 mm), Grade 270 prestressing strand.

In terms of analysis of the bond tests, the main goals were to 1) compare and evaluate the consistency of two types of pullout tests designed to assess bond-ability of prestressing strand, and 2) determine if pullout test values can be correlated to measured transfer lengths.

For the transfer and development length testing portion of the study, the goals were to 1) determine if a significant difference was seen between bond performance of prestressing strand in SCC vs. conventional concrete, 2) compare experimental transfer and development length results to values calculated from equations in the AASHTO and ACI codes to determine if the equations that are being used in design are conservative for both conventional concrete and SCC, 3) evaluate the effect of concrete strength on bond performance, and 4) determine if casting position has a significant effect on transfer length of prestressing strand.

The analyses of results in relation to these research goals are discussed in this section.

5.2. BOND TEST RESULTS

Several different analyses were performed on the results from the NASP tests in mortar and concrete and the LBPT. First, the three strand types were analyzed based on bond acceptance limits of the NASP test in mortar and the LBPT, and then the overall pass/fail and relative rankings from each test were compared to each other to see if both tests produced similar results. The results from the NASP tests in concrete were then analyzed to determine if any differences could be seen between the pullout tests done in conventional concrete versus SCC and also compared to equations based on concrete compressive strength determined by previous research.

5.2.1. Discussion of NASP Test in Mortar Results. The pullout values for 0.1 in. (2.54 mm) and 0.001 in. (0.025 mm) for strand types 101, 102, and 103 are presented in Table 3.8 but are also displayed graphically in Figure 5.1 for ease of comparison and discussion. In Figure 5.1, the error bars represent one standard deviation above and below the average. For reasons discussed in Section 3.3.1, N-101-A and N-101-B were completed with the same strand source but two different mix designs. N-101-B, N-102-B, and N-103-B were directly compared to evaluate relative bond quality of the three sources, and N-101-A was compared to N-101-B to determine the effect of mortar mix design on pullout values.

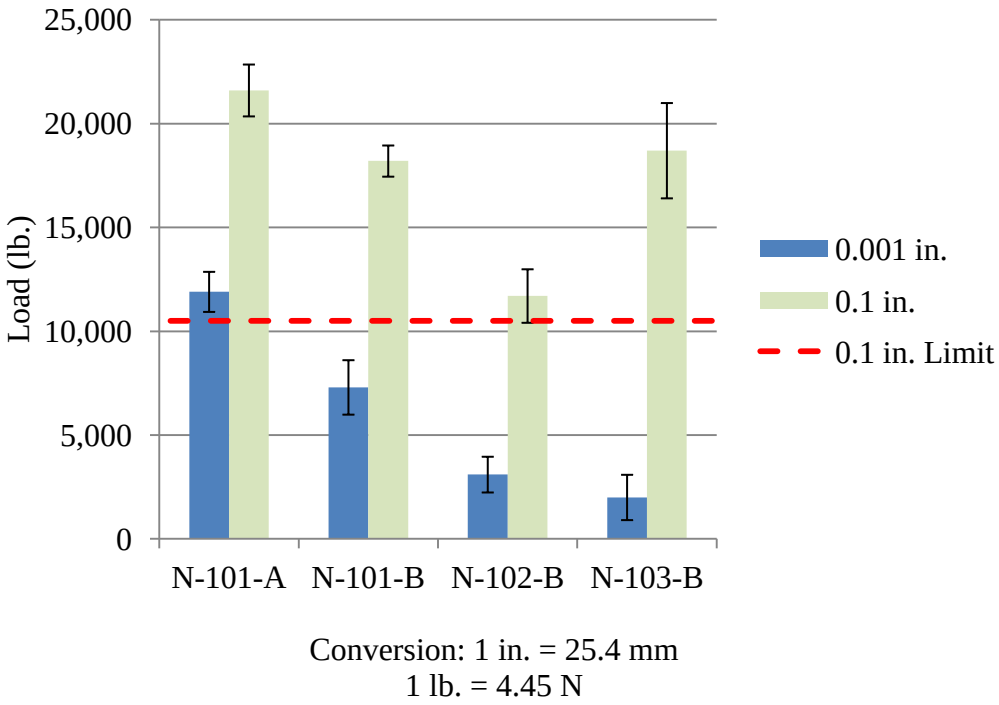

Figure 5.1 – NASP in Mortar Pullout Values

The NASP test specifies that for 0.5-in.-diameter (12.7 mm) strand, the minimum average pullout value at a strand slip of 0.1 in. (2.54 mm) is 10,500 lb (46.7 kN), and no individual test should have a result falling below 9,000 lb (40.0 kN). Strand types 101 and 103 were comparable and showed the best bond quality by exceeding the specified

average minimum pullout value by 73% and 75%, respectively. Strand type 102 also passed, but exceeded the minimum required value by only 11%. Strand type 102 also came close to failing the individual requirement with N-102-B-4 having a 0.1 in. (2.54 mm) pullout value of 9,300 lb (41.4 kN) (Table 3.6). Still, all three strand types exceeded the minimum bond acceptance criteria as specified by the NASP test, and as a result, all sources were deemed to have acceptable bond quality based on the proposed standard.

Although all strands passed strictly based on the criteria, several other observations were noted that could possibly affect analysis of bond quality. First, although the bond acceptance criteria in the proposed standard is based on the 0.1 in. (2.54 mm) slip, in this research, the loads at 0.001 in. (0.025 mm) slip were also recorded so the strands could also be analyzed and compared based on "first slip." Interestingly, in the analysis of the results, it was discovered that N-103-B had the highest average pullout value at 0.1 in. (2.54 mm) but the lowest average pullout value at 0.001 in (0.025 mm), as shown in Figure 5.1. Although strand 103 appeared to have the best bond quality based on the 0.1 in. (2.54 mm) slip load, initial slip was caused by an extremely low load compared to the other two strand types. First slip is caused by the sudden loss of adhesion, or the chemical bond that forms between the strand and mortar or concrete. Currently, the proposed standard bases acceptance only on the 0.1 in. (2.54 mm) pullout load, but the low 0.001 in. (0.025 mm) pullout load could possibly indicate a problem with adhesion, which could affect bond performance, or at least warrant more investigation.

Additionally, analysis of the load vs. slip plots of the three strand types showed a trend that could help distinguish acceptable from poor bond quality. The load vs. slip plots for N-101-B, N-102-B, and N-103-B are presented in Figures 5.2, 5.3, and 5.4, respectively. Strand types 101 and 103 both had average pullout values that exceeded the minimum required average by over 70%, and both load vs. slip plots, shown in Figures 5.2 and 5.4, indicate that for each specimen, the loads were still increasing at a slip of 0.1 in. (0.025 mm). However, strand type 102, which only exceeded the minimum average by 11%, shows a distinct plateau, or softening, and eventually a gradual decrease in load as slip continues to increase (Figure 5.3). The plateaus in loads for strand type 102, which were not seen in the load vs. slip plots for types 101 and 103, which clearly had high

bond quality, is a sign that strand type 102 may still have questionable bond quality even though the strand type passed based on the threshold values. This concern was also noted by Hawkins and Ramirez in their due diligence study performed on the four rounds of NASP testing (2010).

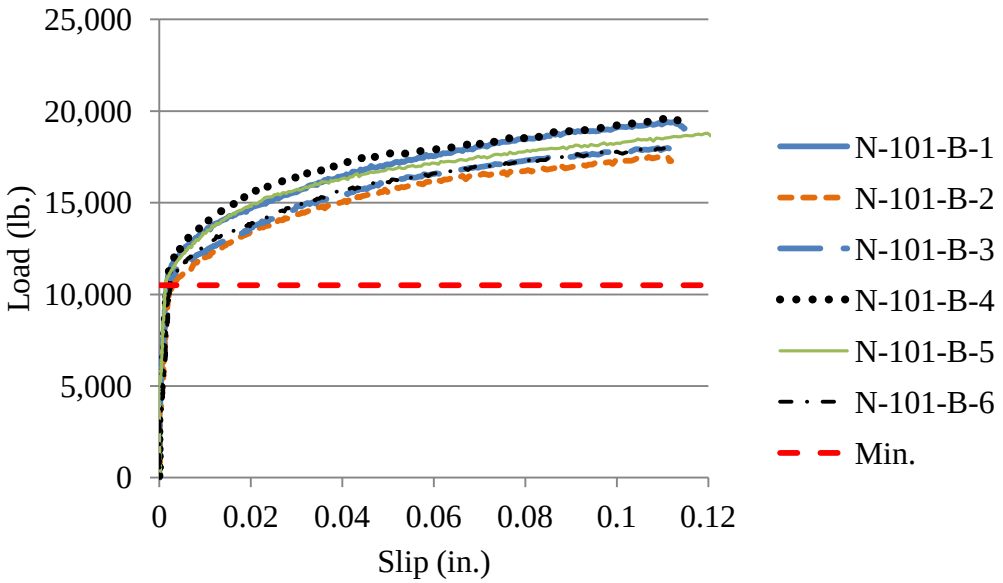

Conversion: 1 in. = 25.4 mm
1 lb = 4.45 N

Figure 5.2 – N-101-B Load vs. Slip

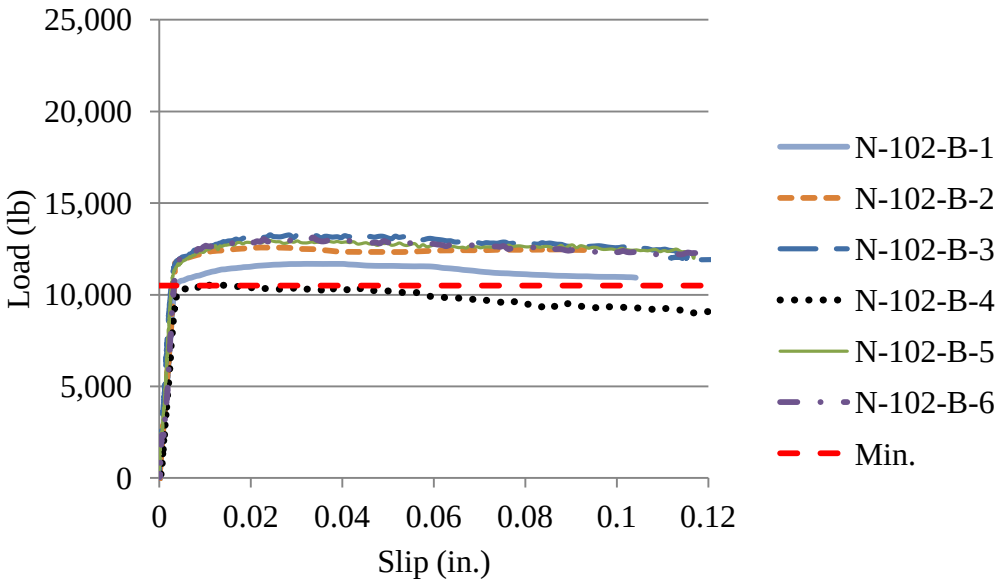

Conversion: 1 in. = 25.4 mm
1 lb = 4.45 N

Figure 5.3 – N-102-B Load vs. Slip

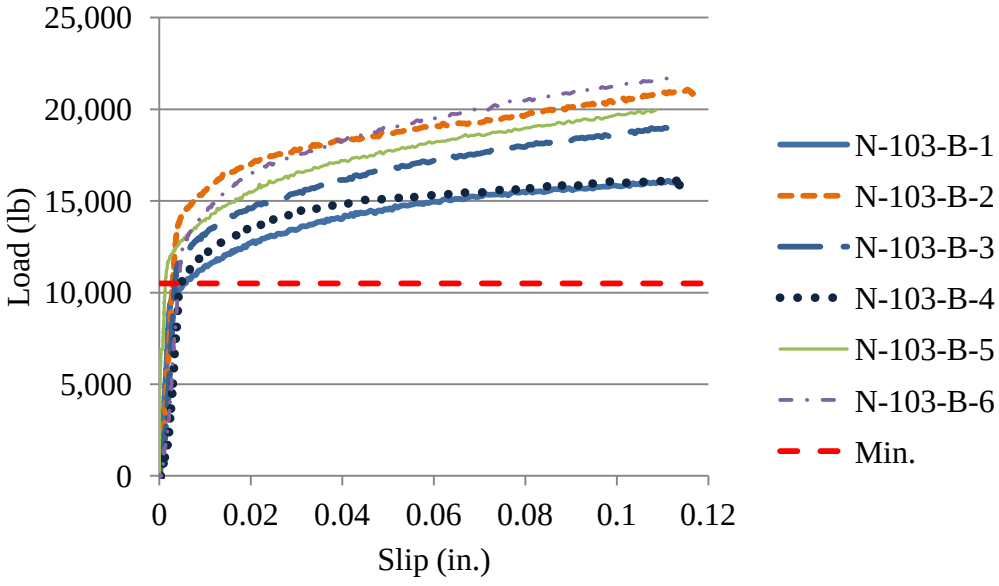

Conversion: 1-in. = 25.4 mm
1 lb = 4.45 N

Figure 5.4 – N-103-B Load vs. Slip

While no known previous bond testing had been done on strand type 101, NASP tests had been completed on strand types 102 and 103 during NCHRP 10-62, and samples of the two strand types were sent to Missouri S&T to be blindly tested to see if similar NASP test results could be obtained. After testing was completed at Missouri S&T, the previous results from NCHRP 10-62 were acquired and compared to the results from this test program. The 0.1 in. (2.54 mm) average pullout value results from NCHRP 10-62 and Missouri S&T for strands 102 and 103 and the percent differences are displayed in Table 5.1.

Table 5.1 – Average Pullout 0.1-in. (2.54 mm) Pullout Values from Missouri S&T and NCHRP 10-62 for Strands 102 and 103

Strand ID	NCHRP 10-62 Pullout Load (lb)	Missouri S&T Pullout Load (lb)	Percent Difference
102	10,600	11,700	9.9%
103	13,300	18,700	33.8%

Conversion: 1 lb = 4.45 N

The results from Missouri S&T were higher than the results from NCHRP 10-62, and the values from strand type 102 had a difference of 9.9% while there was a 33.8% difference between the pullout values for strand type 103. The differences between the average pullout values from NCHRP 10-62 and Missouri S&T could be explained by several factors. First, the strands were sent to Missouri S&T months after the initial testing, and that time could have allowed the strand surface quality to degrade. Also, the mix designs and compressive strength and flow properties of the mixes used for the tests conducted for NCHRP 10-62 were unknown. Even if the compressive strengths and flow values for the tests done by NCHRP 10-62 were within the acceptable ranges, as were the mixes used by Missouri S&T, differences in mix designs, such as the water/cement ratio or amount and angularity of the sand could have affected the pullout loads.

While the proposed standard only specifies compressive strength and flow ranges and has no restrictions on mix proportioning, the round robin testing completed for the development of the NASP test indicated that the desired mix properties can usually be

obtained by using a mix design with a 0.45 water/cement ratio and a sand/cement ratio of around 2:1 (Hawkins and Ramirez 2010). Most literature from other research where the NASP test was completed indicates the use of mix designs similar to this. However, with the materials available, Missouri S&T was unable to create a mix with the desired properties using the conventional mix proportions and instead used a mix with a water/cement ratio of 0.395 and a sand/cement ratio of 0.9:1, which is drastically different than the proposed typical proportions. There are many unknowns regarding the treatment of the strands between tests and the mix designs, but on the surface, the noticeable differences appear to indicate that in this case, the test did not seem to be reproducible between sites.

The effect of differences in mix proportioning was tested to an extent through comparing pullout values from strand type 101 in mortar Mix A and mortar Mix B. Strand type 101 was initially tested months before types 102 and 103, and the mix design that had originally been used for type 101, mortar Mix A, did not give the same flow properties when tested in trial batches again before testing 102 and 103, most likely due to changes in the sand. A new mix design, mortar Mix B, which also met the strength and flow properties was developed. The mix designs for Mix A and Mix B were discussed in Section 3.3.1 and can be found in Table 3.2. Mix B had a slightly higher water/cement ratio and a much lower sand/cement ratio compared to Mix A. After testing was completed on types 102 and 103 with Mix B, it was decided that remaining samples of type 101 should be tested in Mix B as well, so all pullout values could be directly compared. The samples of strand 101 were wrapped in plastic and stored in a closed container for the six months between the initial and final testing.

The pullout values for strand type 101 in mortar mixes A and B are shown in Table 5.2. Both the 0.001 in. (0.025 mm) and 0.1 in. (2.54 mm) pullout loads were consistently lower in Mix B compared to Mix A. The 0.1 in. (2.54 mm) average pullout value for Mix B was 15.7% lower than Mix A, and the 0.001 in. (0.025 mm) average pullout value for Mix B was 38.7% lower. The 0.001 in. (0.025 mm) and 0.1 in (2.54 mm) average pullout loads are presented graphically in Figure 5.5, with error bars representing 95% confidence intervals for each set. When comparing the 0.001 in. (0.025 mm) and 0.1 in. (2.54 mm) pullout loads between the two mixes, the 95% confidence

interval error bars do not overlap at either slip value. Therefore, both the pullout values at 0.001 in. (0.025 mm) and the pullout values at 0.1 in. (2.54 mm) were found to be statistically different between the NASP test completed in Mix A and the NASP test completed in Mix B. As Table 3.8 shows, both mixes had strengths and flows falling within the required ranges, so it is proposed that the differences in mix proportioning was the reason behind the difference in pullout values. One hypothesis is that the significant decrease in sand content in Mix B could have decreased the effects of mechanical interlock and friction on the strand, causing the lower pullout values.

Since the different mix proportioning between Mix A and Mix B seemed to affect the pullout values, it would follow that the NASP tests completed at other sites with the more conventional mix designs should also produce different pullout values from the values determined at Missouri S&T. However, based on previous tests in literature, the mixes used for NCHRP 10-62 most likely had more sand than Mix B used by Missouri S&T, which should increase the pullout values according to the conclusion drawn from the results of strand 101 in Mix A and Mix B. However, this was not the case, as shown in Table 5.1.

Table 5.2 – N-101-A and N-101-B Pullout Loads

Specimen No.	N-101-A (lb)		N-101-B (lb)	
	0.001 in.	0.1 in	0.001 in.	0.1 in
1	12,500	22,100	8,100	19,100
2	10,600	22,900	6,500	17,300
3	12,600	23,000	7,800	17,800
4	11,100	21,100	7,200	19,100
5	13,100	20,600	8,900	18,200
6	11,500	20,000	5,200	17,800
Avg.	**11,900**	**21,600**	**7,300**	**18,200**
Std. Dev.	**978**	**1,242**	**1,304**	**741**
COV	**8.2%**	**5.8%**	**17.9%**	**4.1%**

Conversion: 1 in. = 25.4 mm
1 lb = 4.45 N

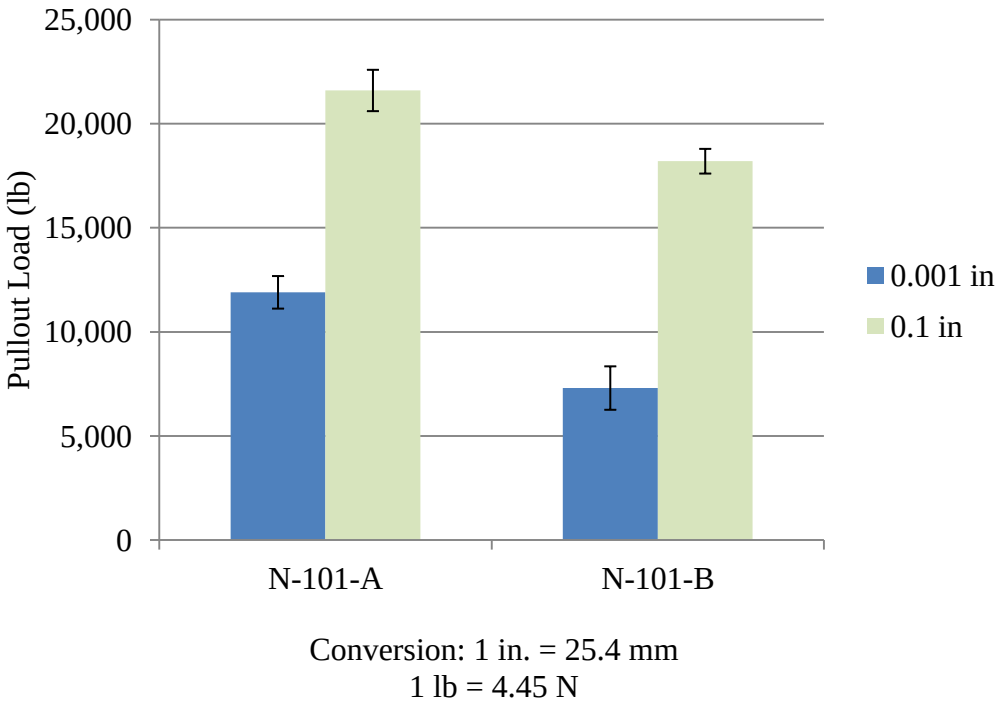

Figure 5.5 – Comparison of N-101-A and N-101-B Pullout Loads

5.2.2. Discussion of NASP Test in Concrete Results. The results from the NASP tests in concrete are presented in Tables 3.9 and 3.10 and are also presented graphically in Figures 5.6 and 5.7 with error bars representing one standard deviation above and below the average. Figure 5.6 displays the 0.001 in. (0.025 mm) and 0.1 in. (2.54 mm) pullout results for C6, S6, C10, and S10 at 1 day, while Figure 5.7 shows the 0.001 in. (0.025 mm) and 0.1 in. (2.54 mm) pullout results for the four concrete mixes at 8 days.

As discussed in Section 2.4.3, concrete strength has been shown to increase bond performance, and Figures 5.6 and 5.7 appear to support this conclusion. At both 1 and 8 days, the high strength conventional concrete 0.1 in. (2.54 mm) average pullout load (N-101-C10) was statistically higher than the normal strength conventional concrete 0.1 in. (2.54 mm) pullout load (N-101-C6). In terms of comparing normal strength to high strength SCC, the 1 day pullout loads showed no statistical difference because the standard deviation of N-101-S10 is so high. However, Figure 5.7 shows that at 8 days, the high strength SCC (N-101-S10) clearly had a higher pullout load than the normal

strength SCC (N-101-S6). The data presented in Figures 5.6 and 5.7 generally show that for a given type of concrete, an increase in concrete strength resulted in a higher pullout value, leading to the conclusion that increasing concrete strength improves bond. This supports the trend that has been noted by previous researchers, specifically, Ramirez and Russell (2008), who also conducted NASP tests in concretes at different strengths. They reported that increasing concrete strength resulted in increased NASP pullout loads, and the pullout loads showed a relatively strong correlation to the square root of the concrete compressive strength (Ramirez and Russell 2008).

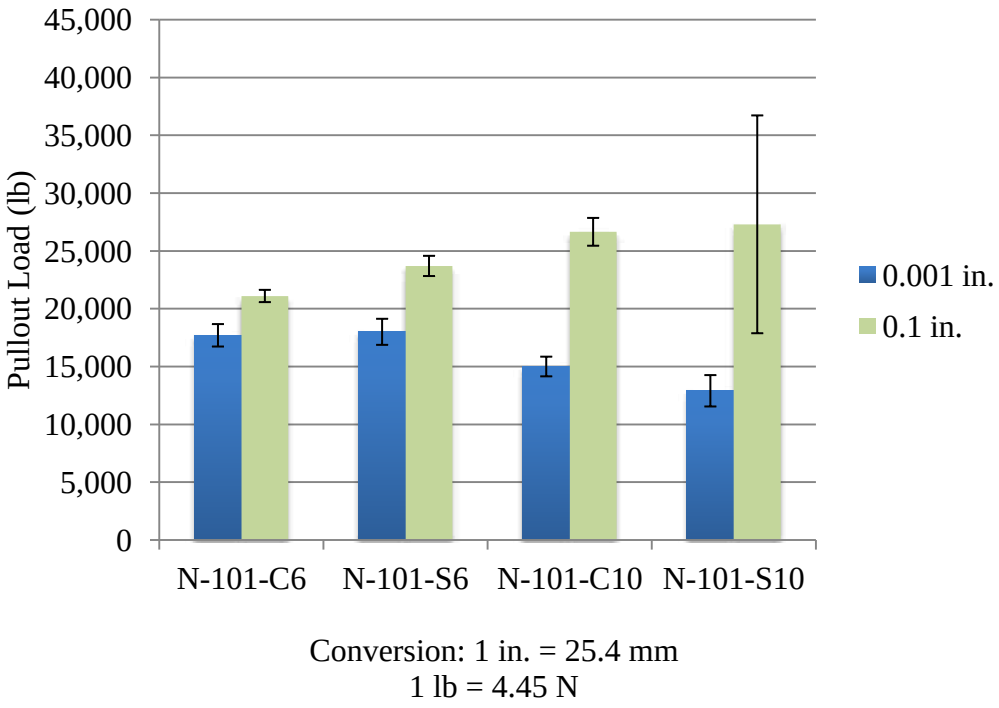

Figure 5.6 – NASP in Concrete Pullout Loads – 1 Day

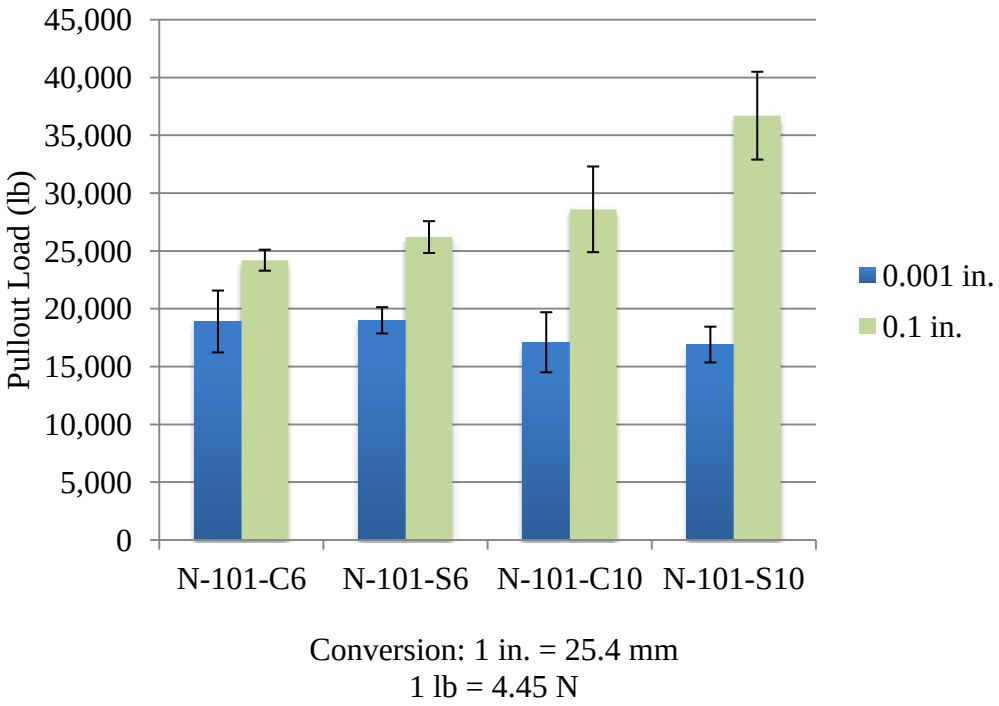

Conversion: 1 in. = 25.4 mm
1 lb = 4.45 N

Figure 5.7 – NASP in Concrete Pullout Loads – 8 Day

In addition to a comparison based on concrete strength, the results from the NASP tests in concrete were also evaluated to determine if the type of concrete affected the pullout loads. In order to directly compare the bond performance of conventional concrete to SCC, the pullout loads were normalized by dividing the pullout value for each mix at each day by the square root of the compressive strength at the time of testing. As discussed, research by Ramirez and Russell (2008) suggested that the NASP pullout loads can be correlated to the square root of concrete strength, so dividing the pullout loads by the square root of the compressive strength negated the effect of the compressive strength on the pullout loads so that the loads could be compared based solely on concrete type. The normalized pullout loads for C6 and S6 are presented in Table 5.3, and the normalized pullout loads for mixes C10 and S10 are shown in Table 5.4. The pullout loads divided by the square roots of the concrete compressive strengths with the standard deviation error bars are graphed in Figures 5.8 and 5.9. Figure 5.8 shows the values for the 1 day tests, and Figure 5.9 contains the results for the 8 day tests.

.

Table 5.3 – NASP in Concrete Results for C6 and S6 Normalized to $\sqrt{f'_c}$

Mix	Day	Specimen ID	$\sqrt{f'_c}$ (psi)	Load/$\sqrt{f'_c}$ at Slip of 0.001 in.				Load/$\sqrt{f'_c}$ at Slip of 0.1 in.			
				Load/$\sqrt{f'_c}$ (lb$\sqrt{psi}$)	Avg. Load/$\sqrt{f'_c}$ (lb/$\sqrt{psi}$)	Std. Dev. (lb.)	COV	Load/$\sqrt{f'_c}$ (lb$\sqrt{psi}$)	Avg. Load/$\sqrt{f'_c}$ (lb/$\sqrt{psi}$)	Std. Dev. (lb.)	COV
C6	1 Day	N-C6-1	69.35	243.7	255.7	14.0	5.48%	301.4	304.2	7.6	2.51%
		N-C6-2		252.3				298.5			
		N-C6-3		271.1				312.9			
	8 Day	N-C6-4	74.97	242.8	252.6	35.7	14.14%	332.1	323.3	12.1	3.74%
		N-C6-5		222.8				328.1			
		N-C6-6		292.1				309.5			
S6	1 Day	N-S6-1	75.23	248.6	239.3	15.0	6.26%	317.7	314.6	11.6	3.69%
		N-S6-2		247.2				324.3			
		N-S6-3		222.0				301.7			
	8 Day	N-S6-4	81.79	221.3	232.7	13.9	5.98%	302.0	320.3	16.8	5.25%
		N-S6-5		228.6				324.0			
		N-S6-6		248.2				335.0			

Conversion: 1 in. = 25.4 mm
1 lb = 4.45 N
1 psi = 6.89 kPa

Table 5.4 – NASP in Concrete Results for C10 and S10 Normalized to $\sqrt{f'_c}$

Mix	Day	Specimen ID	$\sqrt{f'_c}$ (psi)	Load/$\sqrt{f'_c}$ at Slip of 0.001 in.				Load/$\sqrt{f'_c}$ at Slip of 0.1 in.			
				Load/$\sqrt{f'_c}$ (lb$\sqrt{psi}$)	Avg. Load/$\sqrt{f'_c}$ (lb/$\sqrt{psi}$)	Std. Dev. (lb.)	COV	Load/$\sqrt{f'_c}$ (lb$\sqrt{psi}$)	Avg. Load/$\sqrt{f'_c}$ (lb/$\sqrt{psi}$)	Std. Dev. (lb.)	COV
C10	1 Day	N-C10-1	75.30	185.9	198.8	11.3	5.68%	N/A	353.9	16.0	4.51%
		N-C10-2		203.2				365.2			
		N-C10-3		207.2				342.6			
	8 Day	N-C10-4	89.16	173.8	191.8	29.2	15.20%	273.7	321.1	41.6	12.95%
		N-C10-5		176.1				338.7			
		N-C10-6		225.4				351.0			
S10	1 Day	N-C10-1	79.56	170.9	161.7	17.1	10.55%	364.5	342.7	118.4	34.55%
		N-S10-2		142.0				214.9			
		N-S10-3		172.2				448.7			
	8 Day	N-S10-4	92.74	199.5	182.6	16.7	9.16%	427.0	395.7	41.0	10.35%
		N-S10-5		166.1				410.8			
		N-S10-6		182.2				349.4			

Conversion: 1 in. = 25.4 mm
1 lb = 4.45 N
1 psi = 6.89 kPa

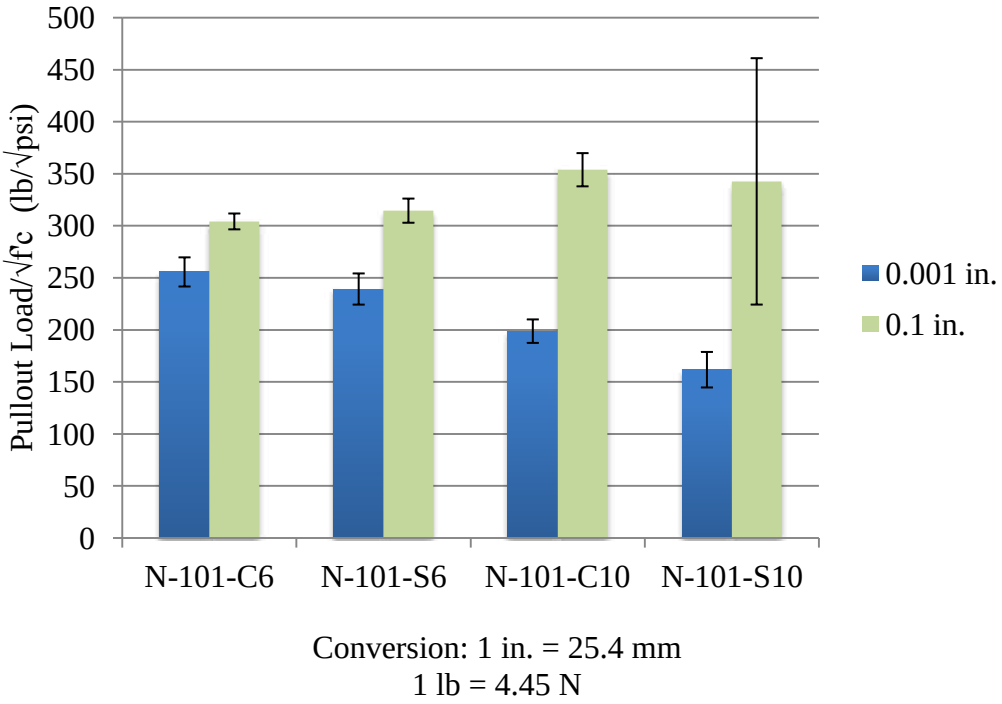

Figure 5.8 – NASP in Concrete Pullout Loads $\sqrt{f'_c}$ – 1 Day

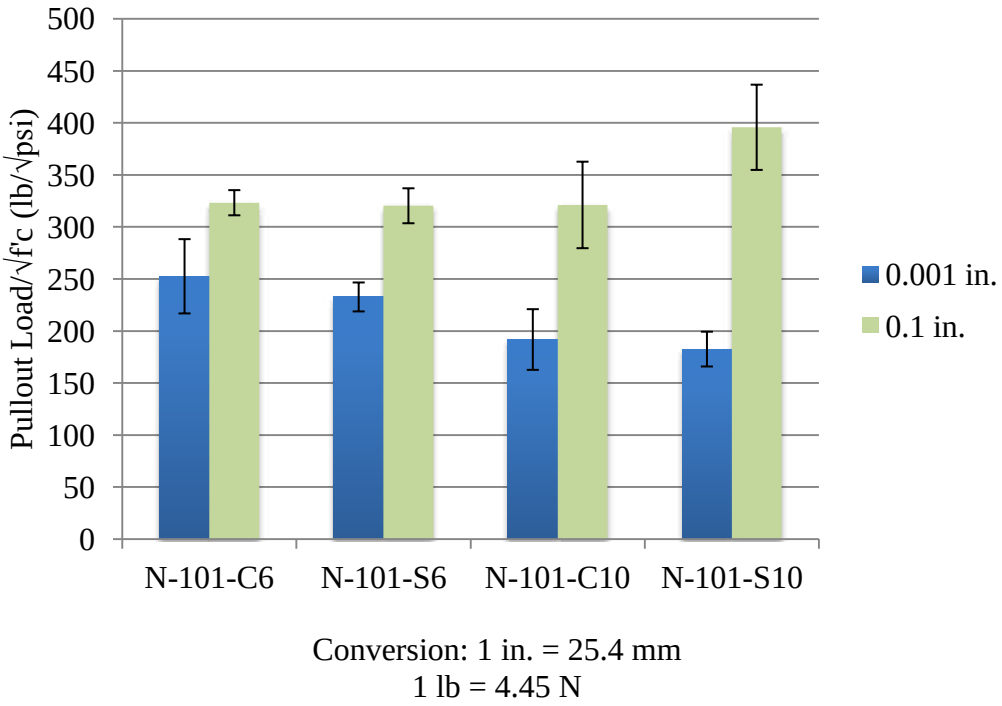

Figure 5.9 – NASP in Concrete Pullout Loads $\sqrt{f'_c}$ – 8 Day

According to Figure 5.8, at 1 day, there was virtually no difference between bond performance of the normal strength conventional concrete and SCC (C6 and S6) at either 0.001 in. (0.025 mm) or 0.1 in. (2.54 mm) of slip. However, in terms of the high strength mixes, the conventional concrete mix (C10) appeared to have slightly better bond in terms of first slip, but there was no difference at 0.1-in. (2.54 mm) pullout loads, mostly due to the high standard deviation in the results from the S10 mix.

Regarding the 8 day results, Figure 5.9 shows that once again, there was no difference in bond performance between the normal strength conventional concrete and SCC (C6 and S6) at either 0.001 in. (0.025 mm) or 0.1 in. (2.54 mm) of strand slip. According to Figure 5.9, at 8 days, there was also no difference in bond performance between the high strength conventional and SCC mixes (C10 and S10). Based on the averages, the S10 mix did appear to somewhat out-perform the C10 mix at the 0.1-in. (2.54 mm) slip benchmark, but error bars overlapped slightly, so that conclusion could not be definitively drawn.

In conclusion, for the NASP test performed with concrete instead of mortar, generally no difference was noted between the bond performance of SCC vs. conventional concrete. However, one conclusion that could be drawn from analysis of Figures 5.8 and 5.9 is that the high strength mixes (C10 and S10) consistently had lower pullout loads at 0.001 in. (0.025 mm) of slip than the conventional strength mixes (C6 and S6), and since the loads had been normalized with respect to concrete strength, this observation is most likely due to other factors affecting the concrete, such as mix design. Based on previous discussion, the low first slip load is likely due to a change in the adhesion between the strand and the concrete, indicating that the high strength mixes had lower adhesion with the strand than the normal strength mixes. The only major differences that was noted between the high strength and normal strength mix designs was that the high strength mixes contained some fly ash replacement and higher cementitious content, while the normal strength mixes did not, and this could be a possible factor affecting the adhesion.

5.2.3. Discussion of LBPT Results. The LBPT procedure is described in Section 3.4, and the results for all specimens can be found in Table 3.13. The average first slip load and peak load results, along with the standard deviation and coefficient of variation (COV), for each strand type are presented in this section in Table 5.5.

Table 5.5 – LBPT Results Statistical Summary

Strand ID	First Slip Load			Peak Load		
	Avg. Load (k)	Std. Dev. (k)	COV	Avg. Load (k)	Std. Dev. (k)	COV
101	19.1	2.3	12.27%	36.6	2.1	5.76%
102	12.7	1.7	13.53%	27.8	2.9	10.40%
103	19.3	3.3	17.16%	34.5	4.6	13.30%

Conversion: 1 kip = 4.45 kN

The average load values were compared to the limits set forth by Logan (Logan, personal communication, October 20, 2011). Logan recommends that in order for a strand to have acceptable bond quality, the average first slip load must exceed 16 kips (71.1 kN), and the average peak load value must be greater than 36 kips (160.1 kN). Additionally, Logan set the maximum allowable coefficient of variation for the peak loads at 10%. The average first slip load and peak load for each strand type as well as the first slip and peak minimum limits are presented graphically in Figure 5.10. The error bars represent one standard deviation from either side of the mean.

As seen in Figure 5.10, strand type 101 was the only strand type that passed the LBPT with the requirements proposed by Logan. The average first slip load and average peak load exceeded the limits by 19.1% and 1.76%, respectively, and the coefficient of variation for the peak load values was 5.76%, falling well below the 10% coefficient of variation limit. Meanwhile, strand type 103 passed the load at first slip limit, but the average peak load fell short of the 36 kip (160.1 kN) minimum limit. Strand type 102 did not pass either limit. Strand types 102 and 103 also had coefficient of variation values for the peak loads exceeding 10%.

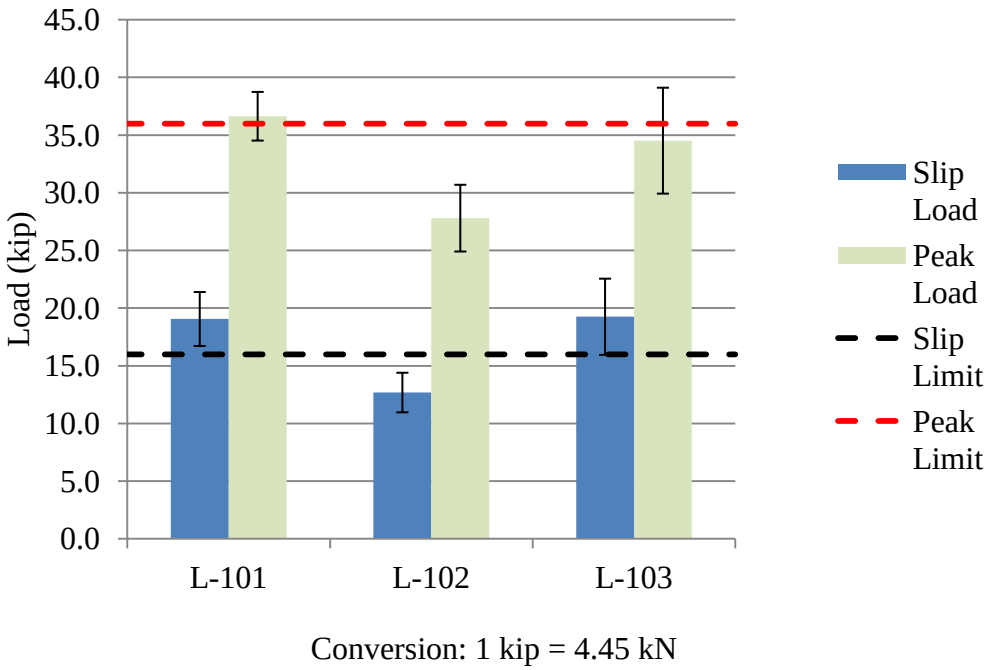

Conversion: 1 kip = 4.45 kN

Figure 5.10 – LBPT Average First Slip and Peak Pullout Loads

Visual observations and results from the towel wipe test, which were presented in Table 3.13, were also compared to the final results to determine if qualitative data could be any indication of the bond performance of the strand. Some researchers have found that rust improves bond quality, yet strand type 102 had the most observed rust and the heaviest residue, but also the lowest average pullout values. However, strand L-102-4 was the only strand that ruptured in the concrete, and this strand was noted to have the highest number of rust spots and heaviest residue out of all the strand samples. Strand types 101 and 103 had very comparable pullout values, and both strands were noted to have light to moderate residue and very little rust. In this project, it appeared that lighter residue led to higher pullout values, but only three strand samples were tested, and due to limited data and the subjective nature of the visual tests, it was determined that no clear correlation existed between amount of rust and residue and strand bond performance.

5.2.4. Comparison of NASP Test in Mortar Results to LBPT Results. One of the purposes of this research program was to compare the NASP test in mortar to the LBPT to determine if one test can be deemed as better or more consistent than the other.

The results from both tests were evaluated to see if the overall results from the different strand types were consistent from test to test.

The pullout results from the NASP in mortar and the LBPT are presented for comparison in Table 5.6. The values presented from the NASP tests are the loads at 0.1 in (2.54 mm) slip from the tests completed in mortar Mix B, while the values presented from the LBPT are the peak pullout loads. Table 5.6 displays the six individual results for each strand and each test as well as the average value, standard deviation, and coefficient of variation for each strand and test.

One observation that can be made from examination of Table 5.6 is that for a given strand type, the coefficient of variation determined from the NASP test and LBPT was remarkably similar (within 1-2%). This would indicate that both the NASP test and LBPT seem to be more or less equal in terms of consistency of results.

In order to determine if a correlation existed between the LBPT and NASP test in mortar performed in this study, the LBPT peak pullout loads and NASP pullout loads at 0.1 in (2.54 mm) slip were plotted against each other. The data was manipulated so that for the results for each strand type, the six NASP pullout loads and six LBPT pullout loads were sorted from lowest to highest within their respective tests. Then, within each strand type, the lowest NASP pullout value was plotted against the lowest LBPT pullout value, and the second lowest values from each test were plotted against each other, and so on. The plot of LBPT pullout loads vs. NASP in mortar pullout loads is presented in Figure 5.11.

The linear trend line through the points in Figure 5.11 yielded an R^2 value of 0.77, which shows there was a somewhat strong correlation between the NASP in mortar pullout loads and LBPT pullout loads in this study. Based on this comparison as well as the previous observation with respect to comparing coefficients of variation for each test method, it appears that either the LBPT or NASP test are equally valid approaches to evaluating bond performance of prestressing strand. However, the limits set on passing may need some refinement, as two of the strand sources passed the proposed NASP standard but did not pass the LBPT requirements.

Table 5.6 – NASP in Mortar and LBPT Pullout Loads

Strand Type	Specimen No. or Statistic	NASP (Mix B) 0.1 in Pullout Load (lb)	LBPT Peak Pullout Load (k)
101	1	19,100	34.3
	2	17,300	34.2
	3	17,800	35.9
	4	19,100	38.8
	5	18,200	38.5
	6	17,800	38.1
	Avg.	**18,200**	**36.6**
	Std. Dev.	**741**	**2.1**
	COV	**4.07%**	**5.76%**
102	1	11,000	27.1
	2	12,400	27.1
	3	12,600	31.0*
	4	9,300	40.1**
	5	12,400	25.1
	6	12,300	31.9
	Avg.	**11,700**	**27.8**
	Std. Dev.	**1,296**	**2.9**
	COV	**11.07%**	**10.40%**
103	1	15,800	33.5
	2	20,500	33.5
	3	18,600	38.7
	4	16,000	35.6
	5	19,700	26.6
	6	21,300	39.2
	Avg.	**18,700**	**34.5**
	Std. Dev.	**2,311**	**4.6**
	COV	**12.36%**	**13.30%**

* - Data collection accidently stopped early, so value determined by observation.
** - Strand fractured, value not included in average or standard deviation.

Conversion: 1 in. = 25.4 mm
1 lb = 4.45 N
1 kip = 4.45 kN

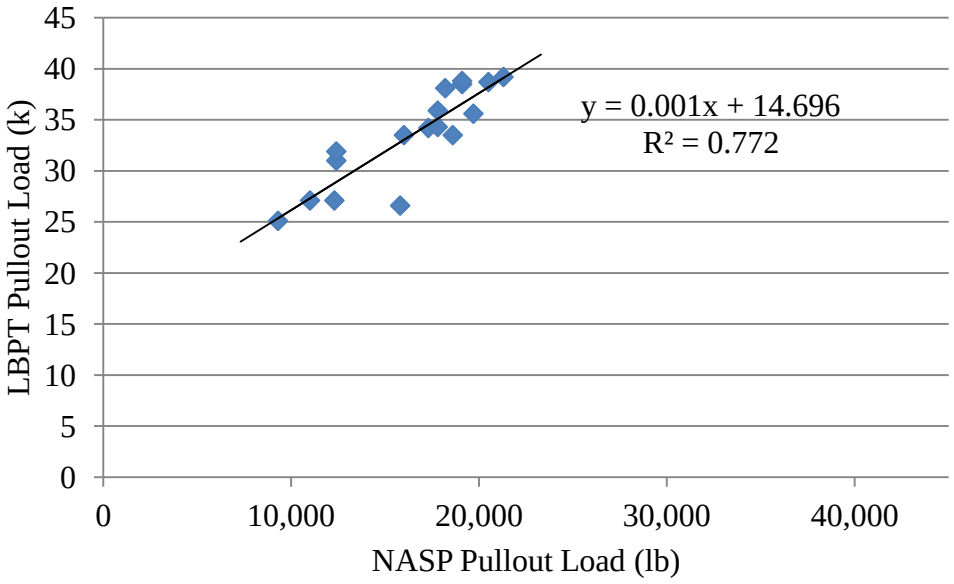

Conversion: 1 lb = 4.45 N
1 kip = 4.45 kN

Figure 5.11 – LBPT Pullout Loads vs. NASP Pullout Loads

As discussed in Sections 5.2.1 and 5.2.3, the NASP test and LBPT results were compared to their respective acceptance limits to determine if each strand passed or failed. The pass/fail results as well as the overall ranking of the strands in terms of bond from each test are presented in Table 5.7. The ranks were based on the load at 0.1 in. (2.54 mm) slip for the NASP test in mortar and the peak pullout load for the LBPT.

Table 5.7 – Pass/Fail Results for NASP in Mortar and LBPT

Strand ID	NASP in Mortar		LBPT	
	Rank	Pass/Fail	Rank	Pass/Fail
101	2	PASS	1	PASS
102	3	PASS	3	FAIL
103	1	PASS	2	FAIL

The correlation between tests was not consistent. As seen in Table 5.7, strand type 101 was the only type that was considered to have acceptable bond performance by both tests. Strand types 102 and 103 both passed the NASP test in mortar but failed the LBPT. The relative bond between strands was also not the same between tests. Strand type 102 had the worst bond performance in both the NASP and LBPT, but strand type 103 had the best performance in the NASP test, while strand type 101 had the best performance in the LBPT. However, strand types 101 and 103 were extremely comparable, and average pullout values between the two types were within 2.7% for the NASP test and 6.0% for the LBPT. Also, error bars show the standard deviations for the two types overlapped significantly for the NASP Test (Figure 5.1) as well as the LBPT (Figure 5.10). Therefore, the differences in rank are not statistically significant for types 101 and 103. The two test methods can be considered fairly accurate with respect to relative bond between strands, but in terms of absolute bond and rejecting or accepting strand based on set limits, the NASP test passed all three types while the LBPT only passed one out of the three.

5.3. TRANSFER LENGTH TEST RESULTS

The transfer lengths determined from DEMEC data and the 95% Average Mean Strain Method, as well as values determined from the end slip values measured by the Synergy data acquisition and steel ruler, are evaluated and discussed in this subsection.

5.3.1. Discussion of 95% Average Mean Strain Transfer Length Results. The primary method used for determining transfer lengths was the 95% Average Mean Strain Method. The process of developing strain profiles based on DEMEC readings and determining the transfer lengths is described in Section 4.4.1. The final individual transfer lengths at 1, 4, 8, 14, 28, and approximately 56 days as determined by the 95% Average Mean Strain Method are presented in Tables 4.3 and 4.4, and the average transfer lengths and the standard deviations for each mix for the top and bottom strands are summarized in Tables 4.5 and 4.6. The averages and standard deviations are based on all of the individual results from each mix, but additional analysis in this section revealed individual measurements that could potentially be removed when comparing averages to

each other to determine if differences between measured transfer lengths from mix to mix are statistically significant.

As discussed in Section 2.4.5, previous research has indicated that a transfer length at a "live end," or end directly adjacent to where the strand is first released, is typically longer than a transfer length at a "dead end," or end not adjacent to the place where the strand is first cut. In this research, the live and dead ends of the strands were not directly monitored. In this research program, for release of each strand, one person was positioned at each location where the strand would need to be cut to separate all the beams in the line, and all locations were attempted to be cut at the same time using bolt cutters, as described in Section 4.3. However, it was very hard for the workers to sever all locations at exactly the same time, and typically one or two locations on one strand were severed before others. It was not noted at the site which location on each strand was cut first, but it was surmised that the linear potentiometer data would be able to indicate which ends were severed first. However, due to the proven unreliability of the potentiometers, the electronically collected data could not reliably indicate the sequence of strand release.

Although there is no hard evidence as to the sequence of release, analysis of the transfer length data does potentially indicate where some of the live ends could have occurred. Figures 5.12 and 5.13 show the casting layouts and initial (1 day) transfer lengths determined by the 95% Average Mean Strain Method at each individual location. The circles indicate locations that have comparatively higher measured transfer lengths, which could possibly indicate the live end locations.

In Figure 5.12, C6-4-1_SE is the only location that appears unusually high, but no definite conclusion could be made regarding a live end because only two transfer lengths out of four were able to be determined for the top strands in the C6 mix. The transfer lengths at C6-4-1_NE and C6-4-1_NW were not established because there were no defined plateaus on the strain profiles. This could be due to faulty DEMEC readings, or the stains were in fact still increasing, which could indicate that those locations were live ends. However, there was no way to come to definite conclusions, so averages were not adjusted for either of the normal strength mixes for two strands or four strands.

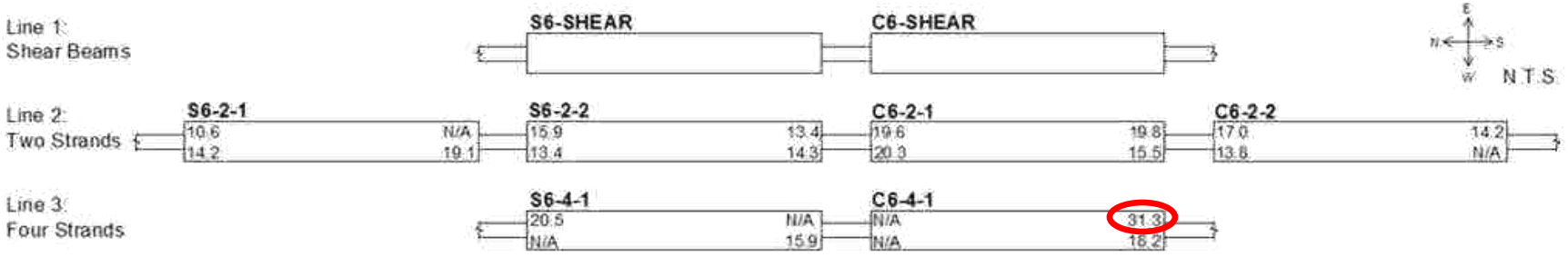

Conversion: 1 in. = 25.4 mm

Figure 5.12 – C6 and S6 Transfer Length Locations

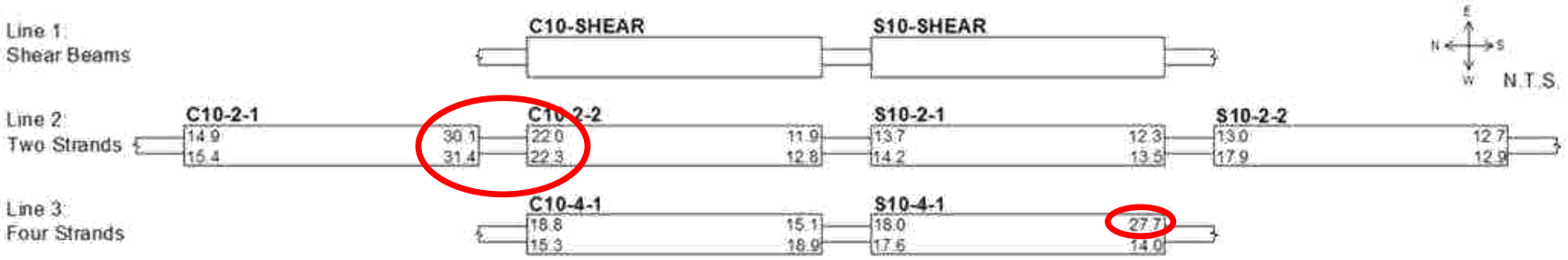

Conversion: 1 in. = 25.4 mm

Figure 5.13 – C10 and S10 Transfer Length Locations

Some more refined conclusions could be made regarding the high strength mixes, based on observations of Figure 5.13. Although S10-4-1_SE was not statistically an outlier, the value was still comparatively high, and several different transfer length averages were calculated for comparison. The standard average transfer length, S10-4, was taken with all four values, and then the potential dead end transfer length average, S10-4 (D), was calculated with the NE, NW, and SW values while the SE value was taken as the live end transfer length, S10-4 (L).

According to Figure 5.13, the four locations that seem to definitively indicate live ends are C10-2-1_SE, C10-2-1_SW, C10-2-2_NE, and C10-2-2_NW. Due to significant and consistent differences in transfer lengths, it appears that the east strand in the two-strand line of high strength beams was first severed between C10-2-1_SE and C10-2-2_NE, and the first cut on the west strand was made between C10-2-1_SW and C10-2-2_NW. Photographic evidence taken at the time of release seems to confirm this determination. Figure 5.14 was taken during release of the east strand of the line of the high strength two-strand beams, and the worker cutting the location between beams C10-2-1 and C10-2-2 is clearly in motion, while the worker between C10-2-2 and S10-2-1 has not started to cut the strand. The person who cut the east strand between C10-2-1 and C10-2-2 also cut the west strand between the two beams, and if he was early on the first strand, chances are reasonable that he was early on the second strand as well. Although the remaining workers cannot be seen, the fact that evidence shows the location between C10-2-1 and C10-2-2 was cut before at least one other location combined with the high transfer length results leads to the assumption that ends C10-2-1_SE, C10-2-1_SW, C10-2-2_NE, and C10-2-2_NW could reasonably be considered the live ends for that line. Therefore, in addition to the standard full C10-2 average for each day, the adjusted average C10-2 (D) was taken for the dead ends, and the adjusted average C10-2 (L) was calculated for the live ends. The different transfer length averages for C10-2 at 1, 4, 8, 14, and 28 days were compared to transfer lengths in the S10 mix.

Figure 5.14 – Release of C10-2 Beams

The standard and modified dead and live end averages, standard deviations, and coefficients of variation for each mix for the bottom and top strands are shown in Tables 5.8 and 5.9, respectively. The "standard" values are the averages and standard deviations calculated based on all reported transfer lengths, and the "modified" values are the live end or dead end averages and standard deviations taken when applicable. C10-2 (L) values in Table 5.8 are the averages at each day for the possible live ends for the bottom strands and include C10-2-1_SE, C10-2-1_SW, C10-2-2_NE, and C10-2-2_NW, while C10-2 (D) values are the dead end averages, which include the remaining ends in the C10-2 beams. S10-4 (L) for the top strands in Table 5.9 is only the S10-4-1_SE value at each day, and S10-4 (D) values are the averages of the remaining three ends. The different averages were compared to determine if there was any statistical difference between transfer lengths measured in the conventional concrete and SCC and then compared to values calculated by AASHTO and ACI equations. Throughout the remainder of this thesis, it should be noted that a mix identification with a "2" suffix indicates bottom strand average, while a mix identification with a "4" suffix indicates a top strand average.

Table 5.8 – Standard and Modified Transfer Length Averages (Bottom Strands)

Bottom Strands		1 Day (in.)	4 Day (in.)	8 Day (in.)	14 Day (in.)	28 Day (in.)	~56 Day (in.)
C6-2	Avg.	17.2	20.4	22.3	23.7	23.6	22.8
	Std. Dev.	2.76	4.07	4.85	5.09	5.69	4.22
	COV	16.1%	19.9%	21.8%	21.5%	24.1%	18.5%
S6-2	Avg.	14.4	18.4	18.2	18.6	19.2	19.2
	Std. Dev.	2.61	3.20	1.90	2.35	2.17	2.21
	COV	18.1%	17.4%	10.5%	12.7%	11.3%	11.5%
C10-2	Avg.	20.1	22.7	23.4	23.2	23.7	23.5
	Std. Dev.	7.63	7.53	7.38	7.38	7.35	8.06
	COV	37.9%	33.2%	31.5%	31.8%	31.0%	34.3%
C10-2 (D)*	Avg.	13.7	16.3	17.2	16.9	17.2	16.4
	Std. Dev.	1.70	2.41	2.31	1.92	1.78	1.90
	COV	12.3%	14.8%	13.4%	11.4%	10.4%	11.6%
C10-2 (L)*	Avg.	26.5	29.1	29.7	29.5	30.3	30.6
	Std. Dev.	4.99	4.22	4.33	4.17	2.69	3.55
	COV	18.9%	14.5%	14.6%	14.1%	8.9%	11.6%
S10-2	Avg.	13.8	16.4	16.3	16.5	16.6	15.9
	Std. Dev.	1.76	2.44	2.04	2.15	2.09	1.71
	COV	12.8%	14.9%	12.5%	13.0%	12.6%	10.7%

* = Modified averages, which include only the assumed dead end (D) or assumed live end (L) transfer length values

Conversion: 1 in. = 25.4 mm

Table 5.9 – Standard and Modified Length Averages (Top Strands)

Top Strands		1 Day (in.)	4 Day (in.)	8 Day (in.)	14 Day (in.)	28 Day (in.)	~56 Day (in.)
C6-4	Avg.	24.8	N/A	27.5	27.6	28.9	26.3
	Std. Dev.	9.25	N/A	3.63	4.98	4.15	N/A
	COV	37.4%	N/A	13.2%	18.0%	14.4%	N/A
S6-4	Avg.	18.2	21.8	22.2	21.1	20.1	22.4
	Std. Dev.	3.26	4.15	0.55	1.50	1.20	0.58
	COV	17.9%	19.0%	2.5%	7.1%	6.0%	2.6%
C10-4	Avg.	17.0	17.2	17.7	17.5	19.0	20.3
	Std. Dev.	2.08	2.95	2.19	2.22	3.59	1.80
	COV	12.2%	17.1%	12.3%	12.7%	18.9%	8.9%
S10-4	Avg.	19.3	17.0	18.6	19.0	18.3	19.5
	Std. Dev.	5.86	3.63	6.50	6.02	6.52	6.46
	COV	30.3%	21.4%	35.0%	31.7%	35.6%	33.1%
S10-4 (D)*	Avg.	16.5	15.6	15.4	16.0	15.1	16.3
	Std. Dev.	2.22	2.80	1.54	1.39	1.35	1.63
	COV	13.4%	18.0%	10.0%	8.6%	8.9%	10.0%
S10-4 (L)*	Avg.	27.7	21.2	28.1	27.9	28.0	29.0
	Std. Dev.	-	-	-	-	-	-
	COV	-	-	-	-	-	-

* = Modified averages, which include only the assumed dead end (D) or assumed live end (L) transfer length values

Conversion: 1 in. = 25.4 mm

5.3.1.1 Comparison of SCC to conventional concrete. In order to determine if the average transfer lengths were statistically different between conventional concrete and SCC, the 90% confidence interval for each mix at each day from 1-28 days was calculated, and then average transfer lengths of mixes were plotted against each other with error bars at each point representing the 90% confidence intervals. Points with overlapping error bars showed the average transfer lengths for those two mixes at a given time after casting were not statistically different. This process of determining statistical significance is based on the data analysis performed by Staton, Do, Ruiz, and Hale in a similar study on transfer length (2009). It should be noted that in the following comparisons, the transfer length averages at approximately 56 days were not included in

the evaluation because the transfer lengths were determined between 48 and 57 days after casting depending on when the four-point flexural testing was completed, so averages were not directly comparable.

The bottom strands in normal strength conventional concrete and SCC mixes (C6-2 and S6-2) are compared in Figure 5.15, and the high strength conventional and SCC mixes (C10-2 and C10-2 (D) and S10) are compared in Figure 5.16 and 5.17. In Figure 5.15, although C6-2 appears to have had higher average transfer lengths, the 90% confidence interval error bars overlap in all cases except at 14 days, meaning that there was really no difference in bottom transfer lengths in normal strength conventional concrete versus SCC. Although there is no overlap at 14 days, the gap is so narrow, that it can be assumed there was no statistical difference at 14 days as well.

On the other hand, Figure 5.16 appears to show there was a statistical difference between the high strength conventional concrete and SCC bottom strand transfer lengths, with C10-2 having the longer transfer lengths. However, the 90% confidence intervals for the C10 mix are very large due to the inclusion of the possible live end transfer lengths. C10-2 (D) is the average of the four possible dead end transfer lengths, and when C10-2 (D) average transfer lengths are compared to the S10-2 average transfer lengths in Figure 5.17, the values are almost identical and there is no statistical difference. S10-2 average transfer lengths were not compared to the C10-2 (L) because it can be assumed that the S10-2 averages are based on dead end transfer lengths, so comparing the S10-2 averages to the live end C10-2 averages would not be a valid comparison.

Overall, the statistical analysis shows that for bottom strands, there was no statistical difference between transfer lengths in conventional concrete and SCC at both normal strength and high strength levels up to 28 days after casting. However, this was only true when the perceived live end transfer lengths were removed from the averages. A summary of the bottom strand transfer lengths from this research for each conventional concrete vs. SCC comparison is presented in Table 5.10. Shaded pairs indicate a statistical difference between the averages.

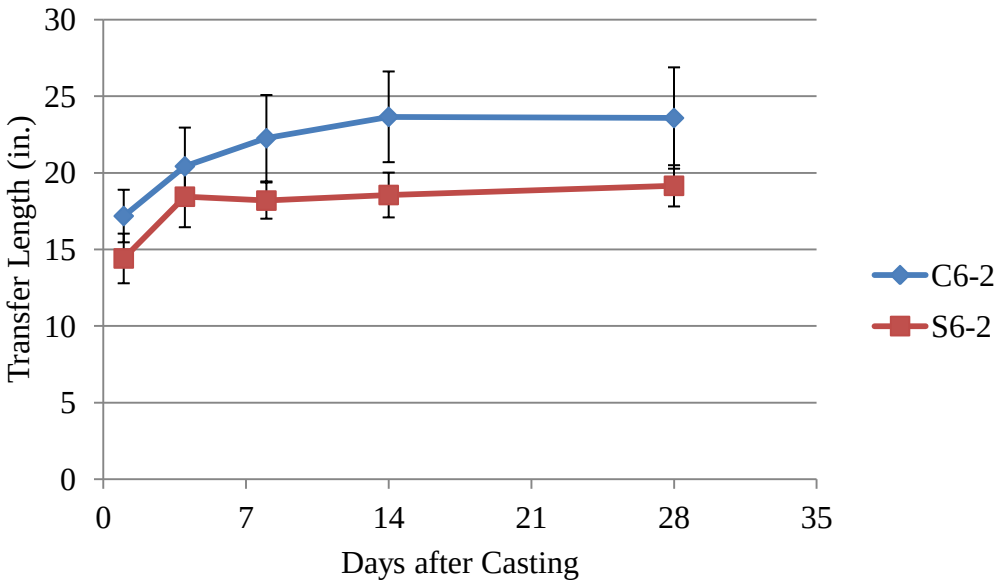

Conversion: 1 in. = 25.4 mm

Figure 5.15 – C6-2 and S6-2 Transfer Lengths with 90% Confidence Intervals

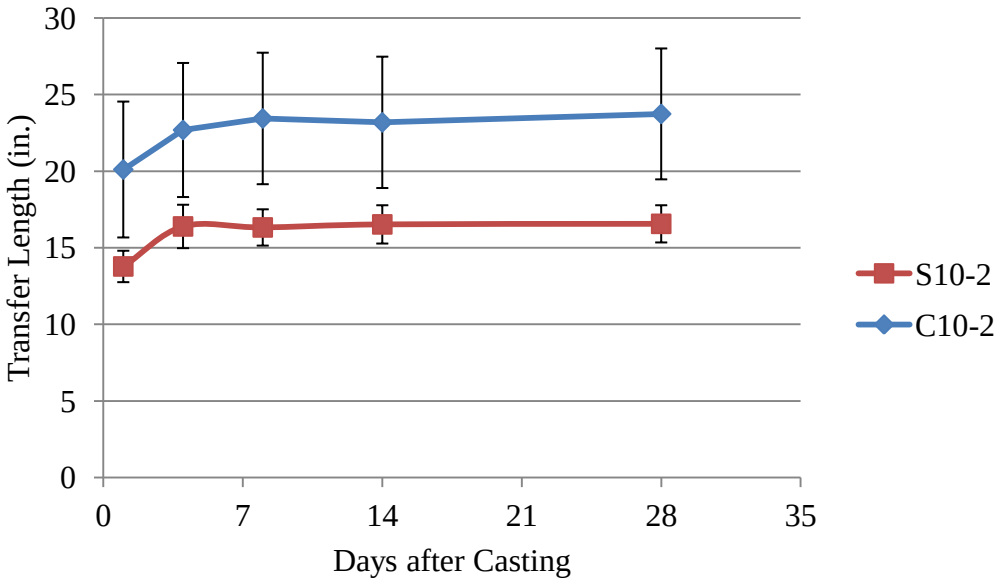

Conversion: 1 in. = 25.4 mm

Figure 5.16 – C10-2 and S10-2 Transfer Lengths with 90% Confidence Intervals

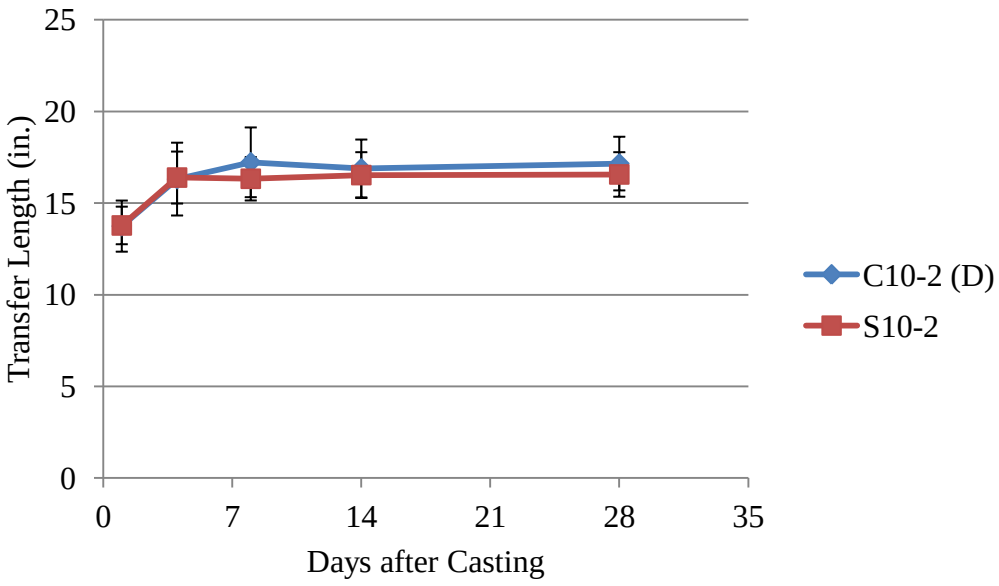

Conversion: 1 in. = 25.4 mm

Figure 5.17 – C10-2 (D) and S10-2 Transfer Lengths with 90% Confidence Intervals

Table 5.10 – Conventional Concrete vs. SCC: Summary of Statistical Differences Between Bottom Strand Transfer Lengths

Combination	1 Day (in.)	4 Day (in.)	8 Day (in.)	14 Day (in.)	28 Day (in.)
C6-2	17.2	20.4	22.3	23.7	23.6
S6-2	14.4	18.4	18.2	18.6	19.2
C10-2	20.1	22.7	23.4	23.2	23.7
S10-2	13.8	16.4	16.3	16.5	16.6
C10-2 (D)	13.7	16.3	17.2	16.9	17.2
S10-2	13.8	16.4	16.3	16.5	16.6

*Shaded pairs indicate statistical difference between values (90% CI)
Conversion: 1 in. = 25.4 mm

The same statistical analysis between transfer lengths in conventional concrete and SCC at the normal and high compressive strength levels was completed for the top strands as well. However, since only one four strand beam was constructed per mix, averages for top strand transfer lengths were based on only four readings, and in many

instances, the DEMEC readings resulted in unreasonable plots where transfer lengths could not be determined. In the cases of the C6-4 and S6-4 beams, the average top strand transfer lengths and standard deviations were only based on two readings each. The top strands in normal strength conventional concrete and SCC mixes (C6-4 and S6-4) are compared in Figure 5.18, and the high strength conventional and SCC mixes [C10-4 and S10-4 and S10-4 (D)] are compared in Figure 5.19 and 5.20.

Figure 5.18 shows overlap of the 90% confidence interval error bars for all days except 28 days for the C6 and S6 mixes. However, these averages and standard deviations for the top strand for these mixes were only based on two readings each, so although the plot indicates that top strand transfer lengths in the normal strength conventional and SCC mixes were generally not statistically different, this conclusion is based on limited data.

In terms of the transfer lengths of top strands in the high strength mixes, the C10-4 transfer lengths are compared to the full S10-4 averages in Figure 5.19 and then compared to the S10-4 (D) averages in Figure 5.20. The 90% confidence intervals overlap in both cases, indicating that there was no difference in top strand transfer lengths in high strength conventional concrete or high strength SCC.

SCC top strand transfer lengths were generally shorter than the conventional concrete top strand transfer lengths, but only a few statistical differences were seen between transfer lengths in the normal strength mixes, and none were seen between either combination of the high strength conventional concrete and SCC averages. A summary of the top strand transfer lengths for each conventional concrete vs. SCC comparison is presented in Table 5.11. Shaded pairs indicate a statistical difference between the averages.

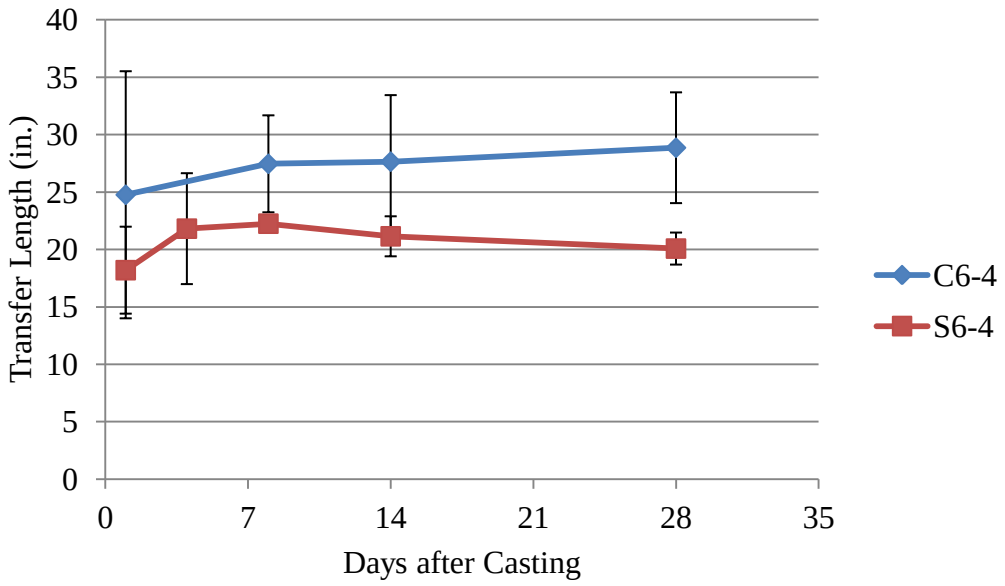

Conversion: 1 in. = 25.4 mm

Figure 5.18 – C6-4 and S6-4 Transfer Lengths with 90% Confidence Intervals

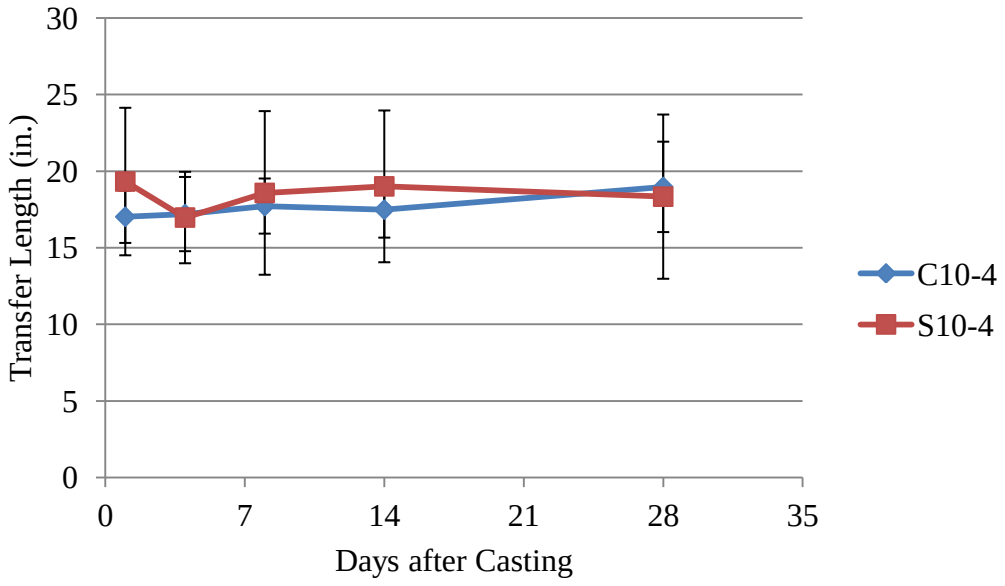

Conversion: 1 in. = 25.4 mm

Figure 5.19 – C10-4 and S10-4 Transfer Lengths with 90% Confidence Intervals

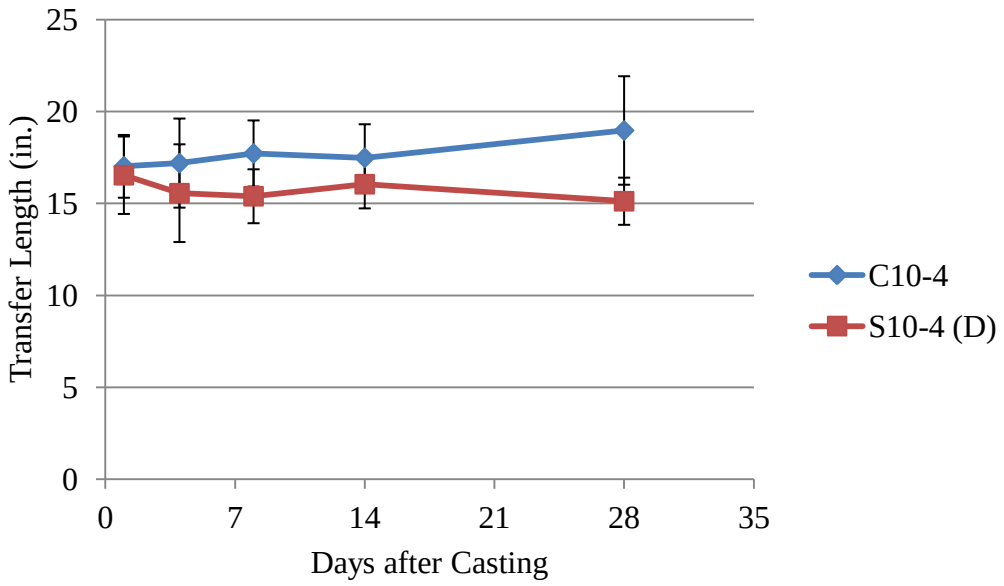

Conversion: 1 in. = 25.4 mm

Figure 5.20 – C10-4 and S10-4 (D) Transfer Lengths and 90% Confidence Intervals

Table 5.11 – Conventional Concrete vs. SCC: Summary of Statistical Differences Between Top Strand Transfer Lengths

Combination	1 Day (in.)	4 Day (in.)	8 Day (in.)	14 Day (in.)	28 Day (in.)
C6-4	24.8	N/A	27.5	27.6	28.9
S6-4	18.2	21.8	22.2	21.1	20.1
C10-4	17.0	17.2	17.7	17.5	19.0
S10-4	19.3	17.0	18.6	19.0	18.3
C10-4	17.0	17.2	17.7	17.5	19.0
S10-4 (D)	16.5	15.6	15.4	16.0	15.1

*Shaded pairs indicate statistical difference between values (90% CI)
Conversion: 1 in. = 25.4 mm

Overall, the results show that there was no significant difference between transfer lengths measured in conventional concrete and SCC of the same strength level from one to 28 days after casting. The plots compare C6 to S6 transfer lengths and C10 to S10 transfer lengths for both top and bottom strands and with the full and modified averages

that include or do not include the possible live end transfer lengths, and although the plots generally show the SCC average transfer lengths were shorter than conventional concrete average transfer lengths, the 90% confidence interval error bars overlap in almost all cases, rendering the differences in transfer lengths statistically insignificant.

Although some previous studies have shown SCC transfer lengths being longer than those in conventional concrete (Girgis and Tuan 2005 and Burgueño 2007), the results from this research matched findings from Staton et al. (2009) and Boehm et al. (2010), who both reported no overall significant difference between SCC and conventional concrete. It should be noted that these previous studies only evaluated bottom strand.

5.3.1.2 Comparison of normal strength to high strength. The top and bottom transfer length values were also analyzed to determine the degree to which concrete strength affects transfer length. The bottom strands in normal strength conventional concrete and high strength conventional concrete [C6-2 and C10-2 and C10-2 (D)] are compared in Figure 5.21 and 5.22, and the normal and high strength SCC mixes (S6-2 and S10-2) are compared in Figure 5.23.

Figure 5.21 shows that there is significant overlap of the 90% confidence interval error bars at all days, so it appears there was no difference between the normal strength and high strength conventional concrete mixes (C6-2 and C10-2). However, when C6-2 average transfer lengths were compared to the averages of the dead end transfer lengths of the high strength conventional concrete [C10-2 (D)] transfer lengths, the transfer lengths in the higher strength concrete were notably shorter than the transfer lengths in the normal strength concrete. Figure 5.22 shows that the 90% error bars do not overlap for the C6-2 and C10-2 (D), so this implies when the live end transfer lengths were removed, there was a statistical difference between the transfer lengths in normal and high strength conventional concretes.

Figure 5.23 shows that the S10-2 transfer lengths appear to be slightly shorter than the S6-2 transfer lengths, but the 90% confidence interval error bars overlap, so according to the data, there was no statistical difference between bottom strand transfer lengths in normal strength and high strength SCC.

Overall, the statistical analysis shows that for bottom strands, an increase in compressive strength resulted in shorter transfer lengths for conventional concrete, especially when the live end transfer lengths were removed from the averages. However, concrete strength did not appear to significantly influence transfer lengths in SCC. A summary of the bottom strand transfer lengths for each normal strength to high strength comparison is presented in Table 5.12. Shaded pairs indicate a statistical difference between the averages.

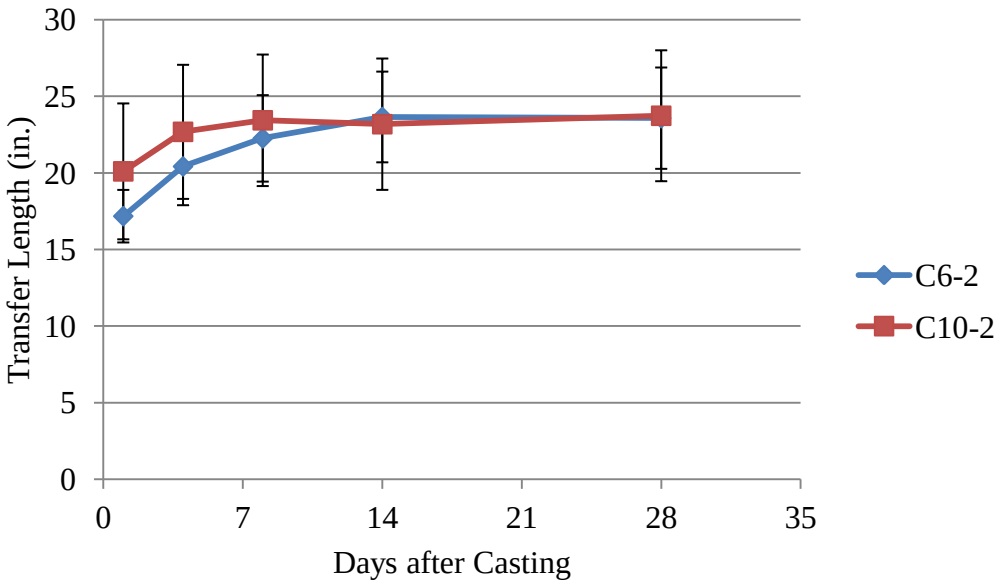

Conversion: 1 in. = 25.4 mm

Figure 5.21 – C6-2 and C10-2 Transfer Lengths and 90% Confidence Intervals

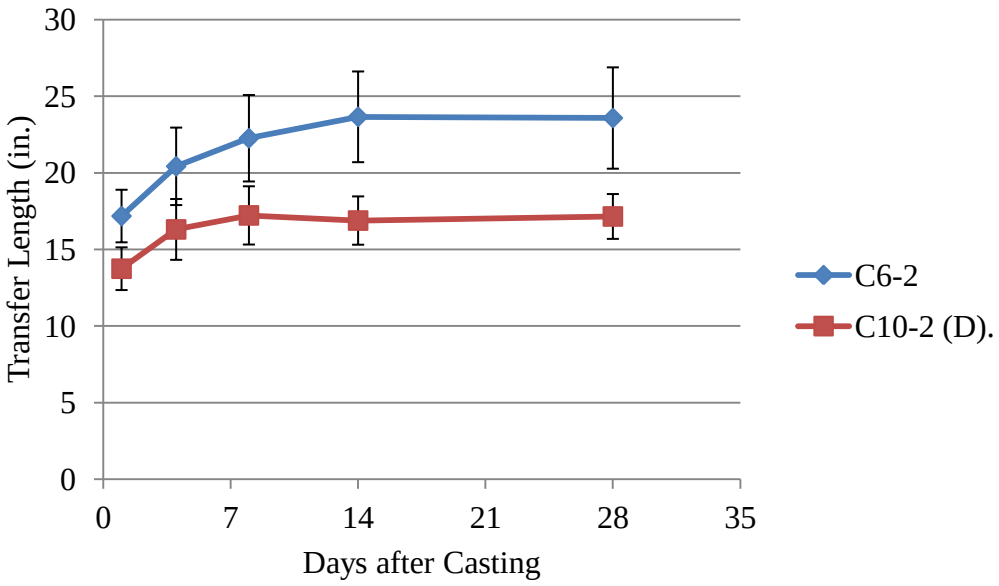

Conversion: 1 in. = 25.4 mm

Figure 5.22 – C6-2 and C10-2 (D) Transfer Lengths and 90% Confidence Intervals

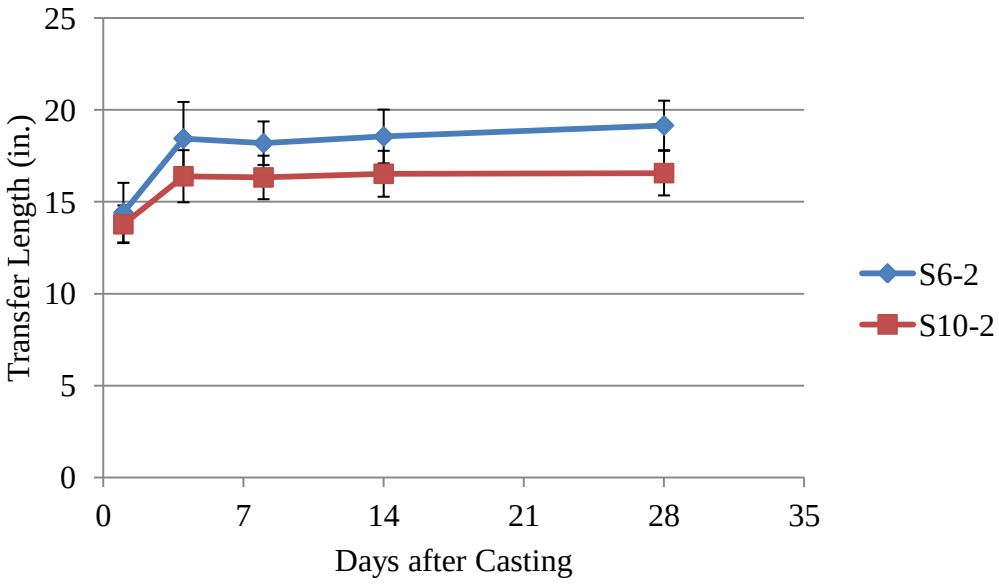

Conversion: 1 in. = 25.4 mm

Figure 5.23 – S6-2 and S10-2 Transfer Lengths and 90% Confidence Intervals

Table 5.12 – Normal Strength vs. High Strength: Summary of Statistical Differences Between Bottom Strand Transfer Lengths

Combination	1 Day (in.)	4 Day (in.)	8 Day (in.)	14 Day (in.)	28 Day (in.)
C6-2	17.2	20.4	22.3	23.7	23.6
C10-2	20.1	22.7	23.4	23.2	23.7
C6-2	17.2	20.4	22.3	23.7	23.6
C10-2 (D)	13.7	16.3	17.2	16.9	17.2
S6-2	14.4	18.4	18.2	18.6	19.2
S10-2	13.8	16.4	16.3	16.5	16.6

*Shaded pairs indicate statistical difference between values (90% CI)
Conversion: 1 in. = 25.4 mm

In terms of the effect of concrete strength on top strand transfer lengths, the 90% confidence interval error bars in Figure 5.24 show that the top strand transfer lengths in the high strength conventional concrete were generally shorter than the top strand transfer lengths in the normal strength conventional concrete. There does not appear to be a statistical difference between the one day transfer lengths, but the 90% confidence interval for C6-4 was fairly large, measuring 10.7 in. (272 mm) above and below the average. Also, the C6-4 average transfer lengths were only based on two values for each day. The transfer lengths in the normal strength conventional concrete did appear to be consistently longer than the transfer lengths in the high strength conventional concrete; however it should be noted that this conclusion is based on limited data.

The top strand transfer lengths in the normal strength and high strength SCC mixes are compared in Figure 5.25 and 5.26. Figure 5.25 shows no statistical difference between the S6-4 and full average of S10-4 transfer lengths. However, when the normal strength SCC transfer lengths are compared to the average dead end high strength SCC transfer lengths in Figure 5.26, this plot indicates that there was no statistical difference at 1 and 4 days, but the S10-4 (D) transfer lengths seemed to be generally shorter than the S6-4 transfer lengths at later ages.

For the top strands in this research program, the increase in concrete strength in conventional concrete generally resulted in shorter transfer lengths, although it should be

noted that the C6-4 average values were only based on two readings. In SCC, when the possible live end was removed from the S10-4 data, the increase in concrete strength also appeared to shorten top strand transfer lengths, specifically at later ages. A summary of the top strand transfer lengths for each normal strength to high strength comparison is presented in Table 5.13. Shaded pairs indicate a statistical difference between the averages.

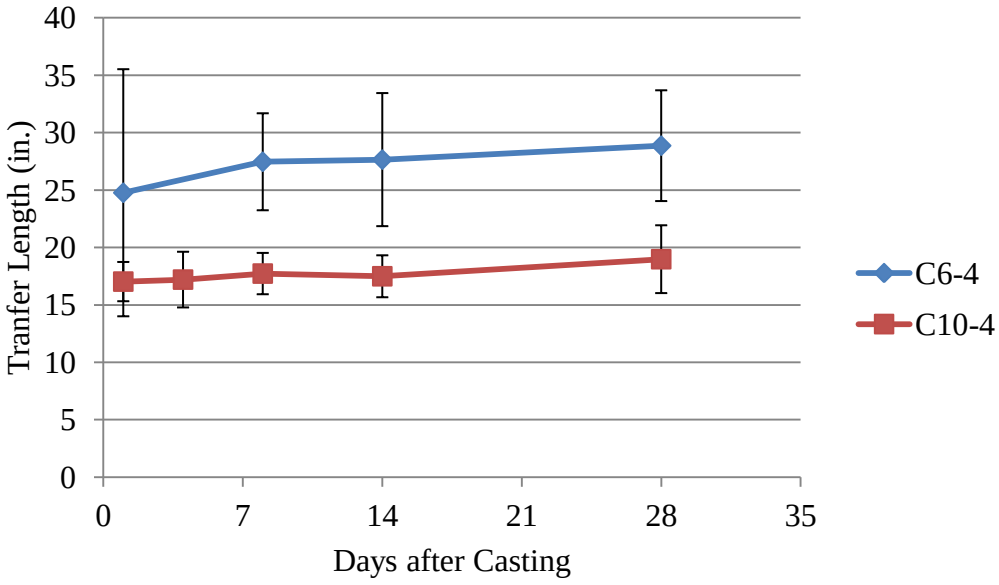

Conversion: 1 in. = 25.4 mm

Figure 5.24 – C6-4 and C10-4 Transfer Lengths and 90% Confidence Intervals

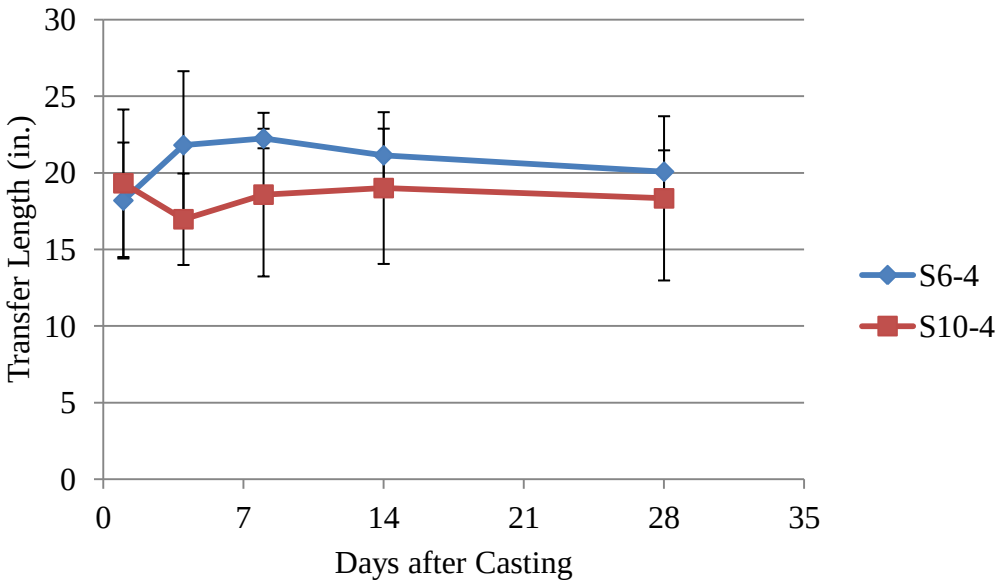

Conversion: 1 in. = 25.4 mm

Figure 5.25 – S6-4 and S10-4 Transfer Lengths and 90% Confidence Intervals

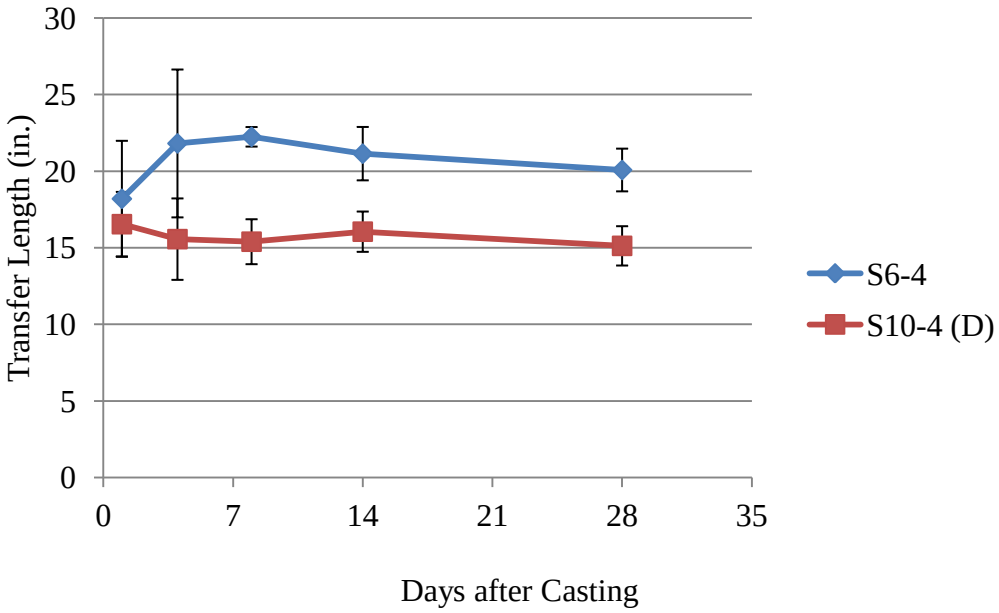

Conversion: 1 in. = 25.4 mm

Figure 5.26 – S6-4 and S10-4 (D) Transfer Lengths and 90% Confidence Intervals

Table 5.13 – Normal Strength vs. High Strength: Summary of Statistical Differences Between Top Strand Transfer Lengths

Combination	1 Day (in.)	4 Day (in.)	8 Day (in.)	14 Day (in.)	28 Day (in.)
C6-4	24.8	N/A	27.5	27.6	28.9
C10-4	17.0	17.2	17.7	17.5	19.0
S6-4	18.2	21.8	22.2	21.1	20.1
S10-4	19.3	17.0	18.6	19.0	18.3
S6-4	18.2	21.8	22.2	21.1	20.1
S10-4 (D)	16.5	15.6	15.4	16.0	15.1

*Shaded pairs indicate statistical difference between values (90% CI)
Conversion: 1 in. = 25.4 mm

Except for the bottom strands in SCC, all comparisons of normal to high strength concretes showed decreased transfer lengths at higher strengths when the live end values were removed from the averages. For the top strands, this was especially true for 8 to 28 days.

As discussed in Section 2.4.3, the idea of transfer length being inversely proportional to concrete strength has been shown by many previous researchers. Mitchell et al. (1993), Lane (1998), Ramirez and Russell (2008), and others have all noted the effect of concrete strength, and except for the bottom strands in SCC, this research mostly upheld the previous findings.

5.3.1.3 Comparison of bottom strand to top strand. For each mix, bottom strand transfer lengths were compared to top strand transfer lengths to determine if significant differences existed. Previous research has indicated that top strands have the potential for longer transfer lengths than bottom strands due to bleed water and air collecting under the top strands and reduced consolidation at the top of a member, thus reducing bond (Peterman 2007, Wan et al. 2002). The same 90% confidence interval approach that was used to compare conventional concrete to SCC and normal strength to high strength was used to evaluate statistically significant differences between top and bottom strand transfer lengths. Top and bottom strand transfer lengths for each mix from 1 to 28 days are plotted in Figures 5.27-5.32.

Figures 5.27-5.29 examine the top and bottom strands in conventional concrete. Figure 5.27 compares the top and bottom strand transfer lengths in the normal strength conventional concrete, while Figures 5.28 and 5.29 compare the high strength full and dead end bottom strand averages to the top strand averages. Figures 5.27 and 5.29 show that the top strand transfer length averages were higher than the bottom strand averages, but the 90% confidence interval error bars overlap in all cases except when comparing C10-2 (D) to C10-4 at one day (Figure 5.29). Although the error bars overlap in Figure 5.28 as well, Figure 5.28 actually indicates in high strength conventional concrete, the average bottom strand transfer lengths (C10-2) were actually longer than the average top strand transfer lengths (C10-4); however, the C10-2 averages include the possible live ends, which would make the averages much higher. Aside from this one anomaly, the comparison of top strand transfer lengths to bottom strand transfer lengths did not appear to show any statistically significant differences in either normal or high strength conventional concrete.

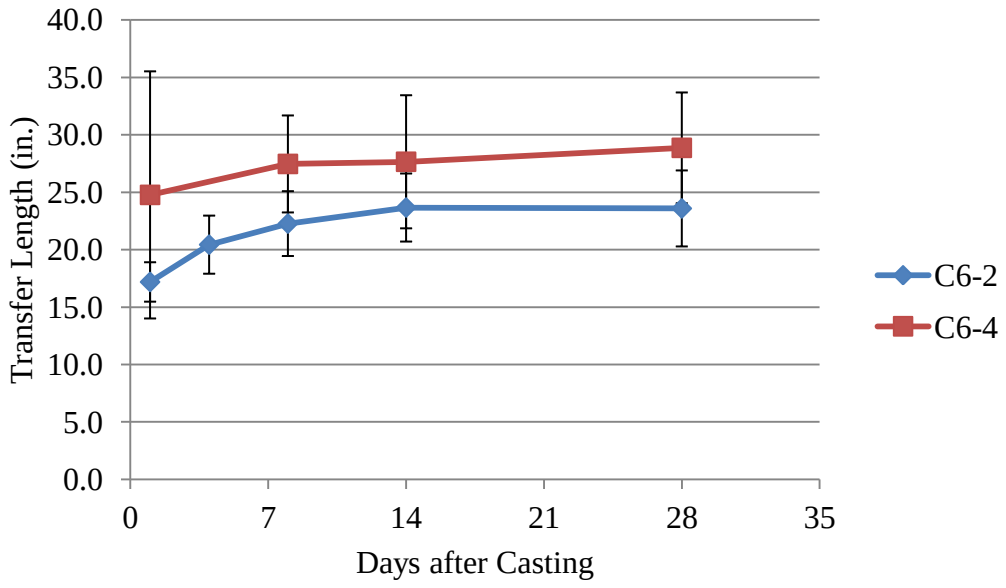

Conversion: 1 in. = 25.4 mm

Figure 5.27 – C6-2 and C6-4 Transfer Lengths and 90% Confidence Intervals

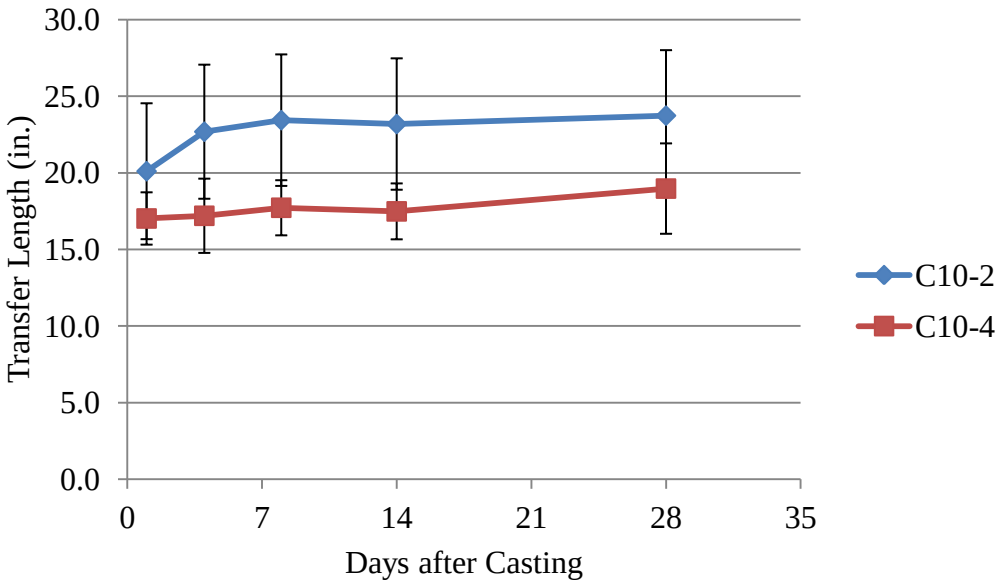

Conversion: 1 in. = 25.4 mm

Figure 5.28 – C10-2 and C10-4 Transfer Lengths and 90% Confidence Intervals

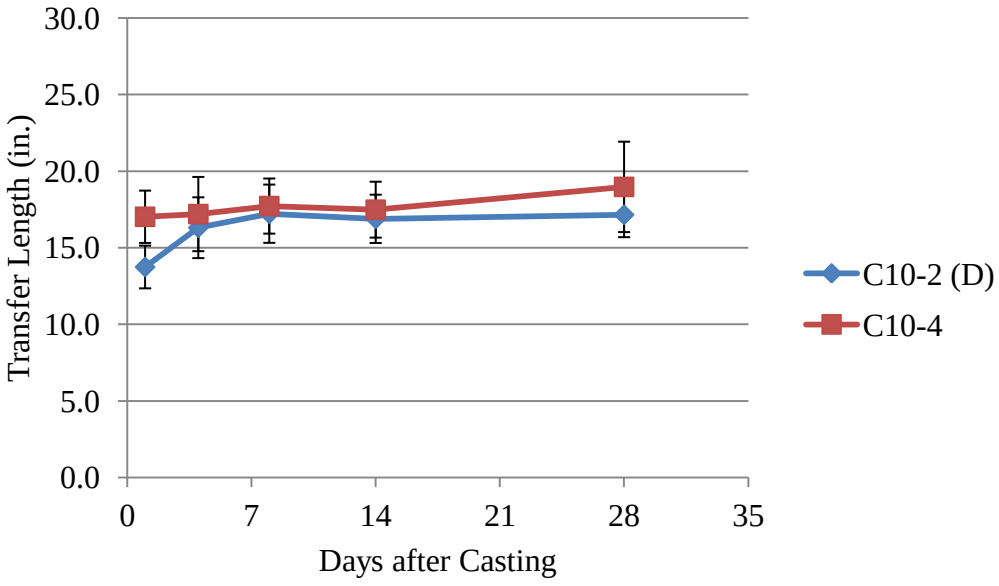

Conversion: 1 in. = 25.4 mm

Figure 5.29 – C10-2 (D) and C10-4 Transfer Lengths and 90% Confidence Intervals

Figures 5.30-5.32 examine the top and bottom strands in SCC. Figure 5.30 compares the top and bottom strand transfer lengths in the normal strength SCC, while Figure 5.31 and 5.32 compare the high strength SCC bottom strand averages to the full and dead end top strand averages. Figures 5.30 and 5.31 show the top strand transfer length averages were higher than the bottom strand averages, but the 90% confidence interval error bars overlap in all cases except when comparing S6-2 to S6-4 at 8 days. For the high strength SCC, when the possible live end was removed from the average top strand transfer length, the transfer lengths appear to be almost identical (Figure 5.32). As was seen with the conventional concrete, aside from one anomaly, almost no statistically significant differences were seen between top and bottom strands in either normal or high strength SCC.

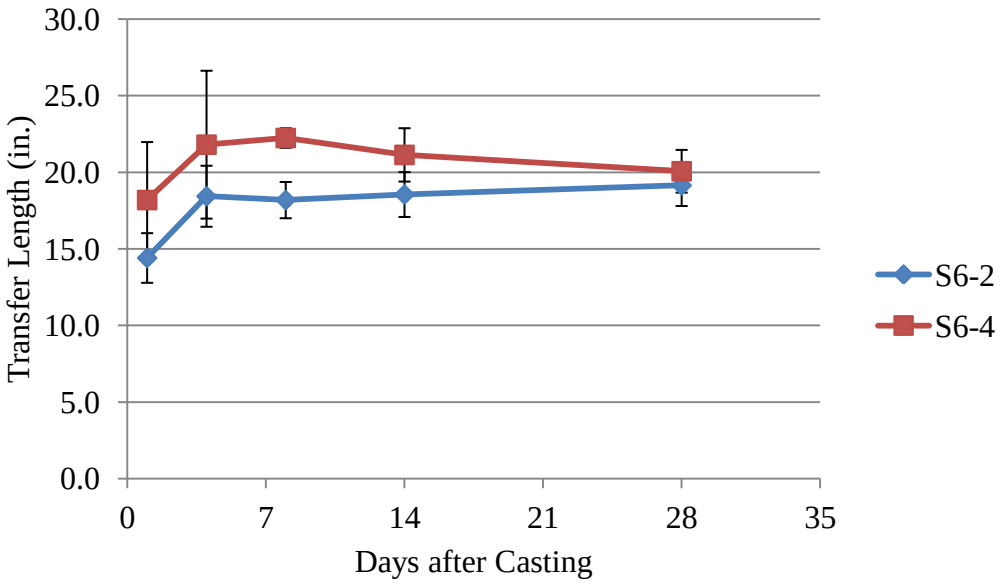

Conversion: 1 in. = 25.4 mm

Figure 5.30 – S6-2 and S6-4 Transfer Lengths and 90% Confidence Intervals

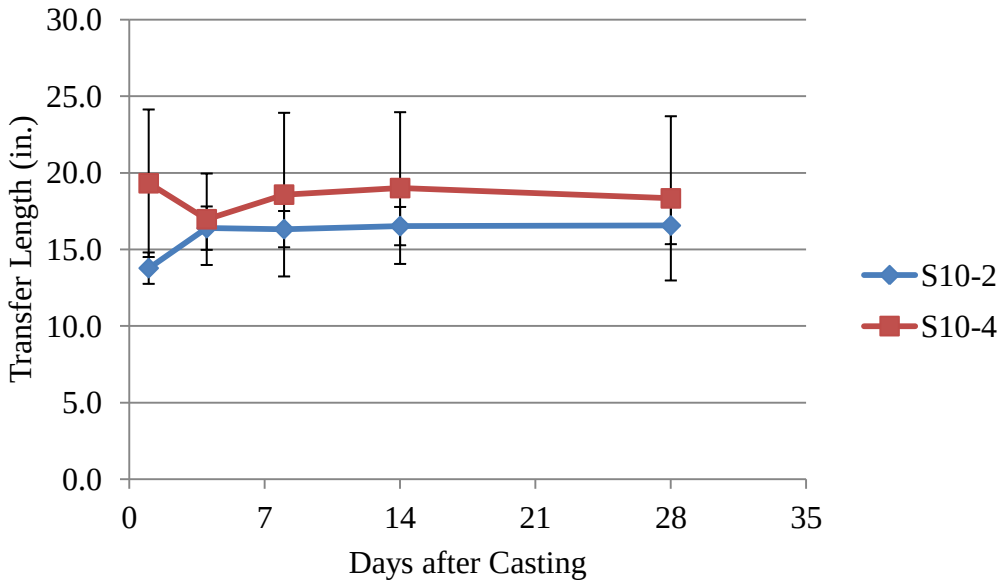

Conversion: 1 in. = 25.4 mm

Figure 5.31 – S10-2 and S10-4 Transfer Lengths and 90% Confidence Intervals

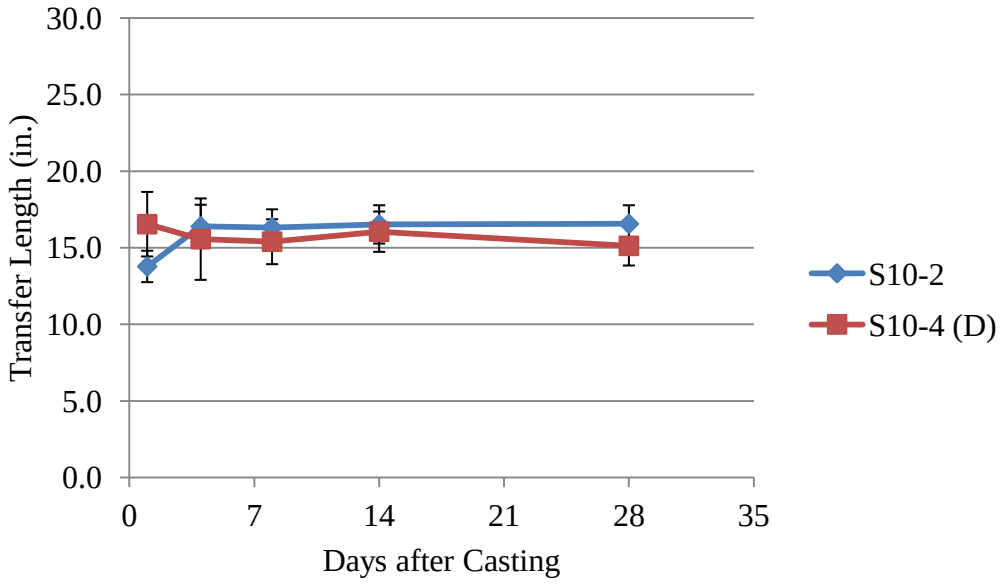

Conversion: 1 in. = 25.4 mm

Figure 5.32 – S10-2 and S10-4 (D) Transfer Lengths and 90% Confidence Intervals

Overall, the top strands generally had longer transfer lengths based on straight averages, but analysis indicated that there were no trends showing statistically significant differences between transfer lengths in top and bottom strands in the same concrete mix. This does not follow previous research findings. As discussed in Section 2.4.6, Wan et al. (2002) and Petrou et al. (2000) both found significantly more slip in top-cast strands compared to bottom-cast strands in piles constructed from conventional concrete. Specifically in terms of SCC, Larson et al. (2007) reported top strand transfer lengths to be 50% longer than bottom strand transfer lengths. However, the top strand transfer lengths in the current study were often longer than those for the bottom strands, especially when live end values were removed from the averages for C10-2, on average 9 to 26% although still within recognized limits of statistical variability.

For this study, a summary of the transfer lengths for each top strand vs. bottom strand comparison for all concrete mixes is presented in Table 5.14. Shaded pairs indicate a statistical difference between the averages, and the lack of shaded pairs indicates that in this research, there was no trend indicating top strand transfer lengths were longer than bottom strand transfer lengths.

5.3.1.4 Change in transfer length over time. As discussed in Section 2.4.4, numerous previous research studies dating back to Kaar, LaFraugh, and Mass (1963) have shown transfer lengths increasing over time, so the data from this study was analyzed to see if the same trend was observed. The percent increases in transfer lengths for top and bottom strands in each mix are presented in Table 5.15. The increases are broken down into initial increases, or the percent increases from 1 to 4 days, and additional increases, or the percent increases from 4 to 28 days, and total increases, or the full percent increases from 1 to 28 days. Negative percent increases indicate the transfer lengths actually decreased.

Table 5.14 – Top Strand vs. Bottom Strand: Summary of Statistical Differences Between Transfer Lengths

Combination	1 Day (in.)	4 Day (in.)	8 Day (in.)	14 Day (in.)	28 Day (in.)
C6-2	17.2	20.4	22.3	23.7	23.6
C6-4	24.8	N/A	27.5	27.6	28.9
C10-2	20.1	22.7	23.4	23.2	23.7
C10-4	17.0	17.2	17.7	17.5	19.0
C10-2 (D)	13.7	16.3	17.2	16.9	17.2
C10-4	17.0	17.2	17.7	17.5	19.0
S6-2	14.4	18.4	18.2	18.6	19.2
S6-4	18.2	21.8	22.2	21.1	20.1
S10-2	13.8	16.4	16.3	16.5	16.6
S10-4	19.3	17.0	18.6	19.0	18.3
S10-2	13.8	16.4	16.3	16.5	16.6
S10-4 (D)	16.5	15.6	15.4	16.0	15.1

*Shaded pairs indicate statistical difference between values (90% CI)
Conversion: 1 in. = 25.4 mm

Table 5.15 – Summary of Increases in Transfer Lengths

Mix ID	Initial Increase (1 Day to 4 Days)	Additional Increase (4 Days to 28 Days)	Total Increase (1 Day to 28 Days)
C6-2	18.9%	15.4%	37.3%
S6-2	28.0%	3.9%	32.9%
C10-2	12.8%	4.6%	18.1%
C10-2 (D)	18.7%	5.2%	24.8%
C10-2 (L)	9.8%	4.3%	14.5%
S10-2	19.0%	1.0%	20.2%
C6-4	N/A	N/A	16.5%
S6-4	19.9%	-8.0%	10.3%
C10-4	1.0%	10.3%	11.5%
S10-4	-12.2%	8.0%	-5.1%
S10-4 (D)	-5.9%	-2.8%	-8.6%
S10-4 (L)	-23.4%	31.9%	1.1%

The bottom strands did show increases in transfer length over time between 1 and 28 days after casting, with total increases ranging from a minimum of 14.5% for C10-2 (L) to a maximum of 37.3% for C6-2. Generally, most of the increase occurred within the first four days, and then the rate of increase appeared to slow significantly from 4 to 28 days. The normal strength mixes appeared to show higher percent increases than the high strength mixes, but no definitive conclusion could be established regarding the performance of conventional concrete to SCC.

The top strands were much more inconsistent. The SCC mixes actually showed decreases in some cases. S6-4 had a decrease from 4 to 28 days, while all combinations of S10-4 transfer length averages showed an initial decrease, and S10-4 and S10-4 (D) also had overall decreases in averages. C6-4 did not have a 4-day average, so the total increase could not be broken down into initial and additional increases. C10-4 had very little initial increase and saw most of the increase occur between 4 and 28 days, which is opposite of what was generally seen in the bottom strands. In conclusion, the top strand transfer lengths did not always increase, and the increases that were seen were generally not as large as the increases that were observed in the bottom strand transfer lengths.

When the increases in bottom strand transfer lengths from this study are compared to results found by recent studies, the 14.5%-37.3% increases are consistent with what has been observed by other researchers. Over 28 days, Staton et al. (2009) observed 8% growth for SCC transfer lengths and 12% growth for high strength conventional concrete transfer lengths. Also, Boehm et al. (2010) reported 28% increases in SCC transfer lengths over 3 months with 38% increases in conventional concrete transfer lengths for the same period. Finally, increases of 10-20% were seen in the bottom strands of SCC beams 21 days after casting in the study conducted by Larson et al. (2007). The only study that assessed increases in top strand transfer lengths was Larson et al. (2007). In that study, increases of 40-45% were seen in the top strand transfer lengths, but the results regarding increases in top strand transfer lengths reported in this thesis were inconclusive.

5.3.1.5 Comparison to AASHTO and ACI equations for transfer length.

After the transfer length averages were compared to each other to determine the effects of concrete type, concrete strength, and strand location, the averages were then compared

to values determined by the AASHTO and ACI equations to ensure the measured values did not exceed the calculated design values. The AASHTO and ACI transfer length equations were presented and discussed in Section 2.5 of this thesis; however, they are repeated here for clarity and convenience.

The AASHTO equation for transfer length is given by Eq. 5.1, where l_t is the transfer length in inches and d_b is the nominal diameter of the strand in inches. For a 0.5-in.-diameter (12.7 mm) strand, l_t as calculated by the AASHTO equation is equal to 30 in. (762 mm).

$$l_t = 60 d_b \tag{5.1}$$

ACI 318-11 presents two equations for transfer length: a general equation and an equation that is used when determining whether a reduced stress in the strand needs to be accounted for when designing for shear near the end of a member. The general ACI transfer length equation that is given in Section 12.9 of the ACI 318-11 code is shown here as equation Eq. 5.2, where l_t is the transfer length in inches, f_{se} is the effective stress in the prestressing strand after losses in psi and d_b is the nominal diameter of the strand in inches. Typical values for f_{se} range from 60 – 65% of f_{pu} depending on the conditions of stressing and losses. In terms of comparison, it was determined that a lower f_{se} value ($0.6f_{pu}$) should be used, so the calculated transfer length would be shorter and more conservative for comparison. Assuming 20% final losses, the 28-day transfer length calculated by Eq. 5.2 would equal 27 in. (686 mm).

$$l_t = \left(\frac{f_{se}}{3000}\right) d_b \tag{5.2}$$

The transfer length equation for shear design from Section 11.3.4 of ACI 318-11 is presented in Eq. 5.3, where l_t is the transfer length in inches and d_b is the nominal strand diameter in inches. For a 0.5-in.-diameter (12.7 mm) strand, this transfer length would equal 25 in. (635 mm).

$$l_t = 50\mathrm{d_b} \quad \textbf{(5.3)}$$

The full average transfer lengths as well as the possible live and dead end averages for each mix are plotted and compared to the values calculated from the AASHTO and two ACI equations for transfer length in Figures 5.33 and 5.34. Figure 5.33 contains the average values for the bottom strands while Figure 5.34 displays the results for the top strands. Each plot contains horizontal lines indicating the transfer length value calculated by each code equation, and the legend labels the values as AASHTO, ACI-1, and ACI-2. AASHTO corresponds to the 30 in. (762 mm) value calculated by Eq. 5.1, ACI-1 represents the 27 in. (686 mm) value determined from Eq. 5.2, and ACI-2 is equal to 25 in. (635 mm), as calculated from Eq. 5.3. Additionally, Tables 5.16 and 5.17 compare the ratios of the calculated AASHTO and ACI values to the average transfer length 28 days after casting for each mix for the bottom and top strands, respectively. In Tables 5.16 and 5.17, a value greater than one indicates that the transfer length calculated from the code equation exceeded the average measured transfer length.

As seen in Figure 5.33, the bottom strands in almost all mixes had average transfer lengths falling below values calculated from all equations. The exception was the possible average live end transfer lengths measured in the C10 mix. The average C10-2 (L) transfer lengths were greater than the transfer lengths predicted by the shear ACI equation (Eq. 5.3) at one day and both ACI equations at 4, 8 and 14 days. The average transfer length at 28 days for C10-2 (L) was 11% greater than the value calculated by ACI-1 and 18% greater than ACI-2 (Table 5.16). The AASHTO equation was conservative for the C10-2 (L) average transfer lengths up to 28 days, where the measured transfer length, which barely exceeded the limit. The code equations applied to the SCC mixes appeared to be more conservative than when applied to the conventional concrete mixes, but as discussed, statistical analysis showed the differences between averages were not statistically significant.

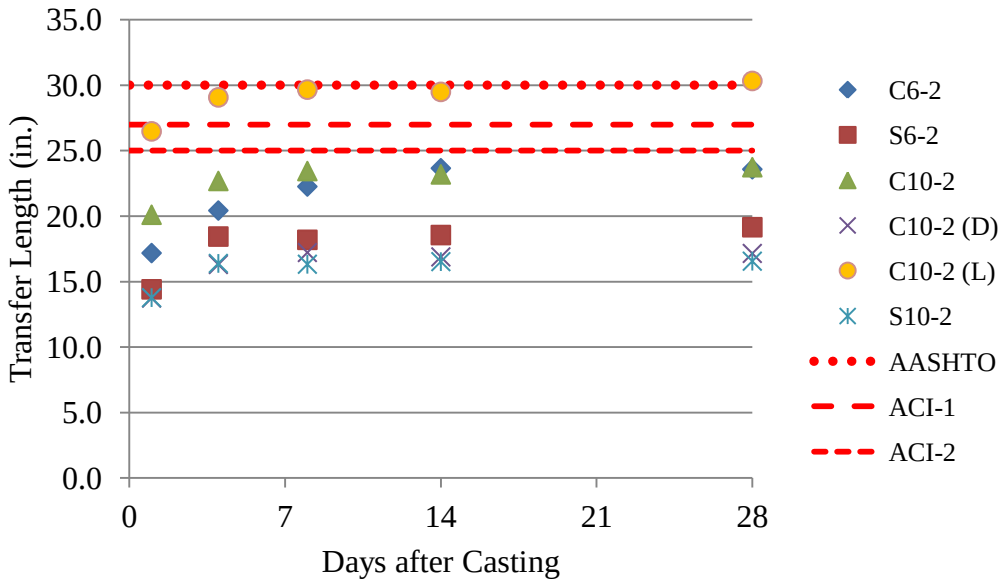

Conversion: 1 in. = 25.4 mm

Figure 5.33 – Average Transfer Lengths Compared to AASHTO and ACI Equations (Bottom Strands)

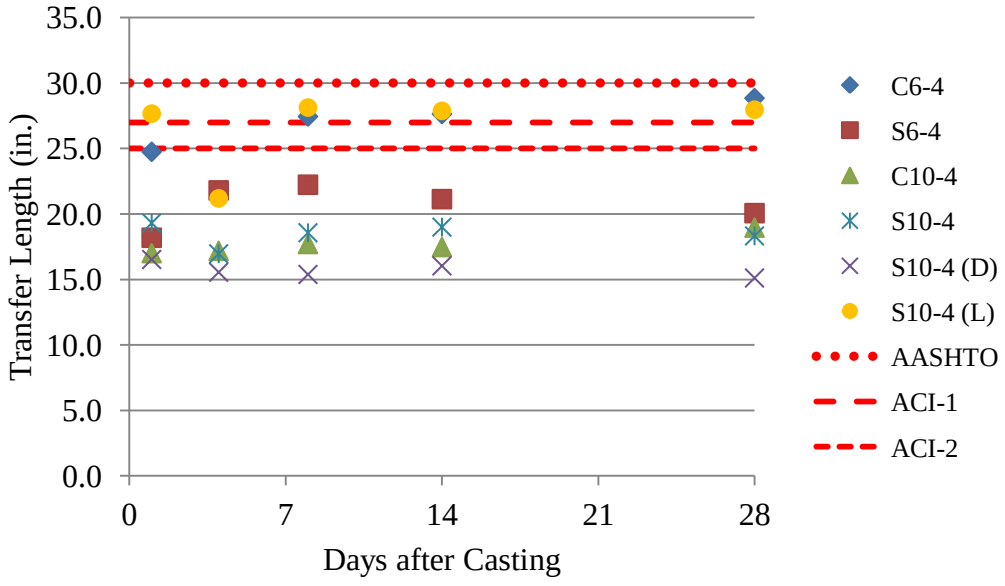

Conversion: 1 in. = 25.4 mm

Figure 5.34 – Average Transfer Lengths Compared to AASHTO and ACI Equations (Top Strands)

Table 5.16 – Ratio of Average Transfer Lengths to AASHTO and ACI Values (Bottom Strands)

	28 Day Avg. (in.)	AASHTO/Avg. (AASHTO = 30 in.)	ACI-1/Avg. (ACI-1 = 27 in.)	ACI-2/Avg. (ACI-2 = 25 in.)
C6-2	23.6	1.27	1.14	1.06
CS6-2	19.2	1.57	1.41	1.31
C10-2	23.7	1.26	1.14	1.05
C10-2 (D)	17.2	1.75	1.57	1.46
C10-2 (L)	30.3	0.99	0.89	0.82
S10-2	16.6	1.81	1.63	1.51

Conversion: 1 in. = 25.4 mm

Table 5.17 – Ratio of Avg. Transfer Lengths to AASHTO and ACI (Top Strands)

	28 Day Avg. (in.)	AASHTO/Avg. (AASHTO = 30 in.)	ACI-1/Avg. (ACI-1 = 27 in.)	ACI-2/Avg. (ACI-2 = 25 in.)
C6-4	28.9	1.04	0.94	0.87
S6-4	20.1	1.49	1.34	1.25
C10-4	19.0	1.58	1.42	1.32
S10-4	18.3	1.64	1.47	1.36
S10-4 (D)	15.1	1.98	1.79	1.65
S10-4 (L)	28.0	1.07	0.97	0.89

Conversion: 1 in. = 25.4 mm

In terms of the average top strand transfer lengths, Figure 5.34 shows a similar trend, with the equations being conservative in most cases. One exception was again the possible live end transfer length, which was greater than the values computed by both ACI equations at all days except day 4. However, the normal strength conventional concrete also had average transfer lengths exceeding both ACI limits at 8, 14, and 28 days. The 28-day average for C6-4 exceeded the ACI-1 and ACI-2 limits by 3% and 11%, respectively (Table 5.17). The AASHTO equation once again proved to be conservative for all mixes.

Other studies have also found the AASHTO and ACI transfer length equations to be largely conservative for SCC as well as conventional concrete. Pozolo and Andrawes (2011) found SCC bottom transfer lengths to be on average 86% below $50d_b$, 72% lower

than $60d_b$, and 69% under $f_{pe}d_b/3$, while Staton et al. (2009) found SCC transfer lengths to be 60% below $f_{pe}d_b/3$ as well. Larson et al. (2007) and Boehm et al. (2010) also found the equations to be conservative for bottom strands and adequate to use with SCC and conventional concrete. However, in terms of top strands, Larson et al. (2007) found top strand transfer lengths in SCC to be 60% longer than predicted by $50d_b$. Here, C6-4 averages were the only top strand averages to exceed the ACI code limit.

5.3.2. Discussion of Initial End Slip Transfer Length Results. Initial transfer lengths were determined by measuring end slips of the strands at release through both electronic and manual means, as discussed in Sections 4.4.2.1 and 4.4.2.2. The transfer lengths determined from the end slips measured by both methods are discussed in this subsection, but overall, the transfer lengths determined by the initial end slips were abandoned because they were deemed unreliable and imprecise compared to the 1 day results determined from the DEMEC readings and the 95% Average Mean Strain Method.

In terms of the end slips measured by the Synergy data acquisition, the gauges that were used in this research program proved to be highly unreliable. The release method appeared to be too violent, and the potentiometers consistently separated from the base plates or slipped on the strands, as discussed in Section 4.4.2.1. The potentiometers were attached to 32 bottom transfer length locations, and only 16 potentiometers yielded what were deemed valid end slips, for a success rate of 50%. The potentiometers were also attached to 10 top transfer length locations, and the potentiometers were unable to yield any readable data from any of these locations. Therefore, for the 42 locations where the potentiometers were installed to collect data, the potentiometers only registered a valid reading 16 times, for a total success rate of only 38%. Also, for the steel rulers, the measurements could only be taken to the nearest $^1/_{32}$-in. (0.79 mm), so precision was a limiting factor.

In light of the unreliability of the potentiometers and the imprecision of the steel ruler measurements, the transfer lengths determined from the 95% Average Mean Strain Method were deemed to be the most consistent and were the transfer lengths that were used for all comparisons of the transfer lengths in the different mixes as well as all comparisons to AASHTO and ACI predicted values. Still, for the sake of comparison, the

transfer lengths determined from the Synergy data and steel ruler end slip measurements are compared to the transfer lengths determined from the 95% Average Mean Strain Method in Tables 5.18 and 5.19. The tables shows the average, standard deviation and the number of readings the average and standard deviation were based on for each method as well as the percent difference between the transfer length from the Synergy or steel ruler data to the transfer length determined from the DEMEC points and 95% Average Mean Strain Method. Table 5.18 contains the comparisons for all bottom strand data, and Table 5.19 contains the comparisons for the top strand data. Although the mixes are labeled with "2" to denote the two strand beams, and consequently the bottom strands, ruler and Synergy data were also taken on bottom strands of the four-strand beams and are included in the averages and standard deviations for the bottom strands.

Table 5.18 shows that for the bottom strands, some of the average Synergy transfer lengths were actually very similar to the DEMEC transfer lengths. The S6 transfer lengths have only a 0.36% differences between averages, but it should be noted that the Synergy average is based on only two values. The Synergy and DEMEC transfer lengths for C10-2 (D) were also very close for this comparison, with only 0.66% difference. Generally all of the Synergy transfer lengths were less than the DEMEC transfer lengths.

The percent differences between the ruler and DEMEC transfer lengths ranged from slightly over 4% to over 76%. The precision for the method was low, which meant that the standard deviations for the transfer lengths for all mixes was high, ranging from around 5 in. (127 mm) to 8.5 in. (216 mm). Overall, correlation between the transfer lengths determined by the steel ruler end slip measurements to the DEMEC transfer lengths was very low, and although there were some isolated instances of steel ruler transfer lengths matching up well to the DEMEC transfer lengths, large differences generally existed between transfer lengths determined by these two methods as well.

Several studies have also measured transfer length through end slips as well as DEMEC readings in conjunction with the 95% Average Mean Strain Method. These studies, including Rose and Russell (1997), Ramirez and Russell (2008), and Boehm et al. (2010), found the transfer lengths calculated from end slips to match fairly well with the transfer lengths determined from DEMEC readings. Unlike these studies, the results

in this thesis did not show a correlation between transfer lengths calculated with the two methods, but this can most likely be attributed to the shortcomings of the methods of end slip data collection in this research program.

All transfer lengths determined by both end slip methods are reported in this thesis, but all values were essentially disregarded in terms of analysis. Only the transfer lengths determined by the 95% Average Mean Strain Method were used for comparative analyses.

Table 5.18 – Comparison of Synergy-DEMEC and Ruler-DEMEC Transfer Lengths (Bottom Strands)

Bottom Strands		Synergy-DEMEC Comparison			Ruler-DEMEC Comparison		
		Synergy (in.)	DEMEC (in.)	% Diff.	Ruler (in.)	DEMEC (in.)	% Diff.
C6-2	Avg.	7.9	17.2	73.48%	17.9	17.2	4.10%
	Std. Dev.	1.08	2.76		8.01	2.76	
	n	4	7		11	7	
S6-2	Avg.	14.5	14.4	0.36%	13.8	14.4	4.10%
	Std. Dev.	0.20	2.61		7.34	2.61	
	n	2	7		11	7	
C10-2	Avg.	13.7	20.1	38.24%	9.0	20.1	76.79%
	Std. Dev.	4.60	7.63		8.17	7.63	
	n	3	8		10	8	
C10-2 (D)	Avg.	13.7	13.7	0.66%	9.5	13.7	36.40%
	Std. Dev.	4.60	1.70		8.44	1.70	
	n	3	4		8	4	
C10-2 (L)	Avg.	N/A	26.5	N/A	6.7	26.5	119.3%
	Std. Dev.	N/A	4.99		9.49	4.99	
	n	0	4		2	4	
S10-2	Avg.	10.2	13.8	29.57%	16.6	13.8	18.33%
	Std. Dev.	6.82	1.76		5.19	1.76	
	n	7	8		10	8	

Conversion: 1 in. = 25.4 mm

Table 5.19 – Comparison of Synergy-DEMEC and Ruler-DEMEC Transfer Lengths (Top Strands)

Top Strands		Synergy-DEMEC Comparison			Ruler-DEMEC Comparison		
		Synergy (in.)	DEMEC (in.)	% Diff.	Ruler (in.)	DEMEC (in.)	% Diff.
C6-4	Avg.	N/A	24.8	N/A	22.4	24.8	10.11%
	Std. Dev.	N/A	9.25		5.17	9.25	
	n	0	2		4	2	
S6-4	Avg.	N/A	18.2	N/A	17.9	18.2	1.63%
	Std. Dev.	N/A	3.26		7.31	3.26	
	n	0	2		4	2	
C10-4	Avg.	N/A	17.0	N/A	9.0	17.0	62.16%
	Std. Dev.	N/A	2.08		3.65	2.08	
	n	0	4		4	4	
S10-4	Avg.	N/A	19.3	N/A	7.8	19.3	84.63%
	Std. Dev.	N/A	5.86		7.64	5.86	
	n	0	4		4	4	
S10-4 (D)	Avg.	N/A	16.5	N/A	7.5	16.5	75.67%
	Std. Dev.	N/A	2.22		9.32	2.22	
	n	0	3		3	3	
S10-4 (L)	Avg.	N/A	27.7	N/A	9.0	27.7	-
	Std. Dev.	N/A	-		-	-	
	n	0	1		1	1	

Conversion: 1 in. = 25.4 mm

5.3.3. Correlation of NASP Test in Concrete Results to 95% Average Mean Strain Transfer Lengths. While results from this study indicated that concrete type (conventional concrete vs. SCC) did not appear to affect transfer lengths, concrete strength did seem to have an effect. The results from this study generally indicated that an increase in concrete strength resulted in lower transfer lengths, which follows the trends of previous research, as discussed in Section 2.4.3. Specifically, Ramirez and Russell (2008) studied the effect of concrete strength on transfer length in an NCHRP study, and based on the results, they proposed new equations for transfer length and development

length, which both incorporate concrete strength as a parameter. The data from this current independent study were compared to the results presented in NCHRP Report 603.

Ramirez and Russell (2008) analyzed pullout loads from the standard NASP test in mortar and modified NASP test in concrete and transfer lengths measured in rectangular and I-beams for three strand types, A, B, and D. The modified NASP in concrete specimens and the beam specimens used for measuring transfer lengths were constructed from conventional concrete with a range of compressive strengths. From the NASP in concrete results, they noted that for each strand type, the pullout load increased as concrete strength increased, and the pullout load increase was proportional to the square root of the concrete compressive strength. The NASP in concrete values were normalized by dividing the NASP in concrete pullout load by the appropriate standard NASP in mortar pullout load for each strand, and then the ratios were plotted against the concrete compressive strength (ksi), as seen in Figure 5.35. The NASP in concrete normalized by NASP in mortar value vs. f'_c confirmed the observation that the bond performance is related to the square root of f'_c, yielding a power trend line equation with an exponent of close to 0.5 (Eq. 5.4).

$$\frac{NASP_{concrete}}{NASP} = 0.49139x^{0.51702} \quad \textbf{(5.4)}$$

Based on this result, NASP in concrete pullout load normalized by the NASP in mortar pullout load ($NASP_{conc}$/NASP) was then plotted against the square root of the compressive strength at one day (ksi), as seen in Figure 5.36. This relationship showed a rather strong linear correlation, with an R^2 value of 0.79. From this plot, a relationship between bond performance and concrete compressive strength was derived and is shown in Eq. 5.5.

$$\frac{NASP_{concrete}}{NASP} = 0.51\sqrt{f'_{ci}} \quad \textbf{(5.5)}$$

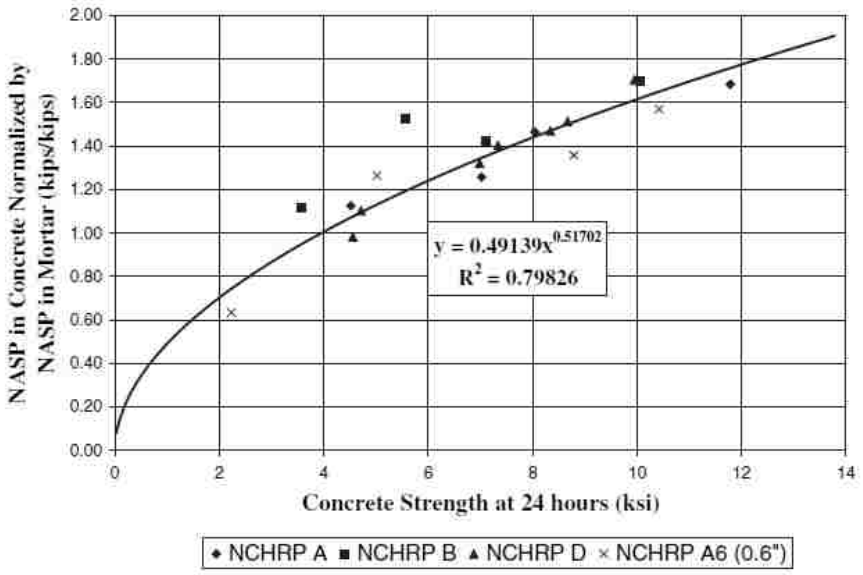

Conversion: 1 kip = 4.45 kN
1 ksi = 6.89 MPa

Figure 5.35 – NCHRP Normalized NASP Pull-out Values vs. Concrete Strength (Ramirez and Russell 2008)

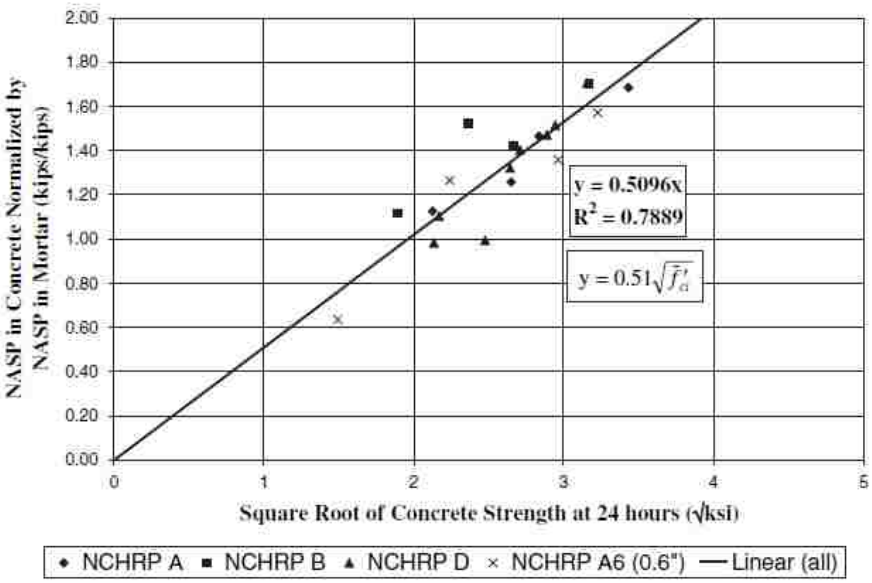

Conversion: 1 kip = 4.45 kN
1 ksi = 6.89 MPa

Figure 5.36 – NCHRP Normalized NASP Pull-out Values vs. $\sqrt{f'_c}$ (Ramirez and Russell 2008)

From this relationship, it can be said that the ratio of the NASP in concrete pullout value to the NASP in mortar value is approximately equal to one half the square root of the concrete compressive strength at 1 day in ksi. Thus, the equation was rearranged, and the normalized NASP value was calculated using Eq. 5.6, where f'$_{ci}$ is the one day compressive strength (ksi) and NASP is the average pullout load determined from the standard NASP in mortar test (k).

$$Normalized\ NASP\ Value = 0.5\sqrt{f'_{ci}}(\text{NASP}) \quad \textbf{(5.6)}$$

Transfer length was then plotted against the normalized NASP value. This relationship is displayed in Figure 5.37, effectively relating concrete strength, standard NASP test in mortar pullout value, and transfer length.

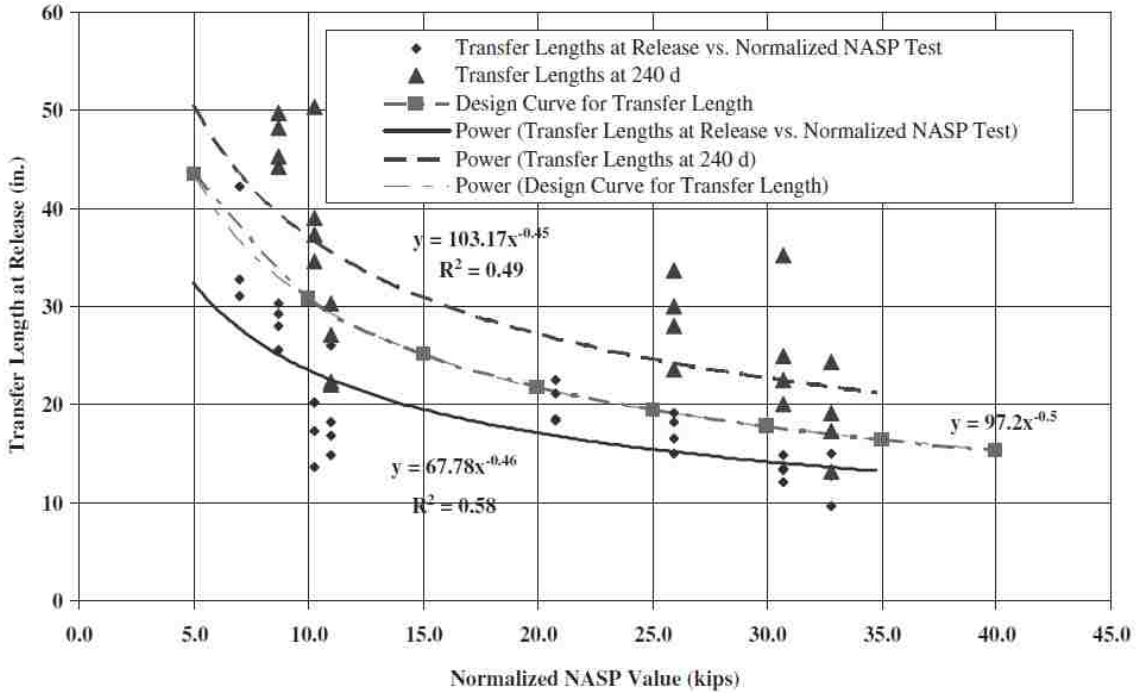

Conversion: 1 kip = 4.45 kN
1 in. = 25.4 mm

Figure 5.37 – NCHRP Transfer Lengths vs. Normalized NASP Bond Values (Ramirez and Russell 2008)

The results produced by the Missouri S&T research program were compared to the results from the NCHRP study to see if these results followed the same trends that were discovered during the NCHRP program. In this study, only one strand type was used for the construction of the transfer length beams (strand type 101), but two standard NASP tests in mortar were run on this strand type, resulting in two different NASP pullout values. Therefore, results from this program were determined using the NASP pullout loads from tests completed with both mortar mixes, N-101-A ($NASP_A$) and N-101-B ($NASP_B$), and both sets of results were presented and compared to the NCHRP results.

The applicable data from this research program that is used for the comparison of Missouri S&T's results to the NCHRP research is summarized in Table 5.20. The one day compressive strength, square root of the one day compressive strength, and pullout value from the modified NASP in concrete tests are presented for each mix. Also, the standard NASP in mortar values for both the tests completed in mortar Mix A ($NASP_A$) and Mix B ($NASP_B$) are presented along with the ratios of the NASP in concrete and NASP in mortar pullout loads.

Table 5.20 – Summary of Data for Comparison with NCHRP Results

Mix	f'_{ci} (ksi)	$\sqrt{f'_{ci}}$ ($\sqrt{ksi}$)	$NASP_{conc}$ (k)	$NASP_A$ [N-101-A] (k)	$NASP_B$ [N-101-B] (k)	$NASP_{conc}/NASP_A$	$NASP_{conc}/NASP_B$
C6	4.81	2.19	21.1	21.6	18.2	0.977	1.159
S6	5.66	2.38	23.7	21.6	18.2	1.097	1.302
C10	5.67	2.38	26.7	21.6	18.2	1.234	1.464
S10	6.33	2.52	27.3	21.6	18.2	1.264	1.500

Conversion: 1 kip = 4.45 kN
1 ksi = 6.89 MPa

In order to compare the data from the two research programs, Figures 5.35, 5.36, and 5.37 were recreated in order for the data from the Missouri S&T research program to be plotted along with the NCHRP data, and these recreated plots are presented in Figures 5.38, 5.39, and 5.40. The results from this research are presented with values calculated

using the NASP in mortar pullout load from N-101-A ($NASP_A$) and also using the NASP in mortar pullout load from N-101-B ($NASP_B$). Although all data is included on each figure, it should be noted that the equations and R^2 values displayed on Figures 5.38-5.40 are calculated based solely on the NCHRP data. Figure 5.38 plots the relationship of $NASP_{conc}$/NASP vs. f'_c, while Figure 5.39 shows the relationship of the $NASP_{conc}$/NASP ratios and $\sqrt{f'_c}$. Figure 5.40 finally relates concrete compressive strength and NASP pullout loads to transfer length by plotting transfer lengths at release vs. normalized NASP values, as calculated by Eq. 5.6. While the original figure in NCHRP Report 603 includes transfer lengths at release and at 240 days, only the data from release as well as the trend line from release is plotted here to have a direct comparison to the transfer lengths measured at release in this research program. This program did not include measuring transfer lengths at 240 days.

For all figures, the trend line equations and R^2 values for just the NCHRP data, the NCHRP data plus the Missouri S&T data with $NASP_A$, and the NCHRP data plus the Missouri S&T data with $NASP_B$ are summarized in Table 5.21. This summary shows how close the results from this research program are to the results of the NCHRP research by showing how little the inclusion of different results change the trend line equations and R^2 values.

Figure 5.38 shows the data from this program appeared to follow the relationship between the $NASP_{conc}$/NASP ratios and concrete compressive strength that was established in the NCHRP research. The $NASP_{conc}$/NASP ratios calculated with the $NASP_A$ values appear to match up well with the NCHRP data ($R^2 = 0.79$), and even though the $NASP_{conc}$/NASP ratios with $NASP_B$ values are on the high end of the scatter, the R^2 value for this data combined with the NCHRP data is still 0.74 (Table 5.21). This is lower than 0.80, which corresponds to the R^2 value for just the NCHRP results, but 0.74 still indicates a fair correlation. Therefore, it can be concluded that for results calculated with $NASP_A$ and $NASP_B$ both fall reasonably within the scatter of the NCHRP results.

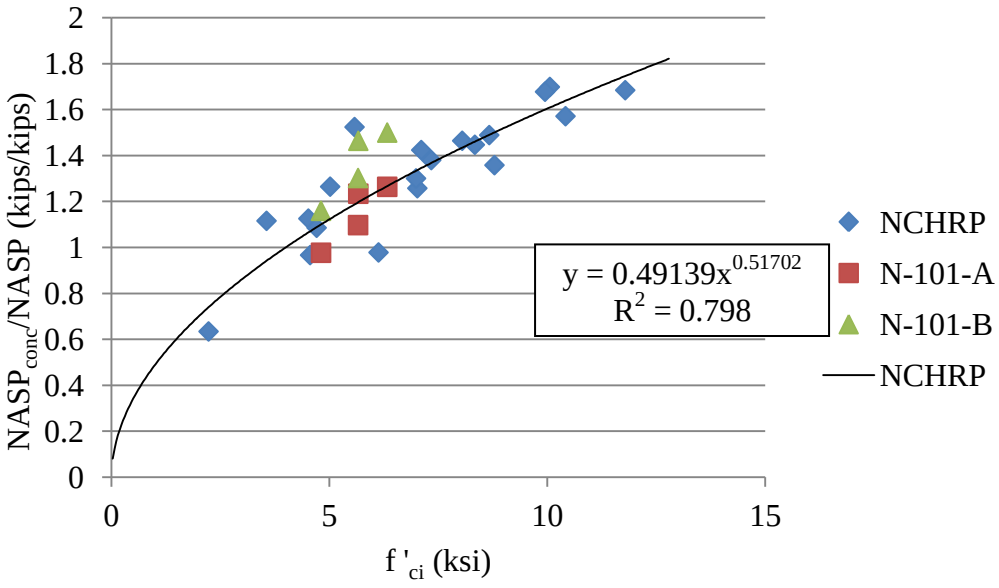

Conversion: 1 kip = 4.45 kN
1 ksi = 6.89 MPa

Figure 5.38 – Normalized NASP in Concrete Pullout Values vs. Concrete Strength (NCHRP and Missouri S&T)

Plotting the $NASP_{conc}/NASP$ vs. $\sqrt{f'_c}$ results from this research program along with the results from the NCHRP program also indicated the results from this program seemed to follow the trend previously established by the NCHRP results (Figure 5.39). The NCHRP data alone had an R^2 value of 0.79, and the NCHRP data combined with the $NASP_A$ Missouri S&T data resulted in and R^2 value of 0.79 as well, while the NCHRP data combined with the $NASP_B$ Missouri S&T data resulted in an R^2 value of 0.72 (Table 5.21). The $NASP_{conc}/NASP$ results with the $NASP_A$ value appeared to more closely fit the data from the NCHRP study, but the $NASP_{conc}/NASP$ ratios with the $NASP_B$ value were still reasonable, even though they were on the high side of the scatter.

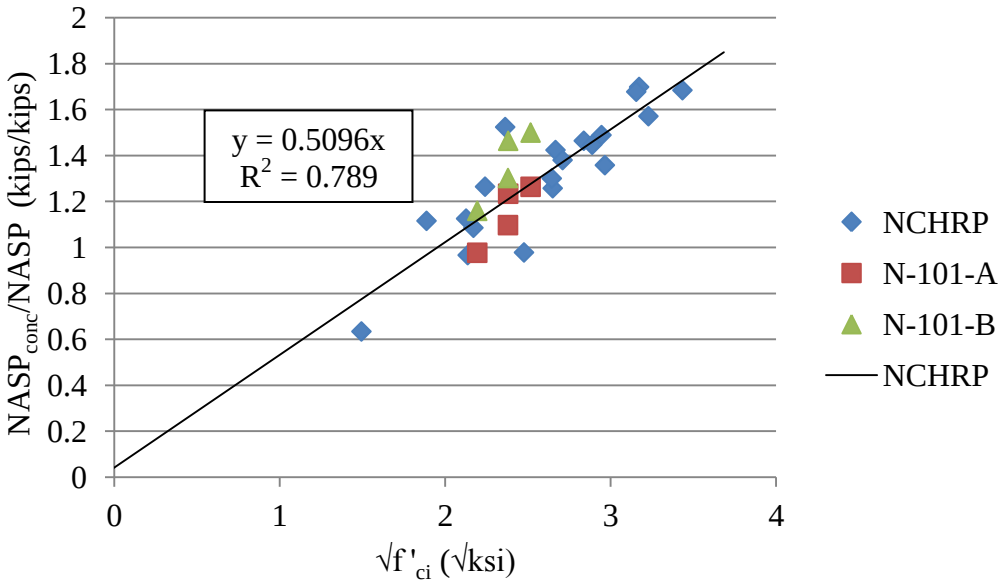

Conversion: 1 kip = 4.45 kN
1 ksi = 6.89 MPa

Figure 5.39 – Normalized NASP in Concrete Pullout Values vs. Square Root of Concrete Strength (NCHRP and Missouri S&T)

The relationship between bond behavior and the square root of compressive strength that was established by the NCHRP research was supported by the results from this research program. Figures 5.38 and 5.39 visually indicate that the results from this research project generally fall within the scatter from the NCHRP research, and Table 5.21 shows that the R^2 values from the NCHRP data alone compared to R^2 values from the NCHRP data combined with results from Missouri S&T are relatively close. Because the relationship was validated, it was deemed acceptable to apply the relationship found in Eq. 5.6 to the Missouri S&T results to calculate a normalized NASP value based on concrete strength and the NASP in mortar values and plot the transfer lengths at release vs. the normalized NASP values from this study along with the values from the NCHRP research (Figure 5.40). The NCHRP data did not have an overly strong correlation to begin with, having an R^2 value of 0.58, but the inclusion of the Missouri S&T data based on the $NASP_A$ or $NASP_B$ values did not seem to significantly alter the trend line equation or R^2 value, showing the results with either NASP test in mortar pullout load follow the

NCHRP trend. Based on the results, transfer length at release could possibly be predicted by the trend line in Figure 5.40, where x is the value corresponding to one-half of the square root of the concrete strength at release in ksi multiplied by the NASP in mortar pullout load in kips.

Based on the results from the NCHRP study, those researchers proposed a new equation for transfer length for the AASHTO code that incorporates the relationship between concrete compressive strength and transfer length (Ramirez and Russell 2008). The proposed transfer length equation is presented here as Eq. 5.7, where f'_{ci} is the concrete compressive strength at release in ksi and d_b is the nominal diameter of the strand in inches. The equation results in a transfer length of $60d_b$ at a concrete strength of 4 ksi (27.6 MPa) and sets a minimum limit of $40d_b$.

$$l_t = \frac{120}{\sqrt{f'_{ci}}} d_b \geq 40d_b \qquad \textbf{(5.7)}$$

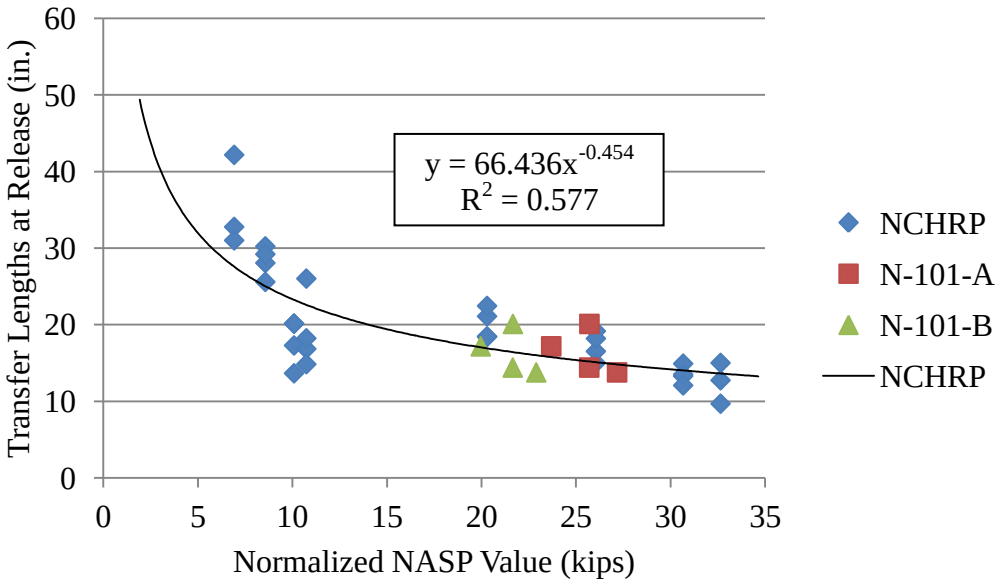

Conversion: 1 kip = 4.45 kN
1 in = 25.4 mm

Figure 5.40 – Normalized NASP Value vs. Transfer Length at Release

Table 5.21 – Summary of Trend line Equations and R2 Values for NCHRP and Missouri S&T Data

	$\frac{NASP_{conc}}{NASP}$ vs. f'_{ci} (Figure 5.35)	$\frac{NASP_{conc}}{NASP}$ vs. $\sqrt{f'_{ci}}$ (Figure 5.36)	Transfer Length at Release vs. Normalized NASP (Figure 5.37)
NCHRP	$y=0.4914x^{0.5170}$ $R^2 = 0.798$	$y=0.5096x$ $R^2 = 0.789$	$y=66.436x^{-0.454}$ $R^2 = 0.577$
NCHRP and Missouri S&T Results with $NASP_A$	$y=0.4753x^{0.5275}$ $R^2 = 0.790$	$y=0.5052x$ $R^2 = 0.786$	$y=65.202x^{-0.445}$ $R^2 = 0.574$
NCHRP and Missouri S&T Results with $NASP_B$	$y=0.5142x^{0.5004}$ $R^2 = 0.740$	$y=0.4722x$ $R^2 = 0.723$	$y = 66.849x^{-0.457}$ $R^2 = 0.577$

Table 5.22 compares the measured transfer lengths for the top and bottom strands in each mix from the current study to the transfer lengths calculated by the current AASHTO code equation and the equation proposed in the NCHRP report. As Table 5.22 indicates, the transfer lengths calculated by the proposed equation are less than the current 30 in. (762 mm), and most of the measured transfer lengths at 1 and 28 days were still less than the values calculated by the proposed equation. The only measured transfer lengths that exceeded the transfer lengths calculated from the proposed equation were the C10-2 (L) and S10-4 (L) averages. The C10-2 (L) 1 and 28 day transfer lengths exceeded the calculated value from the proposed equation by 4.8% and 20.2%, respectively, while the S10-4 (L) 1 and 28 day transfer lengths were 16.4% and 17.6% higher than the value from the proposed equation. However, it should be noted that the S10-4 (L) value is only based on a single value. The transfer length value calculated from the current AASHTO equation was conservative for all measured transfer lengths. In conclusion, while the proposed equation was lower than the values calculated by the current AASHTO equation but still adequately conservative for most of the measured transfer lengths, the proposed equation was not conservative when compared to the live end transfer lengths.

Table 5.22 – Comparison of Measured Transfer Lengths to Values Calculated by Current and Proposed AASHTO Equations

	Measured Transfer Length at 1 day (in.)	Measured Transfer Length at 28 Days (in.)	Current AASHTO $l_t = 60d_b$	Proposed AASHTO $l_t = \frac{120}{\sqrt{f'_{ci}}} d_b$
C6-2	17.2	23.6	30	27.3
S6-2	14.4	19.2	30	25.2
C10-2	20.1	23.7	30	25.2
C10-2 (D)	13.7	17.2	30	25.2
C10-2 (L)	26.4	30.3	30	25.2
S10-2	13.7	16.6	30	23.8
C6-4	24.8	28.9	30	27.3
S6-4	18.2	20.1	30	25.2
C10-4	17.0	19.0	30	25.2
S10-4	19.3	18.3	30	23.8
S10-4 (D)	16.5	15.1	30	23.8
S10-4 (L)	27.7	28.0	30	23.8

Conversion: 1 in. = 25.4 mm

5.4. DEVELOPMENT LENGTH TEST RESULTS

Development length was also evaluated to determine if differences existed in SCC and conventional concrete behavior and also to see if the AASHTO and ACI equations are conservative. The method and procedure for the four-point loading with varying embedment lengths that were used to investigate development length is described in Section 4.5, and the results for each development length test, including visual observations of failure, experimental moment capacity, and average strand slip are presented in Table 4.12. Only bottom strand development length was evaluated, so only the two-strand beams were tested. In each case, the specimen failed due to concrete crushing, reached an experimental moment capacity that exceeded the calculated nominal moment capacity, and showed negligible end slip in the strands. From these results, it was determined that bond failure was not an issue and the strands were fully developed at embedment lengths of both 73 in. (1,854 mm) and 58 in. (1,473 mm), or 100% and 80% of the calculated development length, respectively. Therefore, in this research, the

AASHTO and ACI design equations for development length are conservative because flexural failures occurred even at 80% of the calculated development length.

The calculated and experimental moment capacities are summarized in Table 5.23 and analyzed to see if SCC or conventional concrete resulted in higher increases in actual moment capacities compared to calculated capacities. Overall, all experimental moment capacities were 11-16% above the calculated capacities. The largest discrepancy between SCC and conventional concrete was between C6 and S6 at 58 in. (1473 mm), where S6 had an average moment capacity 16% higher than the calculated value, while C6 only had an average capacity 11% higher. Otherwise, all other comparisons were within approximately 2%.

Table 5.23 – Comparison of Experimental and Calculated Moment Capacities

Mix ID	M_n (k-in)	58 in. (1,473 mm)		73 in. (1,854 mm)	
		M_u (k-in)	M_u/M_n	M_u (k-in)	M_u/M_n
C6	742.7	824.2	1.110	836.2	1.126
S6	757.9	878.8	1.160	860.8	1.136
C10	773.6	877.8	1.135	883.3	1.142
S10	790.7	892.2	1.128	888.0	1.123

Conversion: 1 in. = 25.4 mm
1 k-in. = 113 N-m

As discussed in Section 5.3.3, the results of the NCHRP report showed a correlation between increasing concrete strength and decreasing transfer length. In addition to proposing a new transfer length equation for the AASHTO code, the NCHRP researchers also proposed a new development length equation, which takes into account the effect of concrete strength on development length (Ramirez and Russell 2008). The equation is presented here as Eq. 5.8, where f'_{ci} is the concrete compressive strength at one day in ksi, f'_c is the concrete compressive strength at 28 days in ksi, and d_b is the nominal strand diameter in inches. If the d_b variable is multiplied through, the first term in the equation becomes the proposed transfer length equation, while the second term represents the flexural bond length.

$$l_d = \left[\frac{120}{\sqrt{f'_{ci}}} + \frac{225}{\sqrt{f'_c}}\right] d_b \geq 100 d_b \qquad \textbf{(5.8)}$$

The NCHRP researchers graphically displayed the results of the four-point load test by plotting concrete strength at the time of test vs. embedment length, and each point indicated whether the given test resulted in a flexural, shear, or bond failure (Ramirez and Russell 2008). Figure 5.41 is the NCHRP plot of concrete strength vs. embedment length plot for strands A and B, the strands with high quality bond, in both the rectangular and I-beams. The proposed design equation, Eq. 5.8, was also plotted with the data. For plotting the equation, f'_{ci} was taken as 66.7% of f'_c, which according to the NCHRP report is a reasonable assumption based on general, past experience (Ramirez and Russell 2008). The plot shows that for a given concrete strength, embedment lengths to the right of the line would be conservative and likely result in a flexural failure, while embedment lengths to the left of the line may not be conservative and may result in a bond failure.

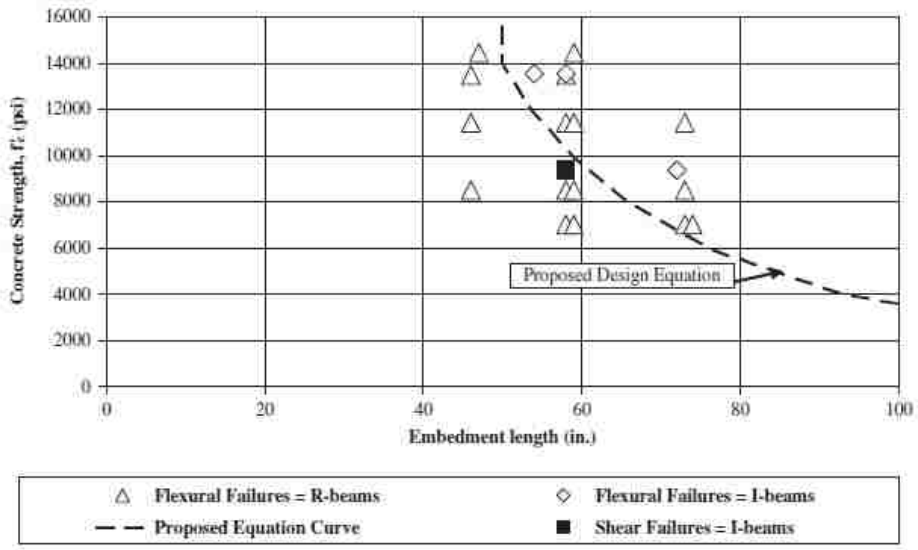

Conversion: 1 psi = 6.89 kPa
1 in. = 25.4 mm

Figure 5.41 – NCHRP Distribution of Bond and Flexural Failures for Strands A/B (Ramirez and Russell 2008)

Figure 5.41 was recreated so that the results from the Missouri S&T research could be plotted with the NCHRP results. This recreated plot of concrete strength vs. embedment length is shown in Figure 5.42. For the NCHRP data presented in Figure 5.42, only the data points from the tests on the rectangular beams were plotted so that the data would be directly comparable to the Missouri S&T data, which was also for rectangular beam sections. Also, points were not designed to differentiate between flexural, bond, or shear failures, because for both the NCHRP and Missouri S&T data shown, all tests failed in flexure. It was chosen to compare the data from this test to the data from the test with strands A and B because strands A and B exhibited high bond quality, as did strand type 101 used in the Missouri S&T research. Figure 5.42 shows that the equation is conservative for strands with high bond quality because even tests with embedment lengths less than the length predicted by the design equation, or points to the left of the curve, resulted in flexural failures.

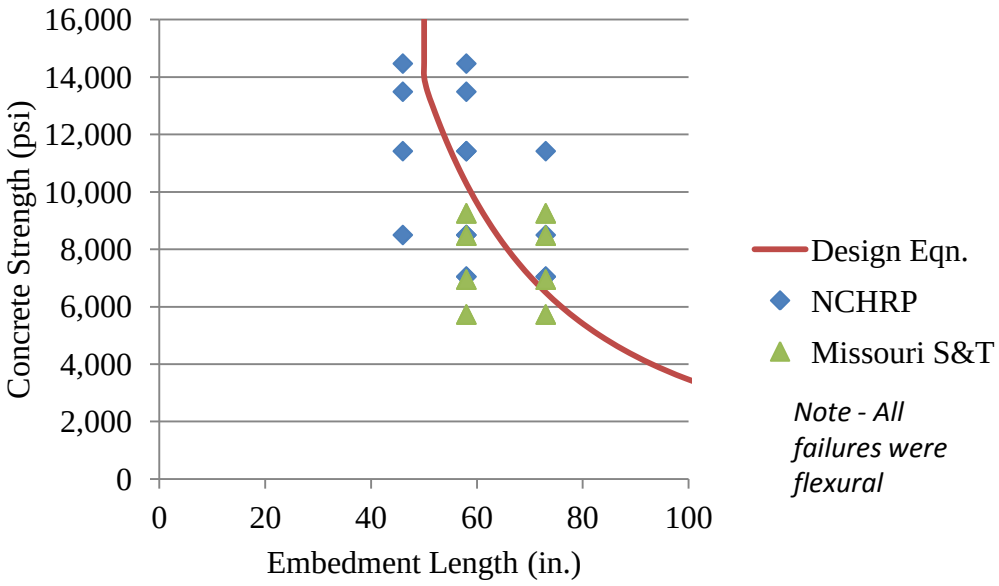

Conversion: 1 psi = 6.89 kPa
1 in. = 25.4 mm

Figure 5.42 – NCHRP and Missouri S&T Concrete Strength vs. Embedment Length Development Test Results

The development lengths for each concrete mix calculated by the current AASHTO equation and the proposed AASHTO equation are presented in Table 5.24. The development length calculated by the proposed AASHTO equation for the C6 mix is actually 102% of the value from the current AASHTO equation, but the other development lengths calculated from the proposed equation range from 83% to 93% of the value calculated by the current AASHTO equation. According to this research, the proposed development length equation appears to be conservative because in this test program, even the development length tests run at an embedment length of 58 in (1,473 mm), which is 80% of the development length calculated from the current AASHTO equation and less than any of the development lengths calculated by the proposed equation, failed in flexure, showing the strand was fully bonded.

Table 5.24 – Comparison of Development Lengths Calculated by Current and Proposed AASHTO Equations

Mix ID	Current AASHTO (in.) $l_d = \left(f_{ps} - \frac{2}{3} f_{pe}\right) d_b$	Proposed AASHTO (in.) $l_d = \left[\frac{120}{\sqrt{f'_{ci}}} + \frac{225}{\sqrt{f'_c}}\right] d_b$
C6	73	74.4
S6	73	67.9
C10	73	63.8
S10	73	60.8

Conversion: 1 in. = 25.4

` Overall, it was found that SCC and conventional concrete performed equally well in terms of adequately bonding with prestressing strand to fully develop the stress in the strand. Additionally, the AASHTO and ACI equations were determined to be conservative. The proposed AASHTO development length equation also appeared to be conservative, except when applied to the live end transfer length averages. Also, while the equations proved to be mostly conservative, it should be noted that the strand used in

these specimens was shown to have exceptional bond quality through the NASP test and LBPT, and using strand with lesser bond quality could result in less conservative, or failing, results.

6. FINDINGS, CONCLUSIONS, AND RECOMMENDATIONS

6.1. FINDINGS

The findings from the bond testing portion of the research as well as the transfer length and development length testing are discussed below.

6.1.1. Bond Test Results. The findings from the NASP test in mortar, modified NASP test in concrete, and LBPT are as follows:

- All three strand types were deemed to have acceptable bond based on the NASP test minimum pullout load requirements.
- The rank of bond performance of strands based on pullout loads at 0.001 in. (0.025 mm) slip was not always the same as the rank determined based on the loads at 0.1 in. (2.54 mm) slip.
- Although strand type 102 passed the NASP test acceptance criteria, the load vs. slip plot displayed a plateau and drop off in load at 0.1 in. (2.54 mm) slip, while strand types 101 and 103, which had much higher pullout values, were still showing increases in load at 0.1 in. (2.54 mm) slip.
- For strand types 102 and 103, the NASP pullout loads from the Missouri S&T testing were significantly higher than the NASP pullout loads determined during the NCHRP testing.
- The two different mortar mixes used to test strand type 101 resulted in a statistically significant difference in average pullout loads.
- Compared to the normal strength concretes, high strength concretes generally had higher 0.1 in. (2.54 mm) pullout loads, but lower 0.001 in. (2.54 mm) pullout loads.
- When normalized to the square root of concrete compressive strength, no statistical difference was observed between the SCC and conventional concrete pullout loads.
- Only strand type 101 passed the first slip and peak load limits of the LBPT. Strand type 102 failed both LBPT limits, while strand type 103 passed the first slip limit but failed the peak load limit.

- No correlation was found between the visual observations and residues on the strands and the final pullout results from the LBPT.
- All three strand types passed the NASP test, while strand type 101 was the only type to pass the LBPT.
- For a given strand type, the coefficient of variation values determined from both tests were very similar.
- Plotting LBPT results vs. NASP test results indicated a linear trend line with an R^2 value of 0.77, meaning there was a fair correlation between the two tests and each one could be an equally valid test.
- Both tests predicted strand type 102 to be the worst, but the NASP test indicated that 103 was the top performer, while the LBPT indicated strand type 101 was the best. However the results for types 101 and 103 were extremely close for both tests.

6.1.2. Transfer Length Test Results. The findings from the transfer lengths determined through the 95% Average Mean Strain Method and the transfer lengths at release calculated by initial end slips are as follows:

- Live and dead ends were not noted at the time of release, but measured transfer lengths indicated some locations where transfer lengths were significantly longer and live ends could be reasonably assumed.
- No significant differences were seen between transfer lengths in SCC and those in conventional concrete for either top or bottom strands from 1 to 28 days when possible live end values were removed from averages.
- In terms of the effect of concrete strength on transfer length, higher strength concrete resulted in shorter transfer lengths for bottom strands in conventional concrete when the possible live end values were removed from the average, but no differences were seen between the transfer lengths in normal and high strength SCC for bottom strands. For top strands, the high strength mixes for both the SCC and conventional concrete had shorter transfer lengths, but only from 8 to 28 days.
- For all concrete mixes at all ages, no statistically significant differences were observed between the transfer lengths of top strands vs. bottom strands.

- For bottom strands, transfer lengths in normal strength concretes increased 33 to 37% over 28 days, while transfer lengths in high strength mixes increased 14 to 24%, and higher increases were observed in transfer lengths in conventional concrete compared to SCC for a given strength level.
- For top strands, no consistent increases were seen over 28 days for any mix or strength, and the high strength SCC mix actually showed decreases in transfer lengths over time.
- For both top and bottom strands, except for the possible live end averages of both the top and bottom strands and top strands in the normal strength conventional concrete, measured transfer lengths were shorter than the values predicted by the two ACI equations. All measured top and bottom transfer lengths, even the possible live end averages, were shorter than the value predicted by AASHTO equation.
- Due to the violent release method, many of the potentiometers did not register valid end slips because the potentiometers either became separated from the plate attached to the strand or the wires connecting the potentiometers to the Synergy data acquisition became disconnected. Only 38% of all potentiometers that were installed registered what could be considered valid end slips.
- The steel ruler measurements had a precision of only $^{1}/_{32}$ in. (0.79 mm) and the same measurements were consistently reported, rendering the steel ruler method of determining end slips imprecise.
- The percent differences between the average DEMEC and Synergy transfer lengths for each mix ranged from 0.36 to 73%. The transfer lengths calculated from the end slips measured by the potentiometers were generally less than the transfer lengths determined from the DEMEC readings.
- The percent differences between the average DEMEC and ruler transfer lengths ranged from 4 to 119%. The transfer lengths calculated from the end slips measured by the steel ruler were generally less than the transfer lengths determined from the DEMEC readings.
- When plotted with results from a similar program by Ramirez and Russell (2008), NASP in concrete pullout loads normalized by NASP in mortar pullout

loads were shown to follow the same correlation to the square root of concrete compressive strength, as was found by Ramirez and Russell. The correlation was not significantly changed whether the results from the NASP test in mortar Mix A or the results from the NASP test in mortar Mix B were used.

- When NASP values normalized to the square root of concrete compressive strength were plotted against transfer lengths at release, the scatter was found to fall within the scatter reported in the NCHRP report, confirming the relationship between the NASP in mortar pullout values, concrete compressive strength, and initial transfer lengths, found by Ramirez and Russell (2008).
- When Ramirez and Russell's proposed transfer length equation was applied to the data from this study, the equation was found to give values shorter than the current AASHTO equation, but the calculated values were still found to generally be conservative, except when compared to the possible live end averages.

6.1.3. Development Length Test Results. The findings from the four-point loading tests performed to evaluate development lengths are as follows:

- All development length test specimens failed in flexure due to concrete crushing.
- All development length test specimens sustained an applied moment that exceeded the calculated nominal moment.
- All development length test specimens showed negligible strand end slip during testing.
- SCC and conventional concrete specimens exceeded the calculated nominal moment capacities by similar amounts and exhibited similar flexural bond behavior.
- When Ramirez and Russell's proposed development length equation was applied to the data from this study, the equation was found to produce development lengths shorter than the AASHTO equation for three of the four mixes. For the normal strength conventional concrete mix, the proposed equation actually resulted in a transfer length longer than the length predicted by the AASHTO equation.

6.2. CONCLUSIONS

Based on the previously stated findings, several conclusions can be drawn regarding the applicability of NASP test in mortar and LBPT bond tests, the bond performance of SCC compared to conventional concrete, and the feasibility of using concrete strength and pullout test results to predict transfer lengths.

1. Based on the linear relationship found between the LBPT and NASP pullout values and the similar coefficients of variation between the two tests for a given strand type, either the LBPT or NASP test are equally valid approaches to evaluating bond performance of prestressing strand. However, the limits set on passing may need some refinement, as two of the strand sources passed the proposed NASP standard but did not pass the LBPT requirements.
2. Proportioning for the mortar mixes did appear to have an effect on NASP in mortar pullout values, and it is hypothesized that a decreased amount of sand could detrimentally affect mechanical interlocking and lead to lower pullout values.
3. While first slips are not required to be monitored in the NASP test, strands with high 0.1 in. (2.54 mm) pullout loads sometimes had the lowest 0.001 in. (0.025 mm) pullout loads, which could indicate a problem with adhesion of the strand.
4. The NASP test in concrete revealed that the high strength concretes had lower first slip values than the normal strength concretes. Compared to their normal strength counterparts, the high strength mixes generally had a lower water/cement ratio, a decrease in coarse and fine aggregate content, an increase in total cementitious material, and an increase in high range water reducer.
5. SCC and conventional concrete were comparable in terms of bond performance, showing few statistical differences between measured transfer lengths or pullout loads between the two types of concrete.
6. Increases in concrete strength generally resulted in shorter, although not always statistically different, transfer lengths, especially if the possible live end values were removed from the averages. Also, top strands only seemed to show statistically significant increases in transfer length at later ages.

7. Transfer lengths of bottom strands tended to increase from 1 to 28 days, with most of the increase occurring between 1 and 4 days. Also, the transfer lengths in normal strength mixes appeared to increase more than those in high strength mixes, and transfer lengths in conventional concrete increased more than transfer lengths in SCC. However, no consistent trends were noted for change in top strand transfer lengths over time.
8. The AASHTO transfer length equation was generally conservative for all mixes for both top and bottom strands, even when compared to possible live end transfer lengths. The ACI equations were generally conservative except when compared to live end transfer lengths or the top strands in the normal strength conventional concrete.
9. The linear potentiometers used in this study were found to be unreliable, and the steel ruler measurements were determined to be imprecise; the transfer lengths determined from the DEMEC readings and 95% Average Mean Strain Method were found to be the most consistent and reliable.
10. Due to the fact that increased concrete strength resulted in decreased transfer lengths and increased NASP in concrete pullout loads, concrete strength does have an effect on bond, and the equation for transfer length should be a function of concrete strength.
11. In this study, transfer length did appear to be related to the square root of concrete compressive strength, which follows the trend noted by Ramirez and Russell (2008) and others.
12. The proposed transfer length equation from Ramirez and Russell (2008) was slightly less conservative than the AASHTO equation, but still mostly conservative when compared to the measured transfer lengths, although the proposed equation was not conservative when compared to the live end transfer lengths.
13. Development length specimens tested at embedment lengths of 80% of the development length calculated from the AASHTO and ACI equations still failed in flexure, so the current AASHTO and ACI equations for development length are conservative.

14. SCC and conventional concrete appeared to exhibit comparable flexural behavior.
15. Ramirez and Russell's proposed development length equation (2008) appeared to be less conservative than the AASHTO and ACI equation but still conservative in three out of the four cases. In this test program, even the development length tests completed at an embedment length of 58 in (1,473 mm), which is 80% of the development length calculated from the current AASHTO equation and shorter than any of the development lengths calculated by the proposed equation, failed in flexure, showing the strand could be fully developed. However, the proposed equation did predict one development length greater than the AASHTO and ACI value for one mix, showing the proposed development length equation may be over-conservative in some cases.

6.3. RECOMMENDATIONS

From the conclusions, the following recommendations for future work and for implementation of tests are listed below:

1. Because differences in bond quality have been shown to vary greatly depending on the source of strand, a standard bond test should be recommended and implemented by MoDOT to ensure strand bond quality before the strand is used in production. Missouri S&T recommends that the NASP Bond test as described in NCHRP Report 603 be prescribed; however, the minimum acceptance criteria loads should be increased to 16,000 lb (71.2 kN) for the average of six specimens and 14,000 lb (62.3 kN) for an individual specimen.
2. The NASP test in concrete should not necessarily be a required test for strand bond because the tests showed pullout strength is mostly a function of concrete compressive strength; however the NASP test in concrete still could be useful for identifying possible effects of mix additions or proportioning on bond.
3. The pullout limits for both the NASP test in mortar and LBPT need refinement. Additional research should be conducted with NASP and LBPT specimens and corresponding transfer length specimens to see if the NASP minimum value should be raised and the LBPT minimum value should be lowered. Specifically, strands with NASP pullout values between 12,000 and 18,000 lb (53 and 80 kN)

and LBPT pullout values between 30.0 and 36.0 kips (133 and 160 kN) should be targeted.

4. The pullout value at first slip, or 0.001 in. (0.025 mm) of slip, should also be reported for the NASP test because low first slip values could indicate problems with adhesion of strand.
5. Additional studies should be completed to investigate the effect of mortar mix proportioning on the pullout values from the NASP test in mortar, and limits should be set for proportioning in addition to strength and flow.
6. More research should be conducted to determine if the contours of the load vs. slip curves for the NASP test in mortar specimens can also be indicators of bond quality. Strand types that show plateaus or drop-offs in load at 0.1 in. (2.54 mm) instead of continuing to increase may not have acceptable bond quality, even if they pass a minimum load limit.
7. The potentiometer and plate method for measuring end slip should be reinvestigated to see if other plate/potentiometer bonding methods or other less violent release methods could yield useable data. However, the steel ruler method should be abandoned, and end slips should be measured with a more precise means, such as a caliper.
8. The current AASHTO and ACI transfer length and development length equations are adequate and conservative for use with conventional concrete as well as SCC.
9. The proposed transfer length equation from Ramirez and Russell (2008) should potentially be reinvestigated because the equation was not conservative for live end transfer lengths.
10. The proposed development length equation from Ramirez and Russell (2008) should also potentially be reinvestigated because the equation might result in overly conservative values in some cases.

APPENDIX A

CONCRETE COMPRESSIVE STRENGTH SUMMARY

Table A.1 – Summary of Concrete Compressive Strengths

Mix ID	Concrete Compressive Strength				
	1 Day (psi)	4 Day (psi)	8 Day (psi)	14 Day (psi)	28 Day (psi)
C6	4,810	5,380	5,620	5,630	5,730
S6	5,660	6,440	6,690	6,910	6,950
C10	5,670	7,890	7,950	8,350	8,480
S10	6,330	8,300	8,600	9,100	9,250

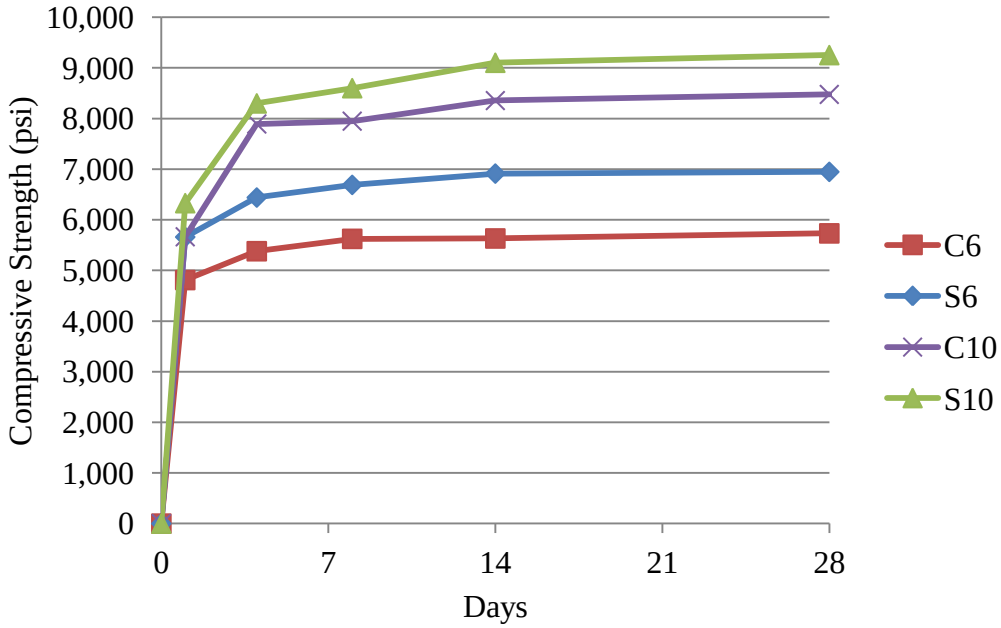

Figure A.1 – Concrete Compressive Strength over Time

APPENDIX B

NASP IN CONCRETE LOAD VS. SLIP PLOTS

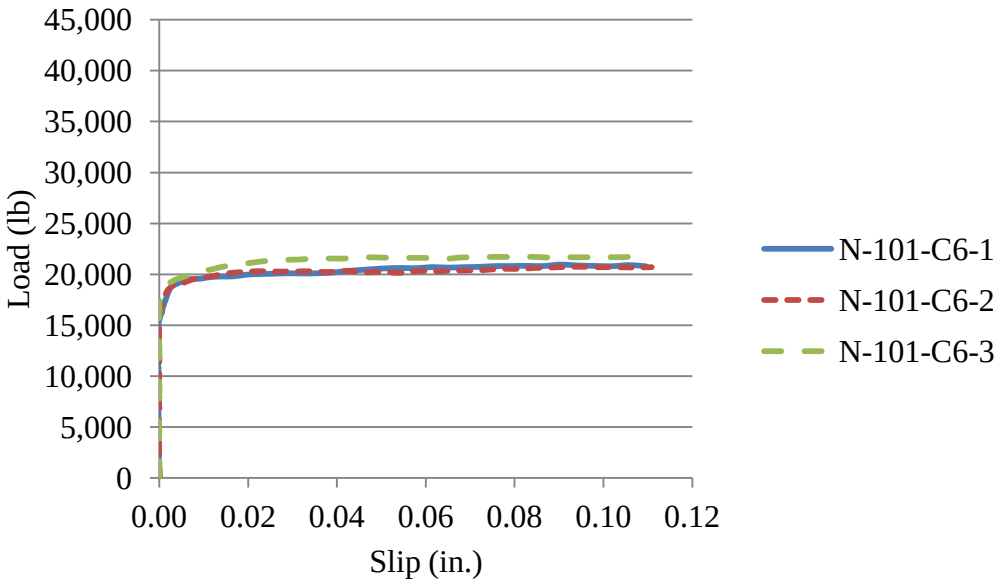

Conversion: 1 in. = 25.4 mm
1 lb = 4.45 N

Figure B.1 – C6 NASP in Concrete – 1 Day

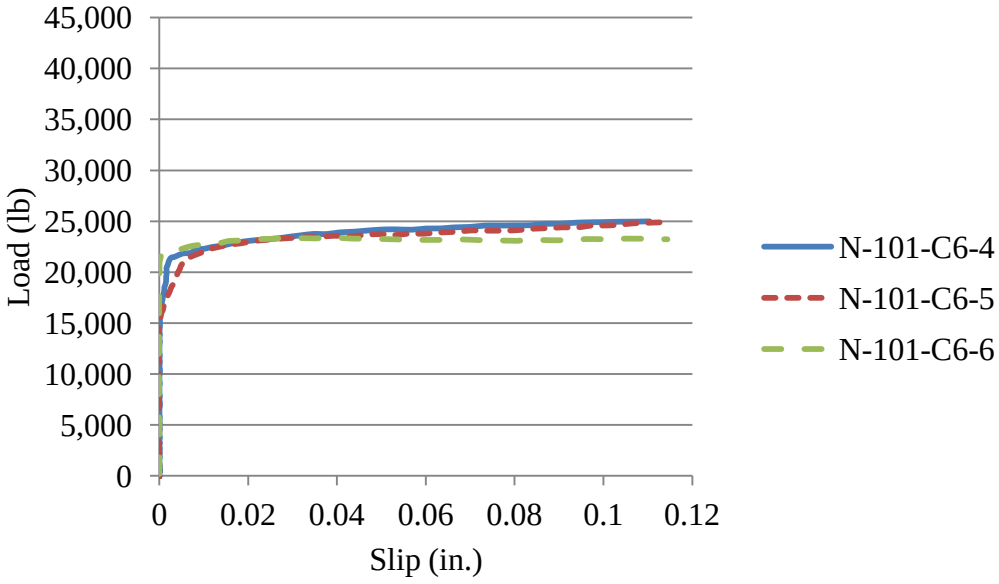

Conversion: 1 in. = 25.4 mm
1 lb = 4.45 N

Figure B.2 – C6 NASP in Concrete – 8 Day

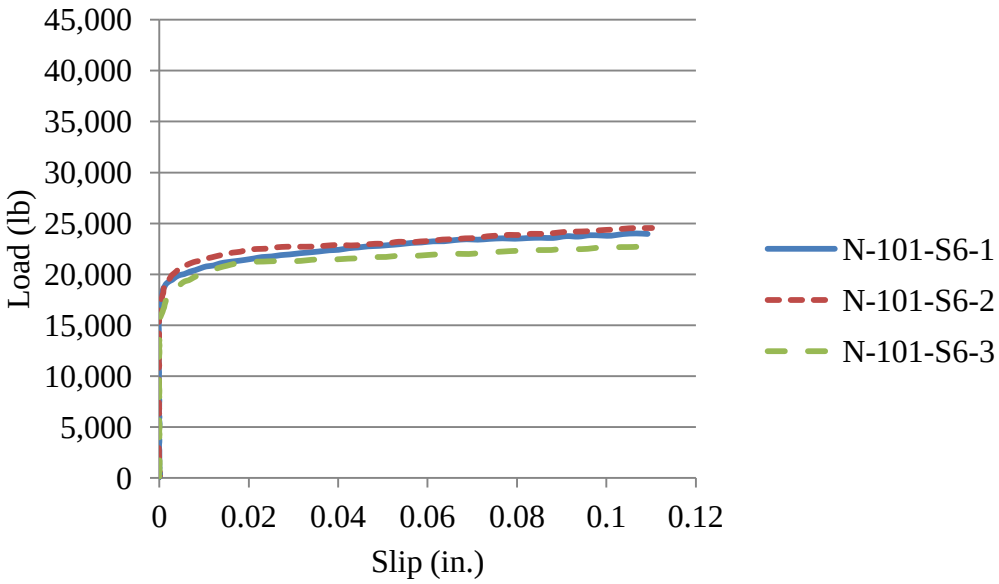

Conversion: 1 in. = 25.4 mm
1 lb = 4.45 N

Figure B.3 – S6 NASP in Concrete – 1 Day

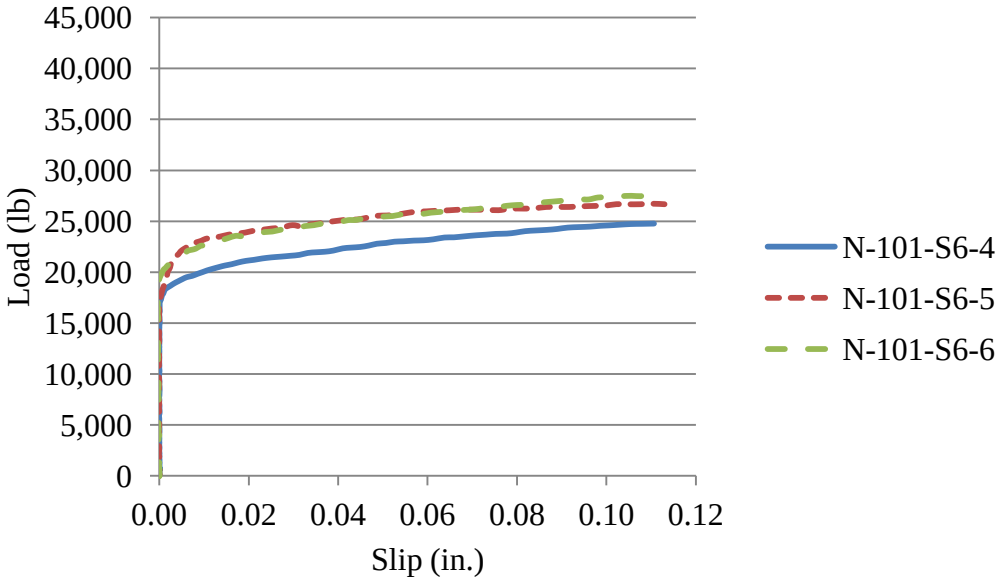

Conversion: 1 in. = 25.4 mm
1 lb = 4.45 N

Figure B.4 – S6 NASP in Concrete – 8 Day

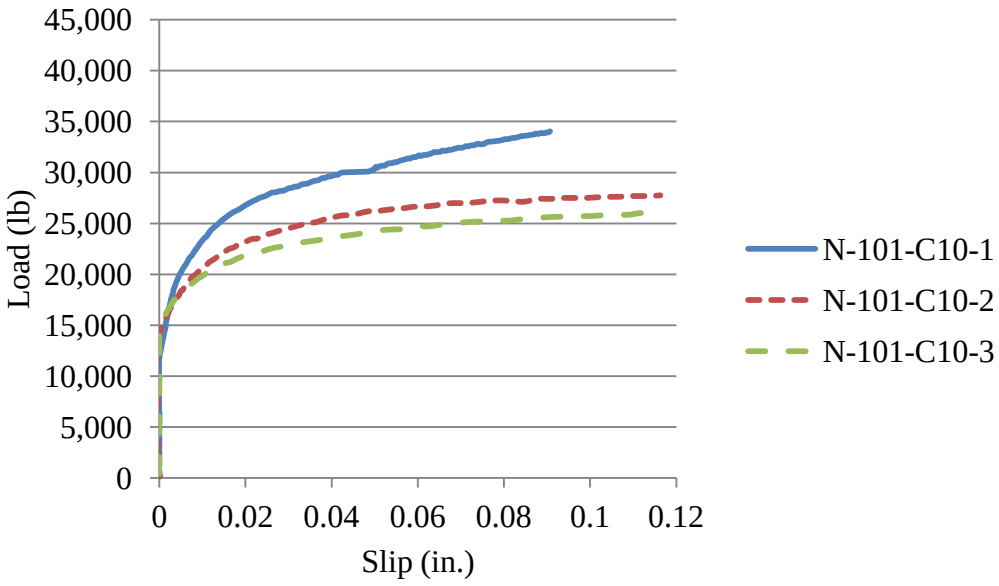

Conversion: 1 in. = 25.4 mm
1 lb = 4.45 N

Figure B.5 – C10 NASP in Concrete – 1 Day

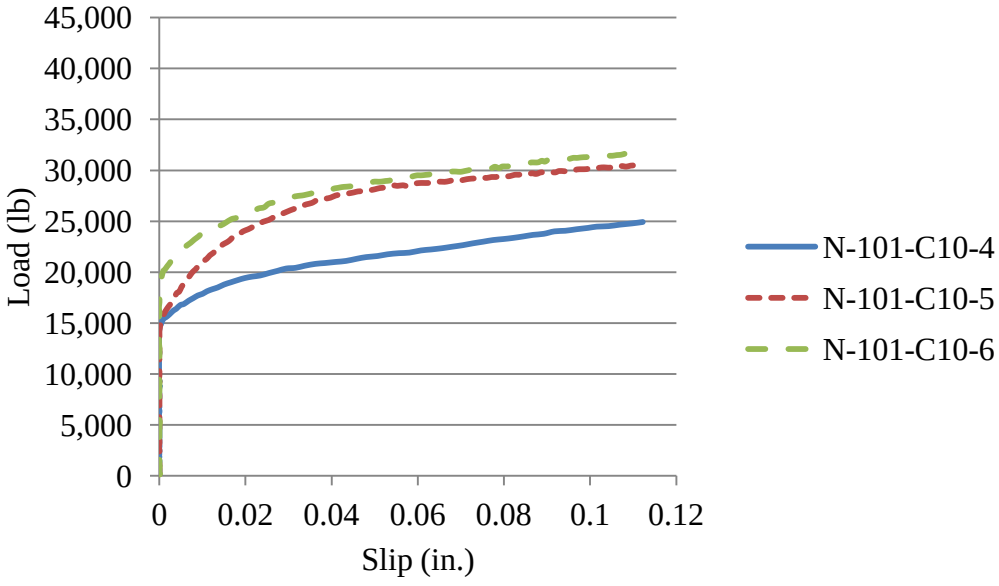

Conversion: 1 in. = 25.4 mm
1 lb = 4.45 N

Figure B.6 – C10 NASP in Concrete – 8 Day

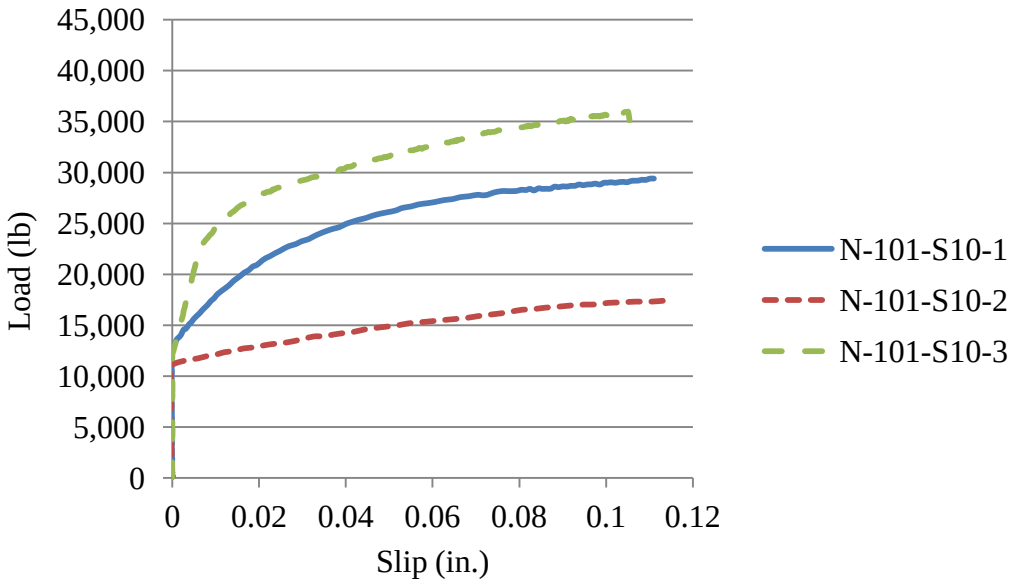

Conversion: 1 in. = 25.4 mm
1 lb = 4.45 N

Figure B.7 – S10 NASP in Concrete – 1 Day

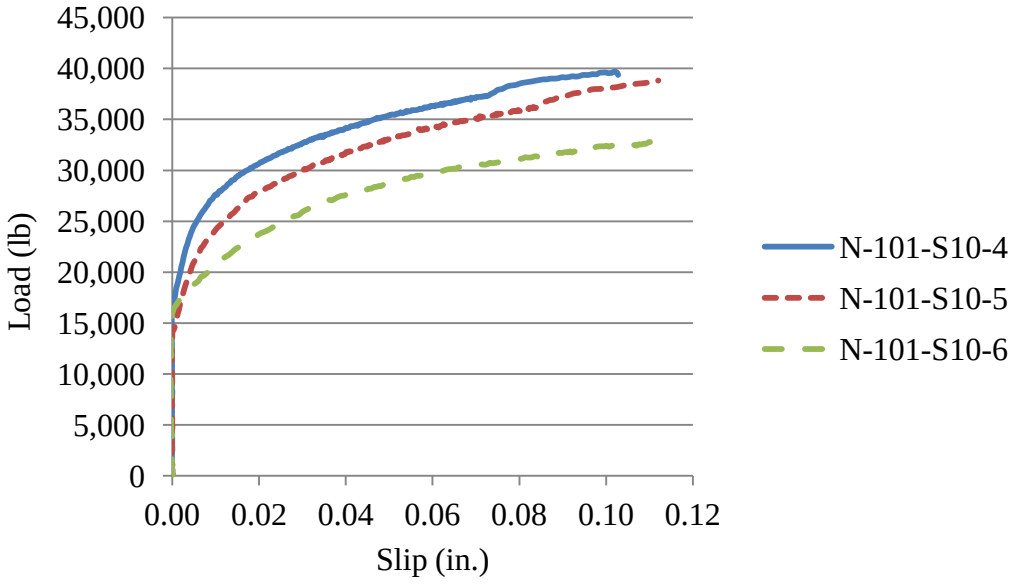

Conversion: 1 in. = 25.4 mm
1 lb = 4.45 N

Figure B.8 – S10 NASP in Concrete – 8 Day

APPENDIX C

LBPT LOAD VS. TIME PLOTS

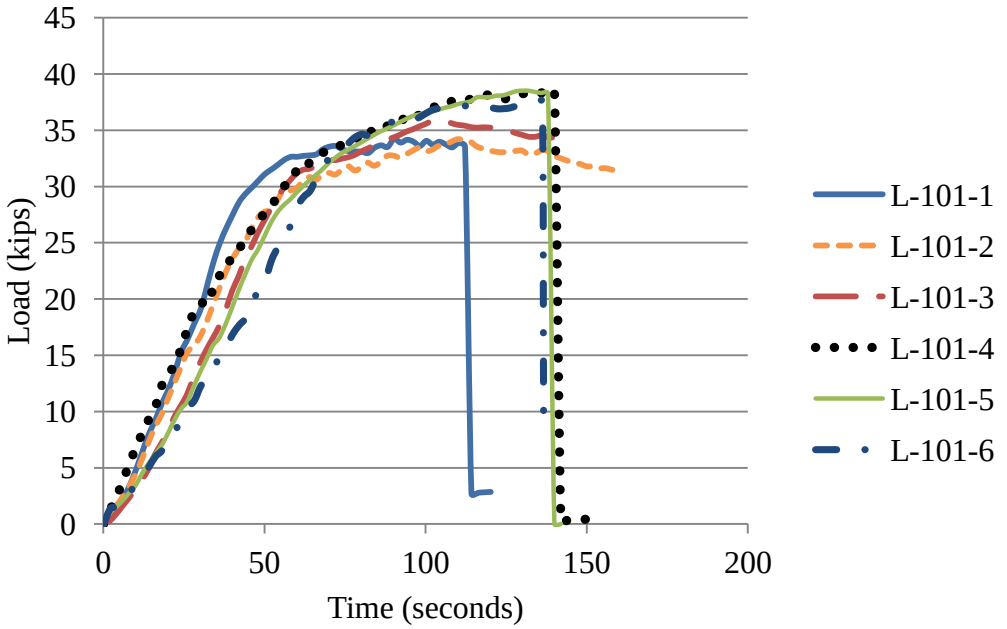

Conversion: 1 kip = 4.45 kN

Figure C.1 – LBPT Results for Strand Type 101

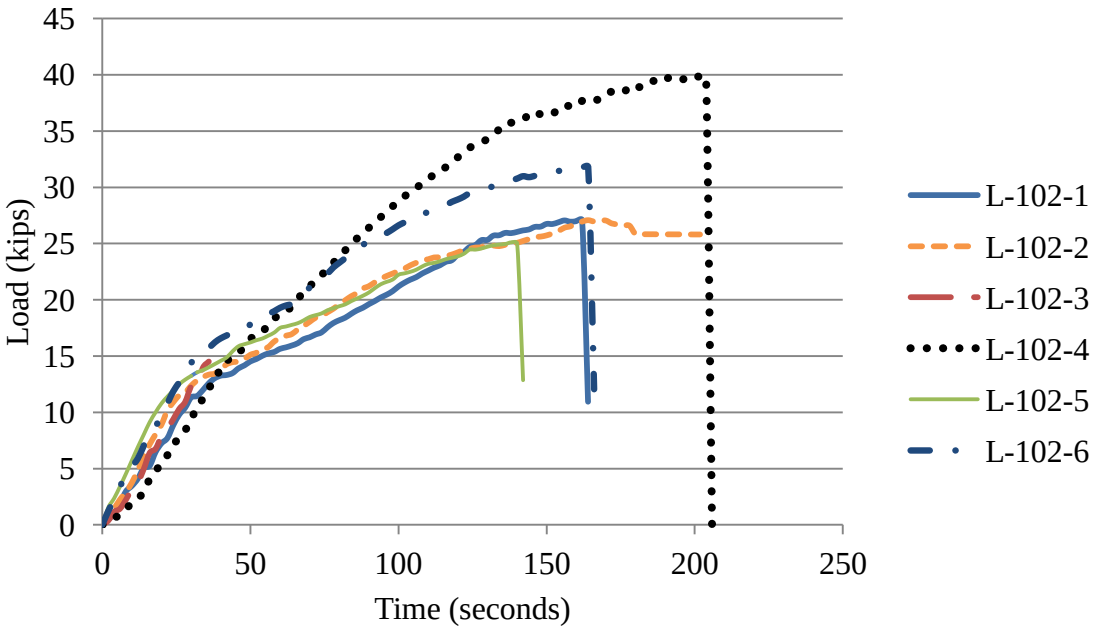

Conversion: 1 kip = 4.45 kN

Figure C.2 – LBPT Results for Strand Type 102

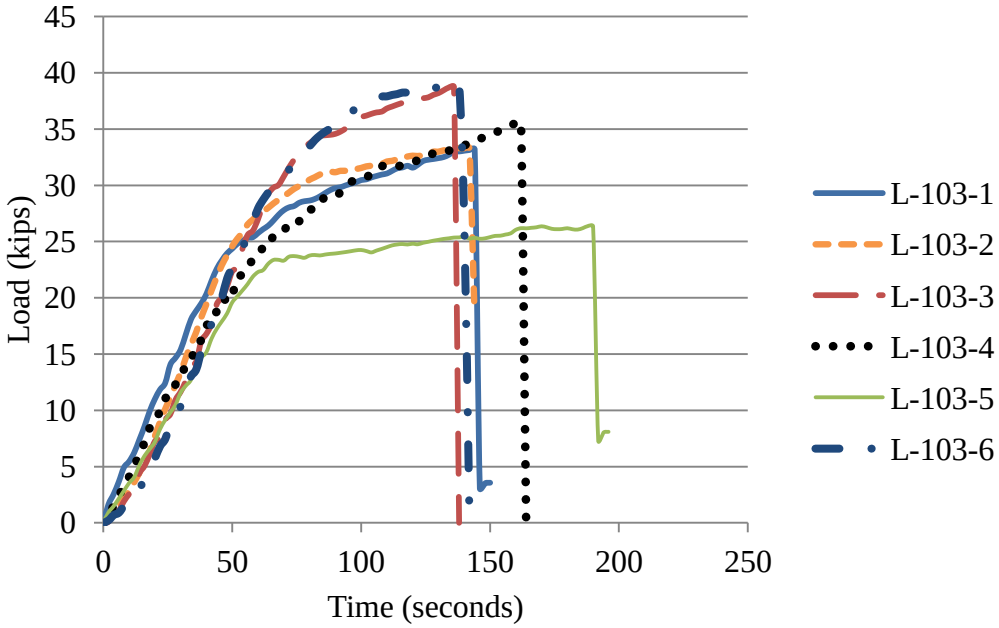

Conversion: 1 kip = 4.45 kN

Figure C.3 – LBPT Results for Strand Type 103

APPENDIX D

95% AVERAGE MEAN STRAIN PLOTS

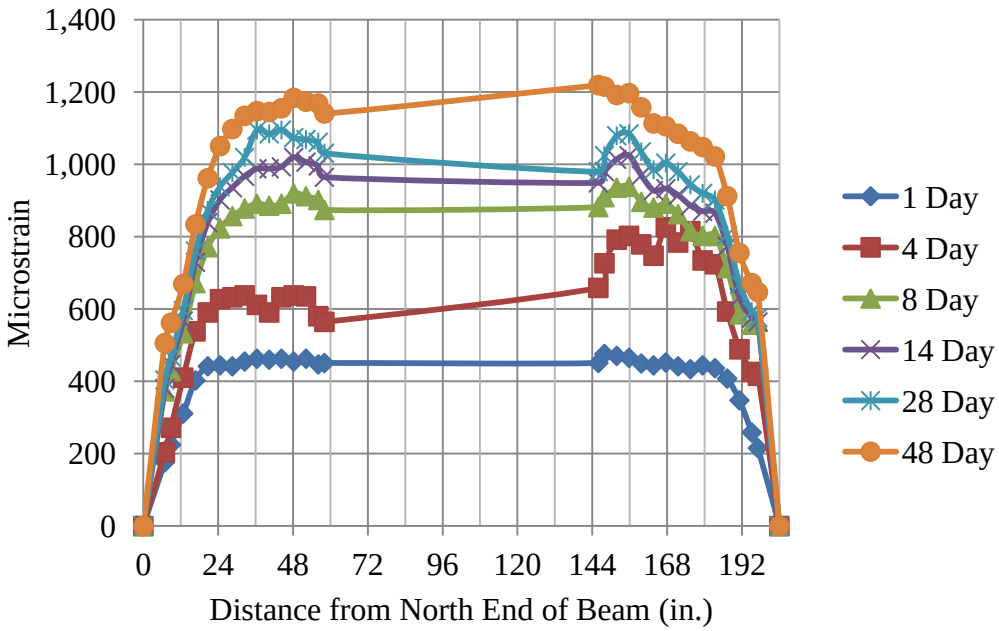

Conversion: 1 in. = 25.4 mm

Figure D.1 – C6-2-1_NE and C6-2-1_SE Average Mean Strains

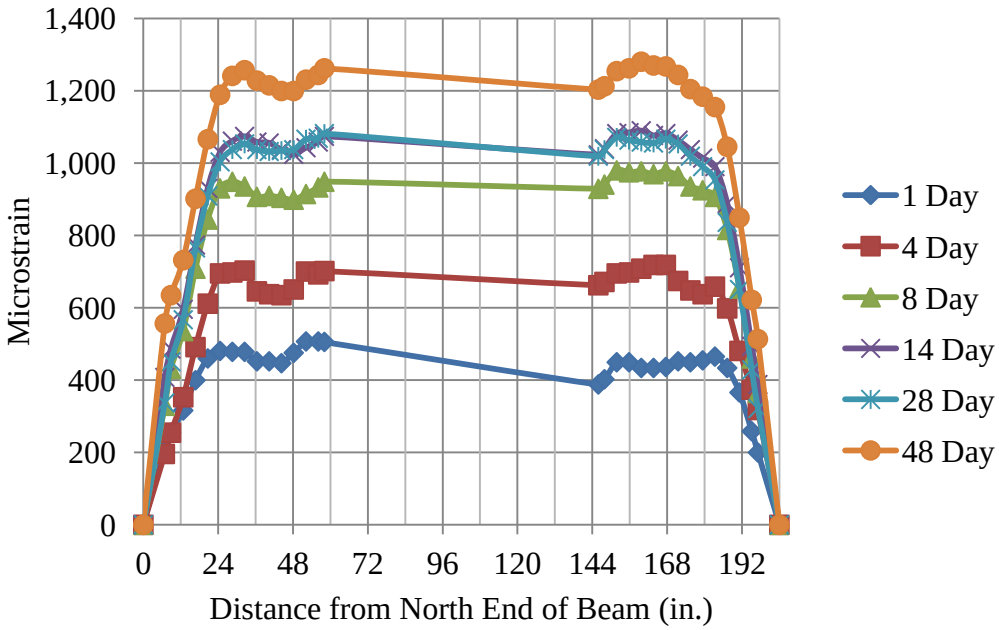

Conversion: 1 in = 25.4 mm

Figure D.2 – C6-2-1_NW and C6-2-1_SW Average Mean Strains

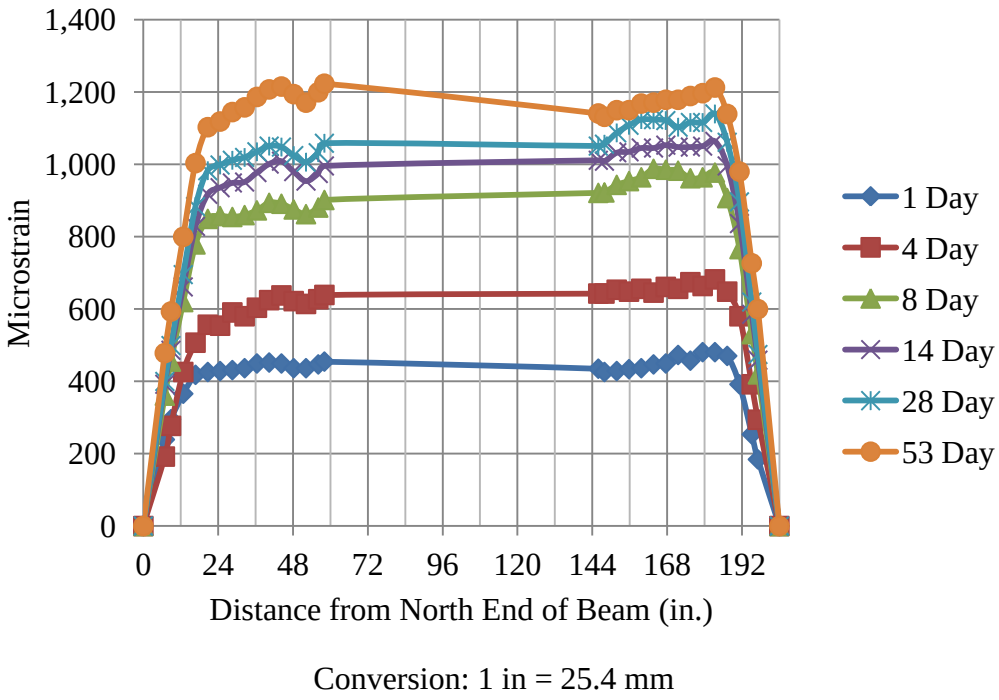

Conversion: 1 in = 25.4 mm

Figure D.3 – C6-2-2_NE and C6-2-2_SE Average Mean Strains

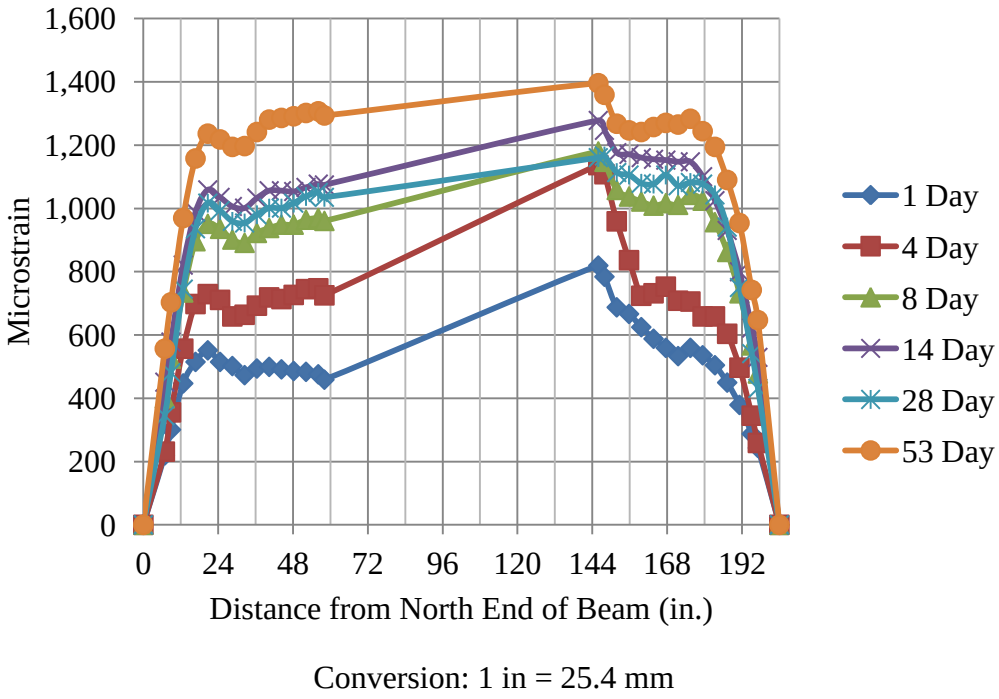

Conversion: 1 in = 25.4 mm

Figure D.4 – C6-2-2_NW and C6-2-2_SW Average Mean Strains

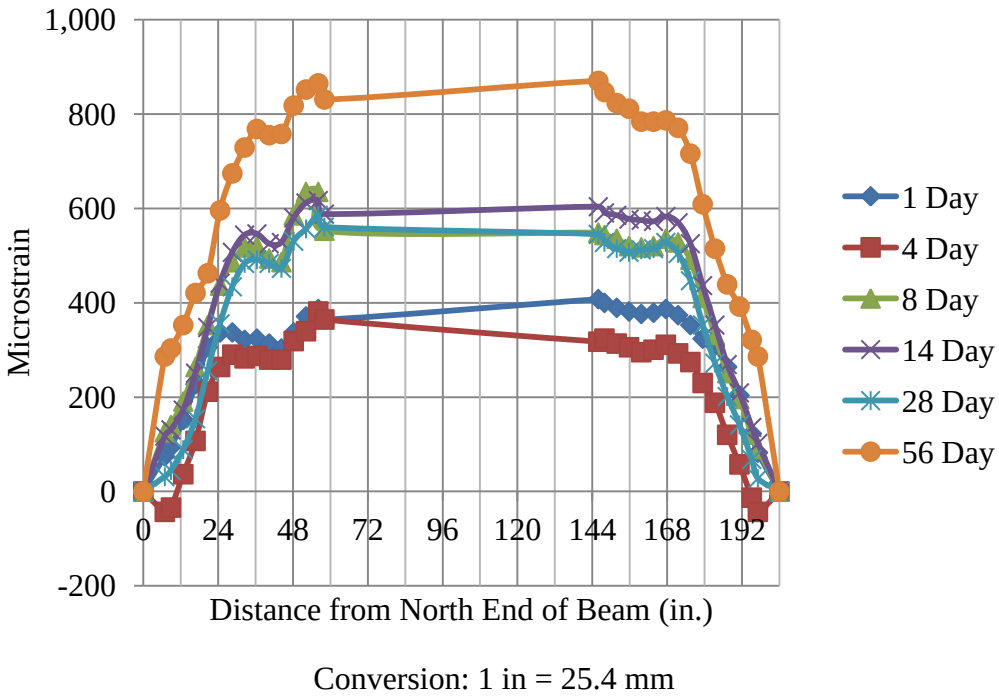

Conversion: 1 in = 25.4 mm

Figure D.5 – C6-4-1_NE and C6-2-1_SE Average Mean Strains

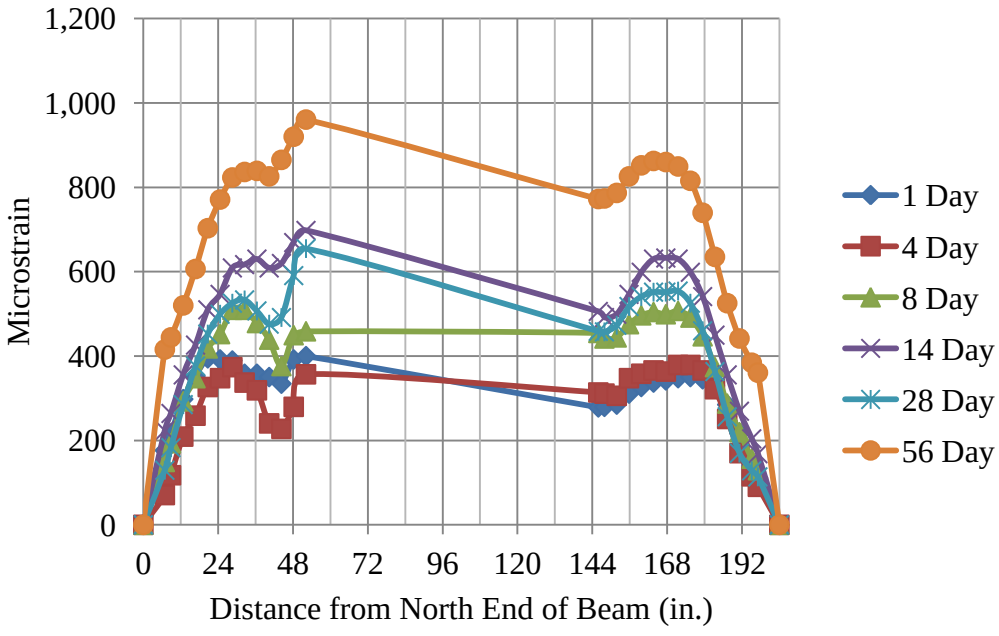

Conversion: 1 in = 25.4 mm

Figure D.6 – C6-4-1_NW and C6-4-1_SW Average Mean Strains

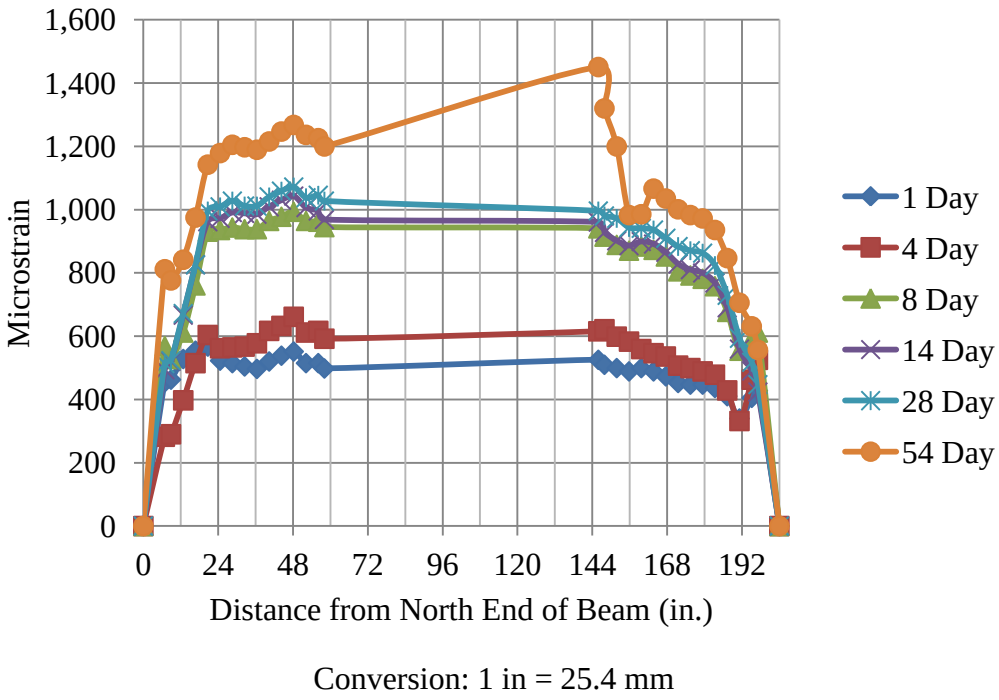

Conversion: 1 in = 25.4 mm

Figure D.7 – S6-2-1_NE and S6-2-1_SE Average Mean Strains

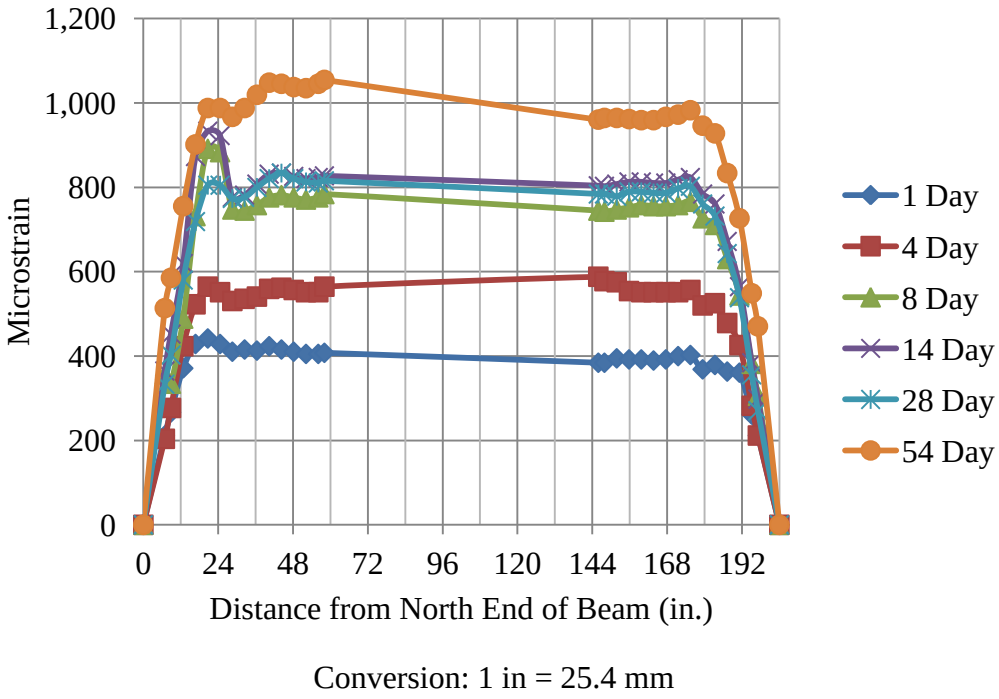

Conversion: 1 in = 25.4 mm

Figure D.8 – S6-2-1_NW and S6-2-1_SW Average Mean Strains

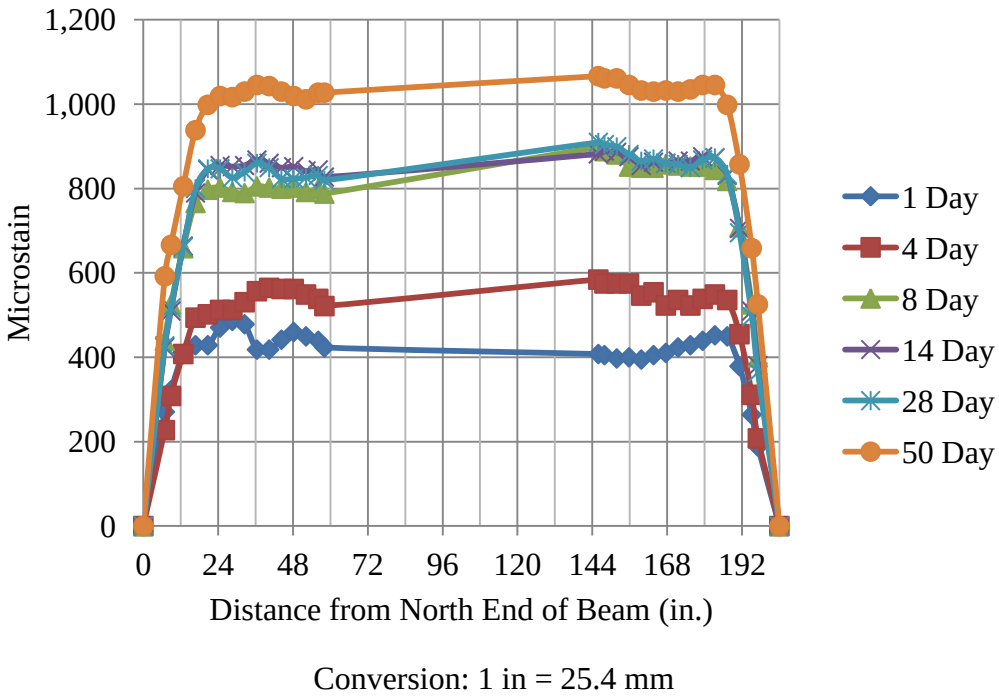

Conversion: 1 in = 25.4 mm

Figure D.9 – S6-2-2_NE and S6-2-2_SE Average Mean Strains

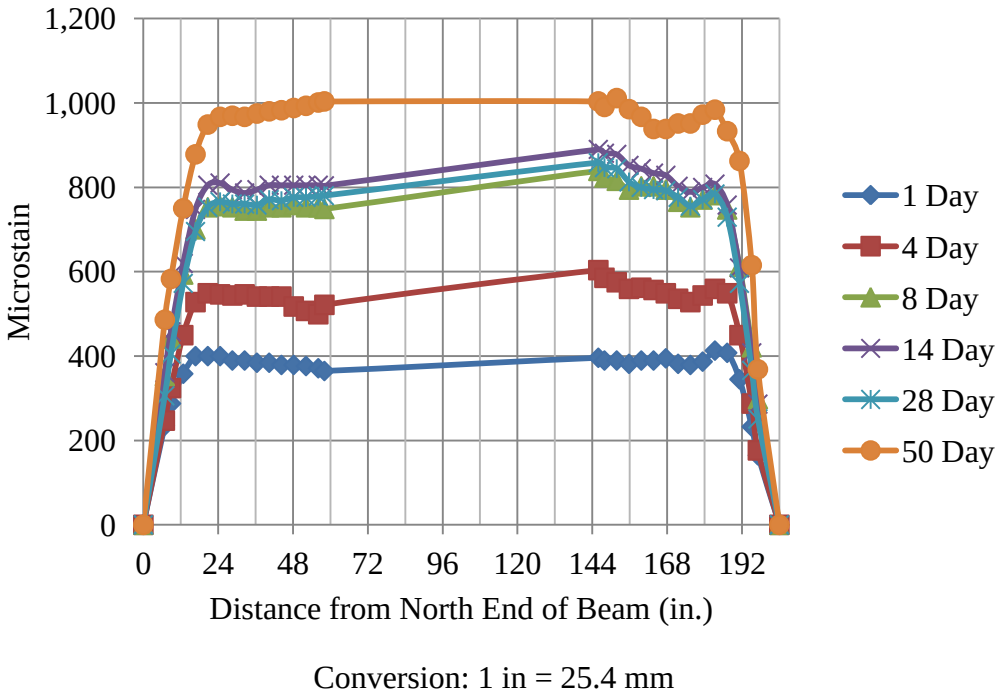

Conversion: 1 in = 25.4 mm

Figure D.10 – S6-2-2_NW and S6-2-2_SW Average Mean Strains

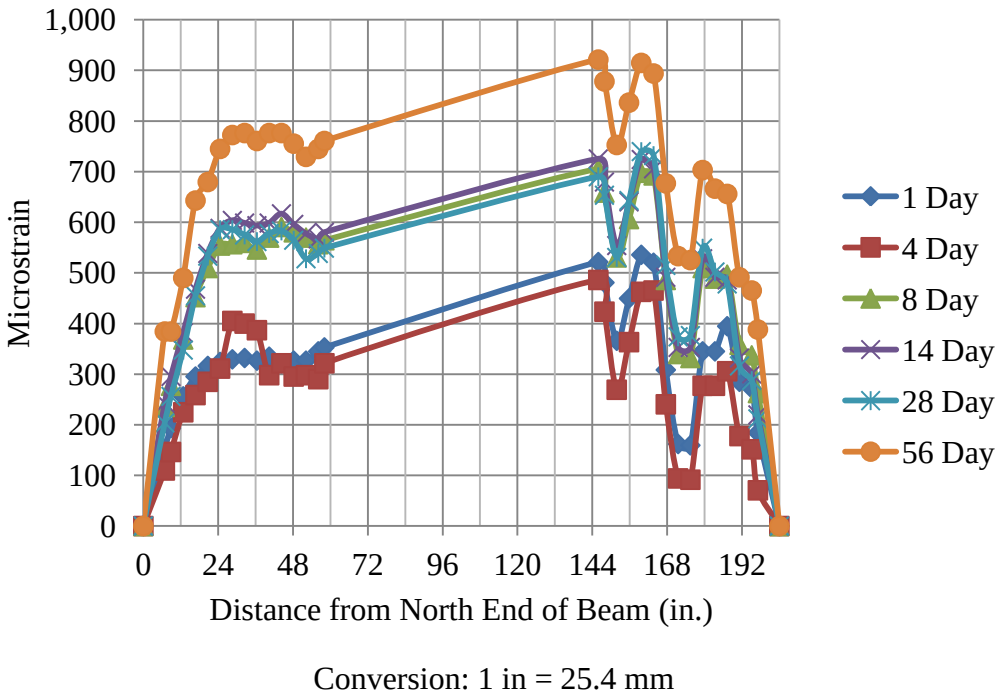

Conversion: 1 in = 25.4 mm

Figure D.11 – S6-4-1_NE and S6-4-1_SE Average Mean Strains

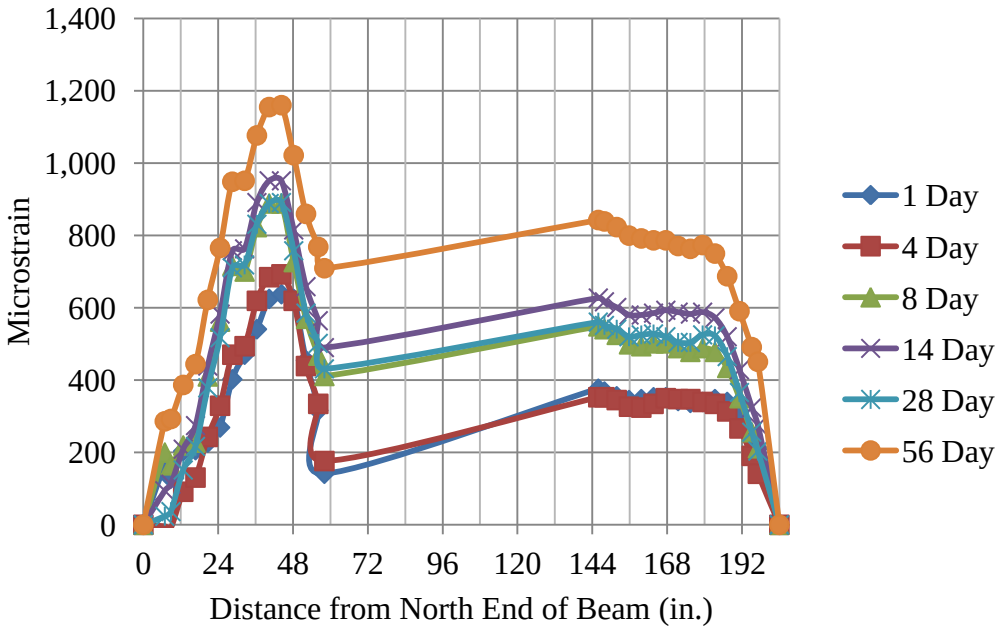

Conversion: 1 in = 25.4 mm

Figure D.12 – S6-4-1_NW and S6-4-1_SW Average Mean Strains

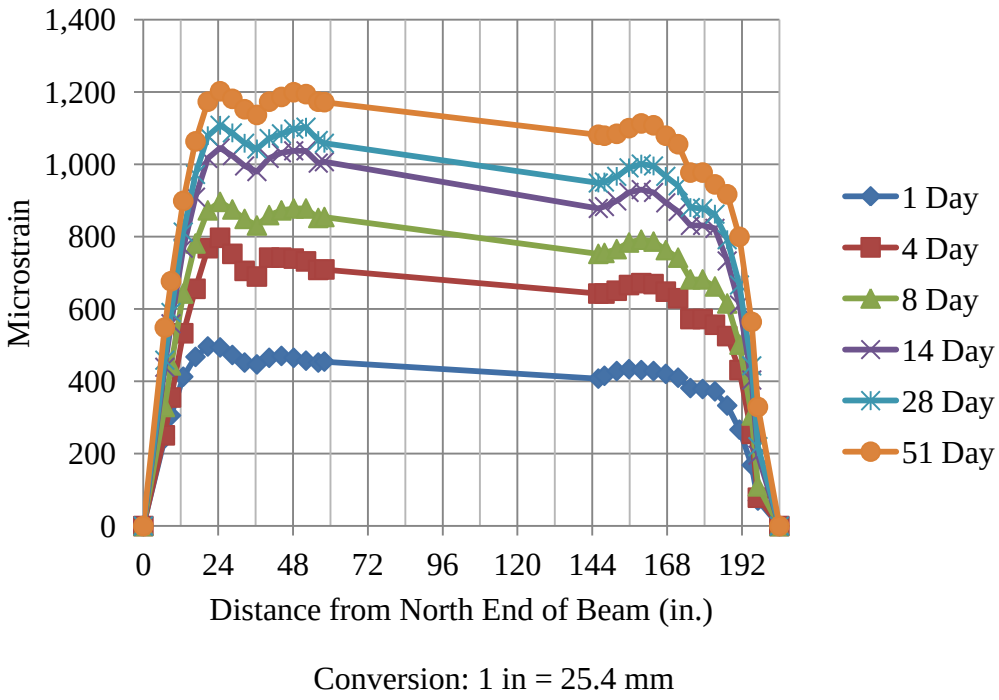

Conversion: 1 in = 25.4 mm

Figure D.13 – C10-2-1_NE and C10-2-1_SE Average Mean Strains

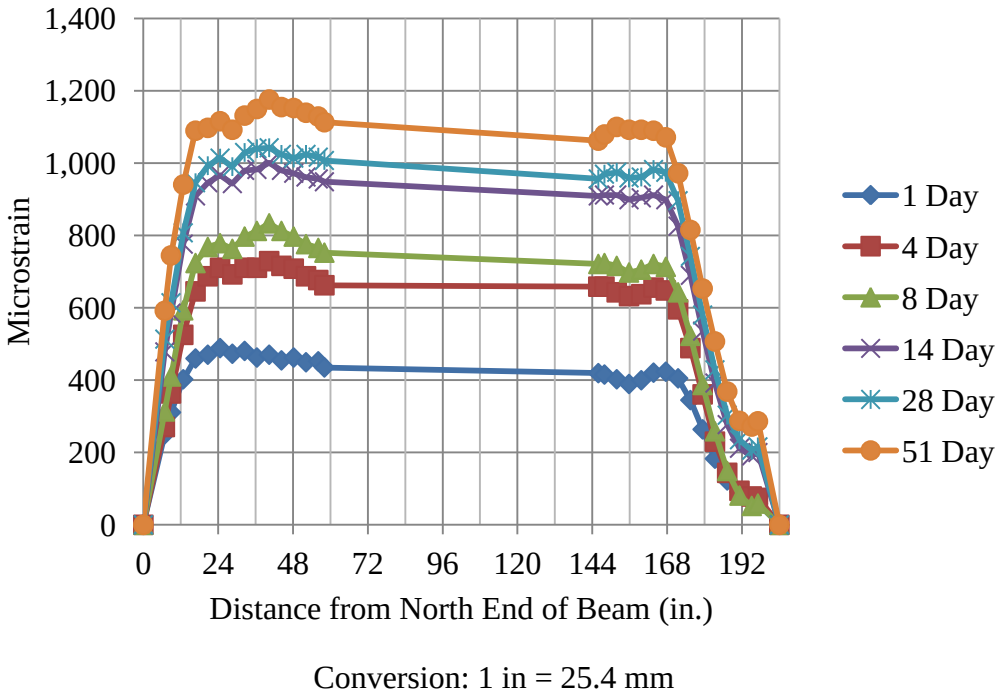

Conversion: 1 in = 25.4 mm

Figure D.14 – C10-2-1_NW and C10-2-1_SW Average Mean Strains

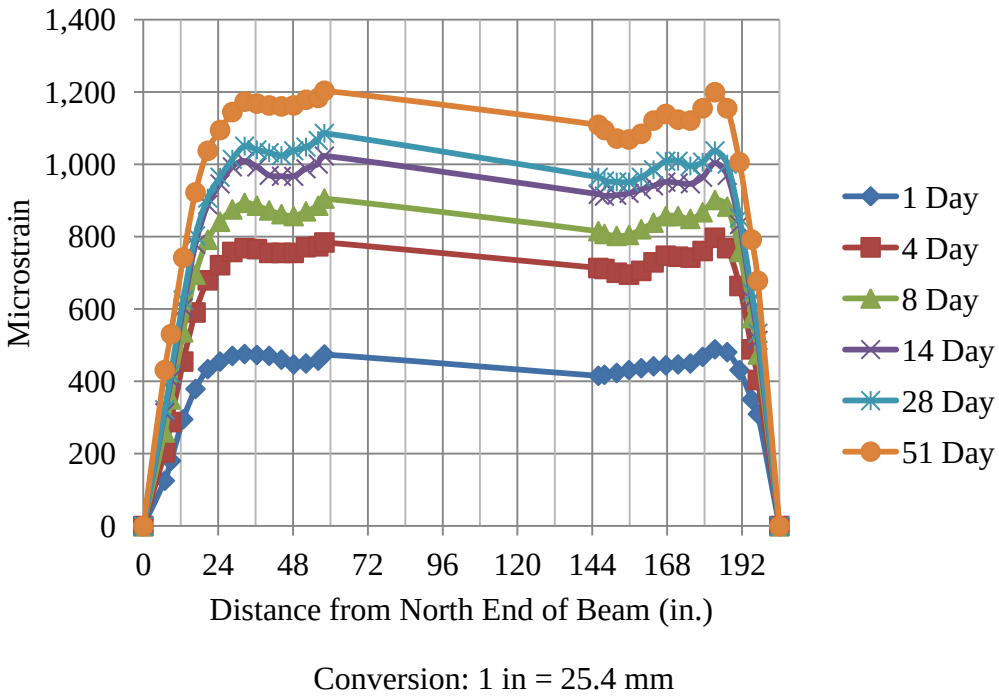

Conversion: 1 in = 25.4 mm

Figure D.15 – C10-2-2_NE and C10-2-2_SE Average Mean Strains

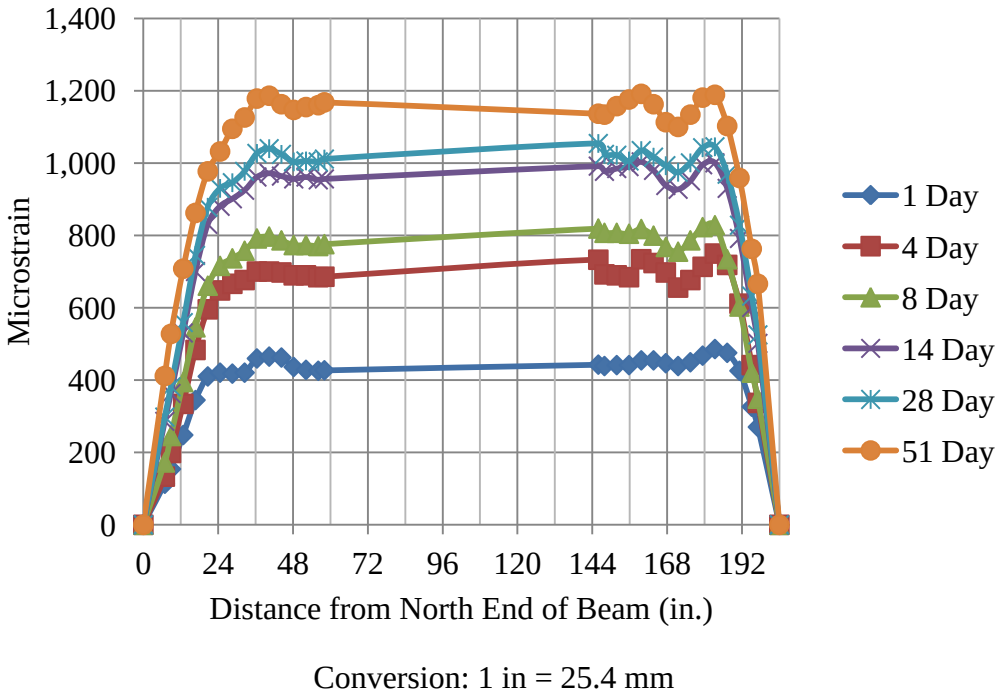

Conversion: 1 in = 25.4 mm

Figure D.16 – C10-2-2_NW and C10-2-2_SW Average Mean Strains

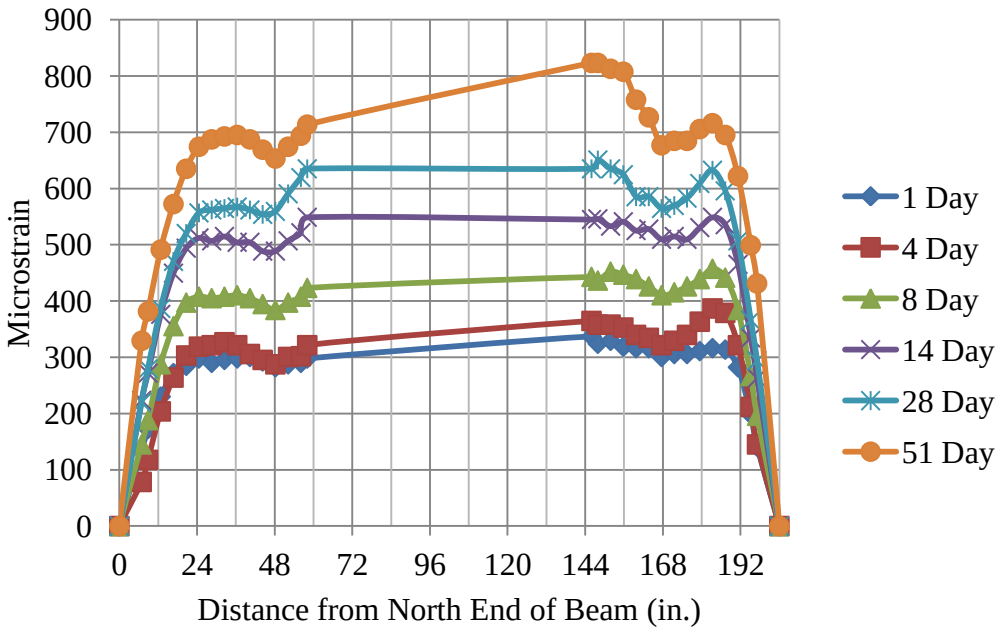

Conversion: 1 in = 25.4 mm

Figure D.17 – C10-4-1_NE and C10-4-1_SE Average Mean Strains

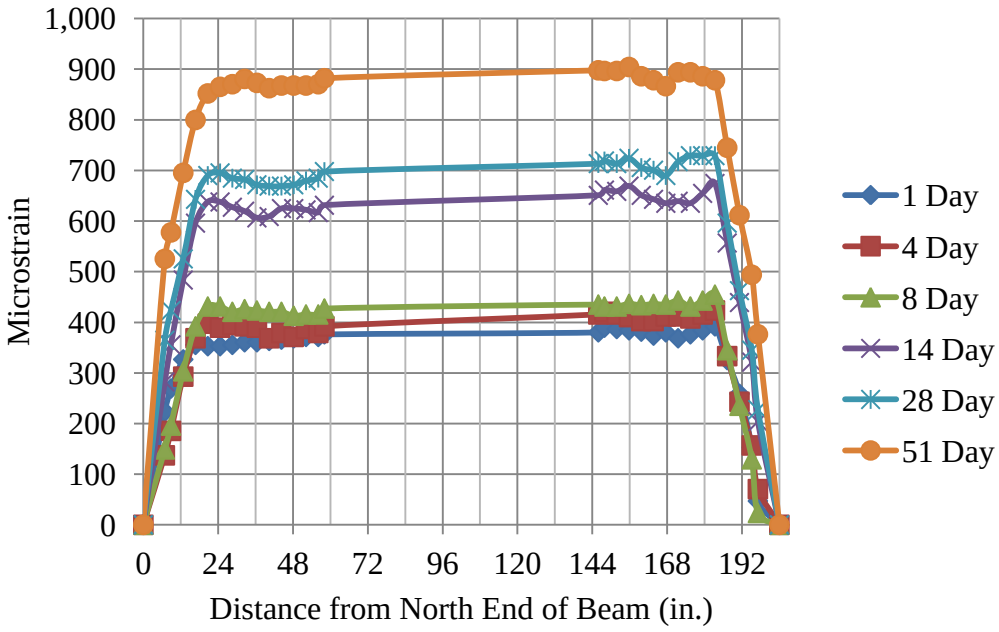

Conversion: 1 in = 25.4 mm

Figure D.18 – C10-4-1_NW and C10-4-1_SW Average Mean Strains

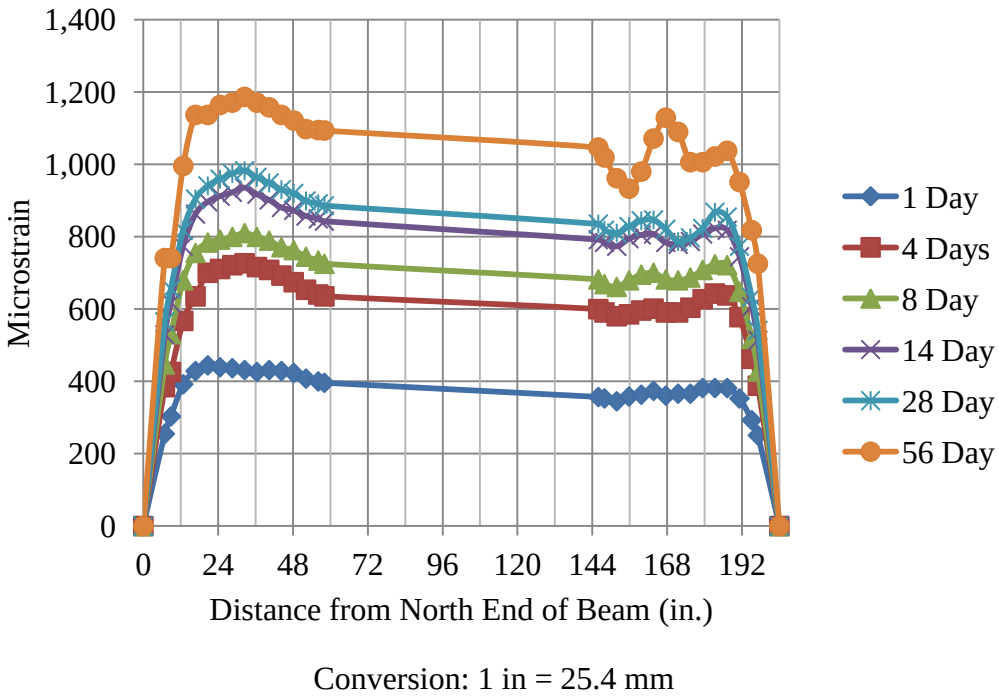

Conversion: 1 in = 25.4 mm

Figure D.19 – S10-2-1_NE and S10-2-1_SE Average Mean Strains

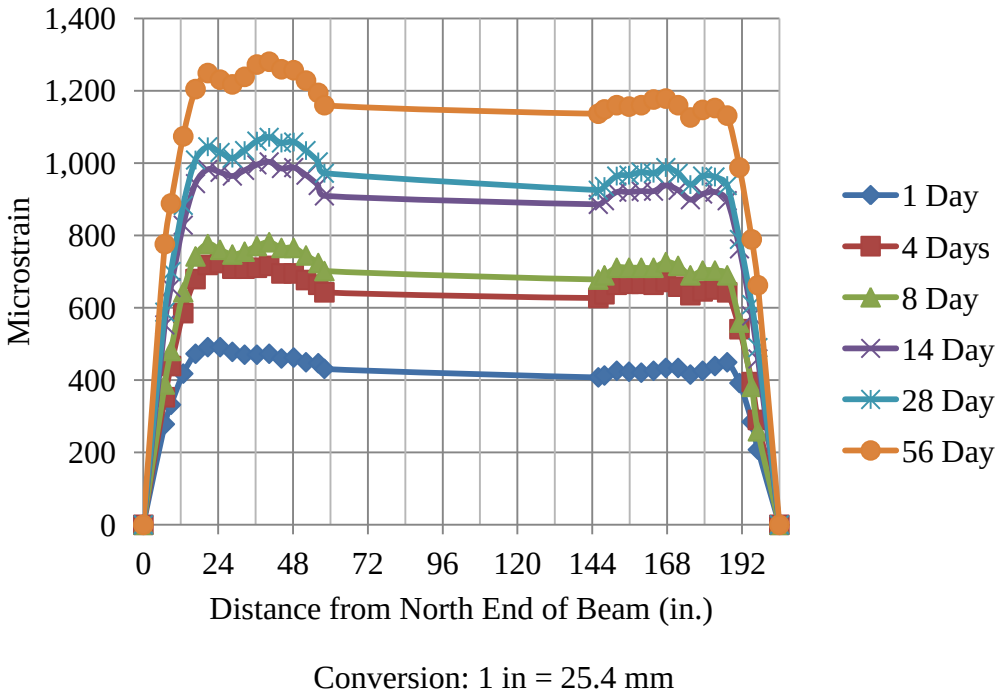

Conversion: 1 in = 25.4 mm

Figure D.20 – S10-2-1_NW and S10-2-1_SW Average Mean Strains

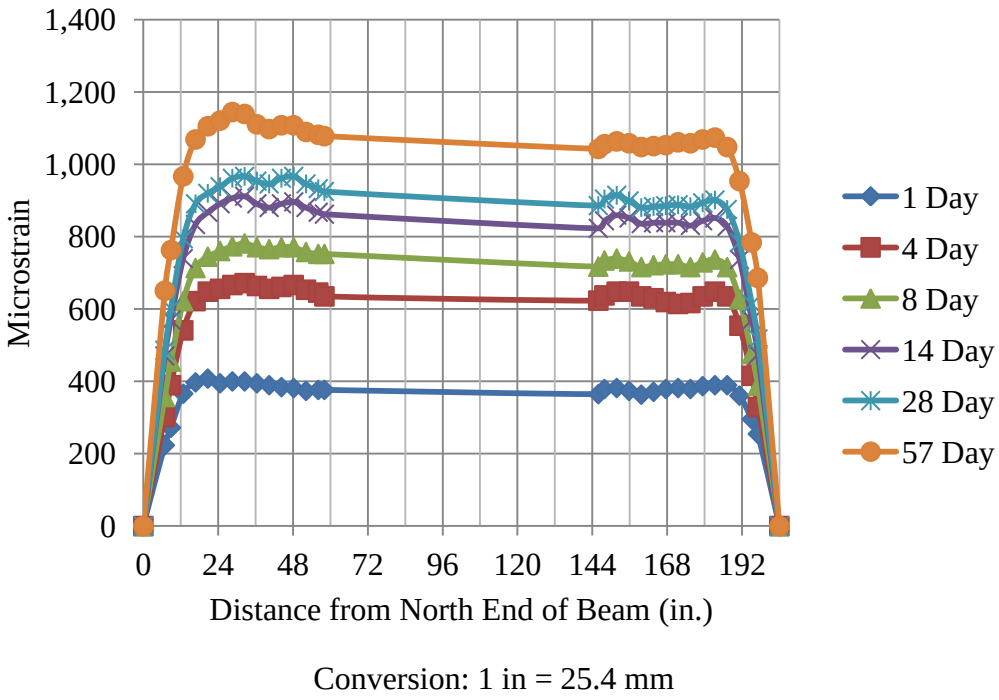

Conversion: 1 in = 25.4 mm

Figure D.21 – S10-2-2_NE and S10-2-2_SE Average Mean Strains

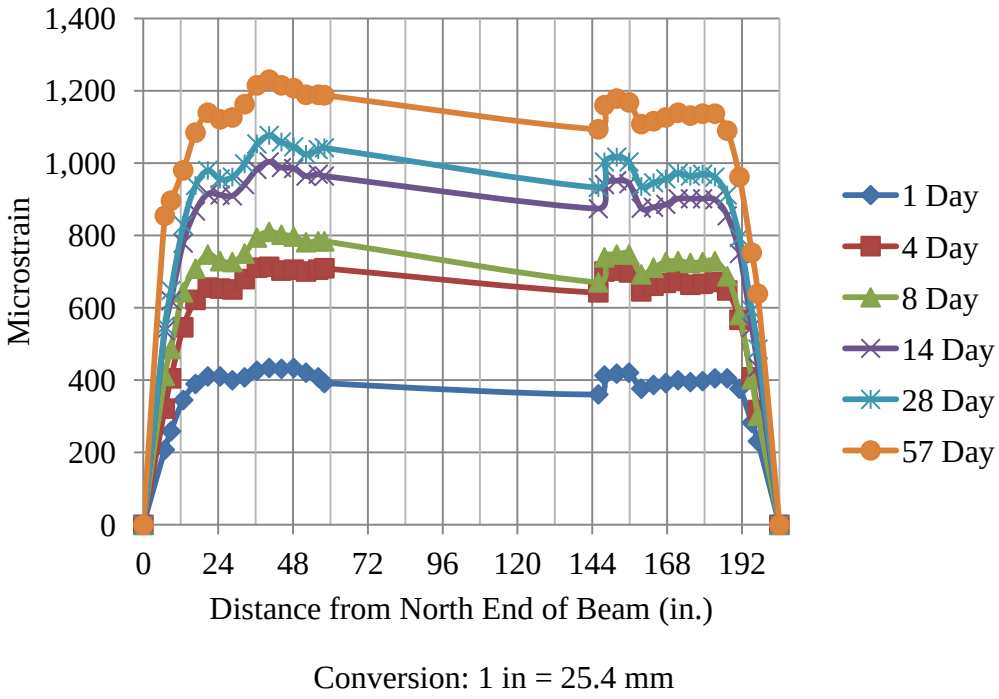

Conversion: 1 in = 25.4 mm

Figure D.22 – S10-2-2_NW and S10-2-2_SW Average Mean Strains

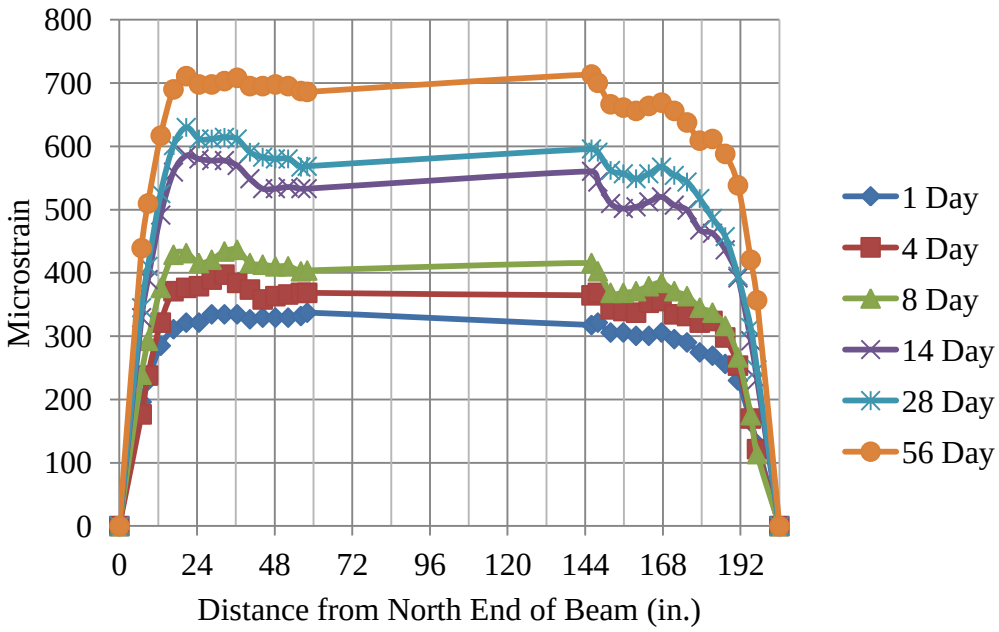

Conversion: 1 in = 25.4 mm

Figure D.23 – S10-4-1_NE and S10-4-1_SE Average Mean Strains

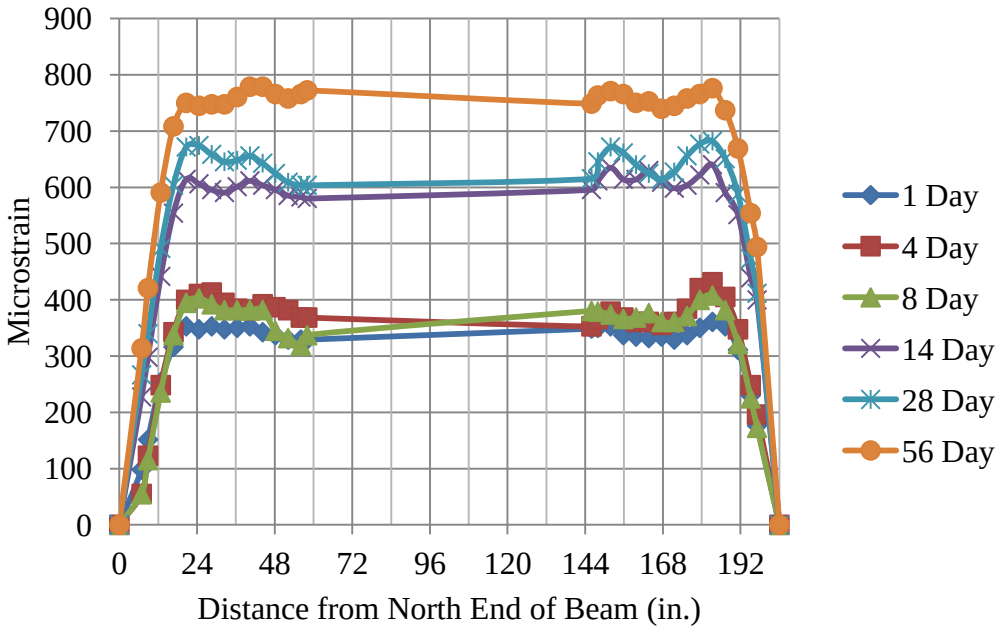

Conversion: 1 in = 25.4 mm

Figure D.24 – S10-4-1_NW and S10-4-1_SW Average Mean Strains

APPENDIX E

LINEAR POTENTIOMETER END SLIP PLOTS

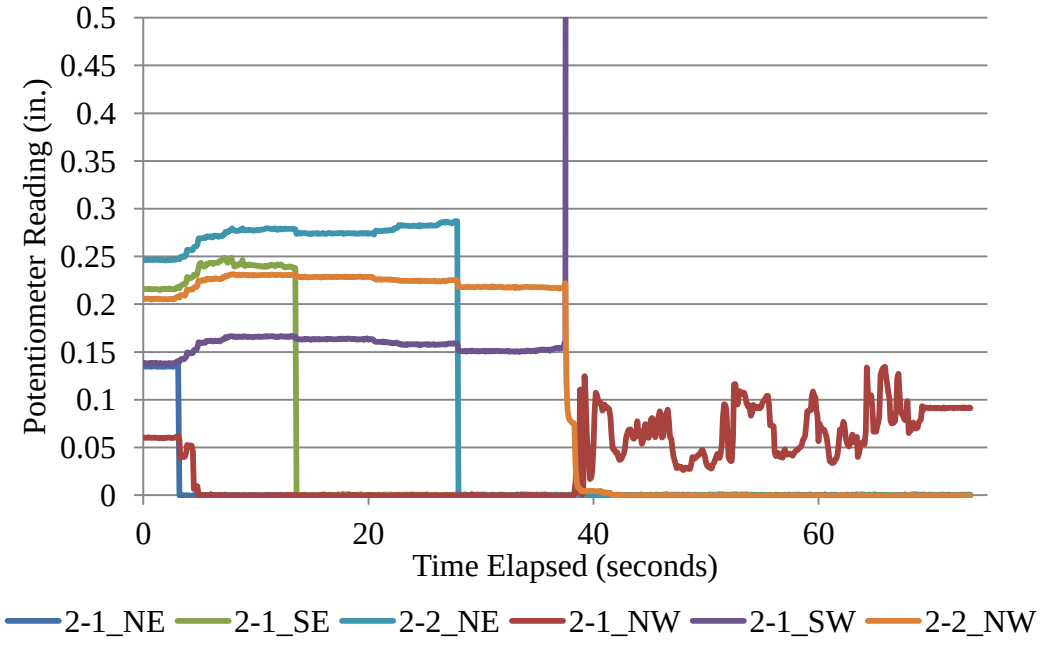

Conversion: 1 in. = 25.4 mm

Figure E.1 – C6-2-1 and C6-2-2 Strands

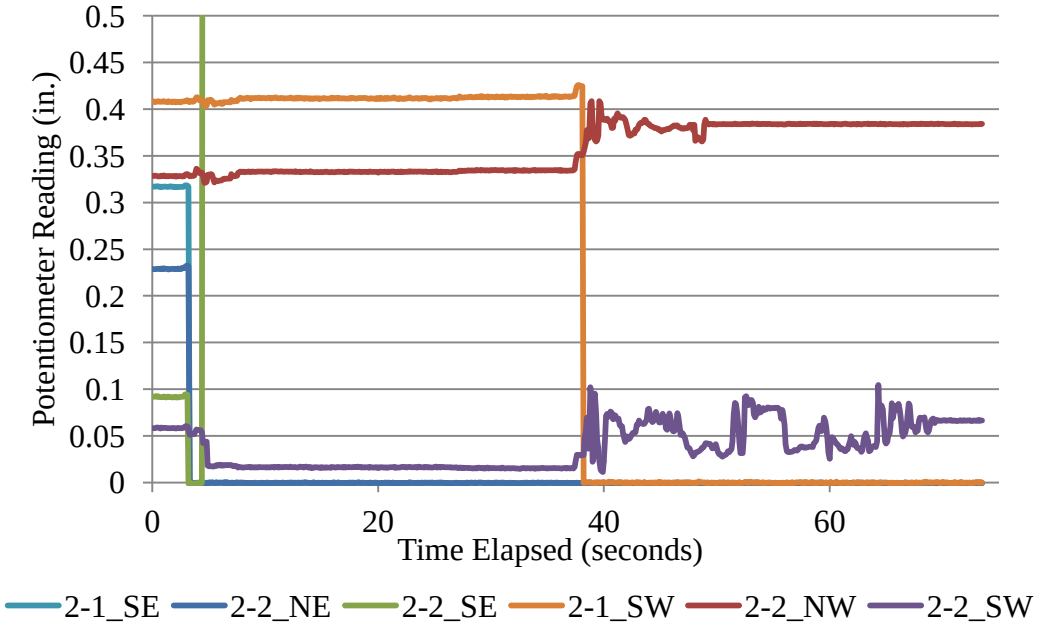

Conversion: 1 in. = 25.4 mm

Figure E.2 – S6-2-1 and S6-2-2 Strands

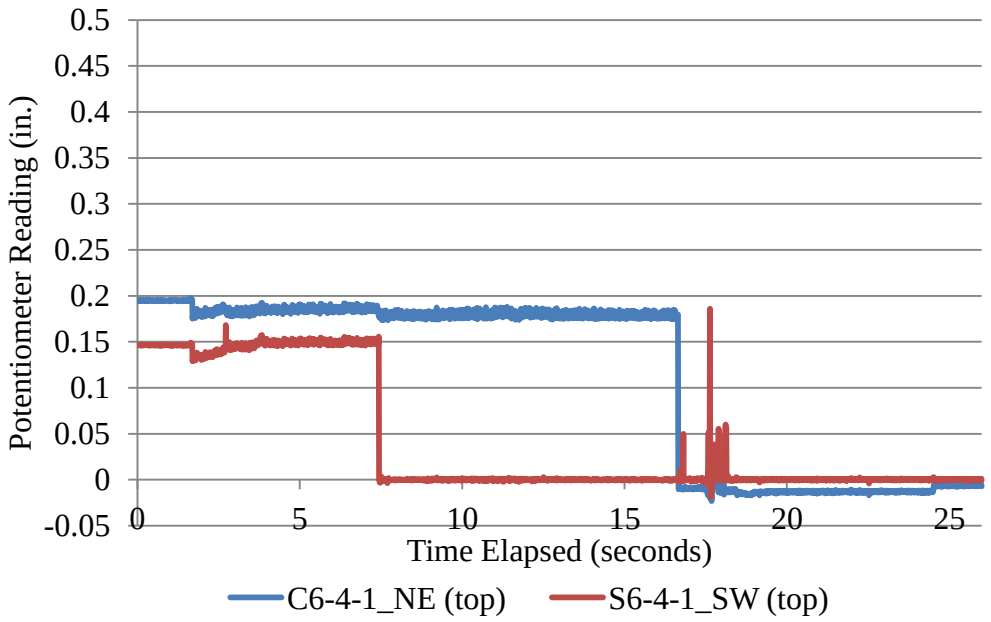

Conversion: 1 in. = 25.4 mm

Figure E.3 – C6-4-1 and S6-4-1 Top Strands

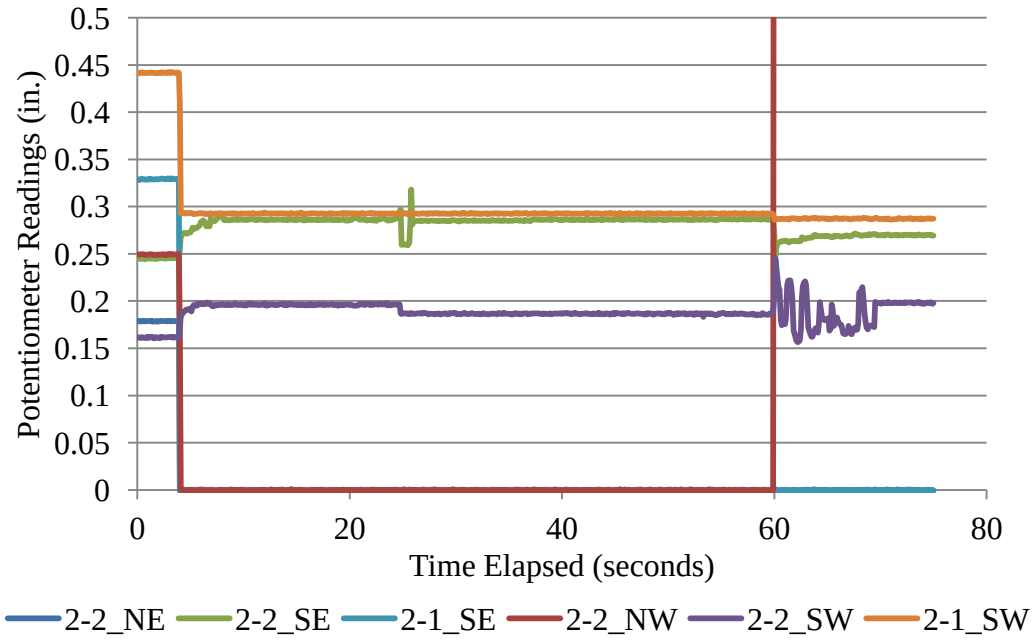

Conversion: 1 in. = 25.4 mm

Figure E.4 – C10-2-1 and C10-2-2 Strands

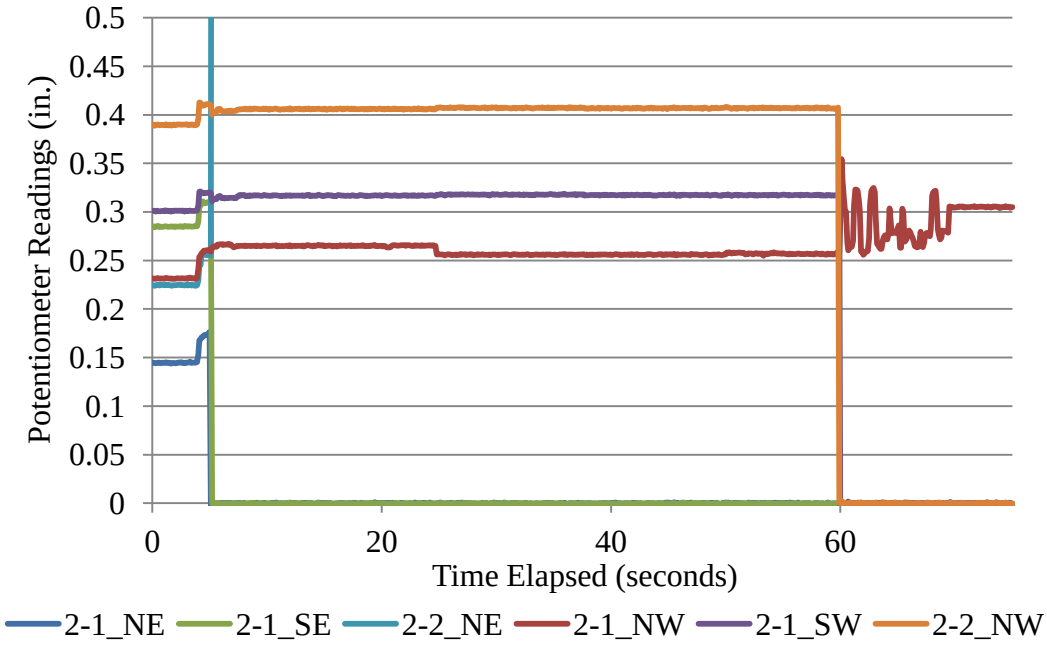

Conversion: 1 in. = 25.4 mm

Figure E.5 – S10-2-1 and S10-2-2 Strands

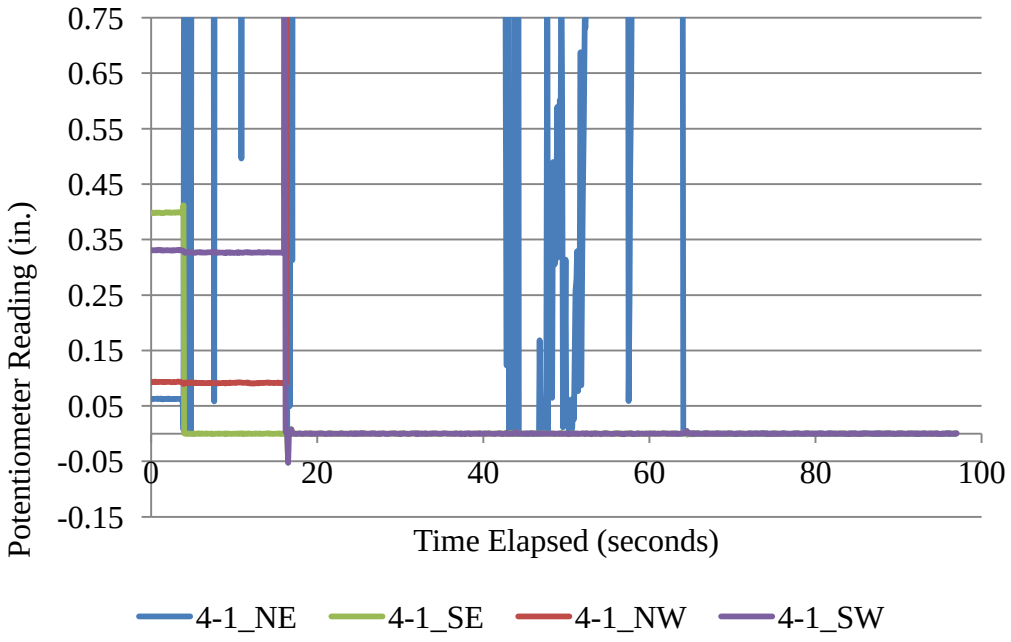

Conversion: 1 in. = 25.4 mm

Figure E.6 – C10-4-1 Top Strands

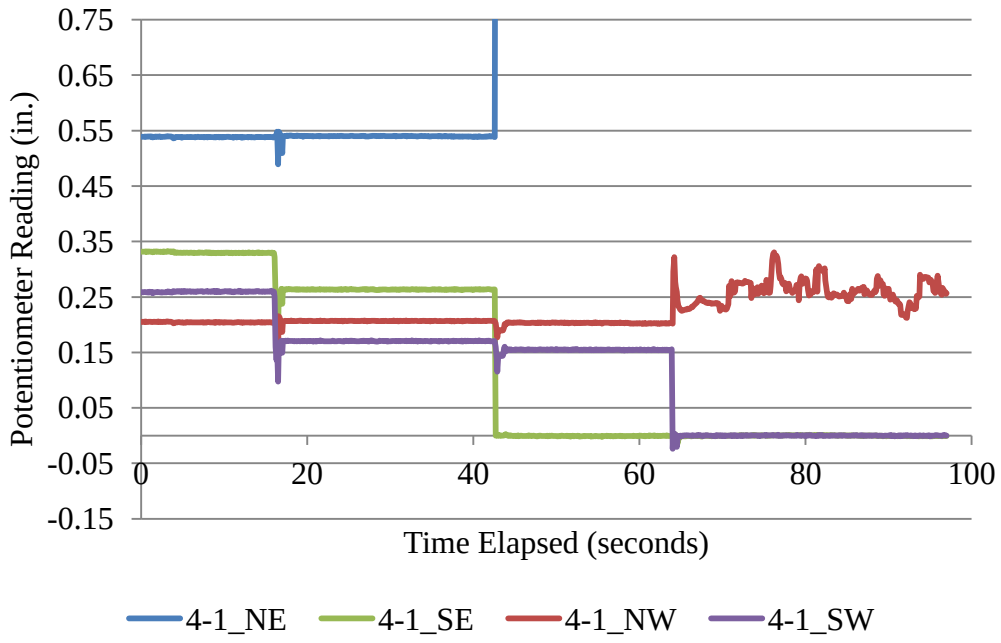

Conversion: 1 in. = 25.4 mm

Figure E.7 – C10-4-1 Bottom strands

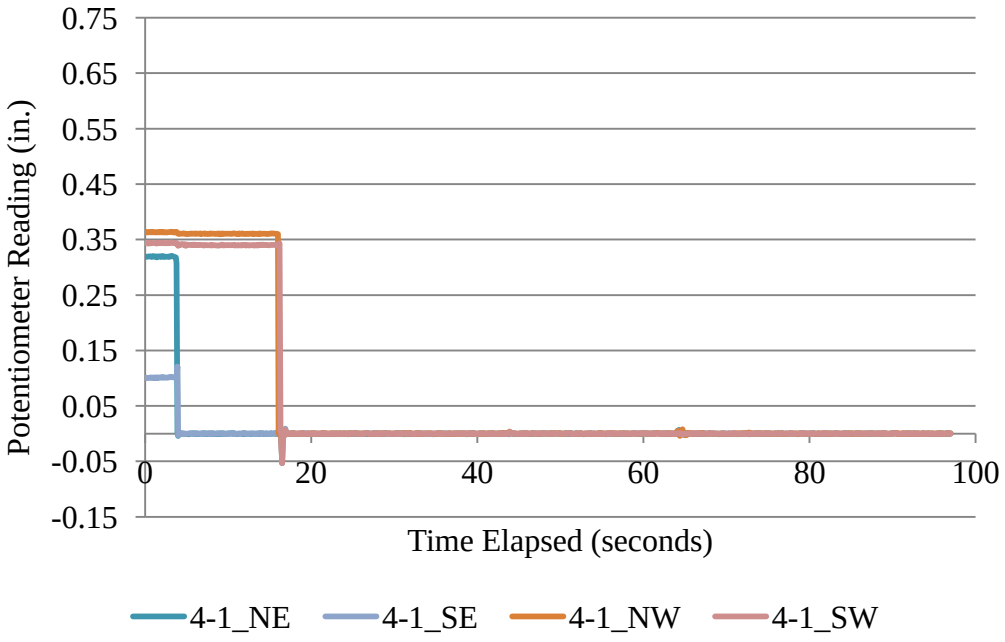

Conversion: 1 in. = 25.4 mm

Figure E.8 – S10-4-1 Top Strands

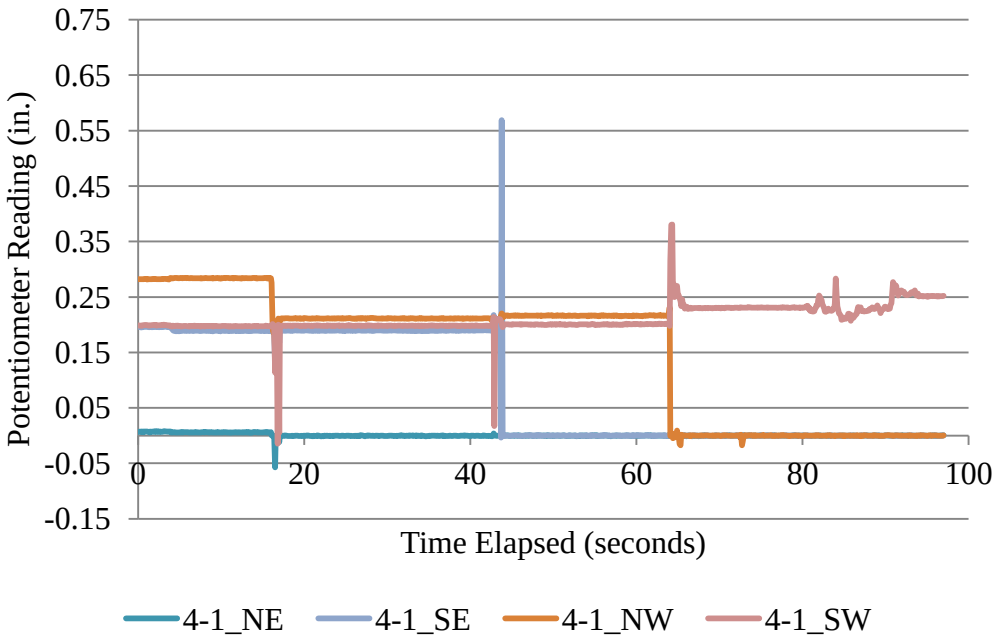

Conversion: 1 in. = 25.4 mm

Figure E.9 – S10-4-1 Bottom Strands

APPENDIX F

DEVELOPMENT LENGTH TEST SUMMARIES

BEAM ID: C6-2-1_58

DATE OF TESTING: 9/7/2011

DAYS AFTER CASTING: 48

Test Summary	
Embedment Length	58 in.
Failure Mode (Flexural or Bond)	Flexural
Beam End	SE/SW
Span Length	132 in.
Deflection at Failure	1.2 in.
Concrete Compressive Strength	5730 psi
Maximum Moment Capacity	
Expected	742.7 k-in.
Actual	811.8 k-in.
Average Transfer Length	
At Release	17.2 in.
At Time of Testing	24.2 in.
Average 0.1 in. NASP Load for Strand 101	
Standard NASP(Mix B)	18200 lb
NASP in Concrete (1 Day)	21100 lb

The test was set up as deflection-controlled, and the beam was initially deflected in increments of 0.02 in. (0.508 mm). Once deflection reached 1.00 in. (2.54 mm), the increments were increased to 0.05 in. (1.27 mm) until failure because at this point, the beam was taking on increasingly less load per deflection increment. At each deflection increment, the load was noted and then the beam was checked for cracks, which were marked with permanent marker.

The first flexural crack was observed directly under the right support at a deflection of 0.30 in. (7.62 mm) and load of about 15.1 kips (67.2 kN). Subsequent flexural cracks in the middle and under the left support appeared at a deflection of 0.32 in. (8.13 mm) and load of 15.9 kips (70.7 kN). These cracks as well as subsequent cracks propagated vertically and then began angling towards the supports. The beam failed due to concrete crushing within the compression zone at a load of 27.8 kips (124 kN) and reached a deflection of 1.2 in. (30.5 mm) at failure. Negligible end slip was observed on both the SE and SW strands.

Figure F.1 – C6-2-1_58 at Failure with Detail of Concrete Crushing

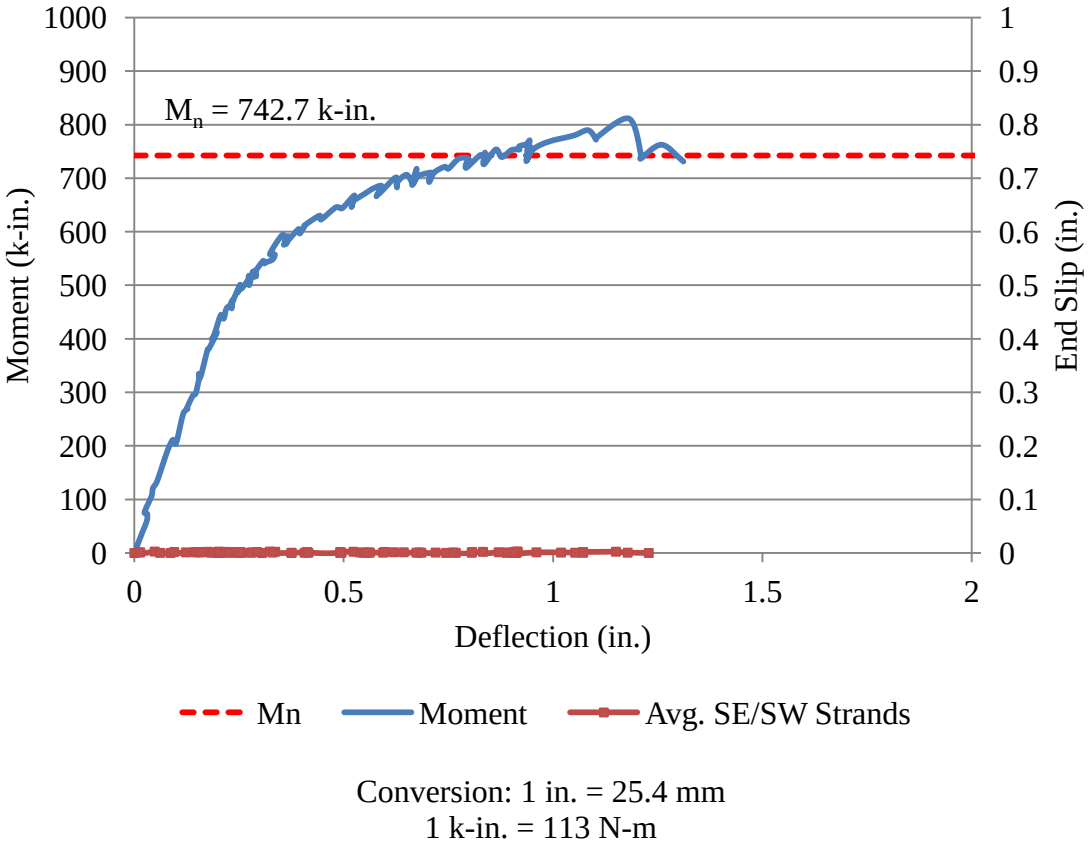

Conversion: 1 in. = 25.4 mm
1 k-in. = 113 N-m

Figure F.2 – C6-2-1_58 Moment vs. Deflection and Strand End Slip vs. Deflection

BEAM ID: C6-2-1_73

DATE OF TESTING: 9/7/2011

DAYS AFTER CASTING: 48

Test Summary	
Embedment Length	73 in.
Failure Mode (Flexural or Bond)	Flexural
Beam End	NE/NW
Span Length	162 in.
Deflection at Failure	1.9 in.
Concrete Compressive Strength	5730 psi
Maximum Moment Capacity	
Expected	742.7 k-in.
Actual	834.8 k-in.
Average Transfer Length (DEMEC)	
At Release	17.2 in.
At Time of Testing	24.2 in.
Average 0.1 in. NASP Load for Strand 101	
Standard NASP (Mix B)	18200 lb
NASP in Concrete (1 Day)	21100 lb

Conversion: 1 in. = 25.4 mm
1 lb = 4.45 N
1 psi = 6.89 kPa

The test was set up as deflection-controlled, and the beam was initially deflected in increments of 0.02 in. (0.508 mm). Once deflection reached 1.00 in. (25.4 mm), the increments were increased to 0.05 in. (1.27 mm) until failure because at this point, the beam was taking on increasingly less load per deflection increment. At each deflection increment, the load was noted and then the beam was checked for cracks, which were marked with permanent marker.

The first flexural cracks were observed under the right support and middle at a deflection of 0.48 in. (12.2 mm) and load of about 12.8 kips (56.9 kN). Subsequent cracks propagated vertically inside and outside the maximum moment zone and then began angling towards the supports. The beam failed due to concrete crushing within the compression zone at a load of 21.6 kips (96.1 kN) and reached a deflection of 1.9 in. (48.3 mm) at failure. Negligible end slip was observed on both the NE and NW strands.

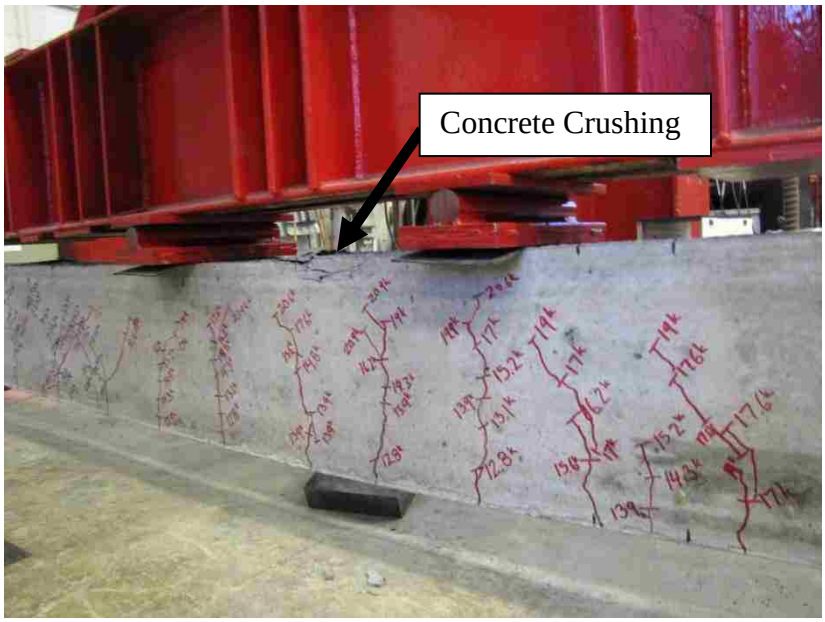

Figure F.3 – C6-2-1_73 at Failure

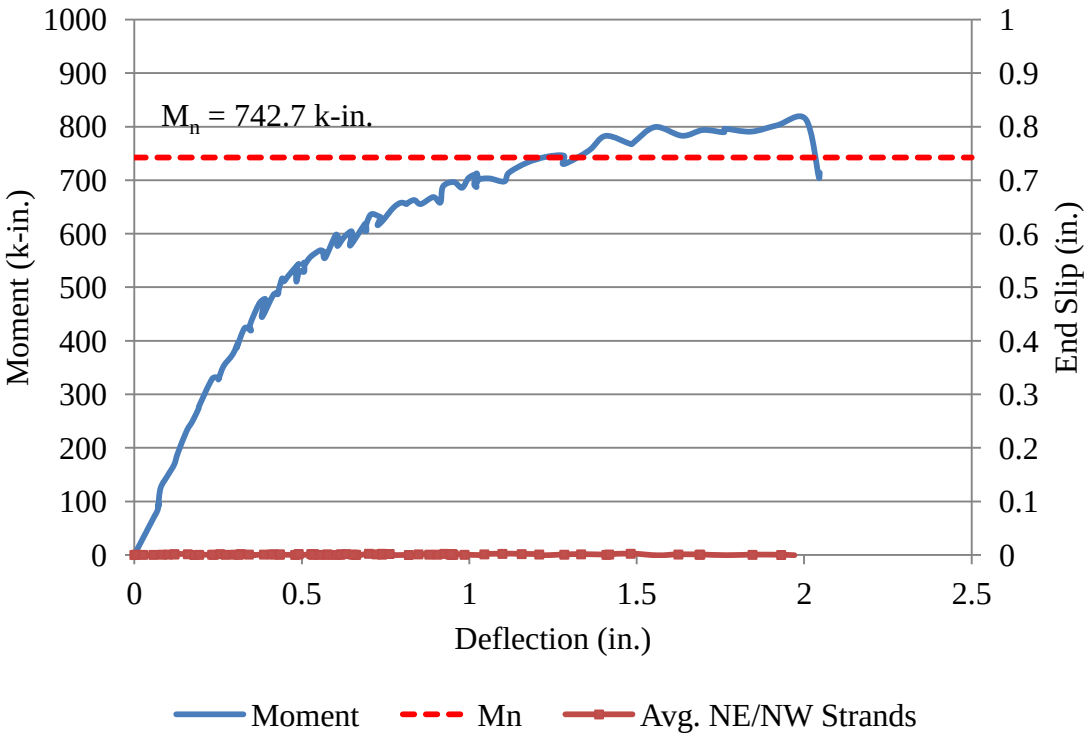

Conversion: 1 in. = 23.4 mm
1 k-in. = 113 N-m

Figure F.4 – C6-2-1_73 Moment vs. Deflection and Strand End Slip vs. Deflection

BEAM ID: C6-2-2_58

DATE OF TESTING: 9/12/2011

DAYS AFTER CASTING: 53

Test Summary	
Embedment Length	58 in.
Failure Mode (Flexural or Bond)	Flexural
Beam End	SE/SW
Span Length	132 in.
Deflection at Failure	1.2 in.
Concrete Compressive Strength	5730 psi
Maximum Moment Capacity	
Expected	742.7 k-in.
Actual	836.6 k-in.
Average Transfer Length	
At Release	17.2 in.
At Time of Testing	24.2 in.
Average 0.1 in. NASP Load for Strand 101	
Standard NASP (Mix B)	18200 lb
NASP in Concrete (1 Day)	21100 lb

Conversion: 1 in. = 25.4 mm
1 lb = 4.45 N
1 psi = 6.89 kPa

The test was set up as deflection-controlled, and the beam was deflected in increments of 0.05 in. (1.27 mm) until failure. The deflection increment was increased to 0.05 in. (1.27 mm) from 0.02 in. (0.508 mm) because it was deemed that 0.02 in (0.508 mm). increments was too slow. At each deflection increment, the load was noted and then the beam was checked for cracks, which were marked with permanent marker.

The first flexural cracks were observed under the supports and middle at a deflection of 0.25 in. (6.35 mm) and load of about 15.6 kips (69.4 kN). Subsequent cracks propagated vertically inside and outside the maximum moment zone and then began angling towards the supports. The beam failed due to concrete crushing within the compression zone at a load of 28.7 kips (128 kN) and reached a deflection of 1.21 in. (30.7 mm) at failure. Negligible end slip was observed on both the SE and SW strands.

Figure F.5 – C6-2-2_58 at Failure

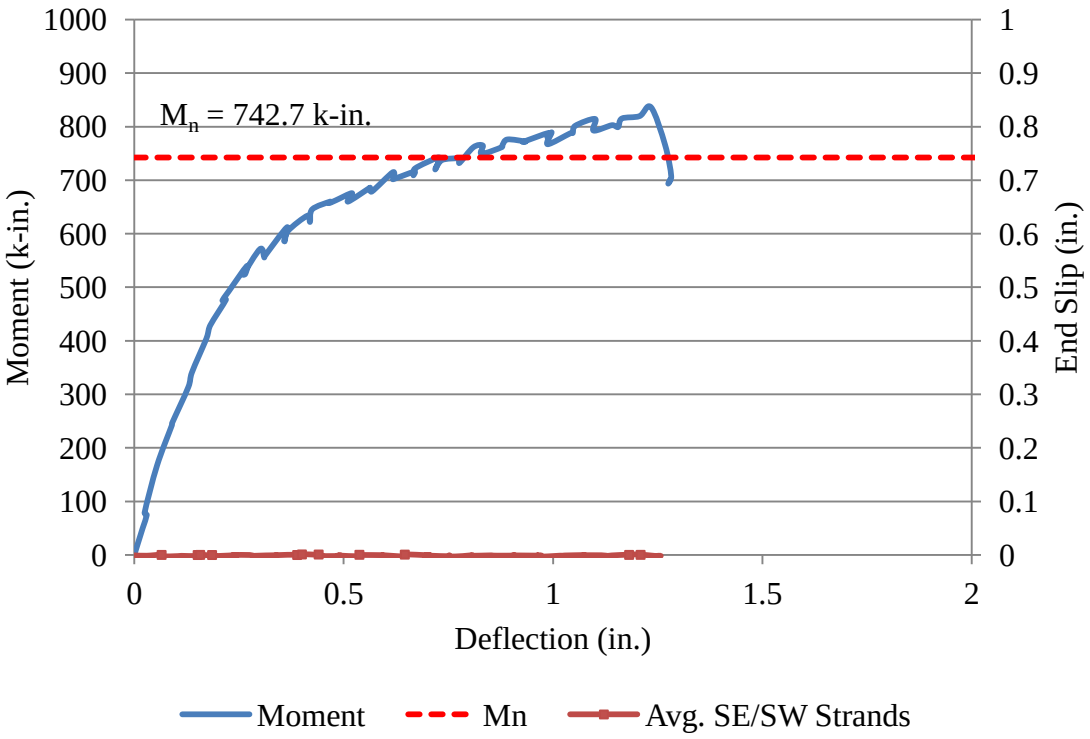

Conversion: 1 in. = 25.4 mm
1 k-in. = 113 N-m

Figure F.6 – C6-2-2_58 Moment vs. Deflection and Strand End Slip vs. Deflection

BEAM ID: C6-2-2_73

DATE OF TESTING: 9/13/2011

DAYS AFTER CASTING: 54

Test Summary	
Embedment Length	73 in.
Failure Mode (Flexural or Bond)	Flexural
Beam End	NE/NW
Span Length	162 in.
Deflection at Failure	1.7 in.
Concrete Compressive Strength	5730 psi
Maximum Moment Capacity	
Expected	742.7 k-in.
Actual	837.6 k-in.
Average Transfer Length	
At Release	17.2 in.
At Time of Testing	24.2 in.
Average 0.1 in. NASP Load for Strand 101	
Standard NASP (Mix B)	18200 lb
NASP in Concrete (1 Day)	21100 lb

Conversion: 1 in. = 25.4 mm
1 lb = 4.45 N
1 psi = 6.89 kPa

The test was set up as deflection-controlled, and the beam was deflected in increments of 0.05 in. (1.27 mm) until failure. The deflection increment was increased to 0.05 in. (1.27 mm) from 0.02 in. (0.508 mm) because it was deemed that 0.02 in. (0.508 mm) increments were too slow. At each deflection increment, the load was noted and then the beam was checked for cracks, which were marked with permanent marker.

The first flexural crack was observed under the right support at a deflection of 0.40 in. (10.2 mm) and load of about 11.9 kips (52.9 kN). Subsequent cracks propagated vertically inside and outside the maximum moment zone and then began angling towards the supports. The beam failed due to concrete crushing within the compression zone at a load of 21.7 kips (96.5 kN) and reached a deflection of 1.73 in. (43.9 mm) at failure. Negligible end slip was observed on both the NE and NW strands.

Figure F.7 – C6-2-2_73 at Failure

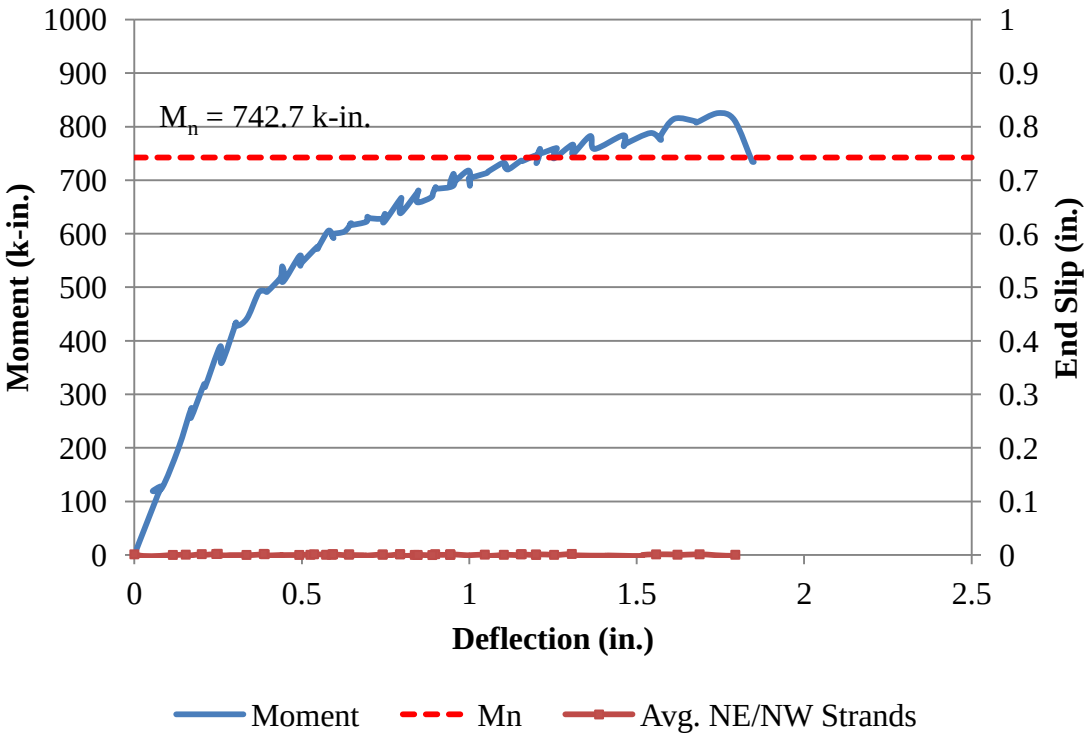

Conversion: 1 in. = 25.4 mm
1 k-in. = 113 N-m

Figure F.8 – C6-2-2_73 Moment vs. Deflection and Strand End Slip vs. Deflection

BEAM ID: S6-2-1_58

DATE OF TESTING: 9/14/2011

DAYS AFTER CASTING: 55

Test Summary	
Embedment Length	58 in.
Failure Mode (Flexural or Bond)	Flexural
Beam End	SE/SW
Span Length	132 in.
Deflection at Failure	1.5 in.
Concrete Compressive Strength	6950 psi
Maximum Moment Capacity	
Expected	757.9 k-in.
Actual	867.7 k-in.
Average Transfer Length	
At Release	14.4 in.
At Time of Testing	19.2 in.
Average 0.1 in. NASP Load for Strand 101	
Standard NASP (Mix B)	18200 lb
NASP in Concrete (1 Day)	23700 lb

Conversion: 1 in. = 25.4 mm
1 lb = 4.45 N
1 psi = 6.89 kPa

The test was set up as deflection-controlled, and the beam was deflected in increments of 0.05 in. (1.27 mm) until failure. The deflection increment was increased to 0.05 in. (1.27 mm) from 0.02 in. (0.508 mm) because it was deemed that 0.02 in. (0.508 mm) increments were too slow. At each deflection increment, the load was noted and then the beam was checked for cracks, which were marked with permanent marker.

The first flexural crack was observed under the right support at a deflection of 0.25 in. (6.35 mm) and load of about 17.1 kips (76.1 kN). Subsequent cracks propagated vertically inside and outside the maximum moment zone and then began angling towards the supports. The beam failed due to concrete crushing within the compression zone at a load of 29.9 kips (133 kN) and reached a deflection of 1.49 in. (37.8 mm) at failure. Negligible end slip was observed on both the SE and SW strands.

Figure F.9 – S6-2-1_58 at Failure

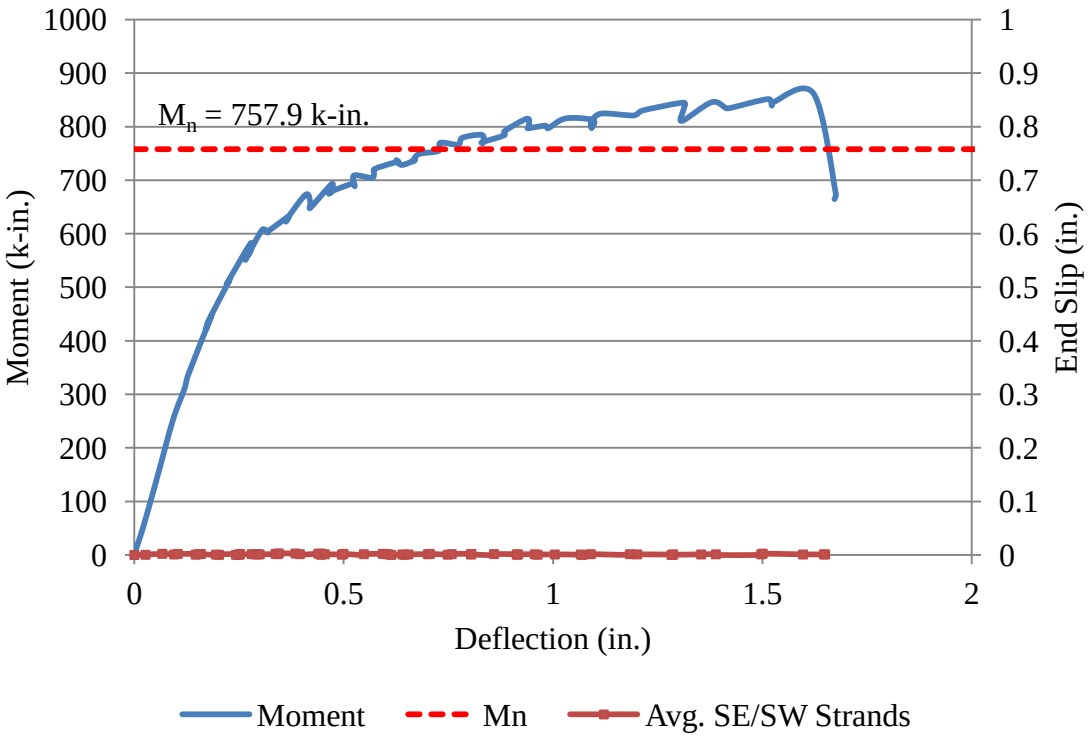

Conversion: 1 in. = 25.4 mm
1 k-in. = 113 N-m

Figure F.10 – S6-2-1_58 Moment vs. Deflection and Strand End Slip vs. Deflection

BEAM ID: S6-2-1_73

DATE OF TESTING: 9/14/2011

DAYS AFTER CASTING: 55

Test Summary	
Embedment Length	73 in.
Failure Mode (Flexural or Bond)	Flexural
Beam End	NE/NW
Span Length	162 in.
Deflection at Failure	2.2 in.
Concrete Compressive Strength	6950 psi
Maximum Moment Capacity	
Expected	757.9 k-in.
Actual	878.4 k-in.
Average Transfer Length	
At Release	14.4 in.
At Time of Testing	19.2 in.
Average 0.1 in. NASP Load for Strand 101	
Standard NASP (Mix B)	18200 lb
NASP in Concrete (1 Day)	23700 lb

Conversion: 1 in. = 25.4 mm
1 lb = 4.45 N
1 psi = 6.89 kPa

The test was set up as deflection-controlled, and the beam was deflected in increments of 0.05 in. (1.27 mm) until failure. The deflection increment was increased to 0.05 in. (1.27 mm) from 0.02 in. (0.508 mm) because it was deemed that 0.02 in. (0.508 mm) increments were too slow. At each deflection increment, the load was noted and then the beam was checked for cracks, which were marked with permanent marker.

The first flexural crack was observed under the midspan and right support at a deflection of 0.45 in. (11.4 mm) and load of about 12.1 kips (53.8 kN). Subsequent cracks propagated vertically inside and outside the maximum moment zone and then began angling towards the supports. Horizontal cracks near midspan at the level of prestressing strand were noted at a deflection of 1.30 in. (33.0 mm) and a load of 19.8 kips (88.1 kN). The beam failed due to concrete crushing within the compression zone at a load of 22.9 kips (102 kN) and reached a deflection of 2.20 in. (55.9 mm) at failure. Negligible end slip was observed on both the NE and NW strands.

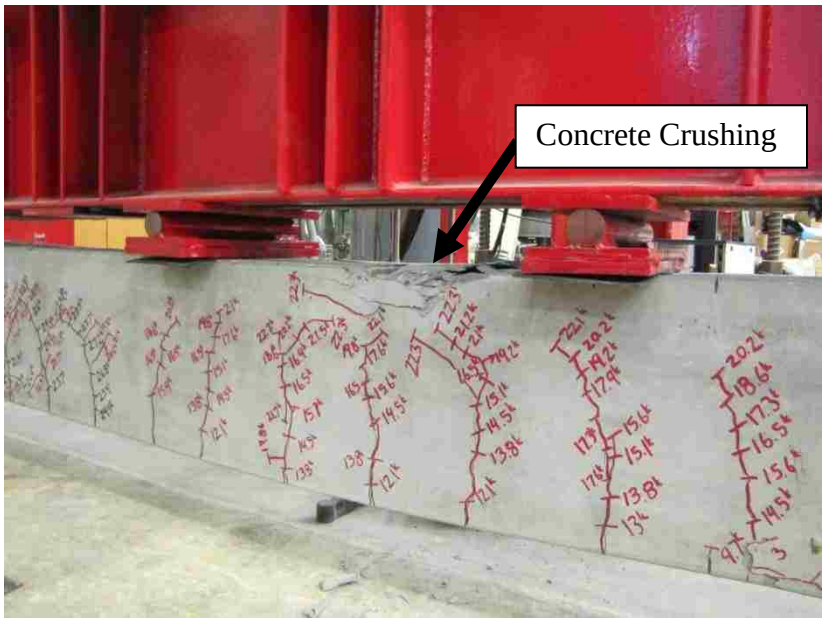

Figure F.11 – S6-2-1_73 at Failure

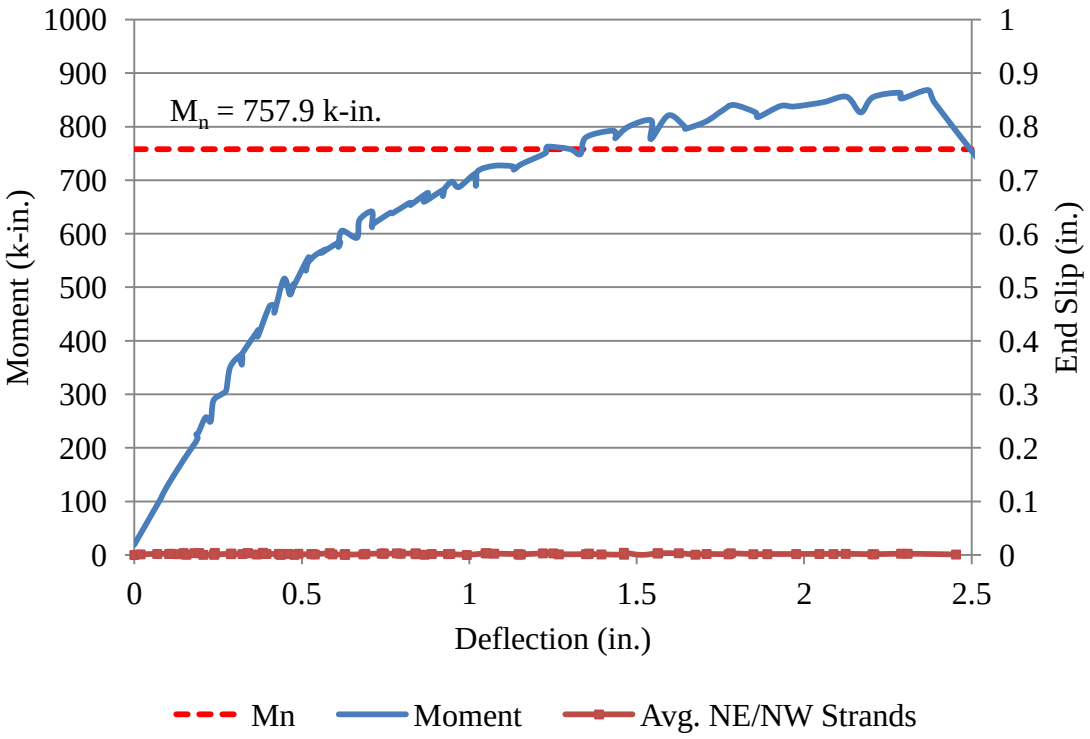

Conversion: 1 in. = 25.4 mm
1 k-in. = 113 N-m

Figure F.12 – S6-2-1_73 Moment vs. Deflection and Strand End Slip vs. Deflection

BEAM ID: S6-2-2_58

DATE OF TESTING: 9/9/2011

DAYS AFTER CASTING: 50

Test Summary	
Embedment Length	58 in.
Failure Mode (Flexural or Bond)	Flexural
Beam End	SE/SW
Span Length	132 in.
Deflection at Failure	1.5 in.
Concrete Compressive Strength	6950 psi
Maximum Moment Capacity	
Expected	757.9 k-in.
Actual	889.9 k-in.
Average Transfer Length	
At Release	14.4 in.
At Time of Testing	19.2 in.
Average 0.1 in. NASP Load for Strand 101	
Standard NASP (Mix B)	18200 lb
NASP in Concrete (1 Day)	23700 lb

Conversion: 1 in. = 25.4 mm
1 lb = 4.45 N
1 psi = 6.89 kPa

The test was set up as deflection-controlled, and the beam was deflected in increments of 0.05 in. (1.27 mm) until failure. The deflection increment was increased to 0.05 in. (1.27 mm) from 0.02 in. (0.508 mm) because it was deemed that 0.02 in. (0.508 mm) increments were too slow. At each deflection increment, the load was noted and then the beam was checked for cracks, which were marked with permanent marker.

The first flexural crack was observed under the right support at a deflection of 0.25 in. (6.35 mm) and load of about 16.3 kips (72.5 kN). Subsequent cracks propagated vertically inside and outside the maximum moment zone and then began angling towards the supports. Horizontal cracks near midspan at the level of prestressing strand were noted at a deflection of 0.75 in. (19.1 mm) and a load of 25.9 kips (115 kN). The beam failed due to concrete crushing within the compression zone at a load of 30.7 kips (137 kN) and reached a deflection of 1.52 in. (38.6 mm) at failure. Negligible end slip was observed on both the SE and SW strands.

Figure F.13 – S6-2-2_58 at Failure

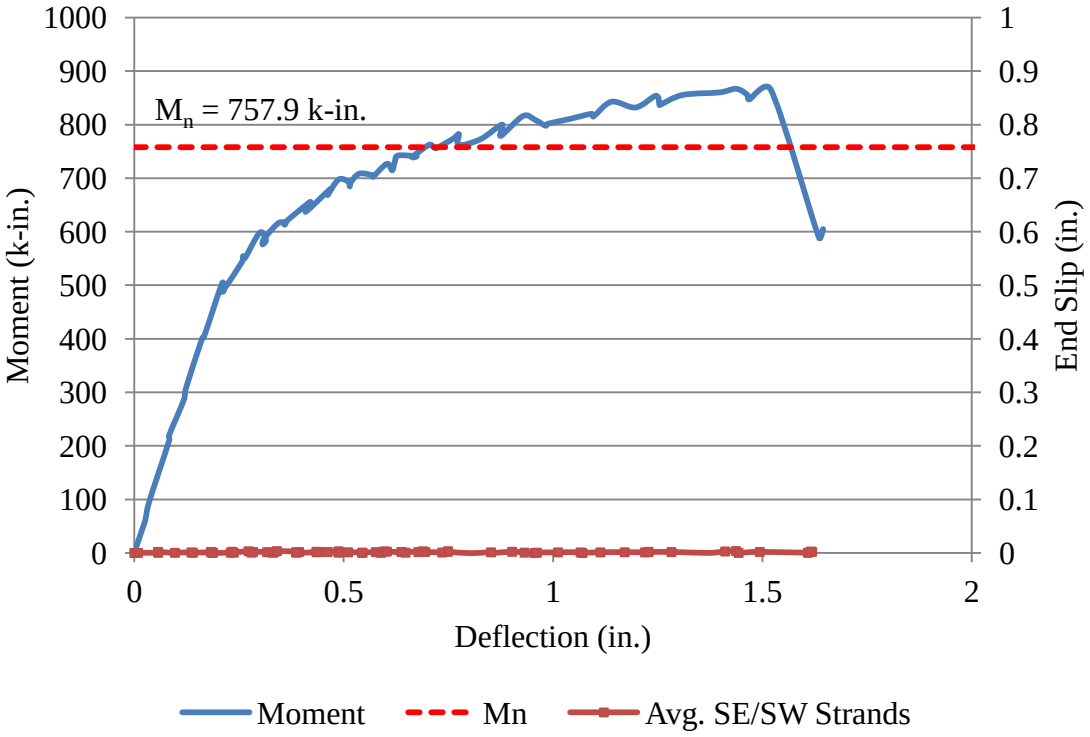

Conversion: 1 in. = 25.4 mm
1 k-in. = 113 N-m

Figure F.14 – S6-2-2_58 Moment vs. Deflection and Strand End Slip vs. Deflection

BEAM ID: S6-2-2_73

DATE OF TESTING: 9/9/2011

DAYS AFTER CASTING: 50

Test Summary	
Embedment Length	73 in.
Failure Mode (Flexural or Bond)	Flexural
Beam End	NE/NW
Span Length	162 in.
Deflection at Failure	1.8 in.
Concrete Compressive Strength	6950 psi
Maximum Moment Capacity	
Expected	757.9 k-in.
Actual	843.1 k-in.
Average Transfer Length	
At Release	14.4 in.
At Time of Testing	19.2 in.
Average 0.1 in. NASP Load for Strand 101	
Standard NASP (Mix B)	18200 lb
NASP in Concrete (1 Day)	23700 lb

Conversion: 1 in. = 25.4 mm
1 lb = 4.45 N
1 psi = 6.89 kPa

The test was set up as deflection-controlled, and the beam was deflected in increments of 0.05 in. (1.27 mm) until failure. The deflection increment was increased to 0.05 in. (1.27 mm) from 0.02 in. (0.508 mm) because it was deemed that 0.02 in. (0.508 mm) increments were too slow. At each deflection increment, the load was noted and then the beam was checked for cracks, which were marked with permanent marker.

The first flexural crack was observed under the left support at a deflection of 0.40 in. (10.2 mm) and load of about 10.8 kips (48.0 kN). Subsequent cracks propagated vertically inside and outside the maximum moment zone and then began angling towards the supports. The beam failed due to concrete crushing outside the compression zone at a load of 21.9 kips (97.4 kN) and reached a deflection of 1.78 in. (45.2 mm) at failure. The failure occurred in the area that had already failed during the 58 in. (1,473 mm) embedment length test, however, it was still deemed a flexural failure by concrete crushing. Negligible end slip was observed on both the NE and NW strands.

Figure F.15 – S6-2-2_73 at Failure

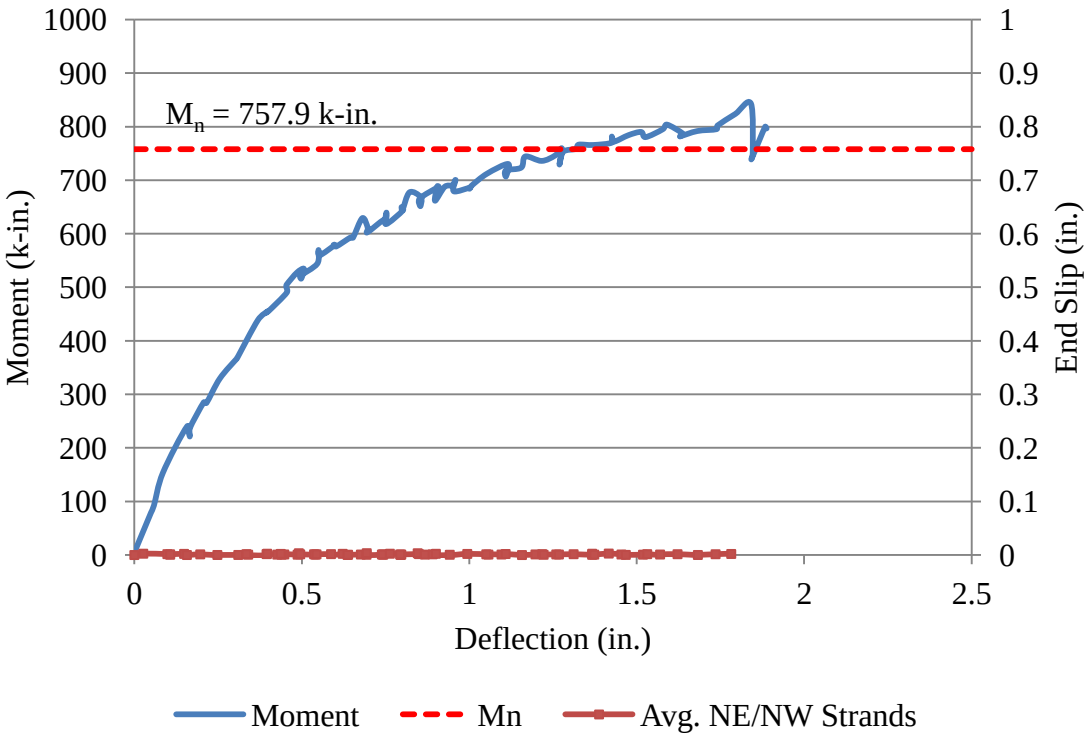

Conversion: 1 in. = 25.4 mm
1 k-in. = 113 N-m

Figure F.16 – S6-2-2_73 Moment vs. Deflection and Strand End Slip vs. Deflection

BEAM ID: C10-2-1_58

DATE OF TESTING: 9/15/2011

DAYS AFTER CASTING: 52

Test Summary	
Embedment Length	58 in.
Failure Mode (Flexural or Bond)	Flexural
Beam End	SE/SW
Span Length	132 in.
Deflection at Failure	1.5 in.
Concrete Compressive Strength	8480 psi
Maximum Moment Capacity	
Expected	773.6 k-in.
Actual	880.3 k-in.
Average Transfer Length	
At Release	20.1 in.
At Time of Testing	23.5 in.
Average 0.1 in. NASP Load for Strand 101	
Standard NASP (Mix B)	18200 lb
NASP in Concrete (1 Day)	26700 lb

Conversion: 1 in. = 25.4 mm
1 lb = 4.45 N
1 psi = 6.89 kPa

The test was set up as deflection-controlled, and the beam was deflected in increments of 0.05 in. (1.27 mm) until failure. The deflection increment was increased to 0.05 in. (1.27 mm) from 0.02 in. (0.508 mm) because it was deemed that 0.02 in. (0.508 mm) increments were too slow. At each deflection increment, the load was noted and then the beam was checked for cracks, which were marked with permanent marker.

The first flexural crack was observed under the midspan and right support at a deflection of 0.30 in. (7.62 mm) and load of about 17.5 kips (77.8 kN). Subsequent cracks propagated vertically inside and outside the maximum moment zone and then began angling towards the supports. Horizontal cracks near midspan at the level of prestressing strand were noted at a deflection of 0.65 in. (16.5 mm) and a load of 24.8 kips (110 kN). The beam failed due to concrete crushing within the compression zone at a load of 30.3 kips (135 kN) and reached a deflection of 1.48 in. (37.6 mm) at failure. Negligible end slip was observed on both the SE and SW strands.

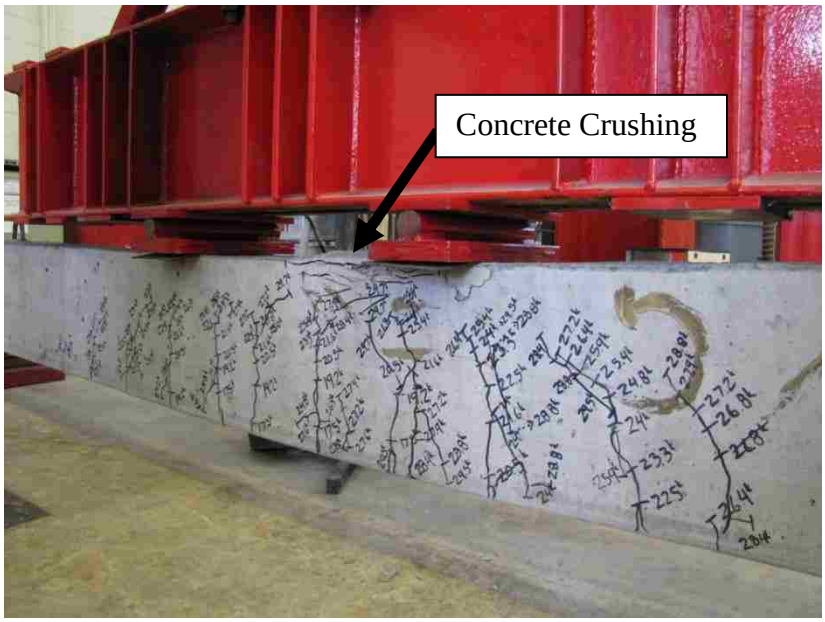

Figure F.17 – C10-2-1_58 at Failure

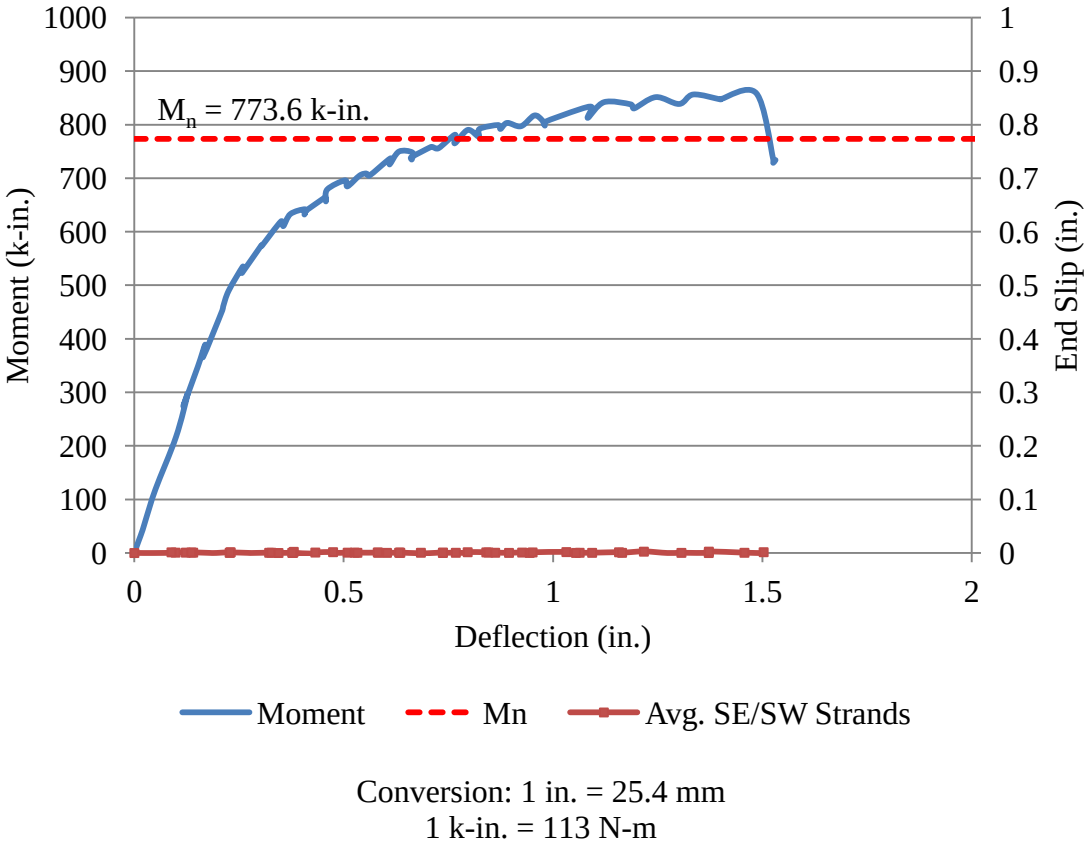

Conversion: 1 in. = 25.4 mm
1 k-in. = 113 N-m

Figure F.18 – C10-2-1_58 Moment vs. Deflection and Strand End Slip vs. Deflection

BEAM ID: C10-2-1_73

DATE OF TESTING: 9/16/2011

DAYS AFTER CASTING: 53

Test Summary	
Embedment Length	73 in.
Failure Mode (Flexural or Bond)	Flexural
Beam End	NE/NW
Span Length	162 in.
Deflection at Failure	2.0 in.
Concrete Compressive Strength	8480 psi
Maximum Moment Capacity	
Expected	773.6 k-in.
Actual	880.7 k-in.
Average Transfer Length	
At Release	20.1 in.
At Time of Testing	23.5 in.
Average 0.1 in. NASP Load for Strand 101	
Standard NASP (Mix B)	18200 lb
NASP in Concrete (1 Day)	26700 lb

Conversion: 1 in. = 25.4 mm
1 lb = 4.45 N
1 psi = 6.89 kPa

The test was set up as deflection-controlled, and the beam was deflected in increments of 0.05 in. (1.27 mm) until failure. The deflection increment was increased to 0.05 in. (1.27 mm) from 0.02 in. (0.508 mm) because it was deemed that 0.02 in. (0.508 mm) increments were too slow. At each deflection increment, the load was noted and then the beam was checked for cracks, which were marked with permanent marker.

The first flexural crack was observed under the midspan and right support at a deflection of 0.40 in. (10.2 mm) and load of about 11.8 kips (52.5 kN). Subsequent cracks propagated vertically inside and outside the maximum moment zone and then began angling towards the supports. Horizontal cracks near midspan at the level of prestressing strand were noted at a deflection of 1.20 in. (30.5 mm) and a load of 19.5 kips (86.7 kN). The beam failed due to concrete crushing within the compression zone at a load of 23.0 kips (102 kN) and reached a deflection of 1.97 in. (50.0 mm) at failure. Negligible end slip was observed on both the NE and NW strands.

Figure F.19 – C10-2-1_73 at Failure

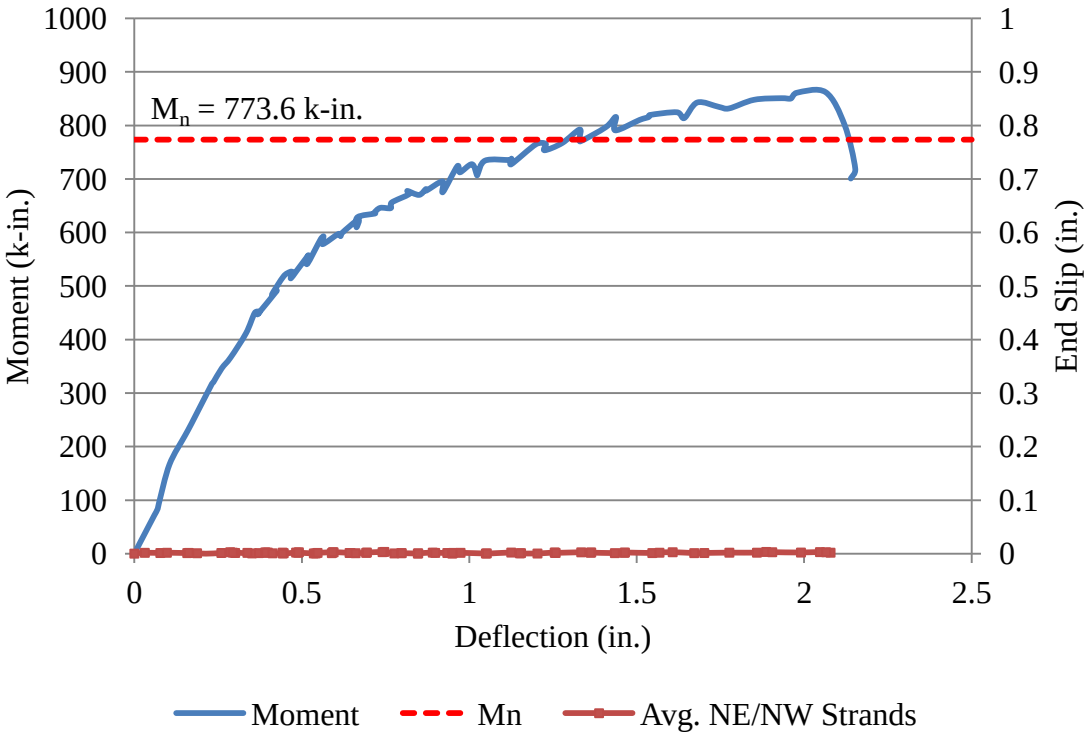

Conversion: 1 in. = 25.4 mm
1 k-in. = 113 N-m

Figure F.20 – C10-2-1_73 Moment vs. Deflection and Strand End Slip vs. Deflection

BEAM ID: C10-2-2_58

DATE OF TESTING: 9/16/2011

DAYS AFTER CASTING: 53

Test Summary	
Embedment Length	58 in.
Failure Mode (Flexural or Bond)	Flexural
Beam End	SE/SW
Span Length	132 in.
Deflection at Failure	1.5 in.
Concrete Compressive Strength	8480 psi
Maximum Moment Capacity	
Expected	875.3 k-in.
Actual	813.6 k-in.
Average Transfer Length	
At Release	20.1 in.
At Time of Testing	23.5 in.
Average 0.1 in. NASP Load for Strand 101	
Standard NASP (Mix B)	18200 lb
NASP in Concrete (1 Day)	26700 lb

Conversion: 1 in. = 25.4 mm
1 lb = 4.45 N
1 psi = 6.89 kPa

The test was set up as deflection-controlled, and the beam was deflected in increments of 0.05 in. (1.27 mm) until failure. The deflection increment was increased to 0.05 in. (1.27 mm) from 0.02 in. (0.508 mm) because it was deemed that 0.02 in. (0.508 mm) increments were too slow. At each deflection increment, the load was noted and then the beam was checked for cracks, which were marked with permanent marker.

The first flexural crack was observed under midspan at a deflection of 0.25 in. (6.35 mm) and load of about 15.0 kips (66.7 kN). Subsequent cracks propagated vertically inside and outside the maximum moment zone and then began angling towards the supports. Horizontal cracks near midspan at the level of prestressing strand were noted at a deflection of 0.85 in. (21.6 mm) and a load of 26.5 kips (118 kN). The beam failed due to concrete crushing within the compression zone at a load of 30.1 kips (134 kN) and reached a deflection of 1.51 in. (38.4 mm) at failure. Negligible end slip was observed on both the SE and SW strands.

Figure F.21 – C10-2-2_58 at Failure

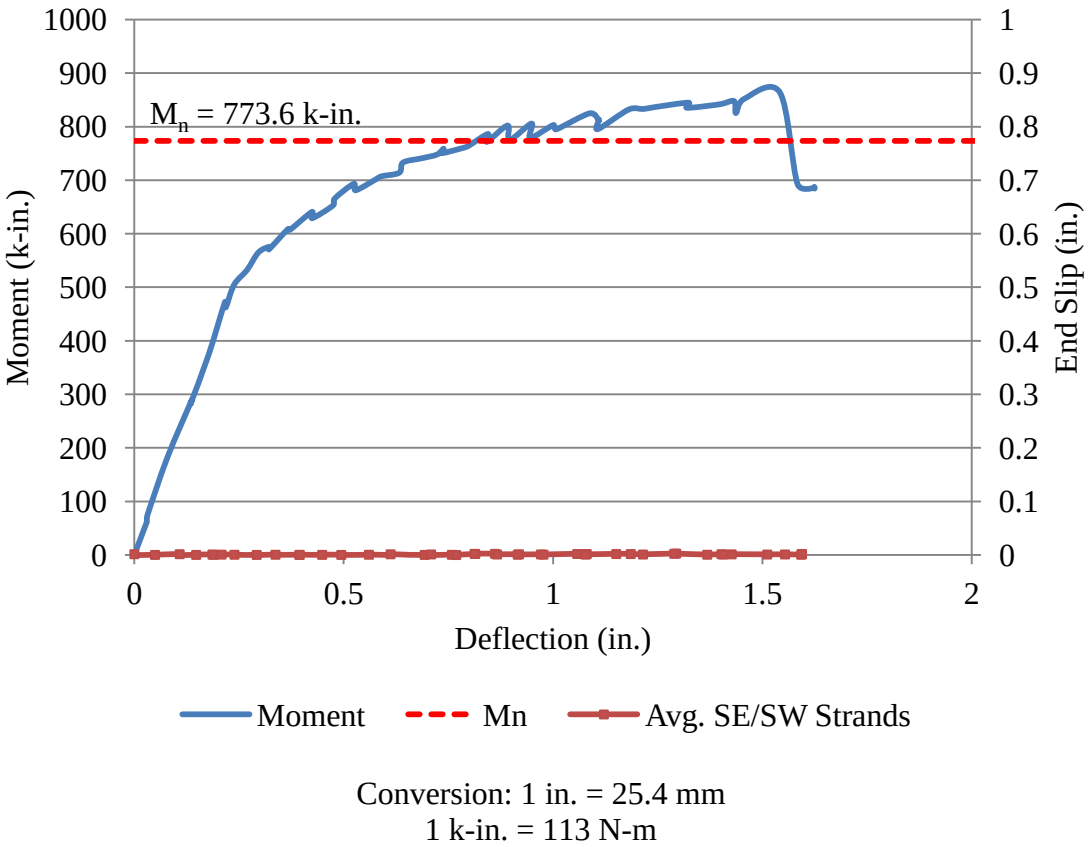

Conversion: 1 in. = 25.4 mm
1 k-in. = 113 N-m

Figure F.22 – C10-2-2_58 Moment vs. Deflection and Strand End Slip vs. Deflection

BEAM ID: C10-2-2_73

DATE OF TESTING: 9/16/2011

DAYS AFTER CASTING: 53

Test Summary	
Embedment Length	73 in.
Failure Mode (Flexural or Bond)	Flexural
Beam End	NE/NW
Span Length	162 in.
Deflection at Failure	2.0 in.
Concrete Compressive Strength	8480 psi
Maximum Moment Capacity	
Expected	773.6 k-in.
Actual	885.8 k-in.
Average Transfer Length	
At Release	20.1 in.
At Time of Testing	23.5 in.
Average 0.1 in. NASP Load for Strand 101	
Standard NASP(Mix B)	18200 lb
NASP in Concrete (1 Day)	26700 lb

Conversion: 1 in. = 25.4 mm
1 lb = 4.45 N
1 psi = 6.89 kPa

The test was set up as deflection-controlled, and the beam was deflected in increments of 0.05 in. (1.27 mm) until failure. The deflection increment was increased to 0.05 in. (1.27 mm) from 0.02 in. (0.508 mm) because it was deemed that 0.02 in. (0.508 mm) increments were too slow. At each deflection increment, the load was noted and then the beam was checked for cracks, which were marked with permanent marker.

The first flexural crack was observed under the midspan at a deflection of 0.45 in. (11.4 mm) and load of about 11.7 kips (52.0 kN). Subsequent cracks propagated vertically inside and outside the maximum moment zone and then began angling towards the supports. Horizontal cracks near midspan at the level of prestressing strand were noted at a deflection of 1.20 in. (30.5 mm) and a load of 18.8 kips (83.6 kN). The beam failed due to concrete crushing within the compression zone at a load of 23.1 kips (103 kN) and reached a deflection of 1.97 in. (50.0 mm) at failure. Negligible end slip was observed on both the NE and NW strands.

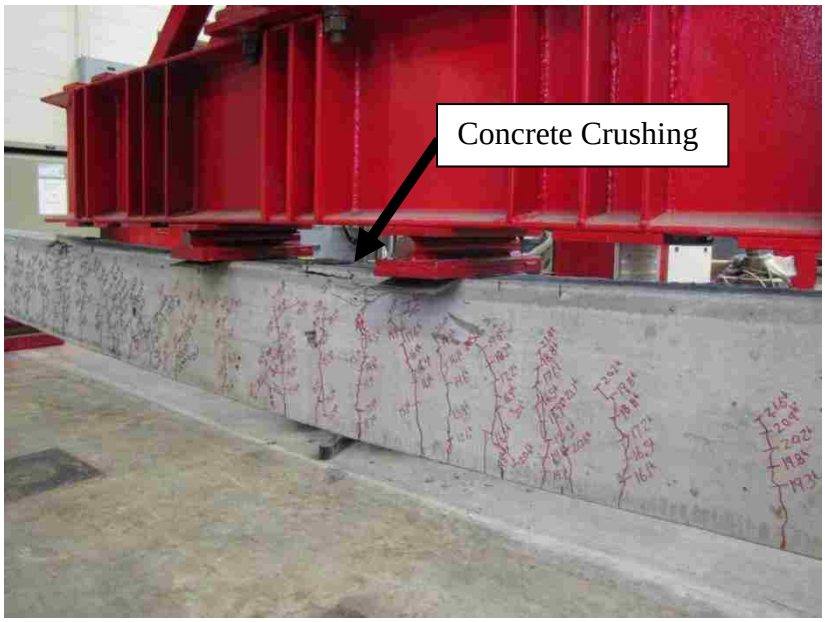

Figure F.23 – C10-2-2_73 at Failure

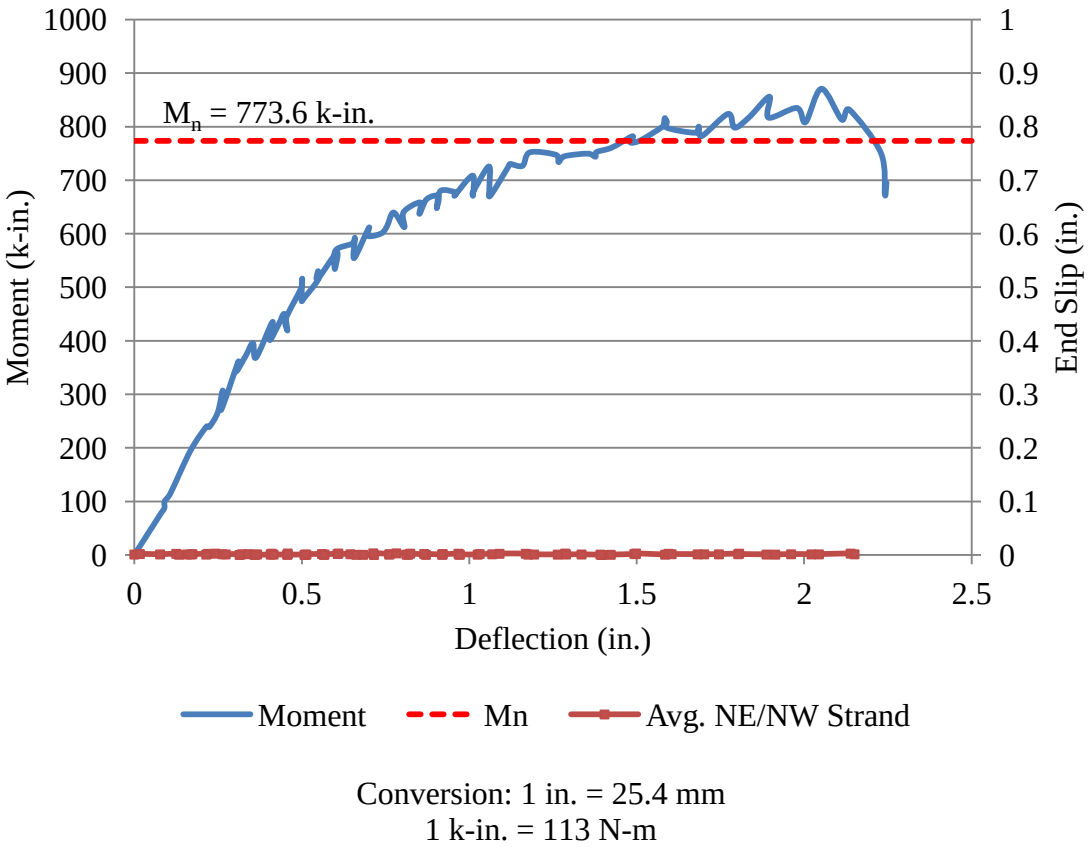

Conversion: 1 in. = 25.4 mm
1 k-in. = 113 N-m

Figure F.24 – C10-2-2_73 Moment vs. Deflection and Strand End Slip vs. Deflection

BEAM ID: S10-2-1_58

DATE OF TESTING: 9/20/2011

DAYS AFTER CASTING: 57

Test Summary	
Embedment Length	58 in.
Failure Mode (Flexural or Bond)	Flexural
Beam End	SE/SW
Span Length	132 in.
Deflection at Failure	1.5 in.
Concrete Compressive Strength	9250 psi
Maximum Moment Capacity	
Expected	790.7 k-in.
Actual	883.3 k-in.
Average Transfer Length	
At Release	13.8 in.
At Time of Testing	15.9 in.
Average 0.1 in. NASP Load for Strand 101	
Standard NASP (Mix B)	18200 lb
NASP in Concrete (1 Day)	27300 lb

Conversion: 1 in. = 25.4 mm
1 lb = 4.45 N
1 psi = 6.89 kPa

The test was set up as deflection-controlled, and the beam was deflected in increments of 0.05 in. (1.27 mm) until failure. The deflection increment was increased to 0.05 in. (1.27 mm) from 0.02 in. (0.508mm) because it was deemed that 0.02 in. (0.508 mm) increments were too slow. At each deflection increment, the load was noted and then the beam was checked for cracks, which were marked with permanent marker.

The first flexural cracks were observed under the midspan and right support at a deflection of 0.25 in. (6.35 mm) and load of about 16.2 kips (72.1 kN). Subsequent cracks propagated vertically inside and outside the maximum moment zone and then began angling towards the supports. Horizontal cracks near midspan at the level of prestressing strand were noted at a deflection of 0.75 in. (19.0 mm) and a load of 25.9 kips (115 kN). The beam failed due to concrete crushing within the compression zone at a load of 30.4 kips (135 kN) and reached a deflection of 1.47 in. (37.3 mm) at failure. Negligible end slip was observed on both the SE and SW strands.

Figure F.25 – S10-2-1_58 at Failure

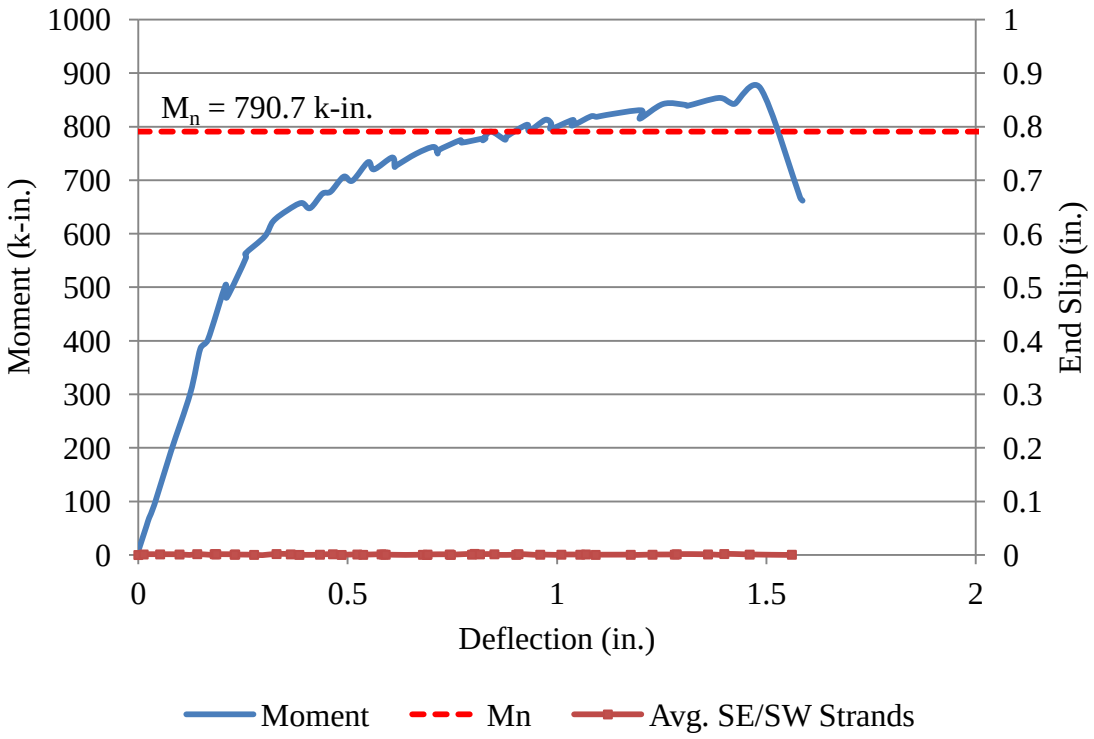

Conversion: 1 in. = 25.4 mm
1 k-in. = 113 N-m

Figure F.26 – S10-2-1_58 Moment vs. Deflection and Strand End Slip vs. Deflection

BEAM ID: S10-2-1_73

DATE OF TESTING: 9/21/2011

DAYS AFTER CASTING: 58

Test Summary	
Embedment Length	73 in.
Failure Mode (Flexural or Bond)	Flexural
Beam End	NE/NW
Span Length	162 in.
Deflection at Failure	2.3 in.
Concrete Compressive Strength	9250 psi
Maximum Moment Capacity	
Expected	790.7 k-in.
Actual	904.2 k-in.
Average Transfer Length	
At Release	13.8 in.
At Time of Testing	15.9 in.
Average 0.1 in. NASP Load for Strand 101	
Standard NASP (Mix B)	18200 lb
NASP in Concrete (1 Day)	27300 lb

Conversion: 1 in. = 25.4 mm
1 lb = 4.45 N
1 psi = 6.89 kPa

The test was set up as deflection-controlled, and the beam was deflected in increments of 0.05 in. (1.27 mm) until failure. The deflection increment was increased to 0.05 in. (1.27 mm) from 0.02 in. (0.508 mm) because it was deemed that 0.02 in. (0.508 mm) increments were too slow. At each deflection increment, the load was noted and then the beam was checked for cracks, which were marked with permanent marker.

The first flexural crack was observed under the midspan at a deflection of 0.40 in. (10.2 mm) and load of about 12.5 kips (55.6 kN). Subsequent cracks propagated vertically inside and outside the maximum moment zone and then began angling towards the supports. Horizontal cracks near midspan at the level of prestressing strand were noted at a deflection of 1.00 in. (25.4 mm) and a load of 18.7 kips (83.2 kN). The beam failed due to concrete crushing within the compression zone at a load of 23.6 kips (105 kN) and reached a deflection of 2.29 in. (58.2 mm) at failure. Negligible end slip was observed on both the NE and NW strands.

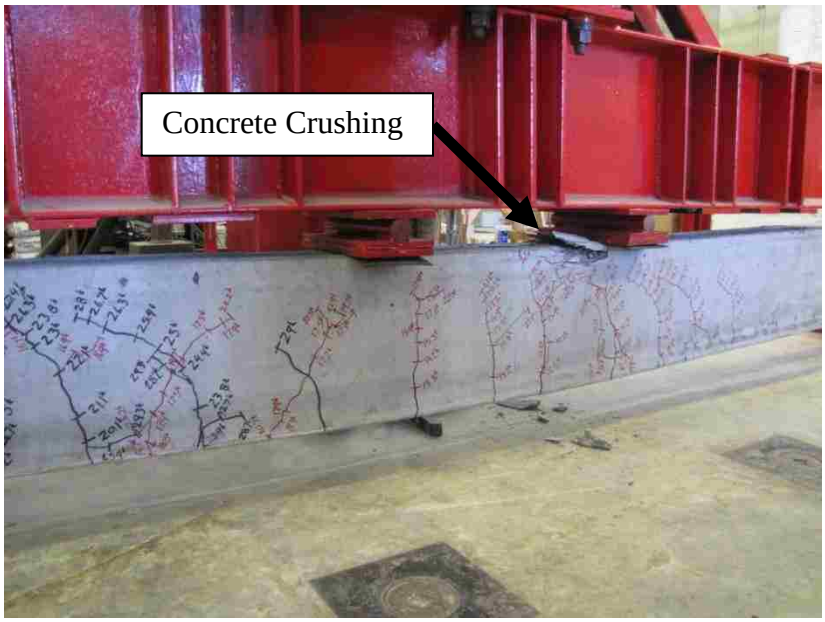

Figure F.27 – S10-2-1_73 at Failure

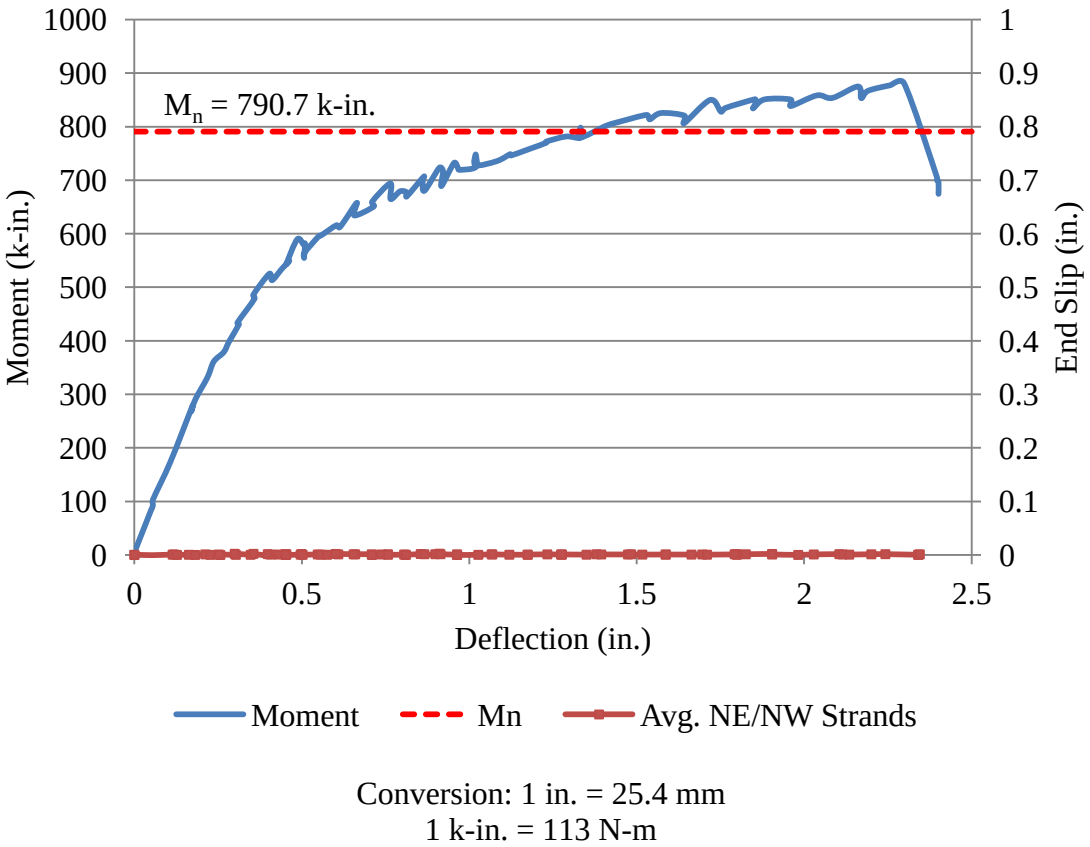

Conversion: 1 in. = 25.4 mm
1 k-in. = 113 N-m

Figure F.28 – S10-2-1_73 Moment vs. Deflection and Strand End Slip vs. Deflection

BEAM ID: S10-2-2_58

DATE OF TESTING: 9/21/2011

DAYS AFTER CASTING: 58

Test Summary	
Embedment Length	58 in.
Failure Mode (Flexural or Bond)	Flexural
Beam End	SE/SW
Span Length	132 in.
Deflection at Failure	1.2 in.
Concrete Compressive Strength	9250 psi
Maximum Moment Capacity	
Expected	790.7 k-in.
Actual	901.2 k-in.
Average Transfer Length	
At Release	13.8 in.
At Time of Testing	15.9 in.
Average 0.1 in. NASP Load for Strand 101	
Standard NASP (Mix B)	18200 lb
NASP in Concrete (1 Day)	27300 lb

Conversion: 1 in. = 25.4 mm
1 lb = 4.45 N
1 psi = 6.89 kPa

The test was set up as deflection-controlled, and the beam was deflected in increments of 0.05 in. (1.27 mm) until failure. The deflection increment was increased to 0.05 in. (1.27 mm) from 0.02 in. (0.508 mm) because it was deemed that 0.02 in. (0.508 mm) increments were too slow. At each deflection increment, the load was noted and then the beam was checked for cracks, which were marked with permanent marker.

The first flexural cracks were observed under the midspan and both supports at a deflection of 0.35 in. (8.89 mm) and load of about 18.2 kips (81.0 kN). Subsequent cracks propagated vertically inside and outside the maximum moment zone and then began angling towards the supports. Horizontal cracks near midspan at the level of prestressing strand were noted at a deflection of 0.80 in. (20.3 mm) and a load of 26.3 kips (117 kN). The beam failed due to concrete crushing within the compression zone at a load of 31.1 kips (138 kN) and reached a deflection of 1.20 in. (30.5 mm) at failure. Negligible end slip was observed on both the SE and SW strands.

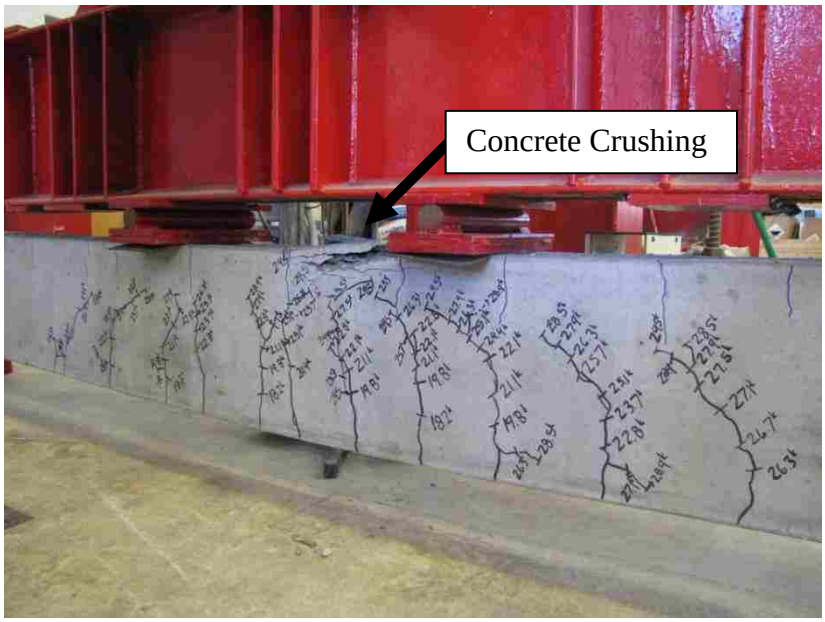

Figure F.29 – S10-2-2_58 at Failure

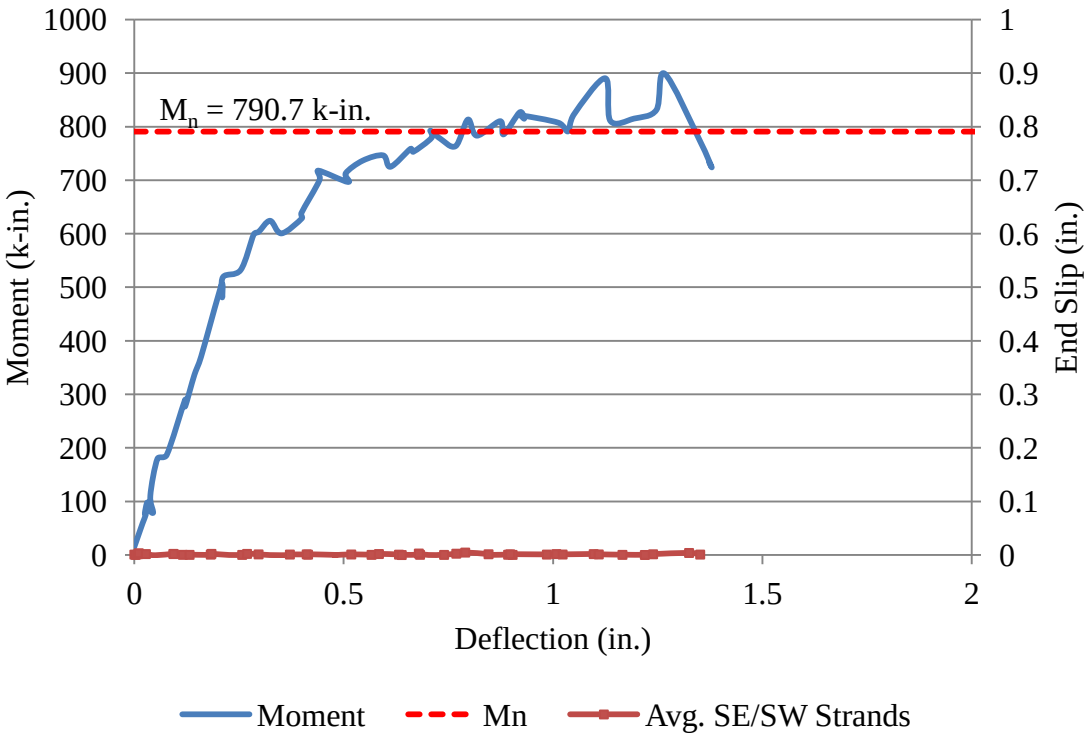

Conversion: 1 in. = 25.4 mm
1 k-in. = 113 N-m

Figure F.30 – S10-2-2_58 Moment vs. Deflection and Strand End Slip vs. Deflection

BEAM ID: S10-2-2_73

DATE: 9/22/2011

DAYS AFTER CASTING: 59

Test Summary	
Embedment Length	73 in.
Failure Mode (Flexural or Bond)	Flexural
Beam End	NE/NW
Span Length	162 in.
Deflection at Failure	2.0 in.
Concrete Compressive Strength	9250 psi
Maximum Moment Capacity	
Expected	790.7 k-in.
Actual	871.7 k-in.
Average Transfer Length	
At Release	13.8 in.
At Time of Testing	15.9 in.
Average 0.1 in. NASP Load for Strand 101	
Standard NASP (Mix B)	18200 lb
NASP in Concrete (1 Day)	27300 lb

Conversion: 1 in. = 25.4 mm
1 lb = 4.45 N
1 psi = 6.89 kPa

The test was set up as deflection-controlled, and the beam was deflected in increments of 0.05 in. (1.27 mm) until failure. The deflection increment was increased to 0.05 in. (1.27 mm) from 0.02 in. (0.508 mm) because it was deemed that 0.02 in. (0.508 mm) increments were too slow. At each deflection increment, the load was noted and then the beam was checked for cracks, which were marked with permanent marker.

The first flexural crack was observed under the midspan at a deflection of 0.40 in. (10.2 mm) and load of about 12.8 kips (56.9 kN). Subsequent cracks propagated vertically inside and outside the maximum moment zone and then began angling towards the supports. Horizontal cracks near midspan at the level of prestressing strand were noted at a deflection of 0.65 in. (16.5 mm) and a load of 16.2 kips (72.1 kN). The beam failed due to concrete crushing within the compression zone at a load of 22.7 kips (101 kN) and reached a deflection of 1.97 in. (50.0 mm) at failure. Negligible end slip was observed on both the NE and NW strands.

Figure F.31 – S10-2-2_73 at Failure

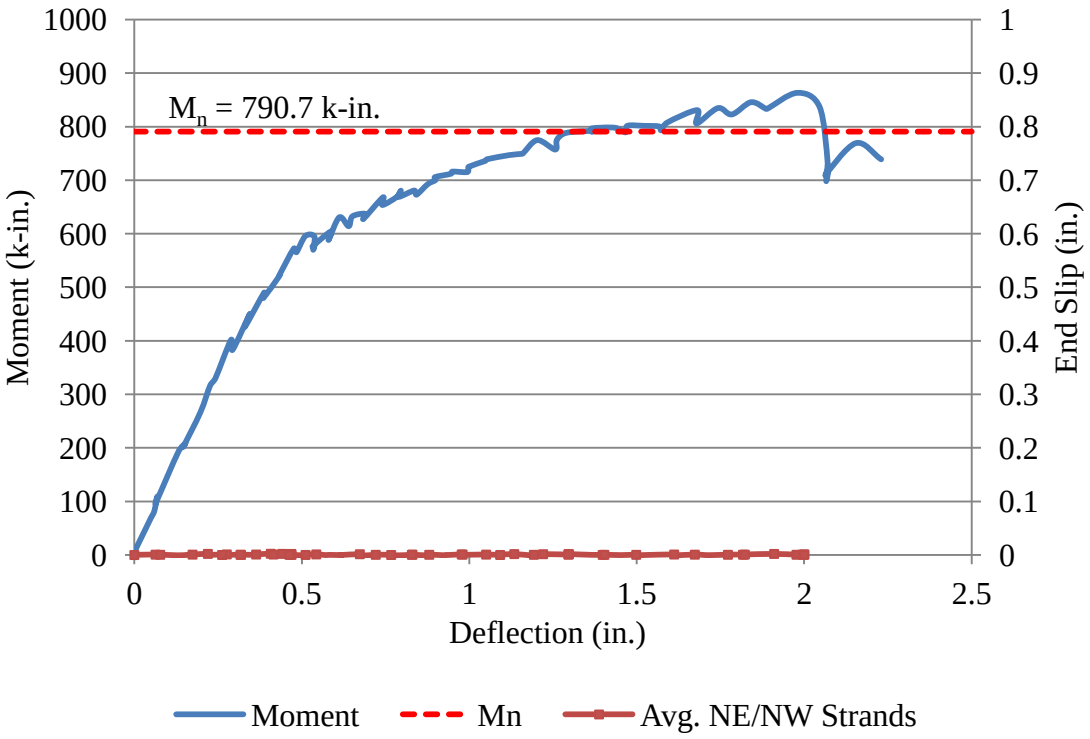

Conversion: 1 in. = 25. 4 mm
1 k-in. = 113 N-m

Figure F.32 – S10-2-2_73 Moment vs. Deflection and Strand End Slip vs. Deflection

BIBLIOGRAPHY

AASHTO (2008). *AASHTO LRFD Bridge Design Specifications: Customary U.S. Units*. 4th ed. Washington D.C.: American Association of State Highway Transportation Officials (AASHTO).

ACI 318 (2011). "Building Code Requirements for Structural Concrete (ACI 318-11) and Commentary (ACI 318R-11)." Farmington Hills, Michigan: American Concrete Institute (ACI).

Anderson, A. R. and Anderson, R. G. (1976). An Assurance Criterion for Flexural Bond in Pretensioned Hollow Core Units." *ACI Journal*, 73 (8), 457-464.

ASTM A 370 (2011). "Standard Test Methods and Definitions for Mechanical Testing of Steel Products." *American Society of Testing and Materials*, West Conshohocken, PA.

ASTM A 416 (2010). "Standard Specification for Steel Strand, Uncoated Seven-Wire for Prestressed Concrete." *American Society of Testing and Materials*, West Conshohocken, PA.

ASTM A 1061 (2009). "Standard Test Methods for Testing Multi-Wire Steel Strand." *American Society of Testing and Materials*, West Conshohocken, PA.

ASTM C 33 (2011). "Standard Specification for Concrete Aggregates." *American Society of Testing and Materials*, West Conshohocken, PA.

ASTM C 39 (2011). "Standard Test Method for Compressive Strength of Cylindrical Concrete Specimens." *American Society of Testing and Materials*, West Conshohocken, PA.

ASTM C 109 (2011). "Standard Test Method for Compressive Strength of Hydraulic Cement Mortars (Using 2-in. or [50 mm] Cube Specimens)." *American Society of Testing and Materials*, West Conshohocken, PA.

ASTM C 138 (2010). "Standard Test Method for Density (Unit Weight), Yield, and Air Content (Gravimetric) of Concrete." *American Society of Testing and Materials*, West Conshohocken, PA.

ASTM C 143 (2010). "Standard Test Method for Slump of Hydraulic Cement Concrete." *American Society of Testing and Materials*, West Conshohocken, PA.

ASTM C 192 (2007). "Standard Practice for Making and Curing Concrete Test Specimens in the Laboratory." *American Society of Testing and Materials*, West Conshohocken, PA.

ASTM C 231 (2010). "Standard Test Method for Air Content of Freshly Mixed Concrete by the Pressure Method." *American Society of Testing and Materials*, West Conshohocken, PA.

ASTM C 469 (2010). "Standard Test Method for Static Modulus of Elasticity and Poisson's Ratio of Concrete in Compression." *American Society of Testing and Materials*, West Conshohocken, PA.

ASTM C 1437 (2007). "Standard Test Method for Flow of Hydraulic Cement Mortar." *American Society of Testing and Materials*, West Conshohocken, PA.

ASTM C 1611 (2009). "Standard Test Method for Slump Flow of Self-Consolidating Concrete." *American Society of Testing and Materials*, West Conshohocken, PA.

ASTM C 1621 (2009). "Standard Test Method for Passing Ability of Self-Consolidating Concrete by J-Ring." *American Society of Testing and Materials*, West Conshohocken, PA.

Barnes, R. W., Grove, J. W., and Burns, N. H. (2003). "Experimental Assessment of Factors Affecting Transfer Length." *ACI Structural Journal*, 100 (6), 740-748.

Boehm, K. M., Barnes, R. W., and Schindler, A. K. (2010). *Performance of Self-Consolidating Concrete in Prestressed Girders*. Auburn University, AL: Highway Research Center and Department of Civil Engineering at Auburn University.

Buckner, C. D. (1995). "A Review of Strand Development Length of Pretensioned Concrete Members." *PCI Journal*, 40 (2), 84-105.

Burgueño, R. and Haq, M. (2007). "Effect of SCC Mixture Proportioning on Transfer and Development Length of Prestressing Strand." ACI Special Publication, 247, 105-116.

Cousins, T. E., Johnston, D. W., and Zia, P. (1990). "Transfer Length of Epoxy-Coated Prestressing Strand." *ACI Materials Journal*, 87 (3), 193-203.

Floyd, R. W., Ruiz, E. D., Do, N. H., Staton, B. W., and Hale, W. M. (2011). "Development Lengths of High-Strength Self-Consolidating Concrete Beams." *PCI Journal*, 56 (1), 36-53.

Girgis, A. F. M. and Tuan, C. Y. (2005). "Bond Strength and Transfer Length of Pretensioned Bridge Girders Cast with Self-Consolidating Concrete." *PCI Journal*, 50 (6), 72-87.

Hawkins, N. M. and Ramirez, J. A. (2010). *Due Diligence Review of NASP Strand Bond Test Method*. Champaign, IL: University of Illinois at Urbana-Champaign, and West Lafayette, IN: Purdue University.

Janney, J. R. (1954). "Nature of Bond in Pre-Tensioned Prestressed Concrete." *Journal of the American Concrete Institute*, 25 (9), 717-736.

Kaar, P. H., LaFraugh, R. W., and Mass, M. A. (1963). "Influence of Concrete Strength on Strand Transfer Length." *PCI Journal*, 8 (5), 47-67.

Lane, S.N. (1998). A New Development Length Equation for Pretensioned Strands in Bridge Beams and Piles. McLean, Virginia: Federal Highway Administration (FHWA).

Larson, K. H., Peterman, R. J., and Esmaeily, A. (2007). "Bond Characteristics of Self-consolidating Concrete for Prestressed Bridge Girders." *PCI Journal*, 52 (4), 44-57.

Levy, K. (2007). "Bond Behavior of Prestressed Reinforcement in Beams Constructed with Self-Consolidating Concrete." M.S. Thesis, Auburn University, Auburn, AL.

Logan, D. R. (1997). "Acceptance Criteria for Bond Quality of Strand for Pretensioned Prestressed Concrete Applications." *PCI Journal*, 42 (2), 52-90.

Mitchell, D., Cook, W. D., Khan, A. A., and Tham, T. (1993). "Influence of High Strength Concrete on Transfer and Development Length of Pretensioning Strand." *PCI Journal*, 38 (3), 52-66.

Peterman, R. J. (2007). "The Effects of As-Cast Depth and Concrete Fluidity on Strand Bond." *PCI Journal*, 52 (3), 72-101.

Petrou, M. F., Wan, B., Joiner, W. S., Trezos, C. G., and Harries, K. A. (2000). "Excessive Strand End Slip in Prestressed Piles." *ACI Structural Journal*, 97 (5), 774-782

Pozolo, A. M. and Andrawes, B. (2011). "Transfer Length in Prestressed Self-Consolidating Concrete Box and I-Girders." *ACI Structural Journal*, 108 (3), 341-349.

Precast/Prestressed Concrete Institute (PCI). (2003). *Interim Guidelines for the Use of Self-Consolidating Concrete in Precast/Prestressed Concrete Institute Member Plants*. 1st. Ed. Chicago, IL: Precast/Prestressed Concrete Institute (PCI).

Ramirez, J. A. and Russell, B. W. (2008) Transfer, Development, and Splice Length for Strand/Reinforcement in High-Strength Concrete. Washington D.C.: Transportation Research Board.

Rose, D. R. and Russell, B. W. (1997). "Investigation of Standardized Tests to Measure the Bond Performance of Prestressing Strand." *PCI Journal*, 42 (4), 56-80.

Russell, B.W. (2006). *Final Report NASP Round IV Strand Bond Testing*. Stillwater, OK: Oklahoma State University.

Russell, B.W. and Burns, N.H. (1993). Design Guidelines for Transfer, Development and Debonding of Large Diameter Seven Wire Strands in Pretensioned Concrete Girders. Austin, TX: Center for Transportation Research at the University of Texas at Austin.

Russell, B. W. and Burns, N. H. (1997). "Measurement of Transfer Lengths in Pretensioned Concrete Elements." *Journal of Structural Engineering*, 123 (5), 541-549.

Russell, B. W. and Paulsgrove, G. A. (1999a). *NASP Strand Bond Testing Round One Pull-out Tests and Friction Bond Tests of Untensioned Strand*. Norman, OK: Fears Structural Engineering Laboratory at the University of Oklahoma.

Russell, B. W. and Paulsgrove, G. A. (1999b). NASP Strand Bond Testing Round Two Assessing Repeatability and Reproducibility of the Moustafa Test, the PTI Bond Test, and the NASP Bond Test. Norman, OK: Fears Structural Engineering Laboratory at the University of Oklahoma.

Shahawy, M. (2001). "A Critical Evaluation of the AASHTO Provisions for Strand Development Length of Prestressed Concrete Members." *PCI Journal*, 46 (4), 94-117.

Staton, B. W., Do, N. H., Ruiz, E. D., and Hale, W. M. (2009). "Transfer Lengths of Prestressed Beams Cast with Self-Consolidating Concrete." *PCI Journal*, 54 (2), 64-83.

Tabatabai, H. and Dickson, T. J. (1993). "The History of the Prestressing Strand Development Length Equation." *PCI Journal*, 38 (6), 64-75.

Wan, B., Petrou, M. F., Harries, K. A., and Hussein, A. A. (2002). "Top Bar Effects in Prestressed Concrete Piles." *ACI Structural Journal*, 99 (2), 208-214.

VITA

Krista Beth Porterfield grew up in Park Ridge, IL. After graduating from Maine Township High School South in 2006, she moved to Rolla, MO to attend University of Missouri-Rolla, now Missouri University of Science and Technology, where she was a four year National Merit Scholar and earned a Bachelor's degree in Civil Engineering. As a freshman, Krista was a walk-on on the UMR/Missouri S&T softball team and played all four years, working her way to an athletic scholarship her senior year and also earning ESPN Academic All District Second Team honors. After receiving her Bachelor's degree, she continued her education at Missouri S&T, completing her Master's degree in Civil Engineering in 2012. As graduate student, Krista was a PCI Daniel P. Jenny Fellowship recipient as well as a Chancellor's Fellowship recipient. Upon the completion of her graduate studies, Krista will begin work as an entry-level structural engineer at Wallace Engineering in Tulsa, OK.